Fate, Transport, and Detection of Poly- and Perfluoroalkyl Substances in Natural and Engineered Environments

Citation

Permanent link

Terms of Use

Share Your Story

Fate, Transport, and Detection of Poly- and Perfluoroalkyl Substances in Natural and Engineered Environments

A DISSERTATION PRESENTED

BY

ANDREA KRISTINA TOKRANOV

TO

THE HARVARD JOHN A. PAULSON SCHOOL OF ENGINEERING AND APPLIED SCIENCES

IN PARTIAL FULFILLMENT OF THE REQUIREMENTS

FOR THE DEGREE OF

DOCTOR OF PHILOSOPHY

IN THE SUBJECT OF

ENVIRONMENTAL SCIENCE & ENGINEERING

HARVARD UNIVERSITY

CAMBRIDGE, MASSACHUSETTS

DECEMBER 2018

Dissertation Advisors: Elsie M. Sunderland and Chad D. Vecitis   Andrea Kristina Tokranov

Fate, Transport, and Detection of Poly- and Perfluoroalkyl Substances in Natural and Engineered Environments

ABSTRACT

Exposure to poly- and perfluoroalkyl substances (PFASs) has been linked to metabolic disruption, immunotoxicity, and cancer in humans, among other adverse health outcomes. The widespread contamination of drinking water arising from the persistence and aqueous mobility of PFASs prompted the U.S. Environmental Protection Agency to issue a lifetime drinking water health advisory for two specific PFASs in 2016: perfluorooctanoic acid (PFOA) and perfluorooctane sulfonate (PFOS). An overview of the intractable PFAS contamination issue is provided in Chapter 1. Given that groundwater is a major source of drinking water, the main objective in Chapter 2 was to investigate geochemical and hydrological processes governing the subsurface transport of PFASs at a former fire training area on Cape Cod, Massachusetts, where PFAS-containing aqueous film-forming foams (AFFFs) were used historically. AFFF is one of the primary sources of groundwater and surface water PFAS contamination in the United States. One of the outcomes from this study was the discovery of mobile perfluoroalkyl acid (PFAA) precursors. PFAA precursors can transform in the human body to terminal compounds such as PFOS and PFOA, but are not included in typical drinking water analysis. Chapter 3 presents an investigation of PFAS transport and the persistence of PFAA precursors across groundwater/surface water boundaries. Although the transport of PFASs through these boundaries was impacted by a complex mixture of hydrogeochemical conditions, the

persistence of precursors in aerobic surface waters and downgradient groundwater (located in residential areas) was established. Chapters 2 and 3 highlight the importance of understanding the total mass of organic fluorine (including precursors) in water. Chapter 4 compliments this by presenting a method to measure total organic fluorine in the surface of consumer products, which are another primary source of PFAS exposure to humans. X-ray photoelectron spectroscopy is demonstrated to be a reliable tool to quantify surficial fluorine in consumer products, can provide important information on the depth distribution of fluorine, and does not require time-intensive extraction procedures prior to analysis, which is an advantage over traditional PFAS analysis techniques.

Table of Contents

viii

List of Figures

List of Tables

Glossary of Terms

4:2 fluorotelomer sulfonate	4:2 FtS
6:2 fluorotelomer sulfonate	6:2 FtS
8:2 fluorotelomer sulfonate	8:2 FtS
Aqueous film-forming foam	AFFF
Fire training area	FTA
Liquid chromatography quadrupole time-of-flight mass spectrometry	LC-QTOF-MS
Liquid chromatography-tandem mass spectrometry	LC-MS/MS
N-Ethyl perfluorooctane sulfonamidoacetic acid	N-MeFOSAA
N-Methyl perfluorooctane sulfonamidoacetic acid	N-EtFOSAA
Particle-induced gamma ray emission	PIGE
Perfluorinated carboxylate	PFCA
Perfluoroalkyl acid	PFAA
Perfluorobutane sulfonate	PFBS
Perfluorobutanoate	PFBA
Perfluorodecane sulfonate	PFDS
Perfluorodecanoate	PFDA
Perfluorododecanoate	PFDoDA
Perfluoroheptane sulfonate	PFHpS
Perfluoroheptanoate	PFHpA
Perfluorohexane sulfonate	PFHxS
Perfluorohexanoate	PFHxA
Perfluorinated sulfonates	PFSA
Perfluorononane sulfonate	PFNS
Perfluorononanoate	PFNA
Perfluorooctane sulfonamide	FOSA
Perfluorooctane sulfonate	PFOS
Perfluorooctanoate	PFOA
Perfluoropentane sulfonate	PFPeS
Perfluoropentanoate	PFPeA
Perfluorotetradecanoate	PFTeDA
Perfluorotridecanoate	PFTrDA
Perfluoroundecanoate	PFUnDA
Poly- and perfluoroalkyl substances	PFASs
X-ray photoelectron spectroscopy	XPS

Acknowledgments

There have been many people whom I would like to thank for their support and friendship throughout my PhD. First, I would like to thank my advisor Dr. Chad Vecitis, who gave me the intellectual freedom to pursue the research I found most exciting and encouraged me to forge my own path, while at the same time providing me with support and guidance when I needed it. I believe this has helped turn me into a stronger researcher, and I am thankful for his mentorship, as well as friendship, over the last several years. I would also like to thank Dr. Elsie Sunderland, who has been incredibly supportive of my research, even before she became my advisor. She has taught me through example how to write more effectively and has provided excellent scientific insight into some of my research conundrums. I'm lucky to have had two advisors that are truly passionate about my research and my future.

Of course, I am also extremely fortunate to have collaborated with the U.S. Geological Survey throughout the course of my PhD. I'm deeply grateful to Denis LeBlanc and Dr. Larry Barber for their scientific guidance on hydrology and biogeochemistry, and everything related to the field sampling in this work. This dissertation would not have been remotely possible if it were not for their collaborative spirit and all the energy they put into making sure my research moved along. I would like to express my heartfelt thanks to Dr. Larry Barber for his mentorship and guidance throughout my PhD, and thank both Larry and Denis for their ceaseless efforts to advance my scientific career. I'd also like to thank the U.S. Geological Survey Cape Cod Toxics group for welcoming me to the team back in my first year when I was still a bit lost as to my project, and for their continued support of my research since then. Special thanks to Robert (Quinn) Hull, Timothy McCobb, Deborah Repert, Richard Smith, Douglas Kent, John Karl Böhlke, Ronald Harvey, John Lane, Martin Briggs, Jeremy Jasmann, and Jennifer Underwood. I am fortunate to have worked with such an amazingly collaborative group of people.

I would also like to express my gratitude to Dr. Zhiming Kuang for his insightful feedback during my qualifying exam, and for dedicating his time to participate as a dissertation committee member. Additionally, the Vecitis and Sunderland groups have made my time here so enjoyable. In particular, I would like to thank Han, Qiaoying, Greg, Marielle, Jenny, Bianca, Carlo, Prentiss, Clifton, Cindy, Ryan, Nicole, Bridger, Kyle, Marie, Charlotte, and Heidi for making the days in the laboratory and the office more fun! And of course, I would like to thank Bram Maasakkers for being a wonderful friend and for climbing with me for 5+ years and not dropping me.

Finally, I would like to thank my parents Karen and Peter Weber, my brothers Erik and Axel Weber, my aunt Carole Wilson, and my parents-in-law Natalya and Vadim Tokranov, for all their support over the years. They were always there through the good times and hard, even if some of them made fun of me for the way I say "experiment". And of course, I am forever grateful for my dear husband Anton, who has been a rock by my side through everything.

Chapter 1

INTRODUCTION AND OVERVIEW

Water quality can be compromised by metals, nutrients, anthropogenic contaminants, and a myriad of other factors. This has been emphasized through the widely publicized lead contamination in Flint, Michigan. Currently, the United States and many other countries are beginning to recognize the breadth and implications of contamination from poly- and perfluoroalkyl substances (PFASs) in the hydrological cycle. PFASs are anthropogenic compounds characterized by the presence of the C_nF_{2n+1} – moiety within the structure, and have been manufactured since the 1940s (>4000 compounds manufactured).[1-3] The multitude of industrial uses for these thermally and chemically stable compounds that have excellent surface tension-lowering properties has led to widespread usage and environmental release.[1, 2]

Health outcomes that have been associated with exposure to various PFAS compounds include dyslipidemia, cancer, obesity, and immunotoxicity in children.[4-7] In 2016 the U.S. Environmental Protection Agency (EPA) set lifetime drinking water health advisories of 70 ng L^{-1} for the combined concentration of perfluorooctanoate (PFOA) and perfluorooctane sulfonate (PFOS).[8, 9] This advisory is low in concentration compared to EPA maximum contaminant level drinking water regulations for other organic pollutants such as trichloroethylene (TCE, 5000 ng L^{-1}) and polychlorinated biphenyls (PCBs, 500 ng L^{-1}). PFOS and PFOA and their precursors have been the focus of international attention because of their extreme persistence and accumulating evidence of adverse health outcomes from epidemiology studies. [1, 8, 9] Health research on other PFASs is ongoing. While PFASs are ubiquitous in the environment, human exposure can vary depending on the indoor environment (air/dust inhalation), and

concentrations in drinking water and food. Currently, there are research gaps in all factors affecting human exposure to PFASs.

1.1   NOMENCLATURE AND STRUCTURAL PROPERTIES

The *per* in *per*fluoroalkyl substances refers to aliphatic compounds where every hydrogen attached to a carbon has been replaced with fluorine (i.e. fully fluorinated).[1] *Poly*fluoroalkyl substances can contain a mix of hydrogen and fluorine attached to carbon.[1] The perfluoroalkyl moiety is thermally and chemically stable, and hydrophobic and oleophobic.[1] The main groups of PFASs discussed here (Figure 1.1) include perfluoroalkyl acids (PFAAs), PFAA precursors (hereon simply referred to as precursors), and fluorinated polymers. Within the PFAA class, the perfluorinated carboxylates (PFCAs), and perfluorinated sulfonates (PFSAs) are differentiated by their anionic headgroup (Figure 1.1). The carboxylate (PFCA) and sulfonate (PFSA) headgroups are hydrophilic and anionic under most environmental conditions (pK_a <1). The combination of the anionic headgroup and hydrophobic tail makes PFCAs, PFSAs, and a range of other PFASs useful as surfactants.[1] PFAAs are frequently grouped by their chain length, as increasing chain length typically results in greater partitioning to solids. "Long-chain length" refers to PFCAs with $n \geq 7$ and PFSAs with $n \geq 6$, where n is the number perfluorinated carbons.[1] Long-chain length PFAAs tend to be more bioaccumulative and typically more toxic than short-chain length PFAAs (although there are not as many studies on the toxicity of short-chain length PFAAs), while short-chain length PFAAs are thought to be more mobile in the environment.[10] Both PFCAs and PFSAs are extremely resistant to biotic and abiotic transformation.[1]
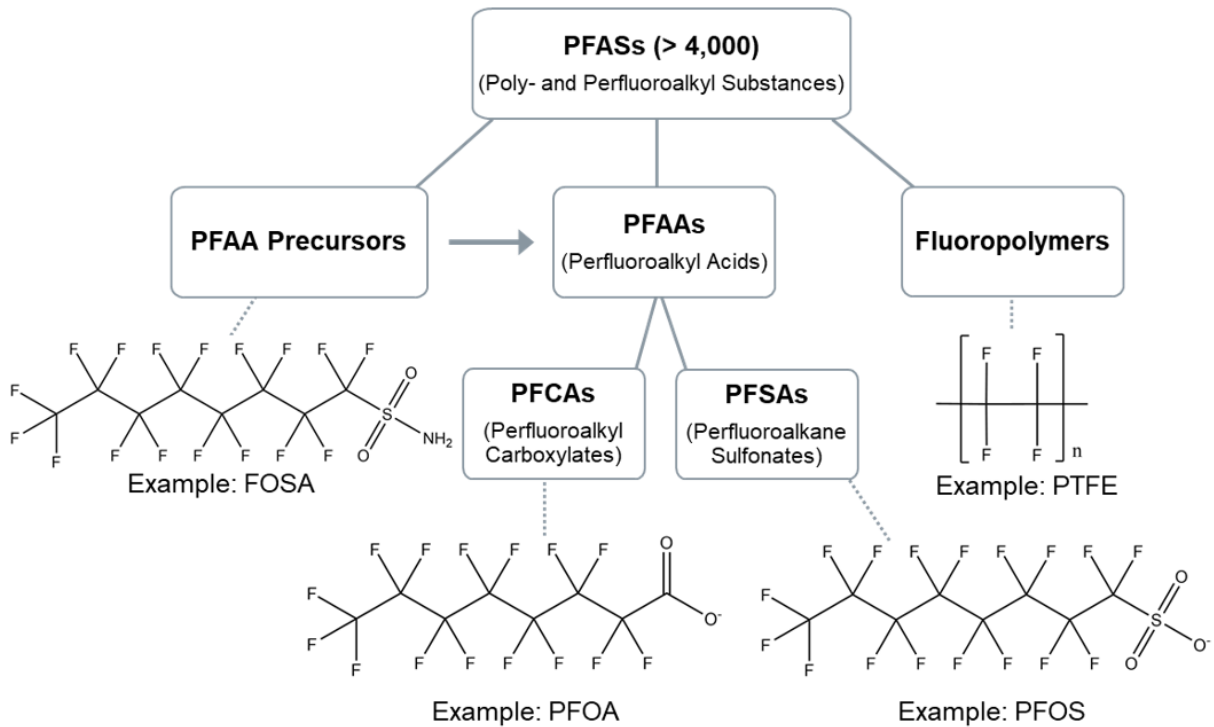
Figure 1.1 Schematic of PFASs discussed in this work. FOSA is perfluorooctane sulfonamide, PFOA is perfluorooctanoate, PFOS is perfluorooctane sulfonate, and PTFE is polytetrafluoroethylene.

1.2   OVERVIEW OF PFAS USES, ENVIRONMENTAL SOURCES, & HUMAN EXPOSURE

Environmental contamination frequently occurs near industries manufacturing or employing PFASs as part of the manufacturing process.[5, 11, 12] PFASs are often used as surfactants, and one significant application is in aqueous film-forming foam (AFFF) used to fight hydrocarbon fuel fires. The low surface tension of the PFAS-containing AFFF allows it to spread over hydrocarbon fuel spills and effectively quench oxygen contact.[13, 14] While AFFFs are still in use today, the PFAS composition has shifted away from PFOS in favor of shorter-chain length PFASs.[14] AFFFs are kept at airports, military bases, municipal fire departments, in the petrochemical industry, and generally in places with risk of hydrocarbon fuel fires.[13] Fire-training

exercises with AFFFs were often conducted repetitively over unlined soils, and these locations have also been shown to be a source of significant environmental PFAS contamination.[15-17]

Additionally, PFASs are often applied as coatings on consumer products (textiles, paper goods, food packaging) for water and oil repellency.[18] As a result of widespread occurrence of PFASs in consumer products, domestic wastewater effluent (and biosolids) and landfills are sources of PFASs to the environment.[19, 20] Wastewater treatment plants are not typically capable of treating for PFAS compounds, and the treatment process has been shown to increase the concentrations of some PFAAs as a result of precursor transformation.[21] Finally, wet and dry atmospheric deposition of PFASs is a non-point source of PFASs to the environment.[19] The multitude of inputs to the environment and the persistence of the perfluoroalkyl moiety has led to the ubiquitous occurrence of PFASs, and a challenging environmental problem.

Similar to the wide variety of sources, human exposure can occur through several pathways. The EPA assumes drinking water has a relative source contribution of 20% to human plasma PFAS concentrations, although exposure can be much higher if the water is from a contaminated source (one study finds median human PFOA serum concentrations 20 times the general U.S. population near a fluoropolymer manufacturing plant).[22] Food (particularly seafood) has also been shown to be a major exposure pathway (up to 84% the median total PFOA intake), as has inhalation of air/dust depending on the indoor environment (up to 50% total PFOA intake).[23, 24] Exposure pathways may also change depending on age. For example, daily intake from dust is estimated to be higher for toddlers than for adults.[25] As children are particularly vulnerable to PFAS exposure,[6] understanding the diverse sources and exposure pathways is critical and is an active area of research.

1.3   THESIS STRUCTURE

This work investigates PFASs in both natural (groundwater and surface water) and engineered (military fire training area and consumer products) environments. Human exposure can be impacted by the PFAS distribution, fate, and transport in/from all these environments and is thus essential to understand. While drinking water is an important human PFAS exposure vector, the fate and transport of PFASs in the hydrological cycle is poorly understood. The first two components of this work focus on the fate and transport of PFASs in groundwater and surface water at a site that has been contaminated with AFFF and wastewater effluent. The first study (Chapter 2) investigates a groundwater PFAS plume as it migrates from the source(s), and concludes that 2.1) the AFFF and wastewater sources can be distinguished based on the PFAS composition near the unsaturated zone, 2.2) despite the assumed mobility of many PFASs, the unsaturated zones remain a source of PFASs for decades following the last inputs, and 2.3) some precursors appear to be mobile, contradicting previously held assumptions. The second body of work (Chapter 3) investigates fate and transport of PFASs between groundwater/surface-water bodies. The previously characterized groundwater plume (Chapter 2) is discharged into a surface water body, where oxygenated conditions prevail (residence time of ~1.6 years), before re-entering groundwater on the downgradient side of the lake. The boundary between groundwater and surface-water is often an area of increased chemical and biological activity, which may impact PFAS fate. Here, the study finds 3.1) transport may be controlled by local hydrogeochemical conditions and may be seasonally and functional-group dependent, 3.2) the air-water interface may have significant effects on PFAS transport, and 3.3). while precursors concentrations decrease, they are persistent in oxygenated environments. Typical measurement techniques target specific PFAS structures and often don't include any precursor structures at all. However, based on the observed aqueous persistence and mobility of precursors within this work, this could underestimate human PFAS exposure.

In the last body of work presented here (Chapter 4), X-ray photoelectron spectroscopy (XPS) techniques were applied to determine whether XPS could provide a more holistic surficial organic fluorine measurement in contrast to traditional PFAS measurement techniques (liquid chromatography-tandem mass spectrometry, or gas chromatography-mass spectrometry). This work naturally extended from the previous two studies: the first two studies highlighted the need to be able to quantify total organic fluorine in water, while this study investigated a method to provide a similar capability for consumer products. Measuring PFAS concentrations in consumer products is particularly difficult owing to challenges such as incomplete PFAS extraction, analysis of only a targeted set of PFAS structures, and matrix effects from the consumer products. However, we find XPS measurement of fluorine is comparatively straightforward, and allows for 4.1) quantification of surficial atomic percent fluorine, 4.2) confirmation of highly fluorinated carbon bonds, and 4.3) fluorine depth resolution in consumer products.

Chapter 2

GEOCHEMICAL AND HYDROLOGIC FACTORS CONTROLLING SUBSURFACE TRANSPORT OF POLY- AND PERFLUOROALKYL SUBSTANCES, CAPE COD, MASSACHUSETTS

2.1   ABSTRACT

Growing evidence that PFASs are associated with negative human health effects prompted the U.S. EPA to issue lifetime drinking water health advisories for PFOA and PFOS in 2016. Given that groundwater is a major source of drinking water, the main objective of this work was to investigate geochemical and hydrological processes governing the subsurface transport of PFASs at a former fire training area (FTA) on Cape Cod, Massachusetts, where PFAS-containing aqueous film-forming foams were used historically. A total of 148 groundwater samples and 4 sediment cores were collected along a 1,200-m-long downgradient transect originating near the FTA, and analyzed for PFAS content. The results indicate that unsaturated zones at the FTA and at hydraulically downgradient former domestic wastewater effluent infiltration beds both act as continuous PFAS sources to the groundwater despite 18 and 20

years of inactivity, respectively. Historically different PFAS sources are evident from contrasting PFAS composition near the water table below the FTA and wastewater-infiltration beds. Results from total oxidizable precursor assays conducted using groundwater samples collected throughout the plume suggest that some perfluoroalkyl acid precursors at this site are transporting with perfluoroalkyl acids.
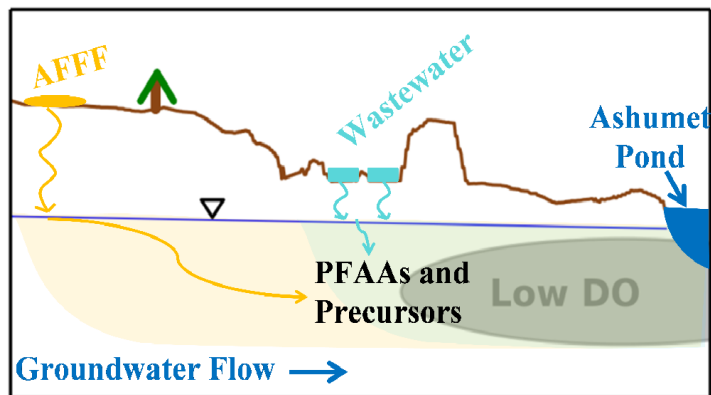
Figure 2.1 Conceptual model of the field site.

2.2 INTRODUCTION

PFASs are common contaminants in the aquatic environment owing to their widespread use in consumer and industrial applications, such as protective coatings, and as a major component in aqueous film-forming foams (AFFFs).[13, 26-28] PFASs have been associated with cancer, immune dysfunction in children, obesity, and thyroid disease, among other adverse health outcomes.[4-6, 29] Given that groundwater is a major source of drinking water and constitutes approximately 22% of total water use in the United States,[30] there is an urgent need to understand the subsurface fate and transport of PFASs.

Groundwater, soil, and surface-water contamination from use of AFFFs during fire-related emergencies and fire-training activities has caused increasing concern for groundwater

quality because AFFFs are a highly concentrated PFAS point source.[28, 31] Fire training areas (FTAs) are potential sources of long-term PFAS influx to the unsaturated zone and groundwater, particularly where hydrocarbon fires were repeatedly extinguished with AFFFs over unlined soil. Studies conducted at several sites impacted by use of AFFFs report groundwater concentrations of PFOS and PFOA above the U.S. EPA lifetime drinking water health advisory level of 70 ng L^{-1} for the combined concentration of PFOS and PFOA, with some sites reaching up to five orders of magnitude above this limit.[8, 9, 16, 32-36] Other PFASs do not presently have EPA health advisories.

AFFF formulations are complex mixtures that generally contain 1-5% w/w PFASs,[31] and are diluted with water before use such that the final solution contains 1-6% v/v of the initial formulation. In 2004, the U.S. inventory of AFFFs was estimated to be $3.75×10^7$ kg.[37] Major users include the military (29%), commercial aviation (16%), fire departments (14%), and the petrochemical industry (39%).[37] Polyfluorinated substances, often a major constituent of AFFFs and other products, can transform into perfluoroalkyl acids (PFAAs), which are extremely recalcitrant to further transformation.[17, 38-43] PFAAs include both perfluorinated sulfonates and carboxylates.

Another significant source of PFASs to the aquatic environment is their use in consumer products and discharge from wastewater treatment plants (WWTPs).[21, 44, 45] PFASs are typically not removed through the treatment process, and some PFAAs have been shown to increase in concentration during treatment as a result of PFAA precursor (from now on referred to as precursor) transformation.[21, 44, 45]

The main objective of this study was to provide information on the factors affecting subsurface mobility of PFASs and the potential for precursor transformation at a site with groundwater contamination from both FTA and WWTP sources. High resolution spatial data at sites contaminated with PFASs are currently lacking and there is limited knowledge of the

9

complex processes controlling PFAS subsurface fate and transport. To address this gap, groundwater samples were collected from wells located along a 1200-m-long transect oriented in the direction of the regional groundwater flow on western Cape Cod, MA. The upgradient wells are located around a former FTA, and 580-690 m downgradient along the flow path is a former WWTP where secondarily treated domestic wastewater effluent was disposed of into infiltration beds. Concentrations of PFASs were measured in groundwater samples collected from wells located at various depths and distances from the FTA to characterize subsurface distributions in a shallow, unconfined sand and gravel aquifer. Sediment cores were collected adjacent to selected groundwater sampling locations and analyzed for PFASs to determine *in situ* sediment/water distribution coefficient (K_d) values. In addition, total oxidizable precursor assays were conducted in the laboratory on selected groundwater samples to determine the presence of precursor compounds and the potential for transformation to PFAAs. The results of this study provide a unique data set on a complex groundwater contamination plume originating from multiple sources.

2.3   METHODS

2.3.1   SITE DESCRIPTION AND HYDROLOGIC SETTING

The study was conducted on western Cape Cod, Massachusetts (Figure 2.2, Figure A1), at the U.S. Geological Survey (USGS) Cape Cod Toxic Substances Hydrology Research Site[46] located on Joint Base Cape Cod. At this site, a groundwater contaminant plume resulting from disposal of treated domestic wastewater has been the subject of long-term hydrogeology and biogeochemistry research.[47-56] The FTA at Joint Base Cape Cod (FTA-1) was used from 1958 to 1985, and records indicate that jet fuel, chlorinated hydrocarbons, transformer oils, paint thinners, and gasoline were released at the site.[57] Use of AFFFs at FTA-1 likely began in 1970

and continued until 1985, with one additional application in 1997.[58, 59] Thermal soil remediation targeting fuel constituents and chlorinated solvents was undertaken at FTA-1 in 1997.[59] The soil was excavated to a maximum depth of 11 m below land surface (the water table is approximately 17 m below land surface) and heated to between 157°C and 204°C before being backfilled.[59] Because PFOA is thermally stable up to 300°C, and perfluorinated sulfonates require even higher temperatures for thermolysis,[60-62] the soil treatment was unlikely to have reduced concentrations of PFAAs. Some precursors may have been thermolyzed to form PFAAs.

FTA-1 is located 580 m upgradient of a WWTP where domestic wastewater produced on the military base was treated from 1936 to 1995 and the effluent disposed of into the sand and gravel aquifer through infiltration beds (Figure 2.2).[63] Wastewater effluent disposal to the aquifer resulted in a large and chemically complex contaminant plume currently characterized by low dissolved oxygen (DO) concentrations and elevated concentrations of dissolved organic carbon (DOC), nitrate, phosphate, ammonium, boron, and organic micropollutants.[51, 52, 55] Boron is used as an indicator for the wastewater plume location (Figure 2.2).[50]

The glacial outwash sediments that comprise the unconfined aquifer at the study site consist of medium to coarse sand and gravel. Hydraulic properties measured during a large-scale tracer experiment at the site include a hydraulic conductivity of 110 m d^{-1}, porosity of 0.39, and average flow velocity of 0.42 m d^{-1}.[64, 65] Recharge to the aquifer from precipitation is 73 cm yr^{-1}.[66] The water table altitude can fluctuate by ~1 m yr^{-1} depending on precipitation[65] and is about 17 m and 6.5 m below land surface at FTA-1 and the infiltration beds, respectively.
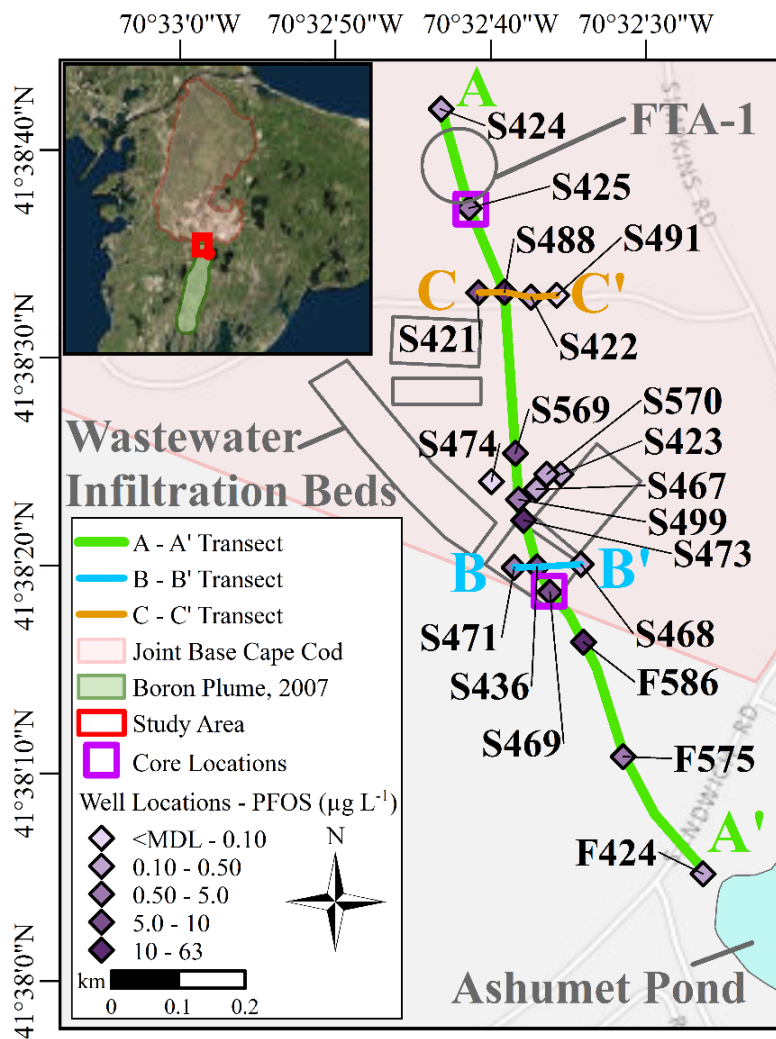
Figure 2.2. Locations and identifiers of groundwater monitoring sites (diamond symbols) sampled during 2015 at the Cape Cod study site. Symbol shading corresponds to the maximum PFOS concentration at each site because PFOS was often the highest PFAS concentration in groundwater samples. Nearly all locations were sampled at multiple depths. The boron plume indicates the extent of the wastewater plume.[50]

2.3.2 GROUNDWATER AND AQUIFER SEDIMENT SAMPLING

Groundwater samples (Figures 2.2 and A1) were collected according to USGS field protocols[67] during 2014 and 2015 from a network of monitoring-well clusters, multilevel

samplers, and continuous multichannel tubing wells (herein, all sampling types are referred to as wells). Sediment cores were collected at S425 (one 1-m core) and at S469 (three 1-m cores) using a piston-type coring device (see Methods section of Appendix A).

A total of 148 groundwater samples were collected during June and December 2014 (19 samples), May-July 2015 (118 samples) and November 2015 (11 samples) from 25 well locations. Note that most well locations (Figure 2.2) have multiple depths associated with each site.[68] The 1,200-m-long A-A' longitudinal transect (Figure 2.2) includes 11 well locations (81 sampling points) along the direction of groundwater flow. There are 9 additional well locations (37 sampling points) located transverse to the A-A' transect (Figure 2.2), including the B-B' and C-C' transects (Figure A2). During June 2014, 5 additional well locations were sampled that are located at greater downgradient distances than the A-A' transect (Figure A1). Unless otherwise noted, the discussion and statistics focus on the major sampling in May-July 2015 to minimize any temporal variability. All distances within the A-A' transect are given along the direction of groundwater flow relative to the estimated center of FTA-1 based on site maps.[57] The transect passes through the infiltration beds and ends near Ashumet Pond (Figure 2.2). Ancillary water quality analyses[53] were conducted and include specific conductance, pH, temperature, DO, phosphate, nitrate, and DOC.[68]

2.3.3 ANALYTICAL MATERIALS

Native and isotopically labeled PFAS standards were purchased from Wellington Laboratories (Guelph, Canada). The PFAS compound names, abbreviations, and key properties are listed in Table 2.1. Details on the analytical internal standards are listed in Table A1. A Barnstead NANOpure Infinity (Lake Balboa, CA) water system provided deionized water (DI) with a resistivity of >18 MΩ cm^{-1}. Other materials are described in Appendix A.

Table 2.1 Compound names, abbreviations, and key properties of poly- and perfluoroalkyl substances and the organic carbon normalized sediment/water partition coefficients (K_{oc}) measured in this study as well as select K_{oc} values from the literature. See referenced work for details. The poly- and perfluoroalkyl substances are reported in anionic form (except for perfluorooctane sulfonamide). K_{oc} values from this study are calculated from measured K_d values and fraction of organic carbon (f_{oc}) values (see Table A2), and may be uncertain based on the difficulty in quantifying low total organic carbon values (<0.0003).

Compound Name	Abbrev.	Mol Formula	Mol Wt	pKa [69,70]	Avg log K_{oc} (this study)	Avg log K_{oc} (lit, laboratory-based)[71-74] low - high range provided	Avg log K_{oc} (lit, field-based)[16,75,76] low - high range provided
Perfluorinated Carboxylates							
Perfluorobutanoate	PFBA	$C_3F_7COO^-$	213	0.4		1.72 ± 0.29 - 1.88 ± 0.11	2.17 ± 1.10
Perfluoropentanoate	PFPeA	$C_4F_9COO^-$	263	-0.1	**2.17 ± 0.77**	1.37 ± 0.46 - 1.71 ± 0.07	1.85 ± 0.70
Perfluorohexanoate	PFHxA	$C_5F_{11}COO^-$	313	-0.16	**2.56 ± 0.17**	1.31 ± 0.29 - 1.90 ± 0.04	1.91 ± 0.39 - 2.06 ± 0.67
Perfluoroheptanoate	PFHpA	$C_6F_{13}COO^-$	363	-0.19	**2.76 ± 0.09**	0.23 ± 0.92 - 1.63 ± 0.15	2.04 ± 0.48 - 2.19 ± 0.65
Perfluorooctanoate	PFOA	$C_7F_{15}COO^-$	413	-0.2	**2.61 ± 0.69**	-0.22 ± 1.26 - 2.4 ± 0.12	1.9 ± 0.1 - 2.31 ± 0.35
Perfluorononanoate	PFNA	$C_8F_{17}COO^-$	463	-0.21	**2.82 ± 0.01**	1.83 ± 0.43 - 2.39 ± 0.09	2.33 ± 0.31 - 2.4 ± 0.1
Perfluorodecanoate	PFDA	$C_9F_{19}COO^-$	513	-0.21	**3.39 ± 0.02**	2.59 ± 0.45 - 2.96 ± 0.15	3.17 ± 0.14 - 3.6 ± 0.1
Perfluoroundecanoate	PFUnDA	$C_{10}F_{21}COO^-$	563	-0.21	**4.31 ± 0.08**	3.30 ± 0.11 - 3.56	4.8 ± 0.2
Perfluorododecanoate	PFDoDA	$C_{11}F_{23}COO^-$	613	-0.21			
Perfluorinated Sulfonates							
Perfluorobutane sulfonate	PFBS	$C_4F_9SO_3^-$	299	0.14		-0.76 ± 0.58 - 1.79 ± 0.10	2.06 ± 0.77
Perfluorohexane sulfonate	PFHxS	$C_6F_{13}SO_3^-$	399	0.14	**2.32 ± 0.15**	0.66 ± 0.65 - 2.05 ± 0.08	2.28 ± 0.70 - 3.6 ± 0.1
Perfluorooctane sulfonate	PFOS	$C_8F_{17}SO_3^-$	499	0.14	**3.37 ± 0.27**	2.40 0.46 - 3.7 ± 0.56	3.14± 0.66 - 3.8 ± 0.1
Perfluorodecane sulfonate	PFDS	$C_{10}F_{21}SO_3^-$	599	0.14	**3.63**	3.53 ± 0.12	
Perfluoroalkyl Sulfonamides							
Perfluorooctane sulfonamide	FOSA	$C_8F_{17}SO_2NH_2$	499	6.52	**4.86**	4.1 ± 0.35	4.3± 0.2

Table 2.1 (Continued)

Compound Name	Abbrev.	Mol Formula	Mol Wt	pK$_a$ [69,70]	Avg log K_{oc} (this study)	Avg log K_{oc} (lit., laboratory-based)[71-74] low – high range provided	Avg log K_{oc} (lit., field-based)[16,75,76] low – high range provided
Fluorotelomer Sulfonates							
6:2 fluorotelomer sulfonate	6:2 FtS	C$_6$F$_{13}$CH$_2$CH$_2$SO$_3^-$	427	0.36	2.62 ± 1.01		
8:2 fluorotelomer sulfonate	8:2 FtS	C$_8$F$_{17}$CH$_2$CH$_2$SO$_3^-$	527		3.65 ± 0.54		

2.3.4   SAMPLE ANALYSIS

Samples were analyzed for PFASs with liquid chromatography-tandem mass spectrometry (LC-MS/MS) using modifications of previously described methods (see Appendix A).[16, 17] All groundwater samples, laboratory DI water blanks, and calibration curve points were prepared in a 50:50 water:methanol solution with internal standards. Samples were analyzed with an Agilent (Santa Clara, CA) 6460 triple quadrupole LC-MS/MS in negative ion mode using an Agilent Poroshell 120 EC-C18 column with mobile phases of 2 mM ammonium acetate in water and 2 mM ammonium acetate in methanol. Duplicate measurements of ~30% of the samples produced good sample reproducibility (<20% relative standard deviation on average) for 6:2 FtS and PFAAs with a chain length of C_9 or less. 8:2 FtS and FOSA had relative standard deviations of 42% and 71% (FOSA concentration near method detection limit), respectively.

2.3.5   TOTAL OXIDIZABLE PRECURSOR ASSAYS

A slightly modified PFAS total oxidizable precursor assay developed by Houtz and Sedlak[77] and Houtz et al.[17] was employed here. For each of the 46 groundwater samples analyzed, 3 mL of a 120 mM potassium persulfate and 250 mM sodium hydroxide solution was added to 3 mL of groundwater sample in an 8 mL HDPE bottle and heated for 6 hr at 85 ˚C in a circulating water bath. Samples were cooled, neutralized with hydrochloric acid, and stored at 4 ˚C until offline solid phase extraction (SPE) and LC-MS/MS analysis (see Appendix A for experimental details and recoveries). Total oxidizable precursor experiments were duplicated for 30% of the samples. The relative standard deviation for duplicates was <15% on average for all PFAAs with C_9 or shorter chain lengths.

2.3.6   PARTITION COEFFICIENT EXPERIMENTS

Sediment cores were collected from the same depths as selected corresponding groundwater samples at the FTA-1 (near well S425) and infiltration bed (near well S469) sites to determine *in situ* K_d values. Subsamples of each sediment core were centrifuged at 4,000 rpm for 20 min, and the pore water was removed for LC-MS/MS analysis. The sediment was dried, sieved to <2.36 mm, homogenized and extracted for PFAS content three times with 0.1% ammonium hydroxide in methanol (see Appendix A for details).[17, 78] Sediment samples were analyzed for PFASs, organic carbon, and mineralogy as described in Appendix A (Tables A2, A3).

2.4   RESULTS AND DISCUSSION

2.4.1   SPATIAL ANALYSIS

Vertical profiles of water chemistry show variations with depth below the water table reflecting aquifer geochemical conditions and source zone influences. The full set of chemical results for all groundwater analysis are presented elsewhere.[68] At well S469, which is located in one of the infiltration beds, concentrations of DOC and phosphate decreased rapidly with depth below the water table, the nitrate peak occurred at an altitude of 8 m, the DO minimum occurred at an altitude of 2-4 m, and total PFASs had a distinct peak at an altitude of 4 m (Figure 2.3A). The vertical relationships at S469 were stable over time, and the maximum PFOS concentrations coincided with the DO minimum (Figure 2.3B). The low DO zone downgradient from S469 (Figure 2.4A) is a distinct characteristic of the wastewater plume from the infiltration beds, that developed from microbial activity during attenuation of the wastewater contaminants.[51, 79, 80]

The A-A' longitudinal transect shows that the sum of PFASs (Figure 2.4B) forms a relatively shallow (<30 m below land surface) plume that originates beneath FTA-1, extends

over 1,200 m downgradient in the direction of groundwater flow, and passes beneath (and mixes with) the PFAS plume that originates at the infiltration beds. The sum of PFASs is referenced here primarily to describe the plume shape, while individual PFASs provide insight to sources, transport, and transformation. The width of the PFAS plume is relatively narrow as evidenced by the transverse B-B' and C-C' cross sections (Figures 2.2 and A2), but may widen downgradient from the infiltration beds. The maximum concentrations of PFOS (63 μg L^{-1}; Figure 2.4C) and sum of PFASs (95 μg L^{-1}; Figure 2.4B) were observed at F586 (780 m downgradient from FTA-1). The maximum PFOA (8.0 μg L^{-1}) and PFHxS (18 μg L^{-1}) concentrations occurred at S488 (210 m downgradient from FTA-1). The molar perfluorinated sulfonate:perfluorinated carboxylate ratios for the groundwater ranged from 0.3 to 14, with a median of 2.8. Except for FOSA, all PFASs are strong acids (Table 2.1) that are anionic at the groundwater pH (ranged from 4.7 to 6.3).[69, 70]
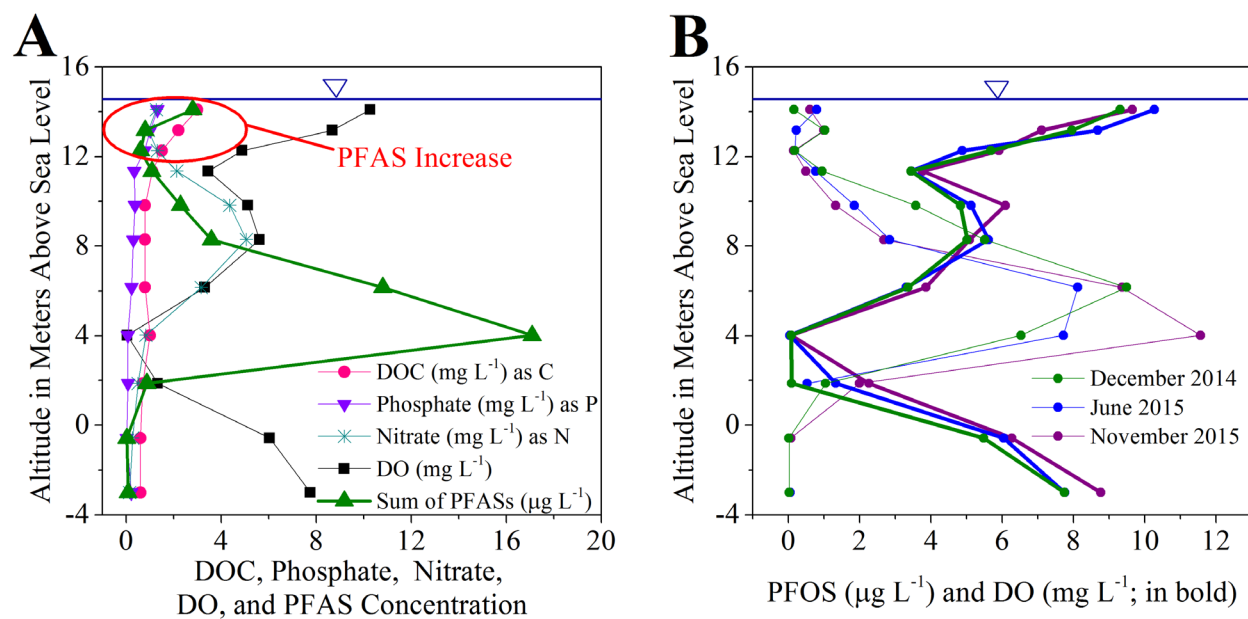
Figure 2.3. Vertical profiles at well S469 located in the wastewater infiltration beds showing (A) geochemical conditions and distribution of the sum of poly- and perfluoroalkyl substances (PFASs) in June 2015, and (B) time series profiles for dissolved oxygen (DO) and perfluorooctane sulfonate (PFOS). In June 2015, PFOS is on average 46% of the total molar concentration of the sum of measured PFASs at well S469. Inverted triangles show the position of the water table.
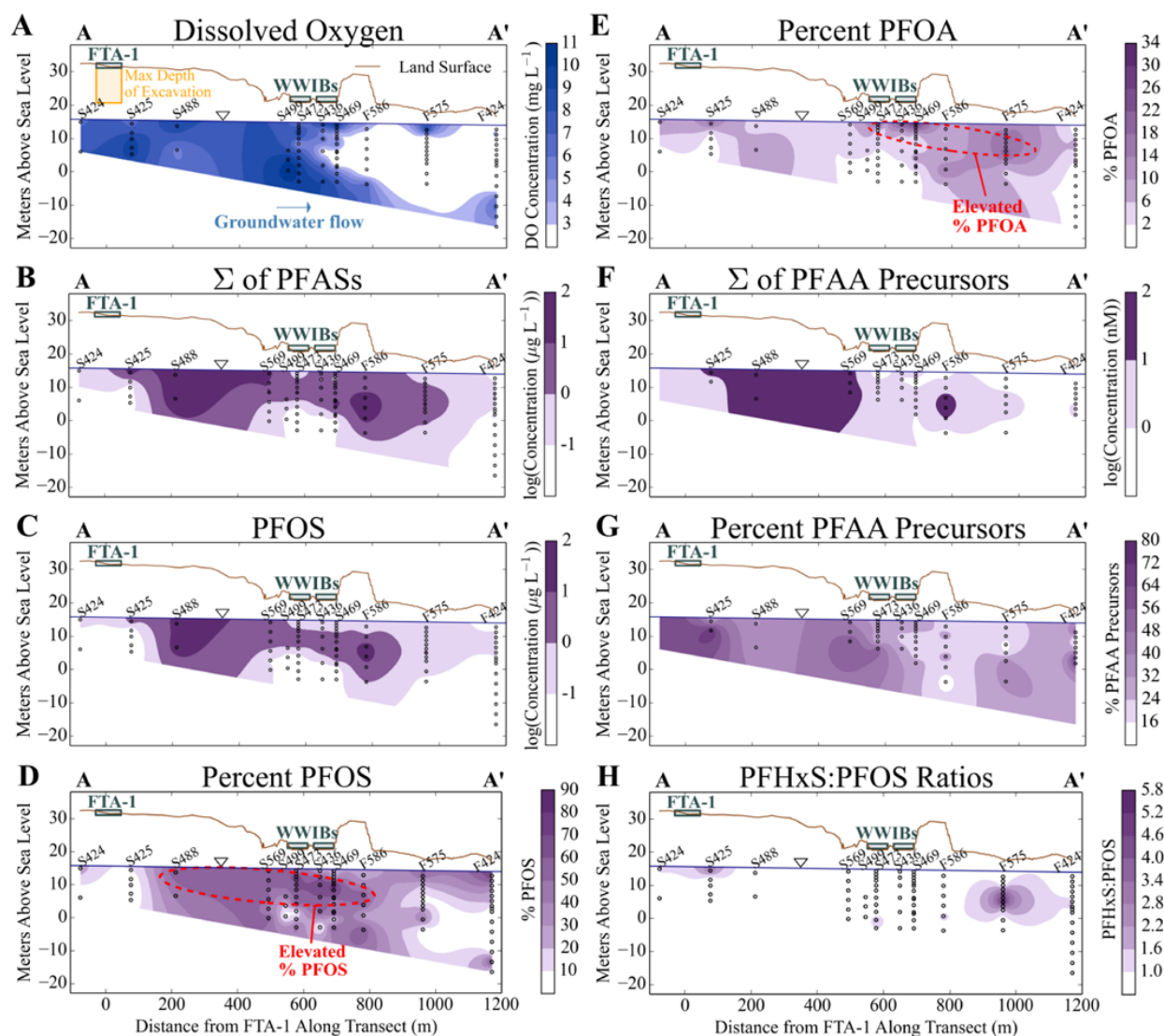
Figure 2.4 Vertical sections along longitudinal transect A-A' showing (A) dissolved oxygen concentrations (max = 11 mg L^{-1}), (B) the sum of poly- and perfluoroalkyl substance (PFAS) concentrations listed in Table 2.1 (max = 95 μg L^{-1}), (C) perfluorooctane sulfonate (PFOS) concentrations (max = 63 μg L^{-1}), (D) PFOS molar percentage of total measured PFASs (max = 82%), (E) perfluorooctanoate (PFOA) molar percentage of total measured PFASs (max = 32%), (F) the molar sum of perfluoroalkyl acid (PFAA) precursors as determined by the total oxidizable precursor assay (max = 78 nM), (G) precursor molar percentage of total PFASs (the sum of precursors and measured perfluoroalkyl acids pre-oxidation) (max = 78%), and (H) the perfluorohexane sulfonate (PFHxS):PFOS ratios (max = 5.8). [Circles indicate sampling sites. Inverted triangles indicate the water table. FTA-1 refers to the fire training area and WWIBs refers to wastewater infiltration beds. Box beneath FTA-1 in panel (A) shows maximum depth of soil excavated and thermally treated in 1997. Vertical exaggeration is 10x for all vertical sections. The lower boundary of the colored areas is the line connecting the maximum sampled depths, and the upper boundary is set at the water table.]

2.4.2 PFAS SOURCES

The distribution of PFASs in the groundwater immediately downgradient from FTA-1, particularly the elevated PFOS concentrations, along with the occurrence of branched isomers (Figure A3) confirms their origin from electrochemical fluorination–based AFFFs, as expected because of the history of electrochemical fluorination–based AFFF military usage.[17, 37, 81] The detection of 6:2 FtS and 8:2 FtS in groundwater similarly indicates that fluorotelomer-based AFFFs also were used at this site,[81] although likely less frequently than electrochemical fluorination-based AFFFs based on the observed prevalence of perfluorinated sulfonates and presence of branched isomers.

The FTA-1 and infiltration beds appear to be two distinct long-term PFAS contaminant sources to the aquifer as evidenced by elevated concentrations just below the water table at both sites (Figures 2.3A and 2.4B). Further, the compositionally distinct PFAS signatures from these locations indicate two different sources. The composition of the shallow groundwater below FTA-1 (S425, 14 m altitude) is consistent with the characteristics of AFFF formulations and precursor transformation (Figure 2.5A). PFHxA and PFHxS, expected products of precursor transformation (since previously investigated AFFFs contained significant quantities of C_6 precursors)[17], account for about 50% of the PFASs, and the remainder is primarily PFOA, PFOS, and 6:2 FtS. The deeper downgradient wells (S488 and F586 at 6.6 and 6.8 m altitude, respectively, Figure 2.5A) reflect an AFFF source based on the high sum of PFAS concentrations, with PFOS ranging from 42 to 59% of the molar sum of PFASs. The predominance of PFOS along the plume (Figure 2.4C and 2.4D), the known history of fire training with AFFF, and the clear outline of the PFOS plume emanating from the FTA (Figure 2.4C) indicates that the high PFAS concentrations (Figure 2.4B) result from the FTA-1 source.

The PFAS composition of shallow groundwater beneath the infiltration beds (S469, 14 m altitude, Figure 2.5B) has a lower proportion of PFHxS and a higher proportion of PFOA than shallow groundwater from the same altitude beneath FTA-1 (S425). Concentrations of total PFASs at S469 were generally greatest at 4-6 m in altitude (from the influence of the upgradient FTA source) and decreased steadily upward before increasing just below the water table (Figure 2.3A), indicating the infiltration beds also are a continuing PFAS source, but with lower concentrations. Domestic wastewater is a well-known source of PFASs.[21, 44, 45, 82] Enrichment of PFOA and other PFAAs in the shallow groundwater beneath and downgradient from the infiltration beds (the percent PFOA is nearly twice that at FTA-1; Figure 2.5) indicates that the secondary treated wastewater had a different PFAS composition than the FTA-1 source. The influence of wastewater can be seen most clearly by the elevated proportions of PFOA in Figure 2.4E. PFOA is a major component of PFASs in wastewater (reaching 1,050 ng L^{-1} in one U.S. wastewater treatment plant) and has been shown to increase in concentration through the wastewater treatment process as a result of precursor transformation.[21, 44, 82, 83] PFNA concentrations also have been shown to increase during treatment as a result of precursor transformation.[21] Notably, PFNA concentrations were highest in the shallow sample from S469 at the infiltration beds (Figure 2.5B).

Formulations of AFFF previously measured by others had PFOS:PFOA ratios ranging from 49 to 110.[17] The historical PFAS composition of the WWTP effluent is unknown, but the profile at S469 indicates that the composition of the shallow, lower concentration groundwater is consistent with a wastewater source and the composition of the deeper, higher concentration groundwater is consistent with a FTA source (Figure 2.3A, 2.5B). In the groundwater downgradient from the infiltration beds the two PFAS sources comingle and the high concentrations emanating from the FTA-1 overwhelm the lower wastewater concentrations. For example, the sampling location at F586 containing the maximum PFOS concentration at the

field site (63 μg L^{-1}) also has 7.5% PFOA, greater than the median value of 4.5% PFOA (Figure 2.4C, 2.4E).

Because domestic wastewater disposal at the infiltration beds ceased in 1995,[51] the persistence of elevated PFAS concentrations near the water table suggests that they are sorbed to the unsaturated and saturated zone sediments beneath the infiltration beds and are slowly being desorbed and transported to the groundwater. Precursors retained in the unsaturated zone also could be transforming into more mobile PFAAs, which then migrate to the saturated zone. Similar processes of sorption, desorption, and precursor transformation in the unsaturated zone and shallow saturated zone are also likely occurring at the FTA-1 source area. Overall, the unsaturated zones continue to be a source of PFASs to the groundwater after 18 years (FTA-1) and 20 years (infiltration beds) of inactivity.
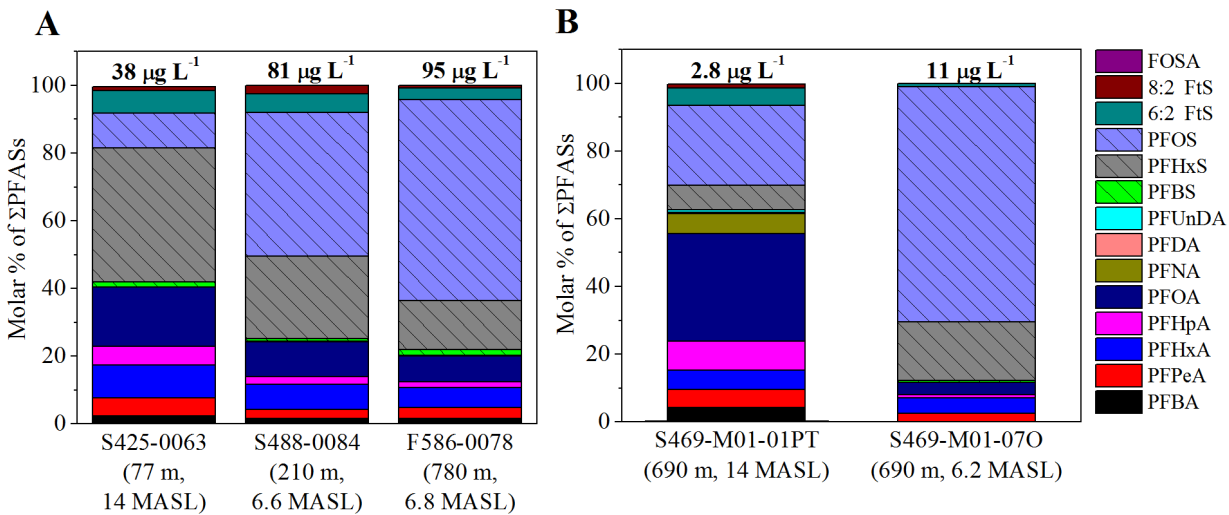
Figure 2.5 Molar percentages of individual poly- and perfluoroalkyl substances (PFASs) in groundwater collected (A) at well S425, located near FTA-1, and wells S488 and F586, located at 210 m and 780 m downgradient from FTA-1, respectively, at the depths with the highest concentrations, and (B) at well S469, located 690 m downgradient from FTA-1 in the wastewater treatment plant infiltration beds, from just below the water table (14 m altitude) and from the deeper (6.2 m altitude) portions of the PFAS plume. [See Table 2.1 for explanation of abbreviations. Total PFAS concentration is shown at the top of each column, and distance from FTA-1 (m) followed by the altitude in meters above sea level (MASL) are shown in parentheses below each well name.]

2.4.3 SORPTION AND ADVECTIVE TRANSPORT

Results from the field-determined *in situ* K_d values were normalized to the fraction of sediment organic carbon (f_{oc} ranged from 0.00013 to 0.0003), and the average log K_{oc} (K_{oc} = K_d/f_{oc}) values ranged from 2.2 to 4.9 L kg C^{-1} (Table 2.1, Table A2, see Appendix A for calculations). The PFAS K_{oc} results from this study are similar to other investigations where observed field-determined values are typically higher than laboratory-derived values. McGuire et al.[16] suggested that higher perfluorinated carboxylate log K_{oc} values may be due in part to carboxylate precursor breakdown during the sediment extraction process. The high K_{oc} values in this study suggest that other sorption mechanisms besides partitioning into sediment organic

carbon are important for low organic carbon sediments. The aquifer mineralogy consists predominantly of quartz and feldspar with only trace amounts of metal oxides and clay minerals (Table A3).

Once PFOS is introduced into the groundwater beneath FTA-1, it is estimated to take 15 yr to travel the 780 m distance to F586, where the highest PFOS concentrations were observed. This estimate is based on simple 1-D advective transport along the transect, a groundwater velocity of 0.42 m d^{-1}, and a PFOS K_d value of 0.45 L kg^{-1} (log K_{oc} = 3.37, f_{oc} = 0.00019%). Based on the estimated 15 yr transport time to F586, the PFOS present at F586 in 2015 was introduced to the saturated zone around 2000. PFOS transport through the 17-m-thick unsaturated zone would have therefore taken between 3 and 30 yr, given that AFFF use occurred between 1970 and 1997. PFOA, PFNA, and PFAAs with C_4-C_7 chain lengths are predicted to be transported farther than PFOS based on lower *in situ* K_{oc} and K_d values (Table 2.1, Table A2). However, the observed distribution of PFOA is similar to PFOS, possibly due to the *in situ* production of PFAAs from precursor transformation. The leading edge of the FTA-1 PFAS plume has likely been transported farther downgradient than the A-A' transect, as suggested by detection of PFOS in wells located up to ~4 km downgradient from FTA-1 (Figure A1).

2.4.4   INFLUENCE OF WASTEWATER DISPOSAL ON GROUNDWATER GEOCHEMISTRY

Following the cessation of treated wastewater disposal at the infiltrations beds in 1995, the mobile components of the wastewater plume, such as boron, have been transported beyond the A-A' transect.[50] However, there is still a residual impact of wastewater disposal on the aquifer, clearly defined by the low DO zone downgradient from the infiltration beds (Figure 2.4A)

more than 20 years after disposal ended. The highest PFOS concentration (Figure 2.4C) occurred in the zone with low DO concentrations.

Historical hydrologic loading of the treated wastewater to the aquifer is estimated to have been between 380 and 5,700 m^3 d^{-1} between 1936 and 1995.[84] Specific conductance of the effluent ranged from 340 to 520 μS cm^{-1} and DOC concentrations ranged from 6.4 to 19 mg L^{-1}.[51, 63] Continuous monitoring of groundwater quality at S469 since the end of wastewater disposal in 1995 has shown slowly decreasing DOC concentrations that continue to persist (3.0 mg L^{-1} during June 2015 sampling, Figure A4A) above background levels because of desorption of organic carbon from the aquifer sediments.[51, 79] Specific conductance also has remained elevated (183 μS cm^{-1} at S469 during June 2015 sampling), and DO concentrations remain low because of persistent biogeochemical oxygen demand (Figure 2.3 and Figure 2.4A).[51]

The persistent wastewater-related geochemical conditions encountered by the FTA-1 PFAS plume as it passed through the residual wastewater plume include elevated concentrations of dissolved ions and sediment organic carbon, both factors that can influence PFAS transport.[71, 72, 85] Groundwater beneath the infiltration beds remained oxic to sub-oxic during the period of wastewater disposal because of the introduction of oxygenated treated wastewater.[79, 80] The oxygenated conditions resulted in stability of iron and manganese oxide grain coatings on the aquifer sediments.[79, 80] The increased sediment organic carbon and ionic interactions resulting from wastewater loading may have enhanced PFAS sorption beneath the infiltration beds through both hydrophobic and electrostatic interactions. The higher K_{oc} values for PFOS indicate greater sorption to the sediments than PFOA and shorter chain length PFAAs.

The PFASs that were sorbed to the aquifer sediments under wastewater disposal conditions were potentially remobilized following cessation of disposal, owing to (1) reduction in dissolved ion concentrations, (2) desorption of sediment organic carbon, and (3) reductive

dissolution of positively charged iron and manganese oxide grain coatings following the onset of anoxic conditions beneath the infiltration beds.[51, 80, 86] Electrostatic interactions with dissolved iron (II) may promote transport of PFOS.[87] The slow desorption of sediment organic carbon beneath the infiltration beds releases DOC and other hydrophobically sorbed contaminants, including PFASs, while a reduction in dissolved ion concentrations may increase the repulsion between the negatively charged quartz and feldspar aquifer sediments (Table A3)[47] and anionic PFASs. A combination of factors likely led to the elevated PFOS concentrations at F586, although elevated concentrations of shorter-chain length PFAAs, such as PFBS at well F586 (Figure A4B), also suggest remobilization.[88]

2.4.5 TOTAL OXIDIZABLE PRECURSOR ASSAYS

The total oxidizable precursor assay can be employed to estimate total PFAA precursor concentrations by oxidizing polyfluorinated compounds into perfluorinated carboxylates and measuring the increase in molar carboxylate concentrations.[17, 77] A sulfonamide precursor with C_n (n = the number of carbons in the chain) is expected to transform into a C_n perfluorinated carboxylate upon oxidation.[17] A range of C_4 to C_{n+1} perfluorinated carboxylates are expected to form from oxidation of fluorotelomer precursors.[17] Following oxidation of selected groundwater samples, PFBA concentrations increased by a factor of 5.0 ± 3.0, PFPeA increased by a factor of 2.9 ± 1.3, PFHxA increased by a factor of 3.7 ± 2.2, PFHpA increased by a factor of 1.5 ± 0.4, PFOA increased by a factor of 1.6 ± 2.2. and PFNA increased by a factor of 1.2 ± 0.3 (Figure 2.6A).

The 6:2 FtS precursor is primarily transformed into PFBA, PFPeA, and PFHxA during oxidation, while 8:2 FtS is primarily transformed into PFPeA, PFHxA, PFHpA, and PFOA.[17, 77] If all of the fluorotelomers measured in the samples were oxidized into the expected PFAAs, 6:2

FtS would account for 9.9±9.3% of the PFBA, PFPeA, and PFHxA increase and 8:2 FtS would account for 9.1±10% of the PFPeA, PFHxA, PFHpA, and PFOA increase. FOSA is expected to transform into PFOA,[17] although pre-oxidation concentrations were so low (≤164 ng/L) that it produced negligible quantities. The additional post-oxidation increase in PFAAs is due to transformation of polyfluorinated compounds that were not quantified here.

Post-oxidation, PFBA, PFPeA, and PFHxA contributed 25 ± 8.5%, 22 ± 9.9%, and 44 ± 17% of the total molar carboxylate increase, respectively, consistent with other studies,[17] and the substantial increase in PFHxA indicates that C_6 precursors were dominant in the original samples. Relatively small increases in PFHpA and PFOA indicate low abundance of C_7 and C_8 precursors. Increases in molar perfluorinated carboxylate concentrations following oxidation provide an estimate of total molar precursor concentrations,[17] which comprised 31 ± 15% of the total PFASs at the Cape Cod site, within the range of what has been previously reported (23% for groundwater, 33 - 63% for wastewater). [17, 89] This suggests that the thermal soil remediation at FTA-1 either did not break down the precursors, or a substantial mass of precursors had passed through the unsaturated zone prior to remediation.

Precursors are co-transporting with the main FTA-1 derived PFAS plume (Figure 2.4F) and show a similar spatial distribution as PFOS (Figure 2.4C). There is a linear correlation between the sum of molar PFAA concentrations pre-oxidation and the calculated sum of molar precursor concentrations post-oxidation from the different sampling locations (Figure 2.6B). This trend does not vary substantially with distance from FTA-1, and precursors exceed 50% of the total PFAS concentration at the farthest downgradient well (Figure 2.4G). Precursors have been suggested to be less mobile than PFAA, although data on this topic are limited and many precursors have yet to be identified.[16, 90] The results indicate that at least some precursor sorption coefficients for the low-carbon Cape Cod aquifer sediments are similar to PFAS sorption coefficients reported in this study (Table 2.1). Some precursors may be less mobile and

retained in the unsaturated zone. A previous study on anaerobic biotransformation of 6:2 and 8:2 fluorotelomer alcohols in digester sludge (methanogenic conditions) reported low levels of PFAAs produced (≤0.4 mol % for PFHxA and PFOA) over the 181-day experiment.[41] If precursor transformation rates decrease under anaerobic conditions, then precursors would be expected to persist during transport in the low DO conditions associated with the wastewater plume downgradient from FTA-1. Overall, the finding of co-transport of PFAA precursors at this field site has implications for water resources, as precursors can increase the total PFAA mass over time through transformation.

The PFHxS:PFOS ratio can be related to the degree of precursor transformation,[16, 17] and electrochemical fluorination-based AFFF formulations from 1988 to 2001 were shown to have ratios between 0.08 and 0.14.[17] The PFHxS:PFOS ratio observed in groundwater near the water table at FTA-1 (S425) was about 3.1 (Figure 2.4H), and increased to 5.8 at F575 (960 m downgradient from FTA-1). Well F575 had minimal percentages of precursors (Figure 2.4G) and elevated PFHxS:PFOS ratios in the same location, suggesting different sources or that precursor transformation contributed to the PFHxS concentrations. Well F424 had PFHxS:PFOS ratios up to 3.8 (Figure 2.4H) and up to 68% precursors (Figure 2.4G), which suggests preferential transport of PFHxS relative to PFOS and mobile precursors (perhaps intermediates).
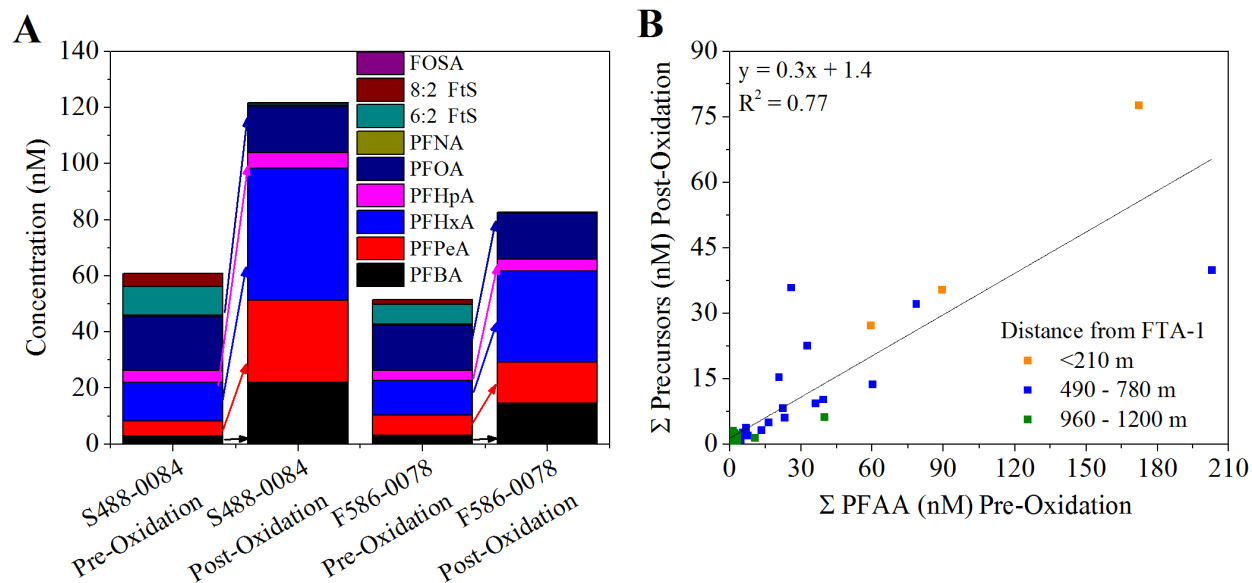
Figure 2.6. Results from the total oxidizable precursor assay conducted on selected groundwater samples. (A) Concentrations of poly- and perfluoroalkyl substances in groundwater samples from wells S488-0084 and F586-0078 pre- and post-precursor oxidation, and (B) linear relationship between the groundwater sample molar sum of perfluoroalkyl acid (PFAA) concentrations pre-oxidation and the molar sum of precursors post-oxidation (n=46). [FTA-1 is the fire training area. Compound abbreviations can be found in Table 2.1.]

2.4.6   DIFFERENTIAL TRANSPORT: CHAIN LENGTH AND HEAD GROUP EFFECTS

The relative mobility of PFASs can be assessed considering (1) the estimation of PFAS-specific retardation factors that are dependent on the sediment characteristics and geochemical conditions, (2) the estimation of precursor retardation factors, and (3) potential biotransformation of precursors into PFAAs.[39, 40, 42, 91, 92] Negligible DO in groundwater downgradient from the infiltration beds may impede current precursor transformation rates, resulting in transport without the confounding factor of *in situ* production. The spatially dependent percentages of each PFAA relative to total PFASs measured suggests that differential transport is occurring, as

29

illustrated by comparing the PFOS distribution (Figure 2.4D) with those of shorter chain PFAAs (Figure A5). Aside from the shallow samples beneath the infiltration beds, the highest percentages of PFOA along the transect (21%) were observed 960 m downgradient from FTA-1, although this is likely a result of wastewater inputs. The proportions of PFHxS were greatest in the groundwater near FTA-1 (S425) and at the deeper altitudes along the transect (Figure A5A). High percentages of PFHpA (12%), PFHxA (20%), and PFPeA (25%) were detected at lower altitudes and farther downgradient at F575 and F424 (Figure A5B−D). These results indicate that shorter chain length PFAAs are more mobile than PFOS both vertically and horizontally. The highest percentages of PFOS (82%) were near the infiltration beds (Figure 2.4D) between 580 and 690 m from FTA-1, indicating that PFOS has not traveled as far compared to shorter chain length PFAAs (log K_{oc} = 2.17-2.76), reflecting its relatively high log K_{oc} value (3.37). These results contrast with those of McGuire et al.[16] who reported no evidence of differential transport, potentially owing to *in situ* biotransformation of precursors. At the Cape Cod site, anoxic conditions may have allowed for the observation of differential transport through the elimination or reduction of *in situ* PFAA production from precursors. While the observed spatial distributions are likely due to a combination of factors including multiple sources, complex hydrological history, differential transport, and precursor transformation, the differences between percentages of PFOS and PFPeA, PFHxA, PFHpA, and PFHxS suggest differential transport is a primary factor determining spatial distributions.

2.4.7   CONCEPTUAL SITE MODEL AND ENVIRONMENTAL IMPLICATIONS

The higher concentration PFAS plume emanating from FTA-1 comingles with the lower concentration PFAS plume emanating from the infiltration beds 580 m downgradient from FTA-1. The unsaturated zones at FTA-1 and the infiltration beds are continuing sources of PFASs to the aquifer decades after source removal. This finding suggests that the unsaturated zones

beneath fire training areas and wastewater infiltration beds at other sites can act as long-term PFAS sources to groundwater over several decades. Furthermore, the shallow groundwaters beneath the two unsaturated zones at this field site are compositionally distinct. The unique profiles observed here may help with source identification in cases where the point source is not known. Another significant component of the conceptual site model is the finding that some precursors are quite mobile at this field site. Therefore, monitoring of precursors downgradient from point sources is essential to accurately predict future PFAA concentrations. Finally, there is evidence of differential transport dependent on chain length and head group, which has not been shown previously at field sites.

2.5   ACKNOWLEDGMENTS

Chapter 3

TRANSPORT, PERSISTENCE, AND SURFACE ENRICHMENT OF POLY- AND PERFLUOROALKYL ACID SUBSTANCES ACROSS GROUNDWATER/SURFACE-WATER BOUNDARIES

3.1   ABSTRACT

Exposure to PFASs has been linked to adverse health effects in humans, drinking water for millions of U.S. residents is above the U.S. EPA health advisory, and sites worldwide have been shown to contain PFASs. PFASs have been detected in groundwater and surface waters near contaminated sites, thus environmental conditions controlling PFAS fate and transport from contaminated sites into the hydrological cycle, and ultimately to drinking water resources, needs to be understood. Here, we investigate whether transport through an oxygenated pond and across the groundwater/surface-water interface, areas characterized by increased biological and chemical activity, results in transformation of perfluoroalkyl acid (PFAA) precursors. Precursors account for 24 ± 1.1% of the total molar PFAS concentration in pond water, and 15 ± 7.7% in downgradient groundwater, suggesting PFAA precursors are slowly transforming when transported across reactive boundaries. PFAS concentrations are observed to be spatially consistent in the pond water. In contrast, the downgradient groundwater exhibits large fluctuations in PFAS composition and concentration. Downgradient sediment/water distribution coefficient (K_d) values for perfluoroalkyl carboxylates are chain-length independent, suggesting a headgroup dependent chemisorption process, whereas perfluoroalkyl sulfonates have chain length dependent values indicating a classical electrostatic and hydrophobic physisorption process, which may explain some of the compositional variation. PFAS concentrations were

observed to increase at the air-pond interface and in shallow groundwater immediately below the water table near the downwelling side of ponds, suggesting enrichment at the pond surface and/or within the unsaturated zone could translate to locally elevated groundwater concentrations.

3.2 INTRODUCTION

PFAS exposure has been linked to diabetes, high cholesterol, and immunotoxicity in children, among other adverse health effects.[6, 93, 94] Drinking water for ~6 million U.S. residents is above the U.S. EPA non-enforceable lifetime drinking water health advisory of 70 ng L^{-1} for the combined concentration of PFOA and PFOS.[8, 9, 95] High drinking water PFAS concentrations near contaminated sites has been shown to result in elevated human serum concentrations.[22, 96] Many sites are highly contaminated from PFAS-containing aqueous film-forming foams (AFFFs) released to the environment during fire emergencies or as part of fire training activities.[15, 16, 32] Both groundwater and surface waters are often impacted through PFAS transport from the original AFFF release point[34] and PFAA precursors in AFFF are known to transform biotically or abiotically to "terminal" PFAAs such as PFOS and PFOA.[39, 43, 92] Therefore, the environmental lifetime and chemical endpoint of PFAA precursors as well as aqueous interfacial sorptive processes affecting PFAS transport must be understood to protect the public from PFAS exposure.

Perfluoroalkyl carboxylate and sulfonate precursors have been detected at AFFF sites,[15-17] and some of these precursors have been observed to be mobile.[15] Studies on several AFFF formulations reveal a complex mixture of anionic, cationic, and zwitterionic PFASs.[90, 97, 98] A total of 57 PFAS classes and 240 individual compounds have been identified in AFFF and groundwater.[97] Precursors in AFFF can account for >99% of the total molar PFAS

concentration,[17] while precursors in groundwater downgradient AFFF use sites account for a lower PFAS percentage (23 – 31%)[15, 17] suggesting environmental precursor transformation. The biotransformation of AFFF precursors such as 6:2 fluorotelomer sulfonate,[42] 6:2 fluorotelomer thioether amido sulfonate,[99] and cationic quaternary ammonium compounds[92] may result in the formation of persistent intermediate precursors,[39, 99] which may have a different environmental mobility than the primary precursor. Anaerobic conditions have been shown to be less conducive to biotransformation of PFAA precursors than aerobic conditions.[42, 99] Therefore, hydrologic exchange between aerobic and anaerobic systems will affect precursor transformation rates and thus the boundary between groundwater and surface water is often an area of increased biologic and chemical activity.[100-103] For example surface water can introduce oxygen and nutrients to groundwater and result in increased microbial activity, while anaerobic groundwater discharged to aerobic surface waters can affect dissolution of metals and precipitation metal hydroxides.[100-103] Thus boundary areas of enhanced biogeochemical activity may stimulate the transformation rates of organic contaminants such as PFAA precursors.

Along with precursor transformation, another process that may affect aqueous PFAA concentrations is sorption to sediment-water and air-water interfaces. Sorption to organic carbon is chain-length and functional group dependent, with the distribution coefficient of perfluorinated sulfonates on average 0.23 log units greater than perfluorinated carboxylates with the same perfluorocarbon chain length.[72] Proteins and iron oxides have been identified as key contributors promoting PFAS sorption in soils.[104] Calcium, pH, and humic acids have also been shown to affect sorption to mineral surfaces and studies have reported a complex mixture of sorption mechanisms driven by electrostatic and hydrophobic interactions.[85, 88] However, most sorption experiments are conducted in the laboratory at concentrations exceeding environmentally relevant conditions (typically in the mg L^{-1} range as compared to the 70 ng L^{-1} EPA drinking water health advisory limit), and therefore it remains unknown whether these

controlled laboratory studies accurately represent the environment. PFAA transport is also known to be affected by chain-length dependent sorption at the air-water interface.[105, 106] However, little is known about how the air-water interface may influence PFAS transport in natural systems, and whether the air-water interface affects groundwater concentrations.

In this study, we investigate transport and transformation of PFASs from a groundwater contamination plume as it discharges to a surface water body (Ashumet Pond), mixes with pond water, and is recharged back into groundwater on the hydraulically downgradient side of the pond. Along this hydrological pathway PFASs encounter aerobic and anaerobic conditions as well as large fluctuations of additional water quality parameters including dissolved organic carbon (DOC), nitrate, and temperature.[51, 79, 107] The study was undertaken to determine whether precursors are degraded rapidly as they (1) pass through the reactive anaerobic to aerobic boundaries between discharging groundwater and surface waters, (2) are exposed to light and predominantly oxic conditions of the pond, and (3) pass from oxic surface water into suboxic to oxic groundwater. Water samples (247) were collected from an upgradient PFAS groundwater contamination plume, the upwelling pore water where groundwater discharges to surface water, the surface water body, the downwelling pore water where surface water recharges the groundwater, and the shallow groundwater downgradient from the discharging surface water. The total oxidizable precursor assay[17, 77] was used to estimate precursor concentration for selected samples. Sediment samples were collected from the upwelling (groundwater flowing into the pond) and downwelling zones (groundwater flowing out of the pond) to calculate sediment/water distribution coefficient (K_d) values. Finally, microlayer samples were collected from the pond surface to determine whether enrichment at the air-water interface could impact downgradient groundwater concentrations.

3.3   METHODS

3.3.1 SITE OVERVIEW

The study was conducted on Cape Cod, Massachusetts, at the U.S. Geological Survey (USGS) Cape Cod Toxic Substances Hydrology Research Site, and focuses on Ashumet Pond and surrounding areas (Figure 3.1).[46] Ashumet Pond is a 0.82 km^2 mesotrophic groundwater-fed kettle-hole pond that has no permanent inflow or outflow rivers and is located in an unconfined sand and gravel aquifer.[107] Ashumet Pond has a maximum depth of 19 m, a volume of 6.26 million m^3,[86] total groundwater outflow of 3.81 x 10^9 L year^{-1},[108] and therefore an estimated hydraulic residence time of 1.6 years. A PFAS groundwater contamination plume, originating from an AFFF fire training area and disposal of secondarily treated domestic wastewater effluent into infiltration beds, is located upgradient and to the northwest of Ashumet Pond.[15] Johns Pond is located to the southeast of Ashumet Pond and is also a groundwater-fed kettle-hole pond with two main outlet rivers (the Quashnet River and the Childs River). Residential houses with septic systems are located around Johns Pond and Ashumet Pond.
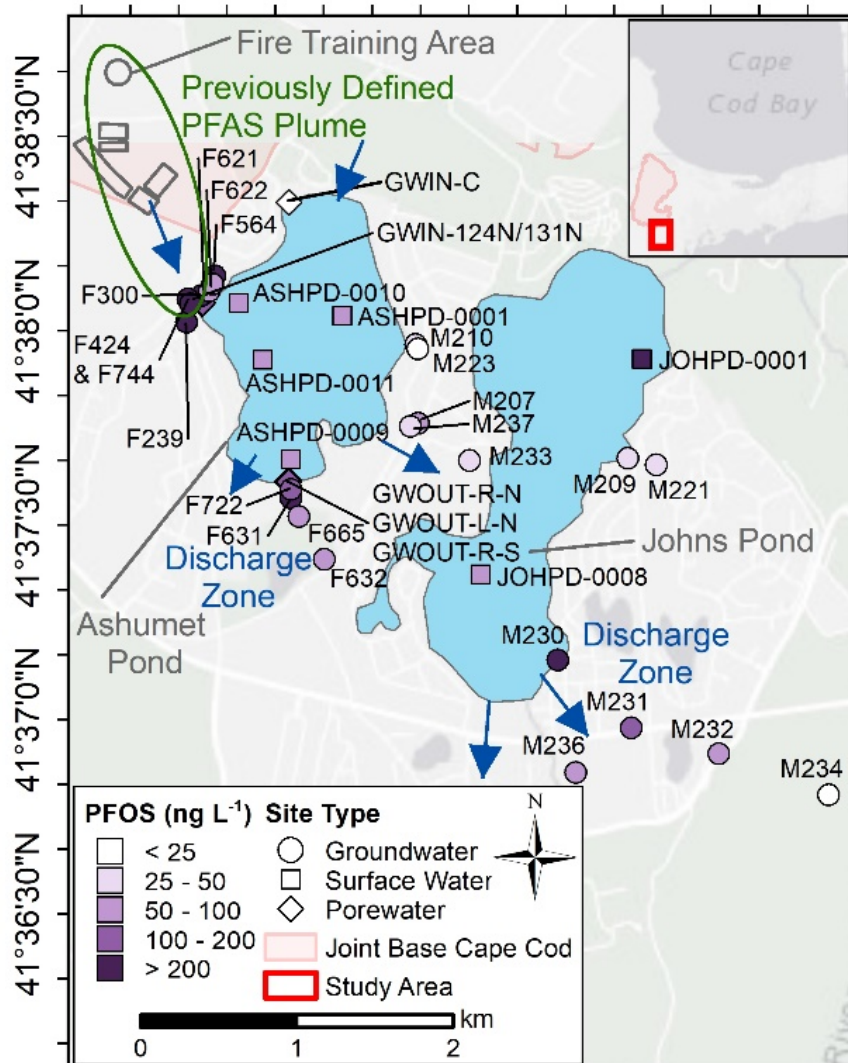
Figure 3.1 Locations and identifiers of samples collected between 2016 and 2018. Note that most locations have multiple sampling depths. Blue arrows indicate groundwater flow directions. Ashumet Pond is recharged near the southeastern edge of the previously defined PFAS plume.[15] The highest PFOS (sum of linear and branched PFOS) concentration is shown for each location. To allow for visualization of groundwater seep sites, the surface water samples are not shown in those locations.

3.3.2 POND, GROUNDWATER, AND SEDIMENT SAMPLING

All water samples were acquired according to USGS field protocols.[67] Water samples for analysis of PFASs were collected in high-density polyethylene (HDPE) bottles with polypropylene caps or low-density polyethylene (LDPE) bottles with PolyCone cap liners that were pre-cleaned with LC-MS grade methanol and deionized (DI) water. DI water equipment blanks were collected for all sampling equipment (see below) by running DI water through the sampling system. All PFAS water samples were unfiltered, stored on ice in the field, and then stored at 4 °C until analysis. A total of 9 DI water equipment blanks and 247 water samples were collected between 2016 and 2018 (Table B1). Field parameters including temperature, specific conductance, pH, and dissolved oxygen (DO) were measured at the time of sample collection (Table B2). Specific conductance was measured using an Orion Star™ A222 meter (ThermoFisher Scientific, Waltham, MA), and pH was measured with an Orion Star™ A221 meter (ThermoFisher Scientific, Waltham, MA), an Orion™ Ross™ Sure-Flow™ 8172 probe, and an Orion™ ATC stainless steel temperature-compensating probe (ThermoFisher Scientific, Waltham, MA). Samples with DO concentrations >31 μM were collected in flushed glass biochemical oxygen demand bottles, stoppered, chilled and measured within 6 hours with a YSI 58 portable DO meter (Yellow Springs, OH) and YSI 5905 self-stirring biochemical oxygen demand probe (Yellow Springs, OH). DO concentrations <31 μM were measured using a CHEMetrics (Midland, VA) V-2000 photometer and K-7553 Vacu-vial self-filling reagent ampoules. Additional water quality analyses included phosphate, nitrate, and DOC.[53]

Groundwater samples were collected from monitoring well clusters or multilevel samplers (MLSs) with either a Grundfos RediFlo2™ submersible pump, Keck SP-81™ submersible pump, or a GeoPump2™ (Geotech, Denver, CO) peristaltic pump as previously described.[15] A minimum of three well volumes were purged before sample collection. Porewater was collected using screened stainless steel pushpoint samplers (MHE Products, East Tawas,

MI) attached to the GeoPump2 ™ peristaltic pump outfitted with Norprene™ tubing after purging three times the tubing volume.

Pond samples were collected using a GeoPump2™ with polyethylene tubing attached to a YSI™ 6920 Multi-Parameter Water Quality Sonde (Yellow Springs, OH) that was extended to the desired sampling depth. DO, temperature, specific conductivity, and pH were measured with the sonde in 2.0 m increments with a starting depth of 0.1 m below the pond surface to ≤2 meters from the pond bottom. The pond surface microlayer was sampled at every location by inserting a 30.5 x 30.5 x 0.5 cm^3 glass plate vertically into the pond water next to the boat and withdrawing at a rate of ~15 cm sec^{-1}.[109] The water surface was generally calm except for the November 2018 sampling (wind and waves). The microlayer was then transferred to the HDPE sample container using a silicone rubber squeegee blade. The blade and plate were rinsed with methanol following every sample to prevent cross-contamination.

Sediment samples from Ashumet Pond were collected near the shore using a 5 cm diameter aluminum barrel that was inserted into the sediment. Sediment samples were divided by depth intervals (0 – 5 cm, 5 – 10 cm, ~10 – 15 cm, and ~15 – 30 cm), transferred to HDPE bottles, kept chilled during collection, and stored frozen at -20 °C until analysis.

The water samples collected in 2016 (75 samples) were all groundwater samples located along a "fence" of well clusters and MLSs along the northwest upgradient side of Ashumet Pond to define the location of the PFAS contamination plume and determine the concentration distribution of PFASs in the groundwater entering the pond. Downgradient groundwater, pond water, and pore water samples at the groundwater-surface water interface (150 samples total) were collected between July and September 2017. An additional 11 pond water samples were collected in November 2017 (ASHPD-0001) and during February 2018 an additional 13 samples (pond water, porewater, and groundwater samples) were collected from F722, GWOUT-L-N, and GWOUT-L-N to evaluate seasonal variations. A total of 16 sediment

39

samples were collected in September 2017 from 4 locations. Additional information is available in Appendix B.

3.3.3   CHEMICALS AND MATERIALS

PFAS standards (25 native compounds and 19 isotopically labeled compounds, Table B3) were purchased from Wellington Laboratories (Guelph, Canada). DI water with a resistivity of >18 MΩ cm^{-1} was obtained from a GenPure™ xCAD Plus UV-TOC system (Thermo Scientific™ Barnstead™, Lake Balboa, CA). Liquid chromatography-mass spectrometry (LC-MS) grade methanol (J.T. Baker, Center Valley, PA) and ACS grade ammonium hydroxide were purchased from VWR (Radnor, PA). ACS grade hydrochloric acid was purchased from Fisher Scientific (Waltham, MA). Reagent grade formic acid, BioUltra ammonium acetate, ACS grade acetic acid, and Supelclean ENVI-Carb (120-400 mesh, 100 m^2 g^{-1} surface area) were obtained from Sigma Aldrich (St. Louis, MO). Oasis WAX cartridges (6 mL, 150 mg, 30 µm particle size) for solid phase extraction (SPE) were obtained from Waters (Milford, MA).

3.3.4   SAMPLE PFAS EXTRACTION AND ANALYSIS

Water samples were warmed to room temperature before analysis, briefly sonicated, and inverted several times before subsampling 20 mL to a 50 mL centrifuge tube. The samples were then spiked with 40 µL of a 0.03 ng µL^{-1} internal standard solution before SPE extraction following established methods.[15, 89, 110] Oasis WAX™ SPE cartridges were preconditioned with 4 mL of 0.1% ammonium hydroxide in methanol, 4 mL of methanol, 4 mL of DI water, and then the 20 mL sample was added to the cartridge and placed under vacuum to yield a flow rate of ~1 drop sec^{-1} followed by a 4 mL DI water rinse before drying the cartridge under vacuum (~30 minutes). The samples were eluted with 4 mL methanol followed by 4 mL of 0.1% ammonium

hydroxide in methanol and the collected eluent was dried using an ultra-high purity nitrogen gas stream, reconstituted in 0.75 mL methanol, heated to 40 °C for 30 min, and vortexed briefly. Finally, 0.75 mL of water was added, the sample was transferred to a polypropylene microcentrifuge tube and centrifuged at 13000 rpm for 20 min, and the supernatant was transferred to a polypropylene autosampler vial for analysis. Every batch of 12 SPE extracted samples included one SPE DI water blank, one sample duplicate, and one native spike (alternating between an environmental sample native PFAS spike of 1.5 ng and a DI water native PFAS spike rotating between 0.15, 1.5 and 15 ng).

Samples were analyzed with an Agilent (Santa Clara, CA) 6460 triple quadrupole liquid chromatograph-tandem mass spectrometer (LC-MS/MS) (see Appendix B for additional information).[15] LC-MS/MS blanks and the calibration curve were prepared with 50:50 MeOH:DI water and internal standard concentrations matching the samples. The 11-point calibration curve ranged from 1 to 10,000 ng L^{-1} and calibration quality controls were included throughout the sample run. Branched and linear PFOS and PFHxS were quantified with individual native isomer calibration curves and the sum is reported. Method detection limits (MDLs) and method quantification limits (MQLs) were the average sample concentrations at which the signal-to-noise ratio was 3 and 10, respectively. See Appendix B for quality assurance/quality control measures (Tables B4 and B5).

3.3.5 TOTAL OXIDIZABLE PRECURSOR ASSAYS

The total oxidizable precursor (TOP) assay[17, 77] was utilized here to estimate total precursor concentrations for selected samples. A 20 mL water sample was combined with 20 mL of a 120 mM potassium persulfate and 250 mM sodium hydroxide in a 60 mL HDPE bottle and maintained at 85 °C overnight in a water bath. Samples were then cooled to room

temperature, neutralized with hydrochloric acid, and extracted as previously described, with the addition of 4 mL of DI water to rinse the sample bottle and cartridge after concentrating the sample. An additional DI water oxidation blank was included in each batch of 12 samples. See Appendix B and Tables B6 – B8 for quality assurance/quality control measures.

3.3.6   SEDIMENT PFAS ANALYSIS

Sediment was extracted following previously developed methods.[15, 17, 78] Frozen sediment samples were thawed, subsampled into 50 mL polypropylene centrifuge tubes and centrifuged at 4000 rpm for 20 minutes. The pore water supernatant was transferred to another container and the sediment was transferred to a new HDPE container and dried at 45 °C for 6 days. The sediment weight before and after drying was recorded to determine the volume of water removed. The sediment was then sieved through a 2.36 mm sieve, homogenized, and 9 g was subsampled into a 50 mL polypropylene centrifuge tube. The sediment sample was then mixed with 18 mL of 0.1% ammonium hydroxide in methanol, vortexed briefly, bath sonicated at 40 °C for 30 minutes, placed on a rotating table for 2 hours, centrifuged at 4000 rpm for 20 minutes, and finally the methanol supernatant was transferred to a 50 mL polypropylene centrifuge tube. The methanol extraction was repeated 3 times, and the combined methanol extracts were dried under an ultra-high purity nitrogen gas stream. Samples were reconstituted with 1.5 mL of 0.1 % acetic acid, heated to 45 °C for 30 minutes, and vortexed briefly before transfer to a polypropylene microcentrifuge tube containing 25-30 mg of ENVI-Carb to remove dissolved organic matter. The methanol-ENVI-carb samples were vortexed, centrifuged at 13000 rpm for 20 minutes, and 710 μL was transferred to a microcentrifuge tube containing 750 μL DI water and 40 μL of a 0.03 ng μL^{-1} internal standard solution. Finally, samples were vortexed and centrifuged at 13000 rpm for 20 minutes before the supernatant was transferred to

a 1 mL polypropylene vial for LC-MS/MS analysis as previously described. A blank sample containing no sediment was included in the extraction.

3.3.7   MODEL OF PFAS FLUX TO ASHUMET POND

The PFAS flux from the FTA PFAS groundwater contamination plume to Ashumet Pond was modeled using the PFAS concentrations in the samples collected from a transect of groundwater samples located upgradient of Ashumet Pond (Figure 3.2B) in conjunction with previously developed estimates of the groundwater flux through the transect toward the pond.[86, 111] Previously, water flux estimates were calculated from a steady-state model using a grid of vertically stacked cells upgradient of Ashumet Pond to determine phosphorus load from the upgradient wastewater contamination plume to Ashumet Pond.[86, 111] The PFAS plume is located within the bounds of this model. PFAS concentrations from the well locations were assigned to each grid cell (16.8 x 16.8 m^2) and interpolated to fill gaps between cells. Water fluxes for each cell were then multiplied by the PFAS cell concentrations to determine the flux of PFAS across each cell, and summed to calculate total PFAS flux to Ashumet Pond. Outside of the transect, it was assumed PFAS concentrations were zero, providing a conservative estimate of total flux to the pond. Uncertainties with this approach include variability in groundwater fluxes and associated model parameters (hydraulic conductivity, recharge, etc.), interpolated/edge PFAS concentrations, and precursor transformation.
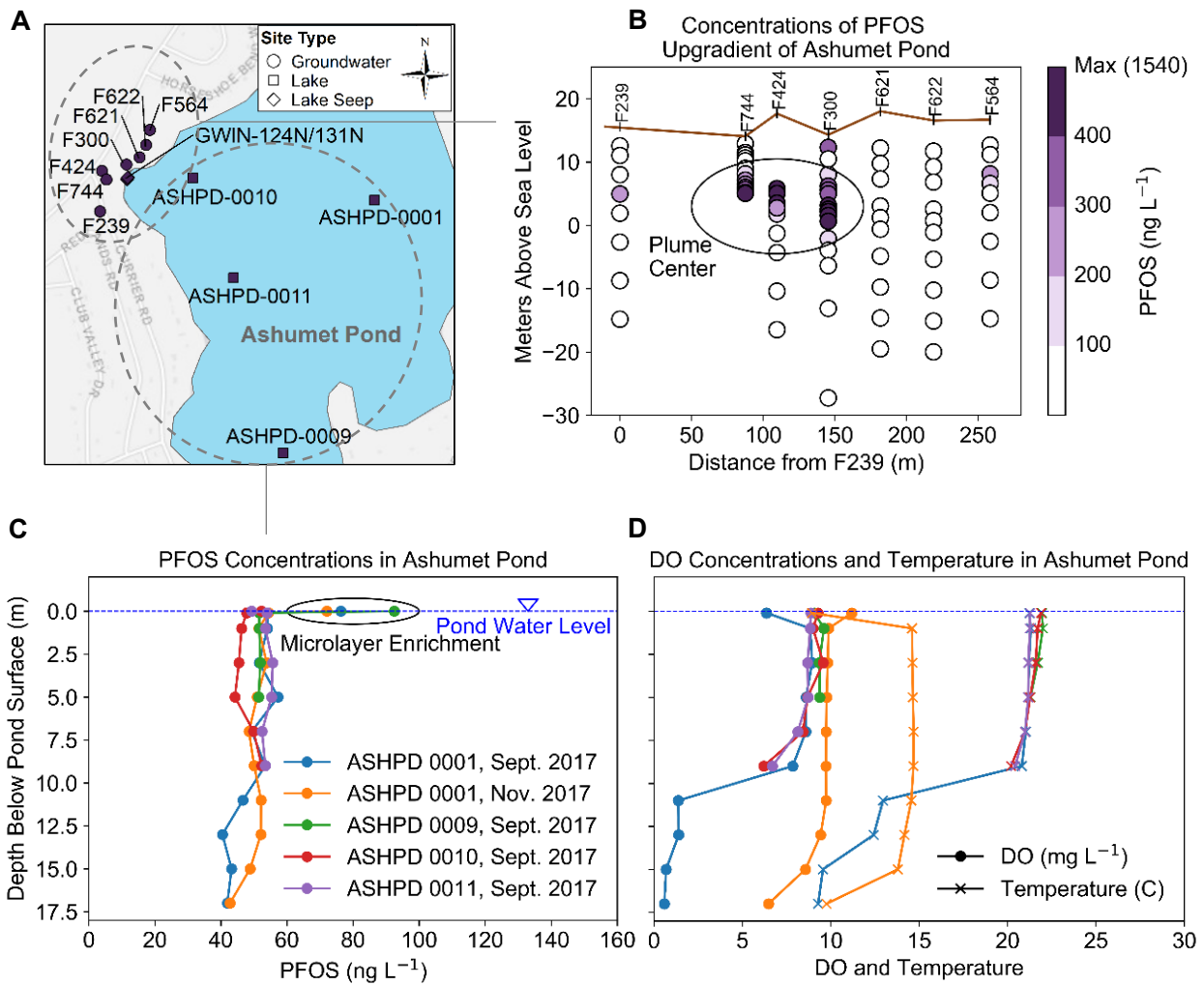
Figure 3.2 (A) Sampling locations, (B) PFOS concentrations in the array of groundwater wells located upgradient of Ashumet Pond, (C) PFOS concentrations in Ashumet Pond in September 2017 at four locations and November 2017 at one location, and (D) associated water quality parameters. The depth of Ashumet Pond is 19 m.

3.4 RESULTS

3.4.1 OVERVIEW OF PFAS CONCENTRATIONS ALONG THE HYDROLOGICAL FLOW PATH

The groundwater samples collected from the fence of wells and MLSs upgradient of Ashumet Pond show a fairly well-resolved plume shape (Figure 3.2B) with the highest concentrations in three adjacent wells F744, F424, and F300. The highest sample concentration in the center of the plume was 3290 ng L^{-1} PFHxS at well F424 (located <100 m upgradient from the shore of Ashumet Pond, Figure B1).

PFAAs downgradient from pond water were hypothesized to be uniform in composition owing to a well-mixed pond water source and high mobility in low organic carbon sediments. Results show PFOS concentrations in Ashumet Pond were fairly homogeneous (51.1 ± 5.0 ng L^{-1}) between sampling locations and sampling dates (Figure 3.2C). In contrast, the surface microlayer samples were enriched by up to 1.8 times the average PFOS concentration. PFOS, PFOA, and PFHxS were the highest concentration PFASs in Ashumet Pond. Across sampling locations and sampling dates the mean concentrations for PFOA and PFHxS were also fairly homogeneous at 29.6 ± 3.1 ng L^{-1} and 74.2 ± 6.3 ng L^{-1}, respectively (Figure B2). Concentrations in the lake were much lower than in the groundwater samples upgradient of the pond (factor of 44 times lesser for PFHxS between the highest concentration sample of 3290 ng L^{-1} and the average pond concentration of 74.2 ng L^{-1}) indicating that the PFAS plume is greatly diluted upon discharge of the upgradient groundwater contamination plume into the large volume pond (see below discussion).

While Ashumet Pond samples were temporally and spatially homogeneous, downwelling porewater and downgradient groundwater were highly variable in concentration and composition despite originating from the pond,[112] as will be discussed below.

3.4.2 FIRE TRAINING AREA PFAS PLUME FLUX TO ASHUMET POND

The total modeled water flux into Ashumet Pond is 5.25 x 10^8 L yr^{-1}.[86] PFAS flux estimates from the FTA PFAS groundwater contamination plume to Ashumet Pond were calculated for PFHxA (14.6 g year^{-1}), PFOS (43.1 g year^{-1}), and the sum of PFAS (191 g year^{-1}). While the water associated with deeper layers (extending to -20 m altitude) in the model could flow underneath Ashumet Pond,[86] the associated PFAS concentrations were so low that removing these values resulted in <1% change in PFAS flux estimates. Assuming a pond volume of 6.26 x 10^9 L[86], and total groundwater outflow of 3.81 x 10^9 L year^{-1},[108] the residence time is ~1.6 years. Therefore, if all PFASs in Ashumet Pond were a result of discharge from the FTA groundwater contamination plume, the diluted pond concentrations would be 3.73 ng L^{-1} PFHxA, 11.0 ng L^{-1} PFOS, and 48.8 ng L^{-1} for the sum of PFAS. Measured mean concentrations in Ashumet Pond were 22.7 ng L^{-1} PFHxA, 51.1 ng L^{-1} PFOS, and 225 ng L^{-1} for the sum of measured PFAS. Measured values are 4.6 – 6.1 times greater than modeled values. Since <25% of the total Ashumet PFAS can be accounted for by the AFFF FTA plume to the northwest it is to be expected there are one or more supplementary sources of PFASs to Ashumet Pond, which could include AFFF-based sources, recreational activity in the lake, and septic systems in the surrounding area. The specific PFAS composition between Ashumet Pond and the upgradient FTA area plume is similar (composed primarily of PFOS and PFHxS), suggesting that the unknown PFAS sources are also AFFF-based. The model mass balance calculation indicates the possibility of multiple PFAS sources at a site where AFFF was frequently used. A mass balance calculation assuming 1) 3.81 x 10^9 L year^{-1} [108] discharges from Ashumet Pond and 2) the average total PFAS concentrations in Ashumet Pond is 225 ng L^{-1} results in a flux of 857 g$_{pfas}$ year^{-1} from Ashumet Pond to the downgradient aquifer.

3.4.3 ESTIMATED TOTAL MOLAR PRECURSOR CONCENTRATIONS ALONG THE FLOW PATH

A total of 53 samples (12 pond water, 1 microlayer sample, 22 downgradient groundwater samples, 10 downwelling pore water samples, and 8 upwelling pore water samples) were analyzed with the TOP assay (Table B12). Precursors were detected in 52 out of 53 samples and PFBA, PFPeA, and PFHxA concentrations increased post-persulfate-oxidation in all samples. The mean increase was 90.4 ± 113% for PFBA, 46.1 ± 27.0% for PFPeA, and 147 ± 126% for PFHxA for samples that had a concentration over the MQL pre- and post-oxidation (22 samples for PFBA, 37 samples for PFPeA, 42 samples for PFHxA). For longer chain length PFCAs ($n \geq 7$, where n is the number of perfluorinated carbons)[2] the median increase was ≤20% (near analytical error), indicating an absence of long chain length PFAA precursors. The sum of measured precursors (4:2 fluorotelomer sulfonate, 8:2 fluorotelomer sulfonate, N-Methyl perfluorooctane sulfonamidoacetic acid, N-Ethyl perfluorooctane sulfonamidoacetic acid, and perfluorooctane sulfonamide) accounted for a maximum of ~8% of precursors from the TOP assay.

The total estimated precursor concentrations are reported in nanomolar units because the original mass of the precursor before oxidation is unknown.[15, 17, 77] The precursor percentage is calculated as the percent of precursors (nM) out of the total molar concentration (ΣPFCAs+ ΣPFSAs + precursors in nanomolar units), where $\sum$PFCAs includes $3 \leq n \leq 13$ perfluoroalkyl carboxylates and ΣPFSAs includes $4 \leq n \leq 10$ perfluoroalkyl sulfonates. The percent precursors was 17 ± 6.2% (mean ± standard deviation) for upwelling pore water, 22 ± 4.2% for Ashumet Pond, 14 ± 4.8% for downwelling porewater, and 15 ± 5.9% for downgradient groundwater. In 2015, precursors from well F424 located directly upgradient the discharge zone exceeded 50% of the molar PFAS concentration,[15] suggesting the 2017 upwelling pore water samples were likely collected axially off-center from where the core of the PFAS plume discharges to the pond

because of their low precursor percentage (17 ± 6.2%). A Mann Whitney test indicates that the percentage of precursors in Ashumet Pond (n = 12) is statistically greater than the percentage of precursors in the downwelling porewater (n = 10, p <0.01) and downgradient groundwater (n = 21, p <0.01). Chain length of the oxidation products does not appear to be influenced by this decrease along the flow path (Figure B3).

For comparison, the average percent precursors measured in 2015 in the upgradient PFAS plume was 31 ± 15%.[15] While the percent of precursors in the samples is moderately declining along the flow path, the persistence of these precursor compounds is notable. The percentage of precursors in Ashumet Pond and downgradient groundwater remains between 10-30% with the exception of 3 out of 53 samples (Figure 3.3A). One study observed indirect photolysis transforms N-ethyl perfluorooctane sulfonamide acetate (N-EtFOSAA) into perfluorooctane sulfonamide (FOSA) and PFOA.[43] However, further breakdown of FOSA was not observed,[43] indicating indirect photolysis may be less effective at breaking down intermediate precursors or that the intermediates are more recalcitrant in general than primary precursors. Ashumet Pond had relatively clear water during sampling, with secchi depths around 5 m, and stratification of the water column around 10 m depth in September 2017 (Figure 3.2D). Despite conditions suitable for indirect photolysis, the (intermediate) precursors are stable, indicating they are more persistent than N-EtFOSAA.
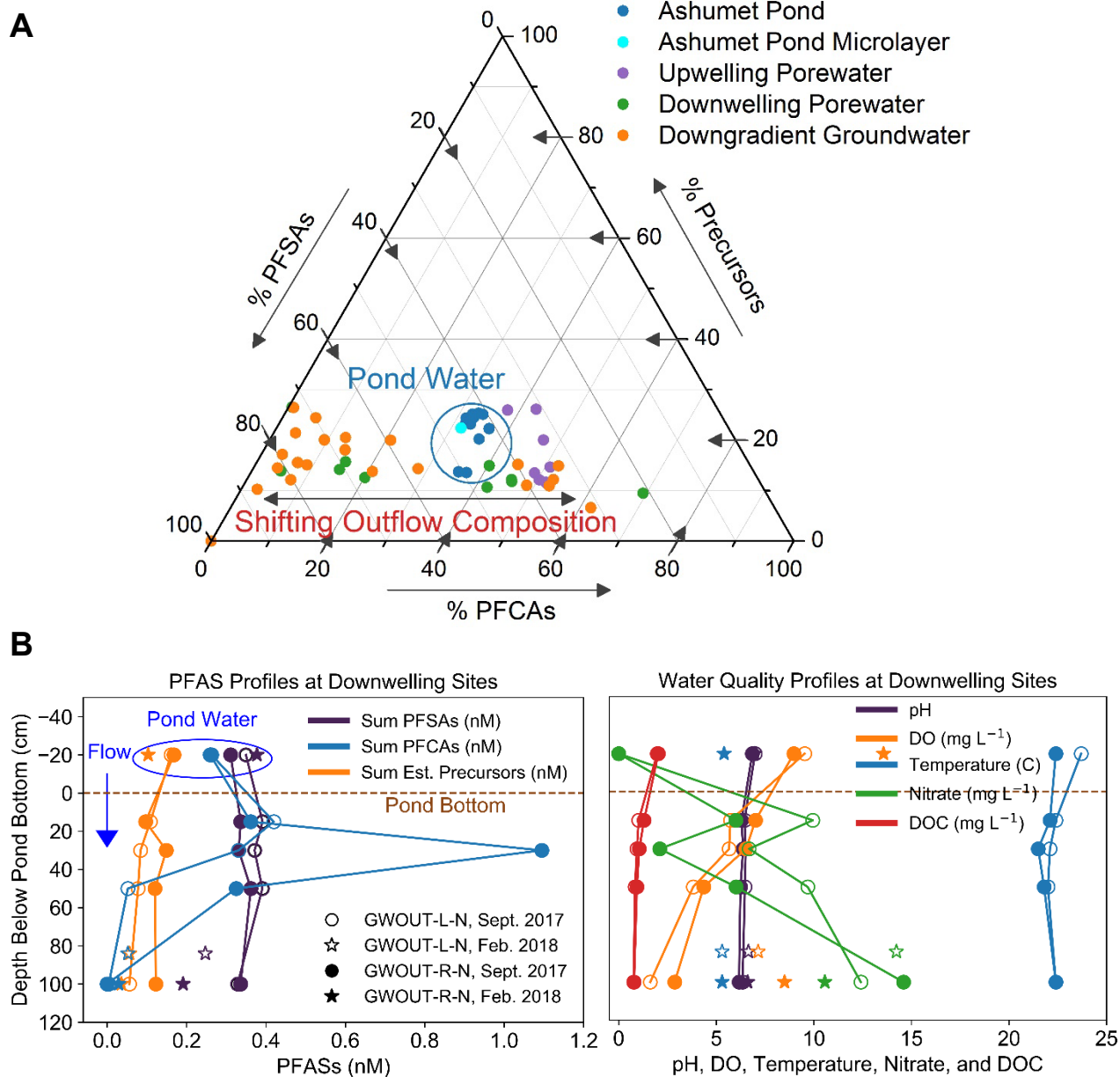
Figure 3.3 (A) Sample PFAS composition measured in nM and converted to percentage for all 53 samples measured with the total oxidizable precursor assay. For each point, PFSAs (%), PFCAs (%), and precursors (%) will sum to 100%. (B) PFCA, PFSA, precursor, and water quality profiles at the downwelling sites.

A wide range of precursor biotransformation rates is reported in the literature.[38, 40, 92] N-ethyl perfluorooctane sulfonamide (EtFOSA) transforms in soil under aerobic conditions with a half-life of 13.9 days when fit with a first order kinetic model.[40] However, negligible transformation of perfluorooctane sulfonamide quaternary ammonium salt (PFOSAmS) was observed over a 180-day soil microcosm study, illustrating the range in biotransformation rates of precursor compounds.[92] Furthermore, the original precursor may undergo several transformations before ultimately forming a PFAA compound. For example, EtFOSA can transform into intermediate precursors EtFOSA alcohol, perfluorooctane sulfonamide acetic acid, FOSA, and terminal PFOS.[40]

Assuming a pseudo-first order kinetic transformation model $[P] = [P_0]e^{-kt}$, where P is the concentration of precursors (nM) at distance x from the lake, P_0 is the lake concentration of precursors (0.195 nM), and t is the time (days) it takes to travel x meters from the lake, the rate constant k (day^{-1}) can be estimated. Well F632 is furthest away from the lake (x = 390m), has an average precursor concentration of 0.051 nM (P), and DO ranging from 0.03 to 5.3 mg L^{-1}. Although biotransformation has been shown to be slow compared to aerobic degradation,[42] there was no statistically significant correlation between precursor concentration and DO in the downgradient groundwater (spearman rho rank correlations, n = 21), and therefore the mean precursor concentration from F632 was used. Applying a flow velocity of 0.42 m d^{-1} [64] and no retardation (to provide a conservative estimate of transformation rates), t is 929 days, and k is 0.0014 day^{-1}. The precursor groundwater half-life ($t_{0.5} = \frac{\ln(2)}{k}$) is therefore 480 days (~200 m transport downgradient), nearly as long as the 1.6 year (584 day) residence time in the lake. This estimate is biased low since it does not account for dilution, retardation, or longer flow paths from deeper in the lake. The half-life estimation suggests precursors are persistent on timescales long enough to allow substantial transport away from point sources.

3.4.4 PFAS TRANSPORT IN POND-INFLUENCED GROUNDWATER

The PFAS composition observed within Ashumet Pond in 2017 is spatially homogeneous (Figures 3.2C, 3.3A). The microlayer sample has a similar composition as the other Ashumet Pond samples since the PFOS increase (25.0 ng L^{-1}) is small compared to the sum of the PFSAs (~180 ng L^{-1}). In comparison, the pond-influenced groundwater PFAS composition on the downgradient side of Ashumet Pond varies considerably (Figure 3.3A). Specifically, there were large compositional variations (PFCAs decreasing to <20% and PFSAs increasing to >80% of the total PFAS composition) between samples (Figure 3.3A). In vertical profiles of porewater in the downwelling pond water to 100 cm depth beneath the surface water/groundwater interface (Figure 3.3B), the PFCA concentrations fluctuated (initially rising then declining with depth), but always had lowest concentrations by 100 cm depth (<0.05 nM for ΣPFCAs, with a maximum individual concentration of 0.03 nM or 6.6 ng L^{-1} PFBA). Aqueous PFSA and precursor concentrations were relatively stable throughout the sediment depth profiles (Figure 3.3B). Temporally, February 2018 samples from the downgradient well closest to Ashumet Pond (F722) had elevated PFCA concentrations (mean 340 ± 200 ng L^{-1}) as compared to the September 2017 sampling (mean 27 ± 33 ng L^{-1}), that had lower concentrations than Ashumet Pond (mean 83 ± 7.5 ng L^{-1}) (Figure 3.4A) suggesting a seasonal dependence of downgradient groundwater PFCA concentration. In contrast, PFSA had more consistent concentrations both spatially and temporally (Figure 3.4B). The downgradient groundwater [PFCA] variability as compared to the [PFSA] consistency suggests a PFAS headgroup specific (carboxylate versus sulfonate) sorption mechanism.
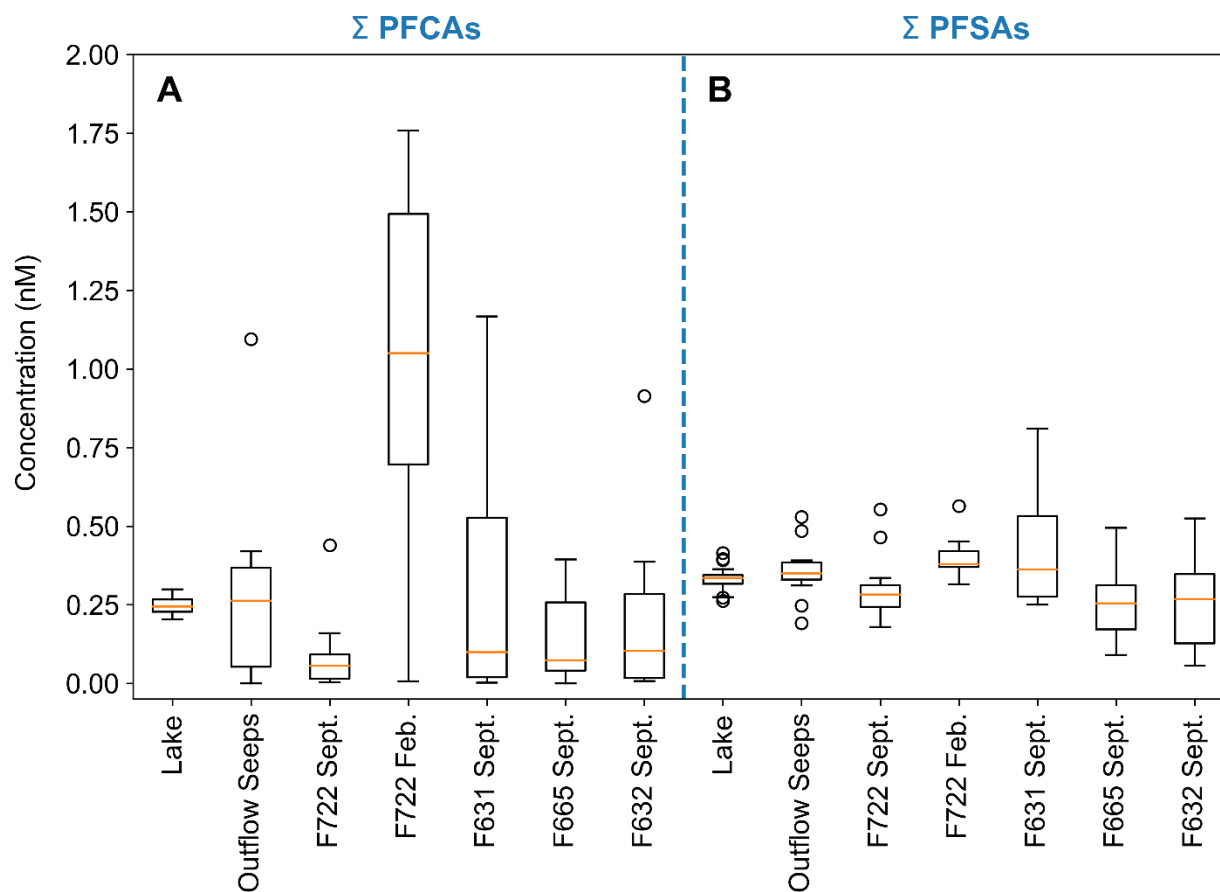
Figure 3.4 (A) PFCA and (B) PFSA concentrations following the hydrological flow path from left to right, with different sampling dates for Well F722. Box encompasses the lower and upper quartiles. The median is the orange line. Whiskers are the 3rd quartile plus 1.5 times the interquartile range (upper bound) or the 1st quartile minus 1.5 times the interquartile range (lower bound). Circles are outside of this range.

Sediment samples acquired from locations corresponding to the upwelling and downwelling pore water samples were extracted to determine K_d values (Table B13, Figure B4). K_d values were higher than those measured previously from the upgradient aquifer (max 0.07 L kg^{-1} for PFOS[15] vs. 18.6 L kg^{-1} for PFOS from Ashumet Pond). PFNA and PFOS both have 8 perfluorinated carbons and can thus be directly compared regarding specific headgroup effects.

In 11 out of 12 samples, PFNA K_d values were larger than PFOS (Table B13, Figure B4), with the largest difference observed in the pond surface sediment at downwelling site GWOUT-R-N (404 L kg^{-1} for PFNA and 14.7 L kg^{-1} for PFOS). At shorter chain lengths, the difference between the upwelling and downwelling sites becomes more apparent. Comparing PFOS to PFCAs with $n \leq 7$, PFOS had the highest measured K_d value of 9.06 at the upwelling sites, while the highest PFCA K_d value was 2.92 (PFHxA). At the downwelling sites, PFOA had the highest K_d value at 105 L kg^{-1}, while the maximum for PFOS was 18.6 L kg^{-1}. At GWOUT-L-N 15 cm all PFCA K_d values exceeded the maximum PFOS K_d (PFBA = 23.6 L kg^{-1}, PFPeA = 32.6 L kg^{-1}, PFHxA = 37.7 L kg^{-1}, PFHpA = 36.5 L kg^{-1}, PFOA = 38.5 L kg^{-1}, PFOS = 18.6 L kg^{-1}) and PFCA K_d values were relatively independent of chain-length. This contrasts the PFSA trend from the same downwelling site, where K_d decreases with decreasing chain length, fitting the typical chain-length dependent sorption framework.[72] Previous studies have found K_{oc} values increase by 0.23 log units for sulfonate as compared to carboxylate functional groups when comparing compounds with equal number of perfluorinated carbons.[72] However, the sediment partitioning at this field site does not fit this model, and the results also do not align with PFAS sorption trends for protein[104], or mineral surfaces[88], which all find PFOS sorption should be greater than PFSAs with shorter chain length and PFCAs with $n \leq 8$, primarily due to increased hydrophobic effects. The disagreement here suggests an alternative PFCA sorption mechanism i.e., specific carboxylate chemisorption as opposed to electrostatic/hydrophobic physisorption.

Sediment extractable metal (Cr, Mn, Fe, Ni, Cu, Zn, Pb) concentrations from the upgradient and downgradient side of Ashumet Pond were measured by inductively coupled plasma mass spectrometry (see Appendix B for extraction and analysis details). In all cases, the Fe and Mn concentrations were highest in sediment from the 0 – 5 cm depth interval and lesser at depth. Fe and Mn were the highest concentration metals detected and concentrations were higher on average at the upwelling sites (250 ± 325 µg g^{-1} for Fe and 643 ± 789 µg g^{-1} for Mn)

and lower at the downwelling sites (99 ± 43 µg g^{-1} for Fe and 24 ± 18 µg g^{-1} for Mn). This indicates that iron and manganese are not likely to be the source of enhanced carboxylate sorption (despite zero point of charge above 7.8 for iron-bearing minerals at the field site[54]), as there are lower iron/manganese concentrations at the downgradient site. Total carbon was previously reported to be 92 ± 1 µmol g^{-1} near the downwelling site studied here and 43 µmol g^{-1} near the upwelling sites,[107] which may explain the higher K_d values seen at the downgradient site. However, PFAS sorption by organic carbon should result in chain-length dependent trends with greater sorption associated with the sulfonate moieties over the carboxylate moieties, in contrast with field measurements.[72]

The increased concentration of PFCAs in February at well F722 (Figures 3.4A and 3.5A) suggests PFCA desorption may occur seasonally, although additional temporal measurements are needed to confirm this. The average temperature in well F722 was 22.0 ± 1.93 °C in September 2017 and 5.30 ± 3.54 °C in February 2018. The specific surface area of the downwelling sediments is 0.28 m^2 g^{-1} [107] (4.6×10^{20} nm^2 L^{-1}, assuming a bulk density of 1.64 g cm^{-3}) [113] and the sum of major anions is ~850 µM (chloride, bromide, sulfate, nitrate, and hydroxide). Assuming an area of 0.35 nm^2 for a hydrated chloride ion (hydrated radius of chloride = 0.332 nm[114]), there are approximately as many anions in solution as there are sorption sites suggesting competitive sorption may be possible. This is especially true when considering that a sorbed PFAS molecule may require a much larger molecular surface area (PFOS = 4.54 nm^2)[115] if there is association of the hydrophobic tail with the particle surface.
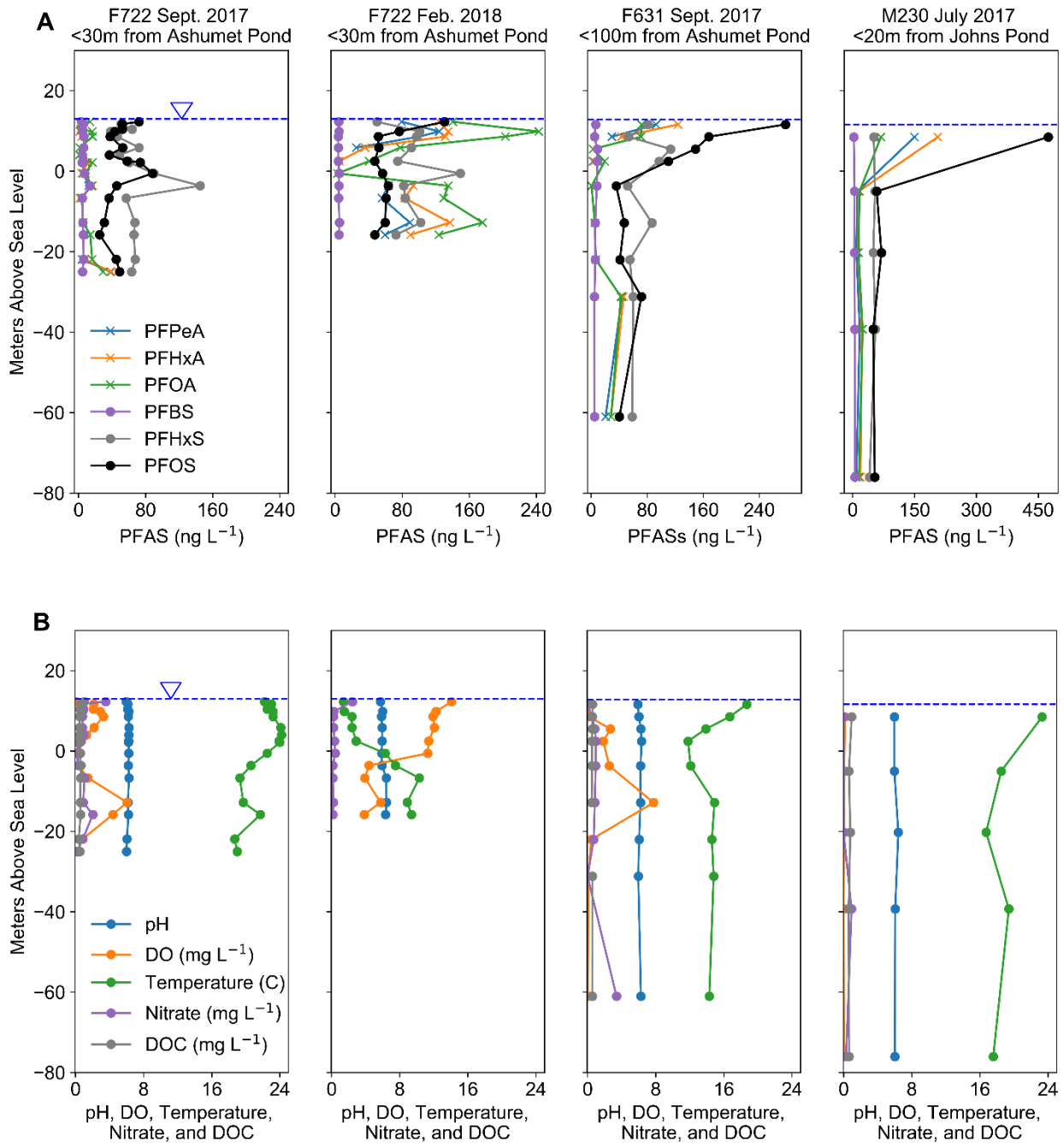
Figure 3.5 (A) Measured PFPeA, PFHxA, PFOA, PFBS, PFHxS, and PFOS concentrations in groundwater wells directly downgradient of Ashumet Pond (F722, F631) and Johns Pond (M230) and (B) pH, dissolved oxygen (DO), temperature, nitrate, and dissolved organic carbon (DOC). Well F722 was sampled in both September 2017 and February 2018.

Quartz has a zero point of charge ranging from 1.8 – 2.4[54] and therefore will be negatively-charged at this field site and not expected to electrostatically attract the carboxylate or sulfonate groups. However, positively charged surfaces such as alumina[116] have been shown to complex with the carboxylate moiety of organic matter,[117] and Al-bearing minerals are found on Cape Cod sediments.[118] PFSA K_d values from this study exhibit chain-length dependence, indicating that a general physisorption process such as hydrophobic effects are a governing mechanism, whereas PFCA K_d values have a relatively weak chain-length dependence, indicating carboxylate functional group complexation may be the dominant sorption mechanism. Gao and Chorover[119] similarly reported different sorption mechanisms for PFOS and PFOA to an iron oxide surface (synthetic hematite). For PFOA, sorption occurred through inner-sphere complexation (specific chemisorption via ligand exchange) between the carboxylate functional group and iron hydroxyl, and electrostatic interaction.[119] PFOS sorption occurred predominantly via general physisorption outer-sphere complexation such as electrostatic interaction and hydrogen bonding.[104, 119] Chemisorption is typically defined by heats of adsorption >20 kJ mol^{-1}, while physisorption has <20 kJ mol^{-1} heats of adsorption.[120] Additional study is needed, but such different sorption mechanisms may be the driver behind diverging PFCA and PFSA concentrations in the downgradient sediment and groundwater (Figures 3.3A, 3.4A, and 3.5A).

3.4.5   AIR-WATER SURFACE ENRICHMENT

Ashumet Pond microlayer samples (top ~50 μm)[109] had PFOS concentrations that were up to 1.8 times the median bulk pond concentration (Figure 3.2C) with 4 out of 5 microlayer samples having enriched PFOS concentrations compared to bulk pond water. In John's Pond, both microlayer samples collected had enriched PFOS concentrations in comparison to bulk pond water, with a maximum enrichment factor of 3.8. Negligible enrichment (less than a factor of 1.4) was observed for all other PFASs, except for PFNA (same number of perfluorinated

carbons as PFOS) in Johns Pond, which had an enrichment factor of 1.9 compared to bulk pond water. A single microlayer sample with enriched PFOS concentrations (1.5-fold enrichment) was oxidized (TOP), but no precursor enrichment was evident. The observed PFOS microlayer concentrations compared to the bulk pond concentrations were well described by Gibb's adsorption isotherm $\Gamma = \frac{-1}{RT} \frac{\partial \gamma}{\partial \ln C}$ (Figure B5 and Appendix B Microlayer Enrichment Theoretical Calculation section).

In groundwater wells near the downgradient shoreline of Ashumet Pond (<100 m, hydraulic travel time of 0.65 years) and Johns Pond (<20 m, hydraulic travel time of 0.13 years), elevated concentrations of PFOS were observed near the water table (Figure 3.5A). Although there was limited PFOS enrichment observed at well F722 in the September 2017 samples, the February 2018 samples from F722 had enriched PFOS concentrations near the water table (Figure 3.5A). PFOS was enriched near the water table (up to ~10x compared to samples from deeper depths in the same well) in all wells that are located immediately downgradient (<100 m) of the southeastern discharge area of the ponds. Wells further away (>100 m) did not display this enrichment.

We hypothesize groundwater table enrichment near the pond could be due to microlayer accumulation in the unsaturated zone due to the high surface area of air-water interface. Fluctuations in the water table height could re-mobilize the concentrated PFASs. Alternatively, wave action on the pond shore could deposit microlayer-enriched PFOS onto the beach sands, which then contribute to elevated PFOS concentrations seen near the water table. A combination of both hypotheses is probable.

PFHxS:PFOS ratios support an air-water interface driven effect. As discussed, PFOS has a higher affinity for the air-water interface than PFHxS based on the Gibbs equation (air-water interface adsorption coefficient of 0.004 cm^3 cm^{-2} for PFOS and 0.00026 cm^3 cm^{-2} for

PFHpA,[105] which has the same number of perfluorinated carbons as PFHxS) and observed pond microlayer concentrations (Figure B5 and Appendix B Microlayer Enrichment Theoretical Calculation section). The PFHxS:PFOS ratio should therefore decrease if the observed PFOS enrichment is due to the air-water interface. For each well (Figure 3.5A), the PFHxS:PFOS ratio was lowest (0.11 – 0.38) in the well port closest to the water table and larger at depth (reaching up to 3.2), providing evidence for air-water interface driven accumulation. The pond PFHxS:PFOS ratio is 1.5. Enrichment close to the water table was also observed for carboxylates down to a perfluorocarbon chain length of 4 (Figure 3.5A), particularly for wells F631 and M230, however, no enrichment was observed for sulfonates with shorter chain lengths (4 to 6 perfluorinated carbons, Figure 3.5A). The results suggest a carboxylate-specific sorption/desorption as discussed in the previous section since carboxylate air-water interface enrichment is not observed in microlayer samples for perfluorocarbon chain lengths less than eight. In summary, the air-water interface PFOS-specific enrichment in groundwater suggests a hydrophobic effect, while the PFCA pulses of sorption and release support a headgroup specific sorption process that may have significant impacts on PFAS fate and transport in groundwater and surface waters.

3.4.6   ENVIRONMENTAL IMPLICATIONS

In this study, we observed that a shallow groundwater plume of limited dimensions discharges and mixes with a surface water body, which subsequently recharges downgradient groundwater with PFAS-contaminated water. The surface water interaction with the plume results in a large groundwater outflow (3.81×10^9 L year^{-1} [108]) from the pond of dilute PFAS concentrations, which is more difficult to remediate than a high concentration at low volume. A mass balance suggests the flux from Ashumet Pond to the aquifer is 857 g_{pfas} year^{-1}. PFAA precursors gradually decline between the pond and downwelling groundwater, but remain highly

persistent (10-30% of total PFAS concentration) despite exposure to photoactive oxic pond water and subsequent transport by downwelling through a biologically reactive surface water/groundwater boundary. The persistence of these precursors and their propensity to transport across pond-groundwater boundaries indicates that precursors need to be considered during monitoring of drinking water to fully understand human exposure risk. While the concentrations and composition of PFASs in Ashumet Pond remained stable over the time period investigated in this study, the downwelling water fluctuated in composition and concentration. Variability may be driven by carboxylate-specific interactions and PFOS sorption at the air-water interface.

3.5   ACKNOWLEDGMENTS

Chapter 4

HOW DO WE MEASURE POLY- AND PERFLUOROALKYL SUBSTANCES (PFASs) AT THE SURFACE OF CONSUMER PRODUCTS?

4.1   ABSTRACT

Exposures to PFASs have been linked to metabolic disruption, immunotoxicity, and cancer in humans. PFASs are known to be present in diverse consumer products including textiles and food packaging. Here, we present a new method for quantifying the atomic percent fluorine (% F) in the surficial 0.01 μm of consumer products using X-ray photoelectron spectroscopy (XPS). The surface of food contact materials and textiles measured in this study contained up to 28% F and 45% F, respectively. PTFE tape was measured to demonstrate XPS accuracy and precision. Depth profiles of fluorine content in consumer products measured using XPS showed the highest levels at the upper-most surface in contact with the surrounding environment and a decrease below the surface. PFASs released in methanol extracts and quantified using traditional liquid chromatography-tandem mass spectrometry typically accounted for <1% of the fluorine measured with XPS in consumer products. We conclude that XPS is a useful technique for characterizing PFASs in consumer products because it can

precisely quantify the surficial fluorine content of materials. XPS also allows identification of CF_2 and CF_3 groups in materials and can elucidate the depth-dependent distribution of fluorine in products.
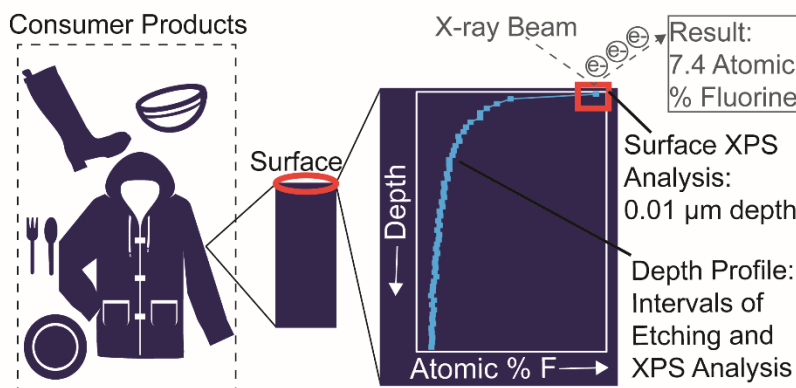
Figure 4.1 Visual representation of XPS analysis of consumer products.

4.2 INTRODUCTION

Elevated exposures to poly- and perfluoroalkyl substances (PFASs) have been linked to many adverse health effects, including diabetes, obesity risk, and immune suppression.[94, 121, 122] More than 4000 PFASs have been produced since the late 1940s and hundreds have been detected in environmental samples.[1-3] PFASs are defined by the presence of the C_nF_{2n+1}- moiety. They are often applied as "nonstick" surface coatings on products,[18] can migrate from treated food contact papers into food or food simulants such as butter, water, vinegar, and water/ethanol mixtures,[1, 2, 18, 123-125] and can leach from textiles into simulated saliva and sweat.[126, 127] While PFASs are often applied as surface coatings on products,[18] quantifying this surficial fluorine remains a challenge.

Traditional methods for measuring PFASs (liquid chromatography-tandem mass spectrometry, LC-MS/MS, or gas chromatography-mass spectrometry, GC-MS) only capture a small fraction of the fluorinated substances present in consumer products.[20] Recently, particle-

induced gamma ray emission (PIGE) has been proposed as a rapid screening technique for measuring the cumulative fluorine in consumer products.[20, 128, 129] PIGE has been validated as a reliable method for detecting the presence of fluorine in the upper 100-250 μm of consumer products but does not distinguish between inorganic and organic fluorine.[20, 128, 129] In addition, measurement techniques that can distinguish between surficial and subsurface fluorine in a product are needed.

Here we investigate the utility of using XPS to quantify surficial (0.01 μm) fluorine content in consumer materials. XPS represents a true surface measurement (surface defined as ≤ 0.1 μm)[130], with a penetration depth 4 orders of magnitude smaller than PIGE (100-250 μm). Penetration depth is important because contact with consumer products (food, skin, children's saliva) typically occurs at the surface of the material. We selected 45 products from a college campus for XPS analysis after determining concentrations of the suite of standardly measured PFASs using LC-MS/MS. XPS measurements were performed before and after a methanol extraction to understand fluorine mobility potential. Finally, we examined heterogeneity in concentrations with depth to determine whether fluorine is concentrated at the surface or evenly distributed with product depth (several micrometers thickness).

4.3   MATERIALS AND METHODS

4.3.1   CONSUMER PRODUCT SAMPLE COLLECTION

With the assistance of the Harvard University Office for Sustainability, we collected 94 consumer products that represent frequently used items on a college campus. These included: 45 food contact materials, 37 textiles, and 12 domestic products such as lens wipes, bandages, masks, and a shower curtain (Table C1 provides a complete sample inventory). All samples

were sealed in low density polyethylene bags for storage at room temperature and cut with methanol-cleaned scissors as needed.

4.3.2 LC-MS/MS AND LIQUID CHROMATOGRAPHY QUADRUPOLE TIME-OF-FLIGHT MASS SPECTROMETRY (LC-QTOF-MS) ANALYSIS

We performed a methanol extraction on products following a method modified from prior work.[20, 125] Methanol is commonly used for consumer product extractions[20, 125, 131, 132] and is optimal for extracting the anionic compounds quantified with LC-MS/MS (see analyte list below). PFAS analysis was performed using an Agilent (Santa Clara, CA, U.S.A.) 6460 triple quadrupole LC-MS/MS with electrospray ionization in negative ion mode, as described elsewhere,[15] with modifications detailed in Appendix C. Native and isotopically labeled PFAS standards were purchased from Wellington Laboratories (Guelph, ON, Canada) (Tables C2 and C3). A total of 16 PFASs were quantified: perfluorobutanoate (PFBA), perfluoropentanoate (PFPeA), perfluorohexanoate (PFHxA), perfluoroheptanoate (PFHpA), perfluorooctanoate (PFOA), perfluorononanoate (PFNA), perfluorodecanoate (PFDA), perfluoroundecanoate (PFUnDA), perfluorododecanoate (PFDoDA), perfluorobutane sulfonate (PFBS), perfluorohexane sulfonate (PFHxS), perfluorooctane sulfonate (PFOS), perfluorooctane sulfonamide (FOSA), 6:2 fluorotelomer sulfonate (6:2 FtS), N-methyl perfluorooctane sulfonamidoacetic acid (N-MeFOSAA), and N-ethyl perfluorooctane sulfonamidoacetic acid (N-EtFOSAA). LC-QTOF-MS analysis was completed for selected samples using a Shimadzu high performance reverse-phase liquid chromatography system coupled with a Sciex 5600 triple QTOF-MS. Samples were scanned in both positive and negative mode. Additional information on analytical methods and quality assurance/quality control measures are provided in Appendix C.

4.3.3   XPS ANALYSIS

A subset of 45 samples (19 food contact materials, 14 textiles, and 12 domestic products) with a wide range of PFAS concentrations (determined by LC-MS/MS analysis) was selected for analysis of surficial percent atomic fluorine (hereon % F will refer to atomic percent fluorine) using a Thermo Scientific Al K-Alpha XPS (Waltham, MA, U.S.A.), 1.4866 keV. The X-rays had a 400 μm spot size. Samples were mounted on carbon tape, and at least two points on each sample were analyzed (we report the average). The instrumental error for atomic composition is ±1%. A survey scan was used to quantify the atomic composition of all samples. A high-resolution scan for carbon (C 1s) and fluorine (F 1s) was completed for samples with detectable fluorine. The "1s" refers to the atomic orbital. The high resolution scan provides information on specific bonds (for example, CF_2 and CF_3 groups) present in the sample.[133] PTFE tape was included as a positive control. Volatile PFASs account for a small fraction (<3%) of total fluorine in consumer products,[20] and we therefore neglect such potential losses during XPS vacuum pump-down.

We used an argon ion beam (ion gun energy = 250 eV) to etch selected samples in 10 s intervals. We performed a survey scan of % F after each etching interval to construct a fluorine depth profile. Details on XPS analysis and sample preparation for XPS measurements pre- and post- methanol extraction are provided in Appendix C.

4.4   RESULTS AND DISCUSSION

4.4.1   LC-MS/MS PFAS ANALYSIS OF METHANOL EXTRACTS

LC-MS/MS is the most commonly used and widely available instrument for aqueous PFAS analysis. Based on this method, at least one PFAS was detected in 43% of the 94 samples examined in this study. PFOA and PFHxA were detected most frequently, with individual detection frequencies of 29%. All LC-MS/MS results are reported in Table C4.

The maximum concentration of any one PFAS was PFOA measured in a carpet sample (sample 60) collected from an actively used faculty office (3200 nmol m^{-2} or 0.38 mg kg^{-1}). Risk-based concentration limits have not been established for most PFASs in consumer products. For comparison, the maximum concentration observed is very close to the New Hampshire Department of Environmental Services Direct Contact Risk Based PFOA soil concentration of 0.5 mg kg^{-1} for young children.[134] A compostable disposable bowl (sample 1) contained the highest single PFAS concentration (PFBA) measured in a food contact material at 960 nmol m^{-2} (0.60 mg kg^{-1}). High concentrations of PFASs detected in numerous compostable food contact materials (Figure 4.2A) suggest potential environmental impacts and requires further evaluation.

Perfluorinated carboxylates (PFCAs) dominated the PFAS composition for both compostable and other food contact materials (Figure 4.2B). Used textiles contained a more diverse composition of PFCAs, perfluorinated sulfonates (PFSAs), and perfluoroalkyl acid (PFAA) precursors (hereon referred to as precursors) than other products. Precursors quantified using LC-MS/MS were N-EtFOSAA, N-MeFOSAA, FOSA, and 6:2 FtS.

Of the compostable food contact materials measured, 50% contained over 64% long-chain PFAAs (Figure 4.2C) ($n \geq 7$ for PFCAs, and $n \geq 6$ for PFSAs, where n is the number of perfluorinated carbons)[2]. Long-chain PFASs have higher bioaccumulation potential than other PFASs and thus are of particular concern.[10] Used textiles were primarily composed of long-chain PFAAs, while new textiles were predominantly composed of short-chain PFAAs (Figure 4.2C). This is consistent with reported shifts in chemical production, where longer-chain PFASs have been replaced by shorter-chain alternatives.[10]
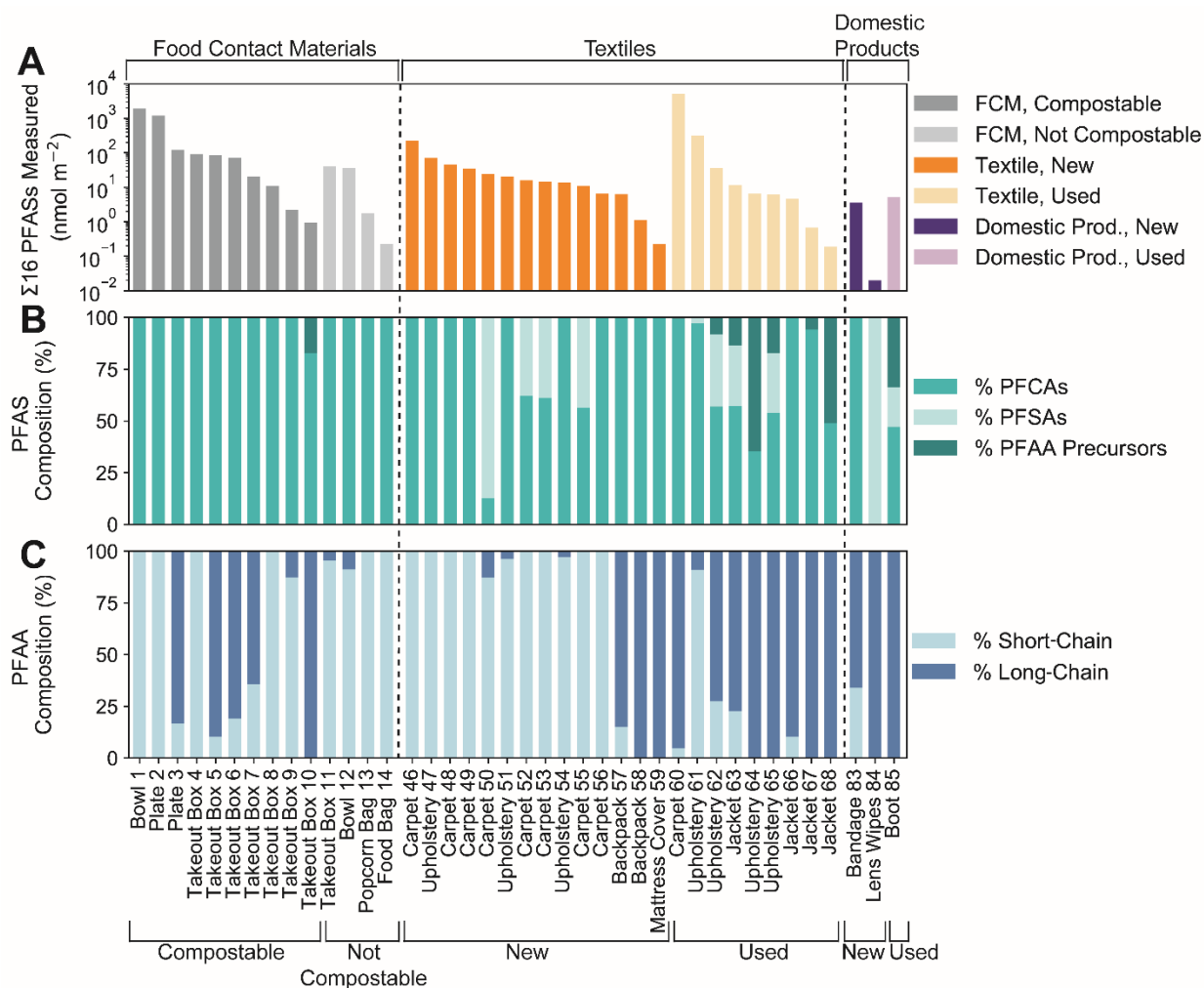
Figure 4.2. Concentrations and composition of 16 PFASs measured in consumer products. Samples include compostable food contact materials, noncompostable (or unknown) food contact materials, new textiles, used textiles, new domestic consumer products, and used domestic consumer products. Panel (A) shows concentrations of the sum of 16 measured PFASs for all samples above detection. FCM denotes food contact material. Panel (B) shows PFAS composition. The PFAA precursors are N-EtFOSAA, N-MeFOSAA, FOSA, and 6:2 FtS. Panel (C) shows the fraction of short- and long-chain PFAAs.

4.4.2 ATOMIC PERCENT FLUORINE (% F)

The highest interfacial fluorine measured in a consumer product was 45% F from a new upholstery sample (sample 51) (Figure 4.3A). The maximum atomic percent fluorine of any food

contact material analyzed was in a disposable food bag (sample 14) that contained 28% F (Figure 4.3A). We did not detect fluorine in any of the domestic consumer products using XPS (detection limit of 1%).

XPS allows identification of CF_2 and CF_3 groups in a sample and can thus confirm the presence of perfluorinated carbons. An example of CF_2 and CF_3 groups identified using a high resolution C 1s scan is shown in Figure 2B. The CF_2 group is usually located at ~292 eV (verified with PTFE tape) and CF_3 at ~293 eV.[133] Out of the 11 samples with detectable fluorine pre-extraction, nine samples displayed peaks at ~292 eV (CF_2 group) and/or at ~293 eV (CF_3 group). The two samples that did not display peaks at ~292 eV or ~293 eV were samples 61 and 68, which had the lowest % F (Figure 4.3A). Further confirming the presence of organofluorine, all 11 samples that had detectable fluorine pre-extraction displayed a peak at ~689 eV in the F 1s scan, which corresponds to the binding energy of highly fluorinated carbon groups (such as CF_2 and CF_3).[135] These results illustrate how high resolution C 1s and F 1s scans can be used to distinguish inorganic from organic fluorine.

The reproducibility of XPS measurements was verified with sample 67 (textile, rough surface). Variability was greatest for spatially independent samples randomly taken from around the textile (relative standard deviation: RSD=27%, n=9). Within a sample (<1 cm^2), RSD decreased to 11.4% (n=10). PTFE tape was measured as a positive control and contained 70% F, which agrees well with the expected value of 67% F for pure CF_2 groups (this value would increase if there were CF_3 groups present). PTFE tape (smooth surface) had a low RSD (0.53%, n=10), indicating that XPS measurements are reproducible and that material coating method/roughness are the main sources of variability.
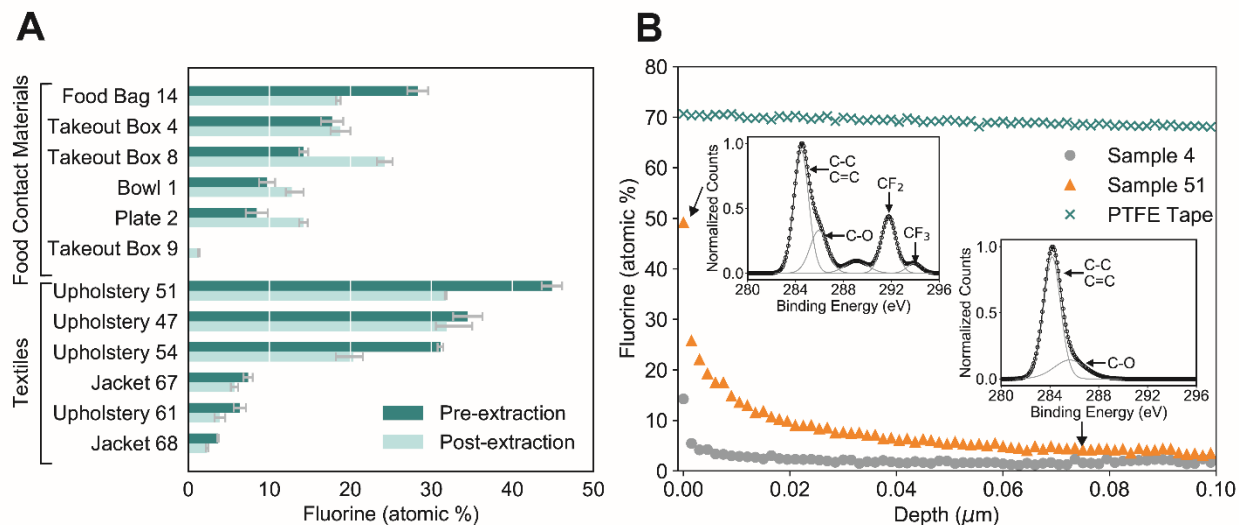
Figure 4.3. (A) XPS results showing % F in food contact materials (n = 6) and textiles (n = 6) that contained detectable fluorine. Sample 9 was included as a blank control but contained fluorine post-extraction (see Methanol Extraction for XPS section in Appendix C). Whiskers are the minimum and maximum measured; the bar is the average % F. (B) Depth profiles of a food contact material (sample 4), a textile (sample 51), and PTFE tape. Each point represents an XPS measurement of atomic percent fluorine, followed by etching with an argon ion beam for 10 s. The depth of etching for a tantalum pentoxide reference is plotted: we estimate the actual maximum total depth etched to be 10 µm. The insets show the high-resolution C 1s scan for two selected data points in sample 51: the surface measurement and one measurement taken at estimated 7.5 µm depth. The inset C 1s scans show the disappearance of the 292 eV peak with depth. The 292 eV peak corresponds with the CF_2 group binding energy.

4.4.3 XPS OF SAMPLES PRE- AND POST-EXTRACTION

Results shown in Figure 4.3A indicate that methanol extraction does not remove most fluorine from consumer materials. The % F measured before and after extraction (n=12) was not statistically different (p > 0.05) based on a two-tailed Wilcoxon signed-rank test. The location of the C 1s peaks associated with perfluorinated carbons did not shift after the methanol extraction, further confirming the persistence of organic fluorine in these materials. Robel et al.[20] also reported that a large fraction of fluorine remains in products post-extraction. These findings suggest substantial quantities of fluorine (perhaps fluorinated polymers and associated

monomers) could be released to landfills or composting facilities at the end of the product's life.[20]

4.4.4   XPS DEPTH PROFILES

Figure 4.3B shows fluorine depth profiles for one food contact material (a takeout box, sample 4), one textile sample (upholstery, sample 51), and PTFE tape as a control. Figure 4.3B indicates the total etching depth reached a maximum of ~0.1 µm based on the etching rate from a tantalum pentoxide reference material. We estimated that the consumer products in this study were etched to a maximum of 10 µm (see Appendix C Sputtering Yield for Consumer Products section for details[136]). A single XPS measurement represents a depth of 0.01 µm, but the depth profiles shown (Figure 4.3B) are composed of >60 individual XPS measurements taken in between etching intervals.

For both products, the % F declined rapidly below the surface before stabilizing (Figure 4.3B). A relatively constant fluorine profile with depth was observed in PTFE tape (Figure 4.3B), reflecting the difference between a coating and a dense polymer. After five rounds of etching (maximum 0.75 µm estimated depth), the % F decreased by 64% in the textile (sample 51) and 77% in the food contact material (sample 4). After etching to a maximum estimated depth of 10 µm, the % F decreased by 93% in the textile and 88% in the food contact material. Depth profiles of additional samples also show decreasing % F with depth (Figure C1). The C 1s spectra displayed a peak at ~292 eV (CF_2 group) at the beginning of the depth profile for sample 51 but not at ~7.5 µm estimated depth where fluorine is detected in small amounts (<5% F) (Figure 4.3B). Three different samples from the same food contact material (sample 4) were subjected to XPS depth profiling to demonstrate reproducibility (Figure C2). XPS depth-profiling

indicates that fluorine is not homogeneously distributed throughout the material and can be heavily concentrated in the near surface (e.g., fluorocarbon coatings).

4.4.5 XPS LC-MS/MS COMPARISON

XPS and LC-MS/MS results were converted to weight percent for comparison (see Appendix C for calculation). The LC-MS/MS results were scaled from the original sample thickness to 0.01 μm for direct comparison to XPS. Scaling the thickness to 0.01 μm provides an upper bound weight percent value for LC-MS/MS since the extraction process likely extracts fluorine from deeper than 0.01 μm (Figure 4.3B).

A maximum of 53% of the fluorine was accounted for using the targeted LC-MS/MS approach based on samples that had detectable fluorine using both LC-MS/MS and XPS (Figure C3). In 7 out of the 11 samples, LC-MS/MS measurements accounted for <1% of the fluorine, indicating that the vast majority remains unmeasured. We did not find a correlation between LC-MS/MS and XPS fluorine (Figure C4), similar to the results reported by PIGE analysis.[20] LC-MS/MS only measures the selected methanol-extractable ionic PFAS fraction, whereas XPS measures the total fluorine content of the material interface, which includes any fluoropolymers or fluoromonomers.

The XPS detection limit is ~1 atomic % (~1.6 wt % F assuming the rest of the material is carbon). LC-MS/MS can detect much lower concentrations, ~4 x 10^{-5} wt % F for PFOA (assuming a representative detection limit of 1 ng g^{-1}, a 1 g sample and the average thickness of 0.055 cm from samples in Figure C3). Therefore, while LC-MS/MS does not capture a large fraction of the fluorine, it does have a significantly lower detection limit. XPS and LC-MS/MS are thus complementary techniques that together provide a more holistic approach to fluorine analysis in consumer products.

We screened for a total of 109 negative and 57 positive PFAS compounds by using LC-QTOF-MS analysis to identify PFASs that contribute to the % F measured using XPS that were not detected using LC-MS/MS. Across all samples, 42 PFASs were detected with LC-QTOF-MS, and 50% were PFAS compounds measured with LC-MS/MS (Table C8). Therefore, it is unlikely that quantitative LC-QTOF-MS analysis of these compounds will close the mass balance between XPS and measured PFAS compounds. Volatile and precursors compounds measured with the total oxidizable precursor assay[17, 77] have also been shown to represent a small fraction of the total fluorine in consumer products.[20] Most research institutions lack the specialized equipment to conduct such investigations. Thus, we propose that widely available analytical techniques such as XPS are useful for screening for total fluorine in the surface of samples.

4.4.6 DISCUSSION

PFASs are often applied as surface coatings to products,[18] which is the component in contact with the surrounding environment. However, the surface-specific (≤ 0.1 μm)[130] fluorine content of consumer products has not previously been characterized. We characterized the total fluorine content in the true surface (0.01 μm) of 45 consumer products using XPS. We find that the surface of the consumer products measured here contain up to 45% F and that fluorine is persistent in the consumer products based on methanol extractions, indicating the potential for long-term environmental impacts.

To the best of our knowledge, PIGE is the only other analytical technique that has been used to determine the presence of total fluorine in consumer products. Both XPS and PIGE could be used to screen products for fluorine content. However, there are important differences between the two techniques. XPS is a surface-specific (0.01 μm) technique that can discern the

71

presence and depth distribution of organic fluorine. PIGE measures the bulk material (100-250 μm) and cannot distinguish between inorganic and organic fluorine and cannot provide depth resolution. XPS systems are commonly available at research universities and could thus be widely leveraged for fluorine analyses. Future work is needed to investigate whether there is a link between surficial fluorine (XPS measurements) and human exposure. We conclude that XPS provides a powerful new method for quantification of % F in the surface of consumer products.

4.5 ACKNOWLEDGMENTS

Chapter 5

SUMMARY AND FUTURE DIRECTIONS

Chapters 2 and 3 present a detailed study of the fate and transport of PFASs at the Cape Cod field site and find:

1. The unsaturated zones beneath the fire training area and wastewater infiltration beds act as long-term PFAS sources to groundwater over several decades, despite the mobility of PFASs in the aqueous phase. This suggests that the source zones must be remediated before groundwater aquifers can recover from the contamination.

2. The shallow groundwaters beneath the fire training areas and wastewater infiltration bed unsaturated zones are compositionally distinct, indicating that "fingerprinting" sources is feasible for source identification. We further show that there is evidence of differential transport dependent on chain length and head group, which previously had only been shown in the laboratory.

3. Some precursor compounds (or intermediates) have been demonstrated to be mobile at this field site, contrary to assumptions that precursors are less mobile than terminal perfluoroalkyl acids.

4. Precursor compounds are not only mobile, but transport across groundwater and surface water bodies and remain persistent even under oxygenated, photoactive conditions and during transport through biologically active layers.

5. Interaction with a surface water body can expand a narrow groundwater plume into a larger, more dilute plume that may be more difficult to remediate (high volume, low concentration).

6. Functional group-specific interactions are likely responsible for sorption and release on the downgradient side of the studied surface water body and may be the cause of observed pulses of high and low concentrations in the groundwater.

7. Sorption to the air-water interface may have significant impacts on shallow groundwater located near the unsaturated zone and near surface water bodies.

The work presented here demonstrates the importance of large-scale, field-based studies. There are fundamental differences between laboratory-based, controlled studies and the complicated hydrogeochemical conditions encountered in the environment, requiring a balance of both laboratory and field-based approaches. While groundwater wells are expensive to drill, future work should be undertaken at study sites with different geology and hydrology than that of Cape Cod to broaden the scope of understanding.

In Chapters 2 and 3 precursors were shown to be an important PFAS constituent in water that must be taken under consideration when evaluating human health risk. As humans are exposed to precursors from consumer products as well, a method to measure total organic fluorine in consumer products was expanded upon in Chapter 4 and demonstrates:

1. XPS is a reliable tool to measure the percent fluorine in the upper 0.01 μm of consumer products and provides an efficient approach to characterizing the total organic fluorine.

2. Depth profiling provides information on the fluorine distribution in products and is able to discern the difference between fluoropolymers and fluorinated coatings.

3. Binding energies can provide confirmation of the presence of CF_2 and CF_3 groups, which define a PFAS molecule.

4. PFASs released in methanol extracts and quantified using traditional LC-MS/MS typically accounted for <1% of the fluorine measured with XPS in consumer products, demonstrating the need for alternative measurement techniques.

All chapters of this work emphasize the importance of a holistic approach to examining PFASs in natural and engineered environments. The continuous shifts in manufacturing compounded with a wide variety of stability, mobility, and transformation rates between compounds requires a complex mixture of field and laboratory studies, and alternative measurement techniques. Exciting future work could focus on fate, transport, and health outcomes using a comprehensive total-organic-fluorine approach that does not rely on quantification of thousands of individual structures. Specifically, it is unknown whether information on the bulk transport of organic fluorine may provide broad insights to help tackle the widespread issue of PFAS contamination.

Appendix A

SUPPLEMENTARY INFORMATION FOR CHAPTER 2

A.1   METHODS

A.1.1   GROUNDWATER AND AQUIFER SEDIMENT SAMPLING

Groundwater samples[68] were collected from monitoring well clusters, multilevel samplers (MLSs),[65, 137] and continuous multichannel tubing wells (CMTs). The monitoring wells consist of 5-cm-diameter PVC casing with 0.9-m-long slotted screens installed at various depths. A Keck SP-81 (Geotech, Denver, CO) submersible pump with an isolation packer and polyethylene discharge tubing was used to collect groundwater samples from monitoring wells. Three well volumes below the isolation packer were purged before sample collection. Each MLS consists of 5-cm-diameter PVC casing with multiple sampling ports located at different depths (0.74 to 4.86 m spacing), allowing detailed vertical profiles to be sampled. Polyethylene tubing (6.4-mm-diameter) extends from each port through the casing to land surface. The CMTs consist of 4.3-cm-diameter polyethylene tubing segmented into 7 discrete channels that are open to various depths (Solinst Canada Ltd., Georgetown, ON). The MLS ports and CMTs were sampled with a GeoPump2 (Geotech, Denver, CO) peristaltic pump and Norprene pump-head tubing after purging three volumes from the MLS tubing or CMT channel. Unfiltered water samples were collected in high density polyethylene (HDPE) or low density polyethylene (LDPE) bottles that were prewashed with methanol and deionized (DI)-water and then rinsed with groundwater from the sample site. The groundwater sampling procedure was quality controlled by pumping DI water through the pumps and tubing to investigate background PFAS contamination. No PFASs were observed above the detection limit.

Sediment cores were collected with a 5-cm-diameter wireline piston core barrel[138] fitted with cellulose acetate butyrate liners and plastic catcher baskets. Cores were sealed with polyethylene caps and electrical tape and were stored at 4 ˚C until analysis. A total of 4 cores were collected at various depths for this study: one near site S425 and three near site S469. See Table A2 for sediment core depths.[68]

A.1.2   ANALYTICAL MATERIALS

Liquid chromatography-mass spectrometry grade methanol (J.T. Baker, Center Valley, PA) and reagent grade sodium hydroxide (Macron Fine Chemicals™, Center Valley, PA) were used. Reagent grade formic acid, ammonium acetate, potassium persulfate, acetic acid, and ammonium hydroxide were obtained from VWR (Radnor, PA) or Sigma Aldrich (St. Louis, MO). Oasis WAX solid phase extraction (SPE) cartridges (6 mL, 150 mg sorbent, 30-μm particle size) were purchased from Waters (Milford, MA) for offline SPE.

A.1.3   SAMPLE ANALYSIS

Groundwater samples were shaken thoroughly and subsampled 5-10 cm below the surface. Sample aliquots (generally 750 μL unless further dilution with DI water was needed), methanol (720 μL), and internal standards (30 μL of a 10 ng/mL solution) were combined in a 1.7 mL polypropylene microcentrifuge tube, vortexed, and centrifuged at 13000 rpm for 20 min in a Heraeus Pico Biofuge (Hanau, Germany), and the supernatant was transferred to a 2-mL polypropylene autosampler vial. Laboratory DI water blanks and the calibration curve were treated the same as samples.

A.1.4   LC-MS/MS CONDITIONS

Separation of the individual PFASs was completed with an Agilent (Santa Clara, CA) 6460 triple quadrupole LC-MS/MS equipped with a Poroshell 120 EC-C18 column (Santa Clara, CA) using mobile phases of 2 mM ammonium acetate in water (A) and 2 mM ammonium acetate in methanol (B) at a flow rate of 0.5 mL min^{-1}. Online SPE was performed for all samples with an Agilent (Santa Clara, CA) 1290 Infinity Flexible Cube using 0.1% aqueous formic acid and 100% methanol mobile phases. The online SPE flow rate was 1 mL min^{-1} and the SPE cartridge was first flushed with 0.1% aqueous formic acid for 0.75 min to load the 300 μL sample onto the cartridge before eluting with the non-SPE mobile phase gradient. The sample was then transferred with mobile phases A and B to the column. To reduce background contamination, all PTFE frits were removed and the majority of the polymer tubing was replaced with stainless steel. Mobile phase filters were removed and an inline reverse phase column (Agilent ZORBAX Eclipse Plus C18) was installed after the pump head to prevent contamination from the aqueous mobile phase. Initial gradient conditions were 97% A and 3% B. From 0.85 to 7.5 min the gradient was linearly increased to 61% B. The gradient was held at 61% B from 7.5 to 8.5 min and then linearly ramped to 100% B at 11.7 min and maintained until the end of the run (14.3 min). Sample was delivered to the triple quadrupole MS/MS, where it was ionized and desolvated using Electrospray Ionization (ESI). The column was operated at a temperature of 55 °C and the source gas temperature was 300 °C with a nebulizer pressure of 45 psi. Table A1 includes the LC-MS/MS parameters.

Similar to a previous study,[17] limits of detection (LOD) were calculated as the average concentration at which the sample signal:noise ratio was 3. The method detection limit (MDL) was twice the calculated LOD because samples were typically analyzed with a dilution factor of 2. The 9-point calibration curve for all samples ranged from 1 to 1200 ng L^{-1}, with the exception of precursor oxidation samples, which had a range from 2.5 to 3600 ng L^{-1}. A typical sample run

included a calibration curve, followed by two blanks (50:50 water:methanol) and then a repeated sequence of six samples and two blanks. One to two samples of the calibration curve were included later in the sample runs as quality control.

A.1.5   TOTAL OXIDIZABLE PRECURSOR ASSAY SAMPLE ANALYSIS

The total oxidizable precursor assay[17] was completed for 46 samples and duplicated for 30% of the samples (Table A4). See the manuscript for a description of the total oxidizable precursor assay procedures. For sample analysis following oxidation, a previously developed method was followed for offline SPE, with some slight modifications.[110] Briefly, the Oasis WAX SPE cartridges were conditioned with ~5 mL of 0.5% ammonium hydroxide in methanol, followed by ~5 mL of methanol and ~5 mL of DI water. Then the 6 mL post-oxidation sample was spiked with internal standards and passed through the cartridge, followed by ~5 mL of 25 mM ammonium acetate in DI water. The PFASs were eluted with ~5 mL of 0.5% ammonium hydroxide in methanol, the extracts were blown down with nitrogen to a final volume of 0.75 mL, and 0.75 mL of DI water was added. Samples were then shaken, diluted as needed, and transferred to 1.7 mL polypropylene microcentrifuge tubes and centrifuged at 13000 rpm for 20 min. The supernatant was transferred to autosampler vials for LC-MS/MS analysis as described above.

The changes in perfluorinated carboxylate concentrations after precursor oxidation are given in Table A4. Recoveries ± standard deviation of PFBS, PFHxS, and PFOS after oxidation were 130±30%, 98±13% and 110±20%, respectively, for samples with a detected concentration before and after oxidation. The average loss of 6:2 FtS after oxidation was 95±3.5% when two outliers with initial concentrations of <10 ng L^{-1} were removed. The average loss of 8:2 FtS after

oxidation was 97±1.9% when one outlier was removed. Quantification of FOSA was difficult due to substantial loss (sorption) of the internal standard throughout the procedure. MDLs were half the calculated LOD because of SPE concentration of 3 mL groundwater to a final volume of 1.5 mL.

A.1.6 SEDIMENT ORGANIC CARBON AND MINERALOGY

Total sediment organic carbon (TOC) analysis was completed with a Shimadzu Total Organic Carbon Analyzer as described elsewhere.[79] The TOC results are summarized in Table A2 and are the average of 3 subsamples.

Mineralogical identification was completed using X-ray diffraction (XRD) and the RockJock program.[139] A 1 ± 0.0005 g representative subsample of each dried sediment core was weighed out and 0.25 ± 0.0005 g corundum was added to each sediment sample as an internal standard before grinding the mixture in a micronizing mill for 5 min with 5 mL of ethanol and yttrium-doped zirconium beads. The ground sediment/corundum mixture was dried overnight at 60 ˚C, transferred to plastic bottles with 3 large nylon beads along with ~400 µl of Vertrel solvent (Wilmington, DE), placed in a mixer for 10 min, and sieved with a 250 µm sieve. Finally, samples were packed into an XRD holder through a slit using tamping and a glass plate to ensure a flat, uniform surface when exposed to the x-ray beam. All samples had no visual cracks or surface texture before XRD analysis. Each sample was run from 5 ˚ to 65 ˚ two theta in 0.02 ˚ intervals on a Siemens D500 XRD (Munich, Germany) and analyzed with the RockJock program. Results are shown in Table A3.

A.1.7 PARTITIONING EXPERIMENTS

Subsamples of sediment and pore water from each core were analyzed for PFASs. Wet sediment (46 to 62 g) was placed in 50 mL polypropylene tubes and centrifuged at 4000 rpm for 20 min. The supernatant (pore water) was removed and centrifuged at 13000 rpm for 20 min before samples were prepared for LC-MS/MS analysis as described above and in the manuscript. The sediment was air dried, heated to 60 ˚C for 48 hr, sieved to <2.36 mm, and homogenized. The sediment extraction method was modified from previous studies[17, 78] and involved placing a 3 g subsample into a 15 mL polypropylene tube along with 6 mL of 0.1% ammonium hydroxide in methanol. The tubes were vortexed (20 sec), sonicated (30 min), placed on a rotating table for 2 hr, centrifuged at 4000 rpm for 20 min, and the supernatant was placed in a new 15 mL polypropylene centrifuge tube.[17] This process was repeated three times for complete PFAS extraction.[17] The extract was dried under flowing nitrogen before adding 1.5 mL of 0.1% acetic acid in methanol followed by vortexing briefly and then heating at 50 ˚C for 30 min.[17] The extracts were then transferred to 1.7 mL polypropylene microcentrifuge tubes and centrifuged at 13000 rpm for 20 min before samples were prepared for LC-MS/MS analysis as described above and in the manuscript.

The sediment/water distribution coefficient (K_d) was calculated as follows:

$$K_d = \frac{C_s}{C_w} \tag{1}$$

where C_s is the concentration on the sediment (μg kg^{-1}) and C_w is the concentration in the aqueous phase (μg L^{-1}).

The K_d data can be normalized to the sediment organic carbon content (K_{oc}) by:

$$K_{oc} = \frac{K_d}{f_{oc}} \tag{2}$$

where f_{oc} is the fraction of organic carbon.

The *in situ* K_{oc} values for PFASs are presented in Table A2.[68] K_{oc} values were not reported if the PFAS concentrations were below the MDL or if negative results were obtained when subtracting residual pore water concentrations from sediment concentrations. Note that the low TOC values may impact the accuracy of K_{oc} results.

A.1.8   ADVECTIVE TRANSPORT CALCULATIONS

The following analysis illustrates the range in uncertainty associated with estimation of travel times through the unsaturated zone and saturated zones along the PFAS transport path.

Estimated travel time through the saturated zone:

PFOS K_d = 0.45 L/Kg (log K_{oc} = 3.37, f_{oc} = ~0.00019)
Porosity (n) = 0.39 reference [64]
Groundwater velocity (v) = 0.42 m d^{-1} reference [64]
Bulk density (ρ_b) = 1.64 g/cm^3 reference [113]
Retardation factor (R):

$$R = 1 + K_d * \frac{\rho_b}{n} = 2.87$$

Time to travel x meters:

$$t = \frac{x * R}{v}$$

Time to travel 780 m through the saturated zone: **5336 days, 15 years**

Estimated travel time through the unsaturated zone:

If the source loading at land surface began in 1970 and the time to travel 780 m from the source through the saturated zone is 15 years (see above), then the travel time from land surface to the water table through the unsaturated zone is estimated to be:

(2015 – 1970) = 45 years -15 years = 30 years

Using the same logic, if the source loading instead began in 1997:

$$(2015 - 1997) = 18 \text{ years } -15 \text{ years} = 3 \text{ years}$$

Assuming more conservative values for porosity and groundwater velocity, n = 0.3 and v = 0.30 m d^{-1}, the retardation factor and estimated travel time through the saturated zone are as follows:

$$R = 1 + \text{K}_d * \frac{\rho_b}{n} = 3.43$$

Time to travel 780 m through the unsaturated zone: **8931 days, 24 years**

The estimated time to travel from land surface to the water table through the unsaturated zone would then be:

$$\text{Source began in 1970: } (2015 - 1970) = 45 \text{ years} - 24 \text{ years} = 21 \text{ years}$$

A.2 TABLES

Table A1. Tandem mass spectrometry parameters for poly- and perfluoroalkyl substances measured in this study. All compounds were measured in negative ion mode. The MS-MS analytical parameters were slightly different for data collected in 2014. Differences include a lack of precursors in sample analysis and one less qualifier ion (represented as Q in the table) for PFHpA, PFHxS, PFNA, and PFUnDA

Analyte	Type	Internal Standard	Precursor Ion Mass	Product Ion Mass	Fragmentor Voltage (V)	Collision Energy (V)
Perfluorinated Carboxylates						
PFBA	Target	[$^{13}C_4$] PFBA	213	169	60	2
PFPeA	Target	[$^{13}C_2$] PFHxA	263	219	60	2
PFHxA	Target	[$^{13}C_2$] PFHxA	313	269	61	2
PFHxA (Q1)				119		2
PFHpA	Target	[$^{13}C_2$] PFHxA	363	319	71	2
PFHpA (Q1)				169		8
PFHpA (Q2)				119		8
PFOA	Target	[$^{13}C_4$] PFOA	413	369	86	2
PFOA (Q1)				169		8
PFNA	Target	[$^{13}C_5$] PFNA	463	419	66	2
PFNA (Q1)				219		12
PFNA (Q2)				169		12
PFDA	Target	[$^{13}C_2$] PFDA	513	469	92	2
PFDA (Q1)				269		2
PFUnDA	Target	[$^{13}C_2$] PFUnDA	563	519	87	5
PFUnDA (Q1)				269		5
PFUnDA (Q2)				169		21
PFDoDA	Target	[$^{13}C_2$] PFDoDA	613	569	92	5
PFDoDA (Q1)				169		25

Table A1 (Continued)

Analyte	Type	Internal Standard	Precursor Ion Mass	Product Ion Mass	Fragmentor Voltage (V)	Collision Energy (V)
Perfluorinated Sulfonates						
PFBS	Target	[$^{18}O_2$] PFHxS	299	80	138	40
PFBS (Q1)				99		24
PFHxS	Target	[$^{18}O_2$] PFHxS	399	80	179	44
PFHxS (Q1)				119		40
PFHxS (Q2)				99		40
PFOS	Target	[$^{13}C_4$] PFOS	499	80	210	55
PFOS (Q1)				99		55
PFDS	Target	[$^{13}C_4$] PFOS	599	80	200	94
PFDS (Q1)				99		94
Fluorotelomer Sulfonates						
6:2 FtS	Target	[$^{13}C_2$] 6:2 FtS	427	407	140	25
6:2 FtS (Q1)				80		35
8:2 FtS	Target	[$^{13}C_2$] 6:2 FtS	527	507	140	30
8:2 FtS (Q1)				80		40
Perfluoroalkyl Sulfonamides						
FOSA	Target	[$^{13}C_8$] FOSA	498	78	180	40
Internal Standards						
[$^{13}C_4$] PFBA	ISTD		217	172	60	2
[$^{13}C_2$] PFHxA	ISTD		315	270	66	2
[$^{13}C_4$] PFOA	ISTD		417	372	91	2
[$^{13}C_5$] PFNA	ISTD		468	423	76	2
[$^{13}C_2$] PFDA	ISTD		515	470	92	2
[$^{13}C_2$] PFUnDA	ISTD		565	520	87	5
[$^{13}C_2$] PFDoDA	ISTD		615	570	97	5
[$^{18}O_2$] PFHxS	ISTD		403	103	184	44
[$^{13}C_4$] PFOS	ISTD		503	80	205	55
[$^{13}C_2$] 6:2 FtS	ISTD		429	81	140	25
[$^{13}C_8$] FOSA	ISTD		506	78	150	50

Table A2. Total sediment organic carbon (TOC) and carbon normalized sediment/water distribution coefficients (K_{oc}) for Cape Cod aquifer sediments. Sediment core depths (in meters below land surface) are given in parentheses. K_{oc} values were not reported if the PFAS concentrations were below the MDL or if negative results were obtained when subtracting residual pore water concentrations from sediment concentrations.

Sample	TOC (fraction)	Log K_{oc} (L/kg)															
		PFBA	PFPeA	PFHxA	PFHpA	PFOA	PFNA	PFDA	PFUnDA	PFDoDA	PFBS	PFHxS	PFOS	PFDS	6:2 FtS	8:2 FtS	FOSA
S425_1 (17.7-18.1 m)	0.0003					1.96							3.33		2.16	3.70	
S425_2 (17.7-18.1 m)	0.0003												2.89			3.08	
S469_1 (6.6-6.9 m)	0.00015		1.63	2.44	2.70	3.33	2.83	3.37	4.37			2.21	3.44		3.54		4.86
S469_2 (6.6-6.9 m)	0.00015		2.72	2.68	2.82	2.54	2.82	3.41	4.25			2.43	3.34	3.63	3.37	4.16	
S469_1 (15.1-15.4 m)	0.00013												3.73				
S469_2 (15.1-15.4 m)	0.00013												3.69				
S469_1 (17.5-17.9 m)	0.00019												3.24		1.42		
S469_2 (17.5-17.9 m)	0.00019												3.34				
Average	**0.00019**		**2.17**	**2.56**	**2.76**	**2.61**	**2.82**	**3.39**	**4.31**			**2.32**	**3.37**	**3.63**	**2.62**	**3.65**	**4.86**
STD	**0.00007**		**0.77**	**0.17**	**0.09**	**0.69**	**0.01**	**0.02**	**0.08**			**0.15**	**0.27**		**1.01**	**0.54**	

86

Table A3. Quantitative X-ray diffraction mineralogy analysis of Cape Cod aquifer sediments collected adjacent to wells S469 and S425. All sediments were sieved to <2.36 mm for mineralogy analysis. The column for well S425 displays the average results for the 125 to 500 μm and 500 μm to 2.36 mm size fractions. Sediment core depths (in meters below land surface) reported in parentheses.

	Weight %			
	S469 (6.6-6.9 m)	**S469 (15.1-15.4 m)**	**S469 (17.5-17.9 m)**	**S425 (17.7-18.1 m)**
Quartz	98.5	94.2	94.6	92.1
Potassium feldspar (ordered microcline)	0.0	2.9	3.6	3.7
Plagioclase (albite, var. cleavelandite)	1.5	3.0	1.7	3.1
Oxides	0.0	0.0	0.0	0.9
Clays	0.0	0.0	0.0	0.2

Table A4. Increases in concentration of perfluorinated carboxylates from the total oxidizable precursor assay. Method detection limit (MDL) values refer to the detection limit during precursor analysis. The increase in concentration is the post-oxidation concentration minus the pre-oxidation concentration. Samples that were duplicated were averaged and are highlighted in bold. Samples for which both pre- and post-oxidation values were below the MDL or samples for which there was a loss after oxidation were set to zero. Samples that were below the MDL before oxidation and had a measurable concentration after oxidation are reported as the concentration after oxidation.

Increase in Concentration (ng L^{-1})

	PFBA	PFPeA	PFHxA	PFHpA	PFOA	PFNA
Minimum MDL	**15**	**3**	**4**	**2**	**5**	**3**
Maximum MDL	**58**	**9**	**9**	**4**	**10**	**7**
Site Name						
MA-SDW 425-0063	2527	1868	5057	0	0	138
MA-SDW 425-0068	24	34	402	50	74	6
MA-SDW 488-0063	1767	1147	4380	167	0	0
MA-SDW 488-0084	4074	6287	10427	455	0	0
MA-SDW 569-M01-CMT01	1032	1392	3595	134	246	0
MA-SDW 569-M01-CMT02	785	731	2710	46	0	0
MA-SDW 569-M01-CMT03	1159	1288	7820	156	10	31
MA-SDW 473-M01-01PT	18	12	15	1	0	0
MA-SDW 473-M01-02GNT	33	17	68	11	10	0
MA-SDW 473-M01-03RT	0	30	260	12	7	0
MA-SDW 473-M01-04BUT	120	126	801	14	4	5
MA-SDW 473-M01-05BKT	209	172	1012	35	0	0
MA-SDW 473-M01-06WT	268	279	2130	87	0	0
MA-SDW 473-M01-07O	120	123	324	60	93	20
MA-SDW 436-M01-01PT	118	277	228	46	68	0
MA-SDW 436-M01-03RT	36	39	67	16	48	1
MA-SDW 436-M01-05BKT	108	85	685	17	21	0
MA-SDW 436-M01-07O	330	279	1679	75	26	0
MA-SDW 469-M01-01PT	109	213	210	105	109	5
MA-SDW 469-M01-02GNT	46	108	93	18	11	0
MA-SDW 469-M01-03RT	38	96	52	24	13	1
MA-SDW 469-M01-04BUT	50	50	47	22	26	0
MA-SDW 469-M01-05BKT	43	52	128	12	11	0

Table A4 (Continued)

Increase in Concentration (ng L^{-1})

	PFBA	PFPeA	PFHxA	PFHpA	PFOA	PFNA
MA-SDW 469-M01-06WT	122	89	292	17	24	0
MA-SDW 469-M01-07O	306	221	1142	21	15	19
MA-SDW 469-M01-08GY	378	507	1990	31	0	23
MA-SDW 469-M01-09Y	71	52	70	1	7	5
MA-FSW 586-0058	33	76	85	14	26	0
MA-FSW 586-0068	140	201	236	23	42	21
MA-FSW 586-0078	2407	1955	6320	251	114	0
MA-FSW 586-0088	1545	2115	5064	200	0	8
MA-FSW 586-0098	731	969	2033	42	0	0
MA-FSW 586-0113	30	18	57	7	0	0
MA-FSW 575-M01-01PT	123	104	326	26	28	8
MA-FSW 575-M01-05BKT	19	14	42	6	2	0
MA-FSW 575-M02-01PT	0	21	14	7	5	3
MA-FSW 575-M02-05BKT	30	45	104	13	21	0
MA-FSW 575-M02-09Y	92	118	144	37	16	0
MA-FSW 575-M02-13BU	361	400	763	57	161	1
MA-FSW 424-M02-04BUT	0	19	9	10	110	10
MA-FSW 424-M02-06WT	32	4	21	11	18	0
MA-FSW 424-M02-08GY	49	29	57	23	31	0
MA-FSW 424-M02-10P	34	60	62	7	17	0
MA-FSW 424-M02-12R	59	86	111	4	23	0
MA-FSW 424-M02-14BK	104	148	241	37	444	0
MA-FSW 424-M01-01PT	99	73	234	5	24	0
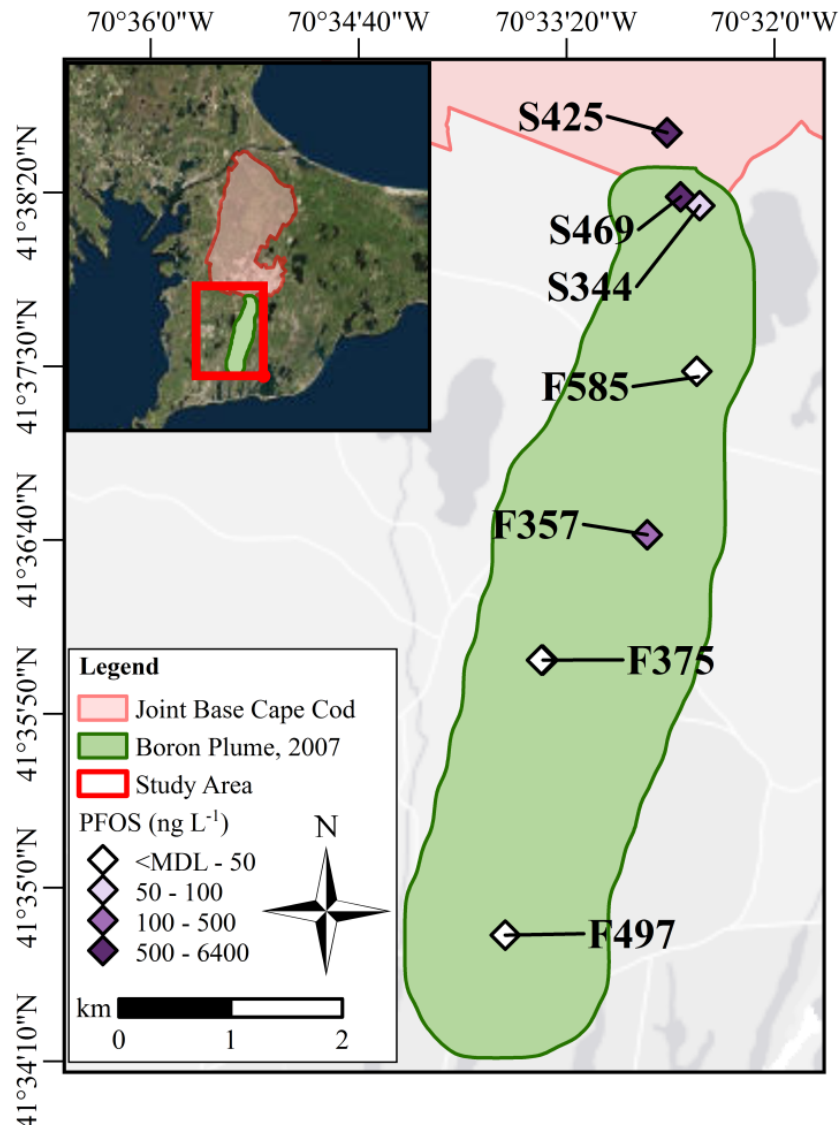
Figure A1. Results for perfluorooctane sulfonate (PFOS) analysis of groundwater samples collected from the Cape Cod well network during June 2014. Shading of symbols corresponds to the maximum PFOS concentration detected at each well. Boron plume extent from Barbaro et al.[50]
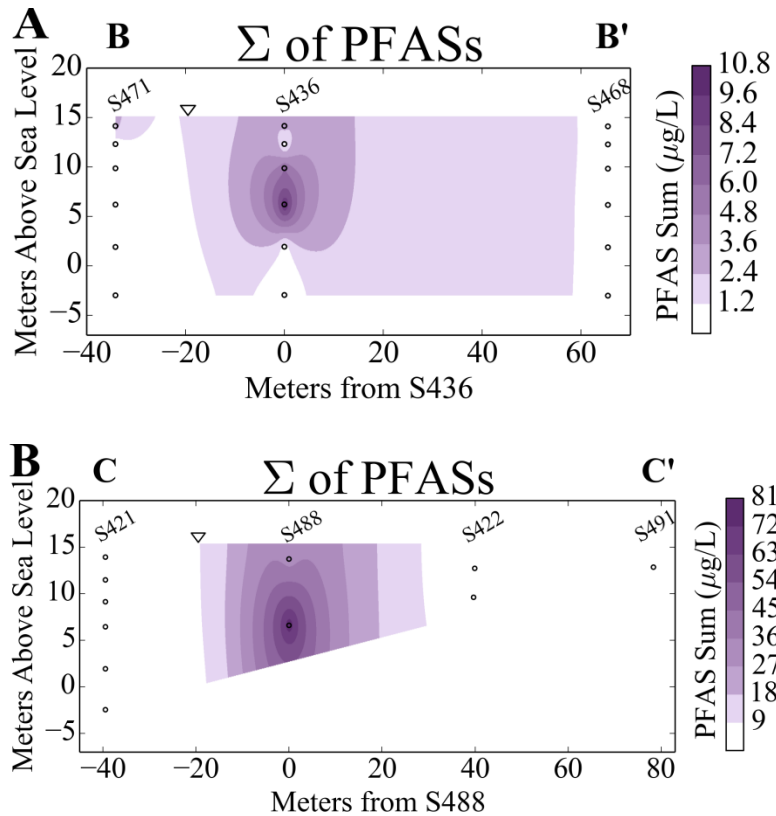
Figure A2. The sum of all poly- and perfluoroalkyl substances (PFASs) in transverse cross sections: (A) B-B' (max = 10.3 μg L^{-1}) and (B) C-C' (max = 81.0 μg L^{-1}). Concentrations are colored according to a linear scale. Circles indicate sampling locations. The inverted triangle indicates the water table.
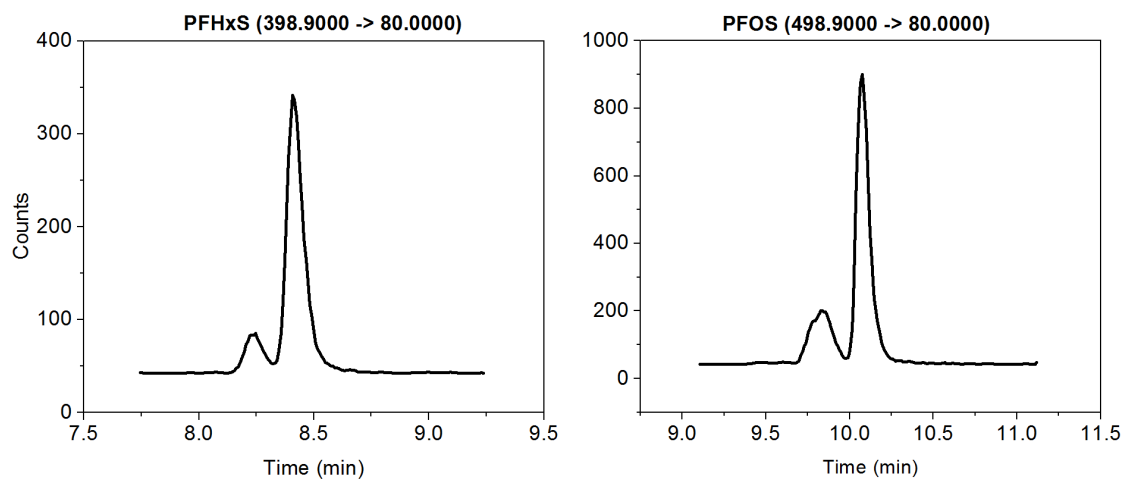
Figure A3. Example liquid chromatography-tandem mass spectrometry (LC-MS/MS) chromatogram of branched and linear perfluorohexane sulfonate (PFHxS) and perfluorooctane sulfonate (PFOS) isomers in a groundwater sample collected from well S469-M01-07. Branched isomers are characteristic of production with the electrochemical fluorination technique, where fluorine replaces hydrogen atoms in the starting compound and results in branched and linear isomers in addition to by-products.[140, 141] Generally the branched isomers (such as monomethyl- and dimethyl-branched isomers) elute more quickly with LC-MS/MS as shown above by the smaller peak that elutes before the larger linear peak.[140] Here, the branched isomers are eluted as a single peak.
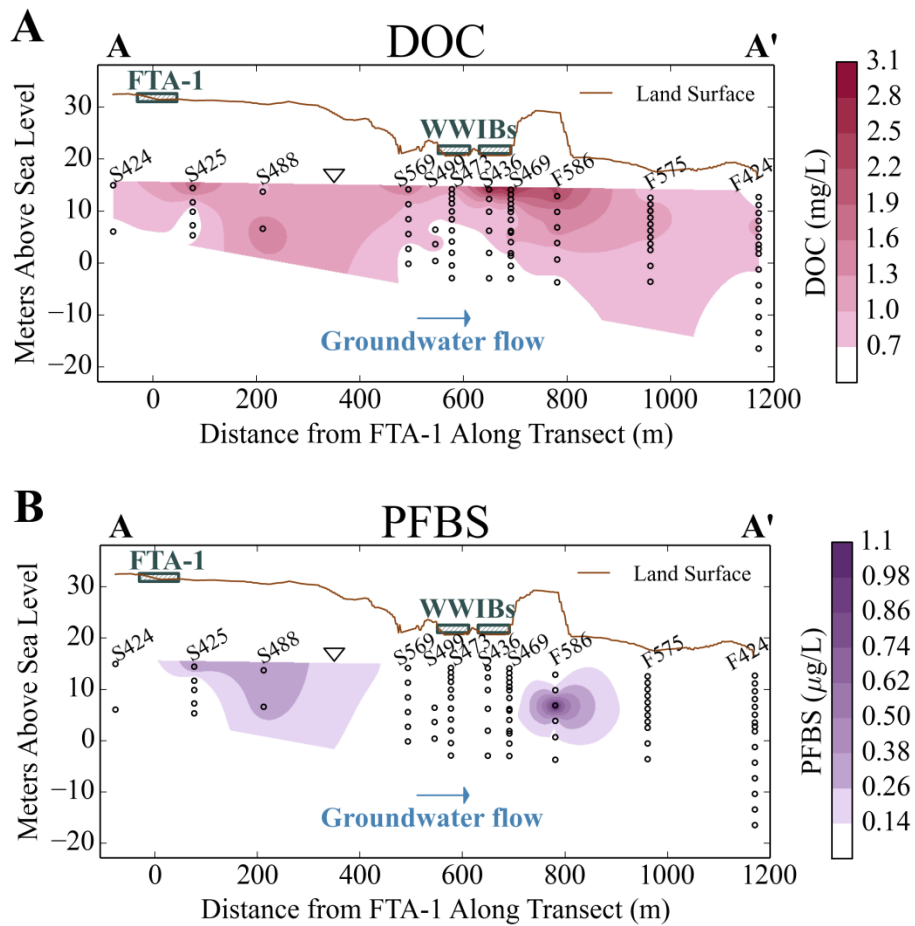
Figure A4. (A) Dissolved organic carbon (DOC) concentrations (max = 3.1 mg L^{-1}) and (B) perfluorobutane sulfonate (PFBS) concentrations (max = 1.1 μg L^{-1}) within the A-A' transect. FTA-1 refers to the fire training area and WWIBs refers to the wastewater infiltration beds. Circles indicate sampling locations. The inverted triangles indicate the water table.
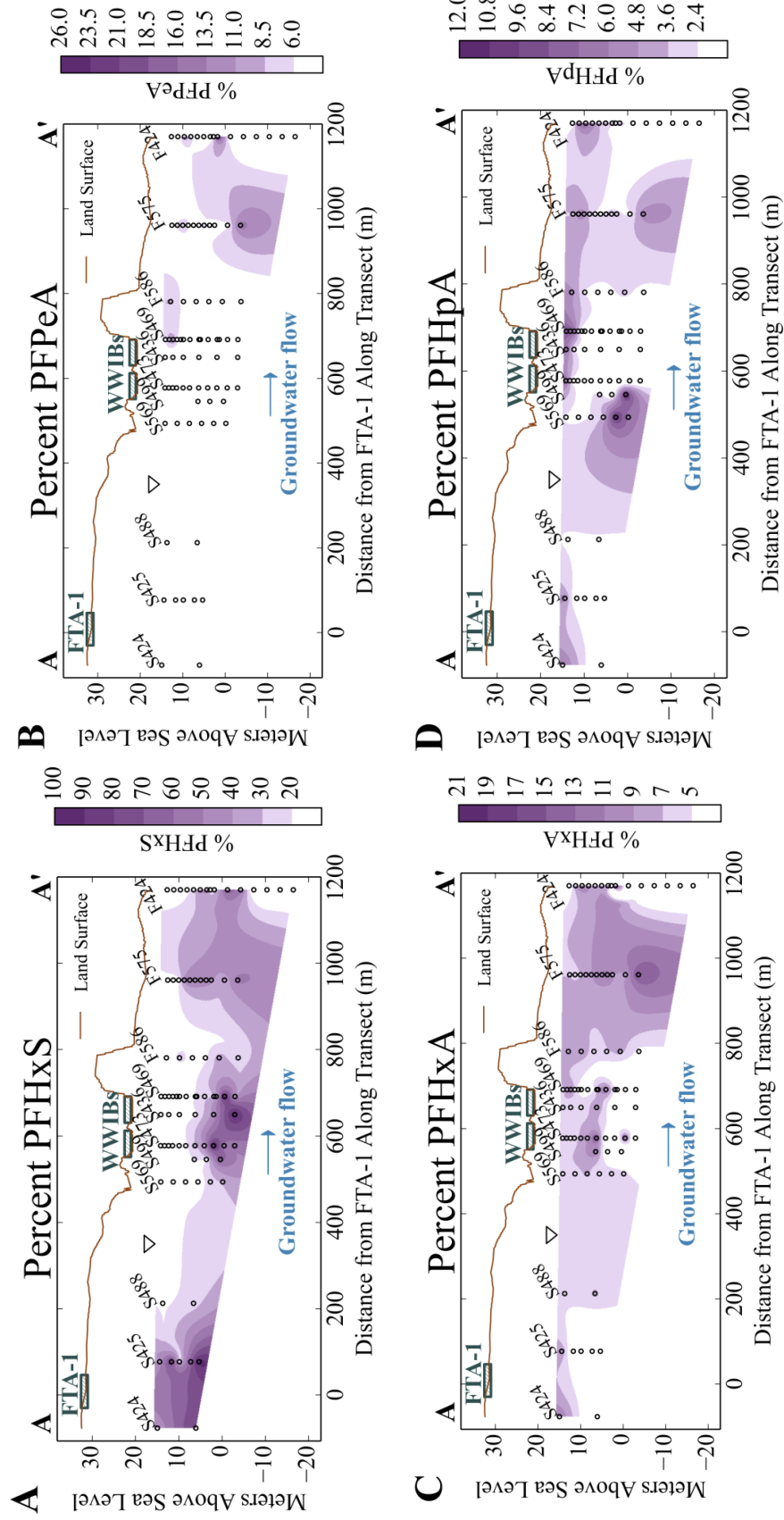
Figure A5. The molar percentages (relative to total measured poly- and perfluoroalkyl substances) of (A) perfluorohexane sulfonate, PFHxS (max = 100%), (B) perfluoropentanoate, PFPeA (max = 25%), (C) perfluorohexanoate, PFHxA (max = 20%), and (D) perfluoroheptanoate, PFHpA (max = 12%). FTA-1 refers to the fire training area and WWIBs refers to the wastewater infiltration beds. Circles indicate sampling locations. The inverted triangles indicate the water table.

Appendix B

SUPPLEMENTARY INFORMATION FOR CHAPTER 3

B.1   METHODS

B.1.1   SAMPLING PROCEDURES

Samples from the Quashnet River were collected and included in analysis, but are not discussed in the thesis, as the focus of the manuscript was on Ashumet Pond. River thalweg and river bank porewater samples were collected using screened stainless steel pushpoint samplers attached to a GeoPump2 (Geotech, Denver, CO) peristaltic pump outfitted with Norprene tubing after purging three times the tubing volume. River samples were collected using a polyethylene syringe with attached Norprene tubing. All types of river samples were collected in 60 mL LDPE bottles and stored at 4 °C until analysis.

B.1.2   LC-MS/MS ANALYSIS

LC-MS/MS analysis was conducted as described previously,[15] with minor modifications outlined here. The gradient was modified to encompass additional compounds. Initial conditions were 97% 2 mM ammonium acetate in water (A) and 3% mM ammonium acetate in methanol (B). From 0.85 to 3.5 minutes the gradient was linearly increased to 54% B. From 3.5 to 16 minutes the gradient was linearly increased to 85% B and then from 16 to 16.5 minutes the

gradient was linearly increased to 100% B and maintained until the end of the run (17.5 min). The column temperature was 50 °C. Mass spectrometry parameters are detailed in Table B3.

B.1.3   QUALITY ASSURANCE AND QUALITY CONTROL.

DI SPE blanks for non-oxidized water analysis were <MQL for all compounds, except for PFBA and one low-level (0.55 ng L^{-1}) detection of FOSA. PFBA was blank corrected using the average quantified concentrations of the SPE DI blanks. All field equipment blanks were below the MQL. Average spike recoveries (75 ng L^{-1} sample matrix spike, 7.5 ng L^{-1} DI water spike, 75 ng L^{-1} DI water spike, and 750 ng L^{-1} DI water spike) ranged from 85% to 125%. The relative percent difference (RPD) was <15% for SPE environmental sample duplicates and <30% for field duplicates for compounds with concentrations over the MQL. The compound 6:2 FtS was removed from sample consideration due to occasional blank contamination.

TOP samples were blank corrected using the average quantified concentration of the oxidation blanks for compounds that had more than 1 instance of blank contamination (PFBA and PFHpA). TOP spike recoveries were between 57.8% and 147% for DI water spikes (7.5 ng L^{-1}, 75 ng L^{-1}, and 750 ng L^{-1} spike) and 75 ng L^{-1} sample matrix spikes (Table B6). The average RPD for TOP environmental sample SPE duplicates was <11% for compounds with concentrations over the MQL. Consistent with other work using the total oxidizable precursor assay,[15, 17, 77, 89] PFSA production from oxidation was minimal, and therefore only PFCAs will be included in precursor concentration calculations.

To ensure precursors were degraded during the oxidation experiments, a groundwater sample and a lake water sample were spiked in triplicate with 3 ng of 6:2 FtS, 8:2 FtS, N-MeFOSAA, N-EtFOSAA, and FOSA. Precursor concentrations were all reduced by >99%.

Average ± relative standard deviation recoveries calculated from $n = 4$ to $n = 8$ carboxylates were 96.3 ± 4.18%.

B.1.4   SEDIMENT METAL ANALYSIS.

A total of 5 g of dried sediments (prepared as described in the manuscript) were weighed out into 50 mL polypropylene centrifuge tubes and extracted with 40 mL 0.5 M HCl for 3 days.[142, 143] The extracts were then centrifuged at 4000 rpm for 10 minutes, and the supernatant was filtered with a 0.45 μm PVDF filter and analysis was completed with a Thermo iCAP Q (Waltham, MA) inductively coupled plasma mass spectrometer (ICPMS) after diluting samples 1:20 (all analytes except Fe and Mn) or 1:400 (Fe and Mn). Internal standards were Sc, Y, and Tb.

B.1.5   MICROLAYER ENRICHMENT THEORETICAL CALCULATION

The Gibb's adsorption isotherm can be used to calculate the surface enrichment expected in microlayer samples:

$$\Gamma = \frac{-1}{RT}\ \frac{\partial \gamma}{\partial \ln C} = K_i C$$

R = gas constant (erg mol^{-1} K^{-1})
T = temperature (K)
γ = surface tension (dyn cm^{-1})
C = concentration of the bulk (mol cm^{-3})
K_i = interfacial tension (cm)
Γ = surface excess (mol cm^{-2})

Parameter Values (calculation example for PFOS):

K_i values (cm^3 cm^{-2}) for different analytes (from Lyu et al.[105])

     PFOS: 0.004

PFHxA: 0.000072
PFHpA: 0.00026
PFOA: 0.00095
PFNA: 0.0035

C (bulk concentration in Ashumet Pond) = 51 ng L^{-1} (1.022 *10^{-13} mol cm^{-3}) for PFOS

Length of PFOS = 1.32 nm[144]

PFOS Calculation:

Γ = (0.004 cm^3 cm^{-2})(1.022 *10^{-13} mol cm^{-3}) = **4.09*10^{-16} mol cm^{-2} (4.09*10^{-12} mol m^{-2})**

Assuming a monolayer with the thickness of PFOS (~1 nm, or 10^{-9} m), the molar concentration at the monolayer surface would be:

(4.09*10^{-12} mol/m^2)/ 10^{-9} m = 0.00409 mol m^{-3} PFOS (**2,040,000 ng L^{-1} PFOS)**

Assuming the microlayer samples were 50 μm (50,000 nm) thick[109], and assuming the concentration underneath the monolayer is equal to the bulk concentration of PFOS in the lake, the expected microlayer concentration is:

Monolayer component: 1/50000 * 2,040,000 ng L^{-1} = **40.8 ng/L**

Bulk Component: 49999/50000 * 51 ng/L = **51 ng/L**

Total Expected Concentration: 51 + 40.8 ng/L = 91.8 ng/L

Table B1. Well names, sample type, sampling date, latitude, longitude, land surface altitude, mid-screen altitude, and depth below water table.

U.S. Geological Survey local site name	Sample Type	Sampling date	Latitude in deg. min. sec. North American Datum of 1927	Longitude in deg. min.sec. North American Datum of 1927	Land surface altitude (m) National Geodetic Vertical Datum of 1929	Mid-Screen Altitude in meters	Depth in meters below water table
DI H2O From Peristaltic Geopump For MLSs	Blank	9/11/2017					
DI H2O From Grundfos Pump	Blank	9/12/2017					
DI H2O From Keck Pump	Blank	9/12/2017					
DI H2O From Henry Sampler	Blank	9/14/2017					
DI H2O From Microlayer Sampling Device	Blank	9/12/2017					
DI H2O From Boat Peristaltic Geopump	Blank	9/12/2017					
DI H2O From Boat Peristaltic Geopump	Blank	11/8/2017					
DI H2O From MA-FSW 631-02GNT	Blank	2/22/2018					
DI H2O From Henry Sampler	Blank	2/22/2018					
MA-MIW 207-0069 (00MW0582B)	Groundwater	7/26/2017	413745.66	703140.45	26.886408	6.59	6.03
MA-MIW 207-0215 (00MW0582A)	Groundwater	7/26/2017	413745.67	703140.45	26.886408	-37.73	50.35
MA-MIW 209-0015 (00MW0584C)	Groundwater	7/21/2017	413740.23	703057.22	13.021056	9.24	2.33
MA-MIW 209-0146 (00MW0584B)	Groundwater	7/21/2017	413740.27	703057.16	13.002768	-30.74	42.31
MA-MIW 209-0286 (00MW0584A)	Groundwater	7/21/2017	413740.23	703057.22	13.021056	-73.39	84.97
MA-MIW 210-0026	Groundwater	7/25/2017	413757.85	703140.97	18.40992	10.51	2.31
MA-MIW 210-0046	Groundwater	7/25/2017	413757.85	703140.97	18.428208	4.59	8.24
MA-MIW 210-0075 (00MW0609B)	Groundwater	7/25/2017	413757.79	703140.96	18.431256	-3.79	16.62
MA-MIW 210-0145 (00MW0609A)	Groundwater	7/25/2017	413757.78	703140.96	18.431256	-24.88	37.71

Table B1 (Continued)

U.S. Geological Survey local site name	Sample Type	Sampling date	Latitude in deg. min. sec. North American Datum of 1927	Longitude in deg. min.sec. North American Datum of 1927	Land surface altitude (m) National Geodetic Vertical Datum of 1929	Mid-Screen Altitude in meters	Depth in meters below water table
MA-MIW 221-0245 (03MW1003B)	Groundwater	7/28/2017	413739.30	703051.25	25.51176	-48.30	59.37
MA-MIW 221-0325 (03MW1003A)	Groundwater	7/28/2017	413739.30	703051.25	25.51176	-72.65	83.72
MA-MIW 223-0111 (03MW1005B)	Groundwater	7/25/2017	413757.16	703140.50	18.42516	-14.65	27.55
MA-MIW 223-0148 (03MW1005A)	Groundwater	7/25/2017	413757.16	703140.50	18.42516	-25.99	38.89
MA-MIW 230-0015	Groundwater	7/20/2017	413709.16	703111.59	12.932664	8.47	3.12
MA-MIW 230-0060	Groundwater	7/20/2017	413709.16	703111.59	12.935712	-5.03	16.63
MA-MIW 230-0110	Groundwater	7/20/2017	413709.16	703111.59	12.941808	-20.26	31.85
MA-MIW 230-0174 (03MW2626B)	Groundwater	7/19/2017	413708.82	703111.95	12.886944	-39.31	50.90
MA-MIW 230-0294 (03MW2626A)	Groundwater	7/19/2017	413708.82	703111.95	12.886944	-76.06	87.65
MA-MIW 231-0040	Groundwater	7/19/2017	413658.68	703056.41	15.24	3.37	6.67
MA-MIW 231-0070	Groundwater	7/19/2017	413658.68	703056.41	15.24	-5.73	15.77
MA-MIW 231-0105	Groundwater	7/19/2017	413658.68	703056.41	15.24	-16.43	26.47
MA-MIW 231-0138	Groundwater	7/19/2017	413658.68	703056.41	15.24	-26.59	36.63
MA-MIW 232-0050	Groundwater	7/18/2017	413654.64	703038.37	20.1168	5.15	4.17
MA-MIW 232-0080	Groundwater	7/18/2017	413654.64	703038.37	20.1168	-4.05	13.37
MA-MIW 232-0115	Groundwater	7/18/2017	413654.64	703038.37	20.1168	-14.63	23.95
MA-MIW 232-0150	Groundwater	7/18/2017	413654.64	703038.37	20.1168	-25.21	34.53
MA-MIW 233-0016	Groundwater	7/26/2017	413739.98	703129.84	13.216128	8.53	3.54
MA-MIW 233-0070	Groundwater	7/26/2017	413739.98	703129.84	13.130784	-7.96	20.04
MA-MIW 233-0174 (00MW0608B)	Groundwater	7/26/2017	413740.08	703129.53	13.011912	-39.32	51.40
MA-MIW 233-0245 (00MW0608A)	Groundwater	7/26/2017	413740.98	703129.53	13.011912	-60.75	72.83
MA-MIW 234-0055	Groundwater	7/20/2017	413648.28	703015.63	20.1168	3.55	3.42
MA-MIW 234-0086	Groundwater	7/20/2017	413648.28	703015.63	20.1168	-5.67	12.65
MA-MIW 234-0120	Groundwater	7/20/2017	413648.28	703015.63	20.1168	-16.18	23.16
MA-MIW 234-0150	Groundwater	7/20/2017	413648.28	703015.63	20.1168	-25.16	32.13
MA-MIW 236-0025 (MAMW0396S)	Groundwater	7/27/2017	413651.77	703107.98	13.36548	8.03	1.41

Table B1 (Continued)

U.S. Geological Survey local site name	Sample Type	Sampling date	Latitude in deg. min. sec. North American Datum of 1927	Longitude in deg. min.sec. North American Datum of 1927	Land surface altitude (m) National Geodetic Vertical Datum of 1929	Mid-Screen Altitude in meters	Depth in meters below water table
MA-MIW 236-0109 (MAMW0296I)	Groundwater	7/27/2017	413651.75	703107.93	13.432536	-18.27	27.71
MA-MIW 236-0189 (MAMW0196D)	Groundwater	7/27/2017	413651.73	703107.88	13.514832	-45.62	55.06
MA-MIW 237-0145 (03MW2620B)	Groundwater	7/27/2017	413745.22	703142.11	25.825704	-17.52	30.34
MA-MIW 237-0254 (03MW2620A)	Groundwater	7/27/2017	413745.22	703142.11	25.825704	-50.80	63.63
MA-FSW 631-M01-01PT	Groundwater	9/12/2017	413734.14	703206.76	16.343376	11.59	1.21
MA-FSW 631-M01-02GNT	Groundwater	9/12/2017	413734.14	703206.76	16.343376	8.53	4.27
MA-FSW 631-M01-03RT	Groundwater	9/12/2017	413734.14	703206.76	16.343376	5.48	7.32
MA-FSW 631-M01-04BUT	Groundwater	9/12/2017	413734.14	703206.76	16.343376	2.43	10.37
MA-FSW 631-M01-06WT	Groundwater	9/12/2017	413734.14	703206.76	16.343376	-3.69	16.49
MA-FSW 631-M01-09Y	Groundwater	9/12/2017	413734.14	703206.76	16.343376	-12.85	25.66
MA-FSW 631-M01-12R	Groundwater	9/12/2017	413734.14	703206.76	16.343376	-22.02	34.82
MA-FSW 631-M01-15W	Groundwater	9/12/2017	413734.14	703206.76	16.343376	-31.19	43.99
MA-FSW 631-0256 (00MW0589A)	Groundwater	9/12/2017	413734.03	703206.76	16.340328	-61.02	73.82
MA-FSW 632-M01-01PT	Groundwater	9/11/2017	413724.69	703159.91	20.007072	10.95	1.32
MA-FSW 632-M01-02GNT	Groundwater	9/11/2017	413724.69	703159.91	20.007072	7.91	4.36
MA-FSW 632-M01-03RT	Groundwater	9/11/2017	413724.69	703159.91	20.007072	4.85	7.42
MA-FSW 632-M01-05BKT	Groundwater	9/11/2017	413724.69	703159.91	20.007072	-1.25	13.52
MA-FSW 632-M01-06WT	Groundwater	9/11/2017	413724.69	703159.91	20.007072	-4.31	16.58
MA-FSW 632-M01-07O	Groundwater	9/11/2017	413724.69	703159.91	20.007072	-7.37	19.64
MA-FSW 632-M01-11GN	Groundwater	9/11/2017	413724.69	703159.91	20.007072	-19.58	31.85
MA-FSW 632-M01-15W	Groundwater	9/11/2017	413724.69	703159.91	20.007072	-31.79	44.06
MA-FSW 632-0195 (00MW0606B)	Groundwater	9/11/2017	413724.75	703159.81	20.028408	-38.65	50.92
MA-FSW 632-0325 (00MW0606A)	Groundwater	9/11/2017	413724.75	703159.81	20.028408	-78.27	90.54
MA-FSW 665-0040	Groundwater	9/12/2017	413731.30	703205.12	17.202912	5.37	7.15
MA-FSW 665-0089	Groundwater	9/12/2017	413731.30	703205.12	17.224248	-9.70	22.23
MA-FSW 665-0139	Groundwater	9/12/2017	413731.30	703205.12	17.254728	-24.80	37.32
MA-FSW 665-0264 (03MW1014B)	Groundwater	9/12/2017	413731.30	703205.12	17.391888	-62.29	74.81
MA-FSW 665-0295 (03MW1014A)	Groundwater	9/12/2017	413731.30	703205.12	17.391888	-71.71	84.24
MA-FSW 722-M01-01PT	Groundwater	9/13/2017	413735.47	703206.71	14.883384	11.69	1.24
MA-FSW 722-M01-02GNT	Groundwater	9/13/2017	413735.47	703206.71	14.883384	9.85	3.09

Table B1 (Continued)

U.S. Geological Survey local site name	Sample Type	Sampling date	Latitude in deg. min. sec. North American Datum of 1927	Longitude in deg. min.sec. North American Datum of 1927	Land surface altitude (m) National Geodetic Vertical Datum of 1929	Mid-Screen Altitude in meters	Depth in meters below water table
MA-FSW 722-M01-06WT	Groundwater	9/13/2017	413735.47	703206.71	14.883384	2.47	10.46
MA-FSW 722-M01-08GY	Groundwater	9/13/2017	413735.47	703206.71	14.883384	-3.63	16.56
MA-FSW 722-M01-09Y	Groundwater	9/13/2017	413735.47	703206.71	14.883384	-6.71	19.64
MA-FSW 722-M01-11GN	Groundwater	9/14/2017	413735.47	703206.71	14.883384	-12.79	25.73
MA-FSW 722-M01-12R	Groundwater	9/14/2017	413735.47	703206.71	14.883384	-15.83	28.77
MA-FSW 722-M01-14BK	Groundwater	9/14/2017	413735.47	703206.71	14.883384	-21.92	34.87
MA-FSW 722-M01-15W	Groundwater	9/14/2017	413735.47	703206.71	14.883384	-25.00	37.93
MA-FSW 722-M02-01PT	Groundwater	9/13/2017	413735.47	703206.71	14.801088	12.26	0.68
MA-FSW 722-M02-03RT	Groundwater	9/13/2017	413735.47	703206.71	14.801088	10.41	2.52
MA-FSW 722-M02-05BKT	Groundwater	9/13/2017	413735.47	703206.71	14.801088	8.58	4.35
MA-FSW 722-M02-08GY	Groundwater	9/13/2017	413735.47	703206.71	14.801088	5.84	7.10
MA-FSW 722-M02-10P	Groundwater	9/13/2017	413735.47	703206.71	14.801088	3.99	8.94
MA-FSW 722-M02-12R	Groundwater	9/13/2017	413735.47	703206.71	14.801088	2.16	10.77
MA-FSW 722-M02-15W	Groundwater	9/13/2017	413735.47	703206.71	14.801088	-0.58	13.51
MA-FSW 722-M01-02GNT	Groundwater	2/23/2018	413735.47	703206.71	14.883384	9.85	3.34
MA-FSW 722-M01-06WT	Groundwater	2/23/2018	413735.47	703206.71	14.883384	2.47	10.71
MA-FSW 722-M01-08GY	Groundwater	2/23/2018	413735.47	703206.71	14.883384	-3.63	16.82
MA-FSW 722-M01-09Y	Groundwater	2/23/2018	413735.47	703206.71	14.883384	-6.71	19.90
MA-FSW 722-M01-11GN	Groundwater	2/23/2018	413735.47	703206.71	14.883384	-12.79	25.98
MA-FSW 722-M01-12R	Groundwater	2/23/2018	413735.47	703206.71	14.883384	-15.83	29.03
MA-FSW 722-M02-01PT	Groundwater	2/23/2018	413735.47	703206.71	14.801088	12.26	0.93
MA-FSW 722-M02-05BKT	Groundwater	2/23/2018	413735.47	703206.71	14.801088	8.58	4.61
MA-FSW 722-M02-08GY	Groundwater	2/23/2018	413735.47	703206.71	14.801088	5.84	7.35
MA-FSW 722-M02-15W	Groundwater	2/23/2018	413735.47	703206.71	14.801088	-0.58	13.77
FS-ASHPD-0001 (ECAMP02) Microlayer	Lake	9/11/2017	413802.32	703156.15			
FS-ASHPD-0001 (ECAMP02) 0.1m	Lake	9/11/2017	413802.32	703156.15			
FS-ASHPD-0001 (ECAMP02) 1.00m	Lake	9/11/2017	413802.32	703156.15			
FS-ASHPD-0001 (ECAMP02) 3.00m	Lake	9/11/2017	413802.32	703156.15			

Table B1 (Continued)

U.S. Geological Survey local site name	Sample Type	Sampling date	Latitude in deg. min. sec. North American Datum of 1927	Longitude in deg. min.sec. North American Datum of 1927	Land surface altitude (m) National Geodetic Vertical Datum of 1929	Mid-Screen Altitude in meters	Depth in meters below water table
FS-ASHPD-0001 (ECAMP02) 5.00m	Lake	9/11/2017	413802.32	703156.15			
FS-ASHPD-0001 (ECAMP02) 7.00m	Lake	9/11/2017	413802.32	703156.15			
FS-ASHPD-0001 (ECAMP02) 9.00m	Lake	9/11/2017	413802.32	703156.15			
FS-ASHPD-0001 (ECAMP02) 11.00m	Lake	9/11/2017	413802.32	703156.15			
FS-ASHPD-0001 (ECAMP02) 13.00m	Lake	9/11/2017	413802.32	703156.15			
FS-ASHPD-0001 (ECAMP02) 15.00m	Lake	9/11/2017	413802.32	703156.15			
FS-ASHPD-0001 (ECAMP02) 17.00m	Lake	9/11/2017	413802.32	703156.15			
FS-ASHPD-0001 (ECAMP02) Microlayer	Lake	11/8/2017	413802.32	703156.15			
FS-ASHPD-0001 (ECAMP02) 0.1m	Lake	11/8/2017	413802.32	703156.15			
FS-ASHPD-0001 (ECAMP02) 1.00m	Lake	11/8/2017	413802.32	703156.15			
FS-ASHPD-0001 (ECAMP02) 3.00m	Lake	11/8/2017	413802.32	703156.15			
FS-ASHPD-0001 (ECAMP02) 5.00m	Lake	11/8/2017	413802.32	703156.15			
FS-ASHPD-0001 (ECAMP02) 7.00m	Lake	11/8/2017	413802.32	703156.15			
FS-ASHPD-0001 (ECAMP02) 9.00m	Lake	11/8/2017	413802.32	703156.15			
FS-ASHPD-0001 (ECAMP02) 11.00m	Lake	11/8/2017	413802.32	703156.15			
FS-ASHPD-0001 (ECAMP02) 13.00m	Lake	11/8/2017	413802.32	703156.15			
FS-ASHPD-0001 (ECAMP02) 15.00m	Lake	11/8/2017	413802.32	703156.15			
FS-ASHPD-0001 (ECAMP02) 17.00m	Lake	11/8/2017	413802.32	703156.15			
FS-ASHPD-0009 (ECAMP01) Microlayer	Lake	9/11/2017	413740.13	703206.86			
FS-ASHPD-0009 (ECAMP01) 0.1m	Lake	9/11/2017	413740.13	703206.86			
FS-ASHPD-0009 (ECAMP01) 1.00m	Lake	9/11/2017	413740.13	703206.86			
FS-ASHPD-0009 (ECAMP01) 3.00 m	Lake	9/11/2017	413740.13	703206.86			
FS-ASHPD-0009 (ECAMP01) 5.00 m	Lake	9/11/2017	413740.13	703206.86			

Table B1 (Continued)

U.S. Geological Survey local site name	Sample Type	Sampling date	Latitude in deg. min. sec. North American Datum of 1927	Longitude in deg. min.sec. North American Datum of 1927	Land surface altitude (m) National Geodetic Vertical Datum of 1929	Mid-Screen Altitude in meters	Depth in meters below water table
FS-ASHPD-0010 Microlayer	Lake	9/11/2017	413804.25	703217.48			
FS-ASHPD-0010 0.1m	Lake	9/11/2017	413804.25	703217.48			
FS-ASHPD-0010 1.00m	Lake	9/11/2017	413804.25	703217.48			
FS-ASHPD-0010 3.00m	Lake	9/11/2017	413804.25	703217.48			
FS-ASHPD-0010 5.00m	Lake	9/11/2017	413804.25	703217.48			
FS-ASHPD-0010 7.00m	Lake	9/11/2017	413804.25	703217.48			
FS-ASHPD-0010 9.00m	Lake	9/11/2017	413804.25	703217.48			
FS-ASHPD-0011 Microlayer	Lake	9/12/2017	413755.52	703212.67			
FS-ASHPD-0011 0.1m	Lake	9/12/2017	413755.52	703212.67			
FS-ASHPD-0011 1.00m	Lake	9/12/2017	413755.52	703212.67			
FS-ASHPD-0011 3.00m	Lake	9/12/2017	413755.52	703212.67			
FS-ASHPD-0011 5.00m	Lake	9/12/2017	413755.52	703212.67			
FS-ASHPD-0011 7.00m	Lake	9/12/2017	413755.52	703212.67			
FS-ASHPD-0011 9.00m	Lake	9/12/2017	413755.52	703212.67			
MI-JOHPD-0001 (ECJNP03) Microlayer	Lake	9/12/2017	413755.62	703054.20			
MI-JOHPD-0001 (ECJNP03) 0.1m	Lake	9/12/2017	413755.62	703054.20			
MI-JOHPD-0001 (ECJNP03) 1.00m	Lake	9/12/2017	413755.62	703054.20			
MI-JOHPD-0001 (ECJNP03) 3.00m	Lake	9/12/2017	413755.62	703054.20			
MI-JOHPD-0001 (ECJNP03) 5.00m	Lake	9/12/2017	413755.62	703054.20			
MI-JOHPD-0001 (ECJNP03) 7.00m	Lake	9/12/2017	413755.62	703054.20			
MI-JOHPD-0001 (ECJNP03) 9.00m	Lake	9/12/2017	413755.62	703054.20			
MI-JOHPD-0001 (ECJNP03) 11.00m	Lake	9/12/2017	413755.62	703054.20			
MI-JOHPD-0001 (ECJNP03) 15.00	Lake	9/12/2017	413755.62	703054.20			
MI-JOHPD-0008 Microlayer	Lake	9/12/2017	413722.35	703127.56			
MI-JOHPD-0008 0.1m	Lake	9/12/2017	413722.35	703127.56			
MI-JOHPD-0008 1.00m	Lake	9/12/2017	413722.35	703127.56			
MI-JOHPD-0008 3.00m	Lake	9/12/2017	413722.35	703127.56			
MI-JOHPD-0008 5.00m	Lake	9/12/2017	413722.35	703127.56			
MI-JOHPD-0008 7.00m	Lake	9/12/2017	413722.35	703127.56			
MI-JOHPD-0008 9.00m	Lake	9/12/2017	413722.35	703127.56			

Table B1 (Continued)

U.S. Geological Survey local site name	Sample Type	Sampling date	Latitude in deg. min. sec. North American Datum of 1927	Longitude in deg. min.sec. North American Datum of 1927	Land surface altitude (m) National Geodetic Vertical Datum of 1929	Mid-Screen Altitude in meters	Depth in meters below water table
ASHPD-GWOUT-L-N-LW	Lake	9/13/2017	413736.09	703207.48			
ASHPD-GWOUT-L-N-015	Downwelling Porewater	9/13/2017	413736.09	703207.48			
ASHPD-GWOUT-L-N-030	Downwelling Porewater	9/13/2017	413736.09	703207.48			
ASHPD-GWOUT-L-N-050	Downwelling Porewater	9/13/2017	413736.09	703207.48			
ASHPD-GWOUT-L-N-100	Downwelling Porewater	9/13/2017	413736.09	703207.48			
ASHPD-GWOUT-R-N-LW	Lake	9/13/2017	413736.11	703207.06			
ASHPD-GWOUT-R-N-015	Downwelling Porewater	9/13/2017	413736.11	703207.06			
ASHPD-GWOUT-R-N-030	Downwelling Porewater	9/13/2017	413736.11	703207.06			
ASHPD-GWOUT-R-N-050	Downwelling Porewater	9/13/2017	413736.11	703207.06			
ASHPD-GWOUT-R-N-100	Downwelling Porewater	9/13/2017	413736.11	703207.06			
ASHPD-GWOUT-R-S-015	Downwelling Porewater	9/13/2017	413735.98	703207.08			
ASHPD-GWOUT-R-S-100	Downwelling Porewater	9/13/2017	413735.98	703207.08			
ASHPD-KIGAM-124N-010E-LW	Lake Upwelling	9/14/2017	413804.51	703226.86			
ASHPD-KIGAM-124N-010E-015	Porewater Upwelling	9/14/2017	413804.51	703226.86			
ASHPD-KIGAM-124N-010E-030	Porewater Upwelling	9/14/2017	413804.51	703226.86			
ASHPD-KIGAM-124N-010E-050	Porewater Upwelling	9/14/2017	413804.51	703226.86			
ASHPD-KIGAM-124N-010E-100	Porewater	9/14/2017	413804.51	703226.86			
ASHPD-KIGAM-131N-011E-LW	Lake Upwelling	9/14/2017	413804.67	703226.80			
ASHPD-KIGAM-131N-011E-015	Upwelling	9/14/2017	413804.67	703226.80			

Table B1 (Continued)

U.S. Geological Survey local site name	Sample Type	Sampling date	Latitude in deg. min. sec. North American Datum of 1927	Longitude in deg. min.sec. North American Datum of 1927	Land surface altitude (m) National Geodetic Vertical Datum of 1929	Mid-Screen Altitude in meters	Depth in meters below water table
ASHPD-KIGAM-131N-011E-030	Porewater Upwelling	9/14/2017	413804.67	703226.80			
ASHPD-KIGAM-131N-011E-050	Porewater Upwelling	9/14/2017	413804.67	703226.80			
ASHPD-KIGAM-131N-011E-100	Porewater Upwelling	9/14/2017	413804.67	703226.80			
ASHPD-GWIN-C-LW	Lake Upwelling	9/11/2017	413819.79	703207.20			
ASHPD-GWIN-C-035	Porewater Upwelling	9/11/2017	413819.79	703207.20			
ASHPD-GWIN-C-100	Porewater Upwelling	9/11/2017	413819.79	703207.20			
ASHPD-GWOUT-L-N-100	Downwelling Porewater	2/23/2018	413736.095	703207.4805			
ASHPD-GWOUT-R-N-LW	Lake Downwelling	2/23/2018	413736.113	703207.0578			
ASHPD-GWOUT-R-N-100	Porewater	2/23/2018	413736.113	703207.0578			
MA-FSW 239-M01-01PT	Groundwater	8/5/2016	413801.33	703228.32	15.57528	12.56	
MA-FSW 239-M01-02GNT	Groundwater	8/5/2016	413801.33	703228.32	15.57528	11.03	
MA-FSW 239-M01-04BUT	Groundwater	8/5/2016	413801.33	703228.32	15.57528	7.99	
MA-FSW 239-M01-06WT	Groundwater	8/5/2016	413801.33	703228.32	15.57528	4.95	
MA-FSW 239-M01-08GY	Groundwater	8/5/2016	413801.33	703228.32	15.57528	1.91	
MA-FSW 239-M01-10P	Groundwater	8/5/2016	413801.33	703228.32	15.57528	-2.65	
MA-FSW 239-M01-12R	Groundwater	8/5/2016	413801.33	703228.32	15.57528	-8.74	
MA-FSW 239-M01-14BK	Groundwater	8/5/2016	413801.33	703228.32	15.57528	-14.82	
MA-FSW 300-M03-01PT	Groundwater	7/7/2016	413805.43	703225.22	14.29512	12.31	
MA-FSW 300-M03-03RT	Groundwater	7/7/2016	413805.43	703225.22	14.29512	10.48	
MA-FSW 300-M03-06WT	Groundwater	7/7/2016	413805.43	703225.22	14.29512	8.04	
MA-FSW 300-M03-09Y	Groundwater	7/7/2016	413805.43	703225.22	14.29512	6.21	
MA-FSW 300-M03-10P	Groundwater	7/7/2016	413805.43	703225.22	14.29512	5.60	
MA-FSW 300-M03-11GN	Groundwater	7/7/2016	413805.43	703225.22	14.29512	4.99	
MA-FSW 300-M03-14BK	Groundwater	7/7/2016	413805.43	703225.22	14.29512	3.16	

Table B1 (Continued)

U.S. Geological Survey local site name	Sample Type	Sampling date	Latitude in deg. min. sec. North American Datum of 1927	Longitude in deg. min.sec. North American Datum of 1927	Land surface altitude (m) National Geodetic Vertical Datum of 1929	Mid-Screen Altitude in meters	Depth in meters below water table
MA-FSW 300-M03-15W	Groundwater	7/7/2016	413805.43	703225.22	14.29512	2.55	
MA-FSW 300-M02-01PT	Groundwater	7/8/2016	413805.43	703225.22	14.29512	2.17	
MA-FSW 300-M02-02GNT	Groundwater	7/8/2016	413805.43	703225.22	14.29512	1.56	
MA-FSW 300-M02-03RT	Groundwater	7/8/2016	413805.43	703225.22	14.29512	0.65	
MA-FSW 300-M02-06WT	Groundwater	7/8/2016	413805.43	703225.22	14.29512	-2.10	
MA-FSW 300-M02-08GY	Groundwater	7/8/2016			14.29512	-3.93	
MA-FSW 300-M02-10P	Groundwater	7/8/2016	413805.43	703225.22	14.29512	-6.37	
MA-FSW 300-M02-14BK	Groundwater	7/8/2016	413805.43	703225.22	14.29512	-13.11	
MA-FSW 300-0138	Groundwater	7/7/2016	413805.43	703225.22	14.365224	-27.25	
MA-FSW 424-M01-01PT	Groundwater	7/26/2016	413804.75	703228.23	17.641824	1.79	
MA-FSW 424-M01-03RT	Groundwater	7/26/2016	413804.75	703228.23	17.641824	-1.26	
MA-FSW 424-M01-05BKT	Groundwater	7/26/2016	413804.75	703228.23	17.641824	-4.30	
MA-FSW 424-M01-09Y	Groundwater	7/26/2016	413804.75	703228.23	17.641824	-10.39	
MA-FSW 424-M01-13BU	Groundwater	7/26/2016	413804.75	703228.23	17.641824	-16.48	
MA-FSW 424-M02-11GN 72-13	Groundwater	7/26/2016	413804.88	703228.12	17.333976	5.81	
MA-FSW 424-M02-12R 72-13	Groundwater	7/26/2016	413804.88	703228.12	17.333976	5.04	
MA-FSW 424-M02-14BK 72-13	Groundwater	7/26/2016	413804.88	703228.12	17.333976	3.51	
MA-FSW 424-M02-15W 72-13	Groundwater	7/26/2016	413804.88	703228.12	17.333976	2.75	
MA-FSW 564-M01-01PT	Groundwater	7/6/2016	413808.47	703222.48	16.675608	12.68	
MA-FSW 564-M01-02GNT	Groundwater	7/6/2016	413808.47	703222.48	16.675608	11.17	
MA-FSW 564-M01-04BUT	Groundwater	7/6/2016	413808.47	703222.48	16.675608	8.13	
MA-FSW 564-M01-05BKT	Groundwater	7/6/2016	413808.47	703222.48	16.675608	6.60	
MA-FSW 564-M01-06WT	Groundwater	7/6/2016	413808.47	703222.48	16.675608	5.08	
MA-FSW 564-M01-08GY	Groundwater	7/6/2016	413808.47	703222.48	16.675608	2.02	
MA-FSW 564-M01-10P	Groundwater	7/6/2016	413808.47	703222.48	16.675608	-2.55	
MA-FSW 564-M01-12R	Groundwater	7/6/2016	413808.47	703222.48	16.675608	-8.65	
MA-FSW 564-M01-14BK	Groundwater	7/6/2016	413808.47	703222.48	16.675608	-14.75	
MA-FSW 621-M01-01PT	Groundwater	7/11/2016	413806.08	703223.67	18.010632	12.20	
MA-FSW 621-M01-02GNT	Groundwater	7/11/2016	413806.08	703223.67	18.010632	9.76	
MA-FSW 621-M01-03RT	Groundwater	7/11/2016	413806.08	703223.67	18.010632	7.32	
MA-FSW 621-M01-05BKT	Groundwater	7/11/2016	413806.08	703223.67	18.010632	3.05	

Table B1 (Continued)

U.S. Geological Survey local site name	Sample Type	Sampling date	Latitude in deg. min. sec. North American Datum of 1927	Longitude in deg. min.sec. North American Datum of 1927	Land surface altitude (m) National Geodetic Vertical Datum of 1929	Mid-Screen Altitude in meters	Depth in meters below water table
MA-FSW 621-M01-06WT	Groundwater	7/11/2016	413806.08	703223.67	18.010632	1.23	
MA-FSW 621-M01-07O	Groundwater	7/11/2016	413806.08	703223.67	18.010632	-0.60	
MA-FSW 621-M01-09Y	Groundwater	7/11/2016	413806.08	703223.67	18.010632	-4.87	
MA-FSW 621-M01-11GN	Groundwater	7/11/2016	413806.08	703223.67	18.010632	-9.75	
MA-FSW 621-M01-13BU	Groundwater	7/11/2016	413806.08	703223.67	18.010632	-14.62	
MA-FSW 621-M01-15W	Groundwater	7/11/2016	413806.08	703223.67	18.010632	-19.50	
MA-FSW 622-M01-01PT	Groundwater	7/11/2016	413807.16	703222.93	16.55064	11.71	
MA-FSW 622-M01-02GNT	Groundwater	7/11/2016	413807.16	703222.93	16.55064	9.27	
MA-FSW 622-M01-03RT	Groundwater	7/11/2016	413807.16	703222.93	16.55064	6.83	
MA-FSW 622-M01-05BKT	Groundwater	7/11/2016	413807.16	703222.93	16.55064	2.57	
MA-FSW 622-M01-06WT	Groundwater	7/11/2016	413807.16	703222.93	16.55064	0.74	
MA-FSW 622-M01-07O	Groundwater	7/11/2016	413807.16	703222.93	16.55064	-1.09	
MA-FSW 622-M01-09Y	Groundwater	7/11/2016	413807.16	703222.93	16.55064	-5.36	
MA-FSW 622-M01-11GN	Groundwater	7/11/2016	413807.16	703222.93	16.55064	-10.24	
MA-FSW 622-M01-13BU	Groundwater	7/11/2016	413807.16	703222.93	16.55064	-15.11	
MA-FSW 622-M01-15W	Groundwater	7/11/2016	413807.16	703222.93	16.55064	-19.98	
MA-FSW 744-0004	Groundwater	7/26/2016	413804.11	703227.58	14.060424	12.88	
MA-FSW 744-0008	Groundwater	7/26/2016	413804.11	703227.58	14.060424	11.50	
MA-FSW 744-0010	Groundwater	7/26/2016	413804.11	703227.58	14.060424	11.13	
MA-FSW 744-0011	Groundwater	7/26/2016	413804.11	703227.58	14.060424	10.64	
MA-FSW 744-0013	Groundwater	7/26/2016	413804.11	703227.58	14.060424	10.20	
MA-FSW 744-0017	Groundwater	7/26/2016	413804.11	703227.58	14.060424	9.00	
MA-FSW 744-0019	Groundwater	7/26/2016	413804.11	703227.58	14.060424	8.14	
MA-FSW 744-0023	Groundwater	7/26/2016	413804.11	703227.58	14.060424	7.14	
MA-FSW 744-0025	Groundwater	7/26/2016	413804.11	703227.58	14.060424	6.50	
MA-FSW 744-0026	Groundwater	7/26/2016	413804.11	703227.58	14.060424	6.00	
MA-FSW 744-0028	Groundwater	7/26/2016	413804.11	703227.58	14.060424	5.67	
MA-FSW 744-0029	Groundwater	7/26/2016	413804.11	703227.58	14.060424	5.18	
MA-FSW 744-0030	Groundwater	7/26/2016	413804.11	703227.58	14.060424	5.04	
Q1 MI-QUARV-00015(QR001)	River	8/15/2017	413807.98	703048.72			
Q3	River	8/15/2017	413759.84	703017.28			

Table B1 (Continued)

U.S. Geological Survey local site name	Sample Type	Sampling date	Latitude in deg. min. sec. North American Datum of 1927	Longitude in deg. min.sec. North American Datum of 1927	Land surface altitude (m) National Geodetic Vertical Datum of 1929	Mid-Screen Altitude in meters	Depth in meters below water table
Q4	River	8/15/2017	413702.78	703001.82			
Q5	River	8/15/2017	413630.39	703007.10			
Q9	River	8/15/2017	413531.86	703027.51			
Q-FC	River	8/15/2017	413607.14	703009.80			
Q-OBR	River	8/15/2017	413727.62	703003.18			
Q-TRIB	River	8/15/2017	413814.27	703025.89			
Quash_HS_Seep1	River	8/16/2017	413636.01	703006.01			
Quash_HS_Seep2	River	8/16/2017	413631.94	703007.73			
QB010	River	8/17/2017	413645.81	703007.57			
QB018	River	8/17/2017	413650.86	703006.47			
QB020	River	8/17/2017	413652.48	703003.88			
QB026	River	8/17/2017	413802.02	703020.02			
QB039	River	8/18/2017	413808.41	703046.81			
DD004	River	8/17/2017	413810.79	703029.45			
DD-12	River	8/17/2017	413809.13	703025.66			
Quash_OV_seep1	River	8/14/2017	413602.94	703010.47			
Quash_OV_seep2	River	8/14/2017	413551.42	703013.92			
Quash_HRTS_seep	River	8/14/2017	413600.32	703011.71			
QT008	River	8/17/2017	413639.22	703004.24			
QT018	River	8/17/2017	413645.43	703007.75			
QT030	River	8/17/2017	413652.32	703004.10			
QT034	River	8/17/2017	413655.01	703002.42			
QT039	River	8/17/2017	413658.35	702959.61			
QT082	River	8/18/2017	413730.07	703003.43			
QT101	River	8/17/2017	413802.04	703019.85			
QT122	River		413811.44	703027.26			
QT142	River	8/18/2017	413809.76	703045.32			
Quash-Spawn1	River	8/16/2017	413628.88	703008.52			
Quash-Spawn2	River	8/16/2017	413627.78	703008.24			
Quash-Spawn3	River	8/14/2017	413537.88	703025.27			

109

Table B2. Specific conductance, pH, dissolved oxygen, and temperature for water samples.

U.S. Geological Survey local site name	Sampling date	Specific conductance in microsiemens per centimeter at 25 degrees Celsius	pH in standard units	Dissolved oxygen in milligrams per liter	Temperature in degrees Celsius
DI H2O From Peristaltic Geopump For MLSs	9/11/2017				
DI H2O From Grundfos Pump	9/12/2017				
DI H2O From Keck Pump	9/12/2017				
DI H2O From Henry Sampler	9/14/2017				
DI H2O From Microlayer Sampling Device	9/12/2017				
DI H2O From Boat Peristaltic Geopump	9/12/2017				
DI H2O From Boat Peristaltic Geopump	11/8/2017				
DI H2O From MA-FSW 631-02GNT	2/22/2018				
DI H2O From Henry Sampler	2/22/2018				
MA-MIW 207-0069 (00MW0582B)	7/26/2017	126.3	6.21	0.033	
MA-MIW 207-0215 (00MW0582A)	7/26/2017	131.9	6.32	0.044	
MA-MIW 209-0015 (00MW0584C)	7/21/2017	669.4	5.16	0.110	
MA-MIW 209-0146 (00MW0584B)	7/21/2017	122.5	6.07	0.214	
MA-MIW 209-0286 (00MW0584A)	7/21/2017	128.3	6.62	2.840	
MA-MIW 210-0026	7/25/2017	129.2	6.22	0.370	
MA-MIW 210-0046	7/25/2017	113.6	5.80	2.660	
MA-MIW 210-0075 (00MW0609B)	7/25/2017	147.3	6.23	7.070	
MA-MIW 210-0145 (00MW0609A)	7/25/2017	144.9	7.20	0.041	
MA-MIW 221-0245 (03MW1003B)	7/28/2017	128.3	6.82	0.317	
MA-MIW 221-0325 (03MW1003A)	7/28/2017	150.6	7.17	0.088	
MA-MIW 223-0111 (03MW1005B)	7/25/2017	118.8	6.35	8.880	
MA-MIW 223-0148 (03MW1005A)	7/25/2017	130.4	5.99	8.230	
MA-MIW 230-0015	7/20/2017	107.9	5.96	0.152	23.3
MA-MIW 230-0060	7/20/2017	114.3	5.96	0.089	18.5
MA-MIW 230-0110	7/20/2017	124.1	6.43	0.060	16.73
MA-MIW 230-0174 (03MW2626B)	7/19/2017	105.5	6.06	0.010	19.4
MA-MIW 230-0294 (03MW2626A)	7/19/2017	103.4	6.02	0.063	17.57
MA-MIW 231-0040	7/19/2017	111.3	6.06	0.052	

Table B2 (Continued)

U.S. Geological Survey local site name	Sampling date	Specific conductance in microsiemens per centimeter at 25 degrees Celsius	pH in standard units	Dissolved oxygen in milligrams per liter	Temperature in degrees Celsius
MA-MIW 231-0070	7/19/2017	103.4	5.84	1.170	
MA-MIW 231-0105	7/19/2017	108.8	6.28	0.096	
MA-MIW 231-0138	7/19/2017	122.4	6.51	0.009	
MA-MIW 232-0050	7/18/2017	85.1	5.62	0.075	
MA-MIW 232-0080	7/18/2017	98.9	6.14	0.052	
MA-MIW 232-0115	7/18/2017	144.6	6.13	0.052	
MA-MIW 232-0150	7/18/2017	187.6	6.68	0.038	
MA-MIW 233-0016	7/26/2017	154.1	5.45	4.260	
MA-MIW 233-0070	7/26/2017	108.8	5.99	0.032	
MA-MIW 233-0174 (00MW0608B)	7/26/2017	152.3	6.78	0.027	
MA-MIW 233-0245 (00MW0608A)	7/26/2017	147.3	6.56	0.013	
MA-MIW 234-0055	7/20/2017	346.0	5.22	0.384	
MA-MIW 234-0086	7/20/2017	145.0	6.67	0.012	
MA-MIW 234-0120	7/20/2017	114.2	6.55	0.075	
MA-MIW 234-0150	7/20/2017	114.8	6.59	0.016	
MA-MIW 236-0025 (MAMW0396S)	7/27/2017	316.9	5.59	0.050	
MA-MIW 236-0109 (MAMW0296I)	7/27/2017	124.5	5.62	0.048	
MA-MIW 236-0189 (MAMW0196D)	7/27/2017	99.3	6.16	0.013	
MA-MIW 237-0145 (03MW2620B)	7/27/2017	109.1	6.37	0.106	
MA-MIW 237-0254 (03MW2620A)	7/27/2017	131.8	6.64	0.037	
MA-FSW 631-M01-01PT	9/12/2017	126.2	5.91	0.066	18.7
MA-FSW 631-M01-02GNT	9/12/2017	128.8	6.04	0.173	16.7
MA-FSW 631-M01-03RT	9/12/2017	128.7	6.26	2.680	13.9
MA-FSW 631-M01-04BUT	9/12/2017	129.9	6.34	1.850	11.8
MA-FSW 631-M01-06WT	9/12/2017	127.2	6.23	2.550	12.1
MA-FSW 631-M01-09Y	9/12/2017	125.4	6.22	7.750	14.9
MA-FSW 631-M01-12R	9/12/2017	123.0	6.05	0.450	14.6
MA-FSW 631-M01-15W	9/12/2017	114.9	5.96	0.077	14.8
MA-FSW 631-0256 (00MW0589A)	9/12/2017	113.6	6.27	0.049	14.3
MA-FSW 632-M01-01PT	9/11/2017	90.8	4.55	5.320	14.1

Table B2 (Continued)

U.S. Geological Survey local site name	Sampling date	Specific conductance in microsiemens per centimeter at 25 degrees Celsius	pH in standard units	Dissolved oxygen in milligrams per liter	Temperature in degrees Celsius
MA-FSW 632-M01-02GNT	9/11/2017	114.5	5.49	7.610	14.0
MA-FSW 632-M01-03RT	9/11/2017	122.5	5.80	4.110	14.2
MA-FSW 632-M01-05BKT	9/11/2017	119.3	5.94	0.040	14.5
MA-FSW 632-M01-06WT	9/11/2017	122.0	5.94	0.069	14.7
MA-FSW 632-M01-07O	9/11/2017	119.1	5.96	0.092	14.8
MA-FSW 632-M01-11GN	9/11/2017	116.3	6.01	0.008	15.0
MA-FSW 632-M01-15W	9/11/2017	104.3	6.22	0.044	15.4
MA-FSW 632-0195 (00MW0606B)	9/11/2017	103.6	5.74	0.009	14.3
MA-FSW 632-0325 (00MW0606A)	9/11/2017	177.6	6.18	0.031	14.4
MA-FSW 665-0040	9/12/2017	123.1	6.21	9.150	19.8
MA-FSW 665-0089	9/12/2017	120.8	6.36	0.244	15.2
MA-FSW 665-0139	9/12/2017	121.8	5.93	0.047	14.8
MA-FSW 665-0264 (03MW1014B)	9/12/2017	109.3	6.55	0.024	15.5
MA-FSW 665-0295 (03MW1014A)	9/12/2017	135.0	6.31	0.042	16.7
MA-FSW 722-M01-01PT	9/13/2017	121.0	6.15	2.140	23.0
MA-FSW 722-M01-02GNT	9/13/2017	123.7	6.26	2.920	23.2
MA-FSW 722-M01-06WT	9/13/2017	125.1	6.24	0.540	23.9
MA-FSW 722-M01-08GY	9/13/2017	126.0	6.21	0.357	20.6
MA-FSW 722-M01-09Y	9/13/2017	126.9	6.28	1.480	19.3
MA-FSW 722-M01-11GN	9/14/2017	124.0	6.17	6.060	19.7
MA-FSW 722-M01-12R	9/14/2017	126.2	6.22	4.390	21.7
MA-FSW 722-M01-14BK	9/14/2017	120.9	6.05	0.829	18.7
MA-FSW 722-M01-15W	9/14/2017	120.4	6.00	0.262	19.0
MA-FSW 722-M02-01PT	9/13/2017	95.5	5.96	0.077	22.2
MA-FSW 722-M02-03RT	9/13/2017	122.5	6.13	2.110	22.5
MA-FSW 722-M02-05BKT	9/13/2017	124.2	6.20	3.290	23.2
MA-FSW 722-M02-08GY	9/13/2017	124.9	6.29	2.180	24.1
MA-FSW 722-M02-10P	9/13/2017	125.2	6.27	1.300	24.2
MA-FSW 722-M02-12R	9/13/2017	124.0	6.23	0.276	24.0
MA-FSW 722-M02-15W	9/13/2017	125.6	6.26	0.077	22.5
MA-FSW 722-M01-02GNT	2/23/2018	127.5	6	12.28	1.5
MA-FSW 722-M01-06WT	2/23/2018	126.9	5.94	11.42	2.9
MA-FSW 722-M01-08GY	2/23/2018	122.6	5.93	4.4	7.5

Table B2 (Continued)

U.S. Geological Survey local site name	Sampling date	Specific conductance in microsiemens per centimeter at 25 degrees Celsius	pH in standard units	Dissolved oxygen in milligrams per liter	Temperature in degrees Celsius
MA-FSW 722-M01-09Y	2/23/2018	122.3	6.43	3.91	10.3
MA-FSW 722-M01-11GN	2/23/2018	120.3	6.45	5.77	8.9
MA-FSW 722-M01-12R	2/23/2018	122.6	6.35	3.85	9.4
MA-FSW 722-M02-01PT	2/23/2018	64.5	5.75	14.09	1.4
MA-FSW 722-M02-05BKT	2/23/2018	126.1	5.87	11.9	2.4
MA-FSW 722-M02-08GY	2/23/2018	126.8	5.95	12.08	2.4
MA-FSW 722-M02-15W	2/23/2018	125.2	5.9	11.29	6.3
FS-ASHPD-0001 (ECAMP02) Microlayer	9/11/2017				
FS-ASHPD-0001 (ECAMP02) 0.1m	9/11/2017	127.0	6.84	6.370	21.24
FS-ASHPD-0001 (ECAMP02) 1.00m	9/11/2017	122.0	6.93	8.850	21.32
FS-ASHPD-0001 (ECAMP02) 3.00m	9/11/2017	122.0	6.92	8.950	21.21
FS-ASHPD-0001 (ECAMP02) 5.00m	9/11/2017	123.0	6.94	8.610	21.17
FS-ASHPD-0001 (ECAMP02) 7.00m	9/11/2017	122.0	6.88	8.590	21.03
FS-ASHPD-0001 (ECAMP02) 9.00m	9/11/2017	123.0	6.77	7.850	20.81
FS-ASHPD-0001 (ECAMP02) 11.00m	9/11/2017	137.0	6.38	1.380	12.96
FS-ASHPD-0001 (ECAMP02) 13.00m	9/11/2017	139.0	6.40	1.400	12.43
FS-ASHPD-0001 (ECAMP02) 15.00m	9/11/2017	141.0	6.44	0.690	9.56
FS-ASHPD-0001 (ECAMP02) 17.00m	9/11/2017	142.0	6.48	0.590	9.29
FS-ASHPD-0001 (ECAMP02) Microlayer	11/8/2017				
FS-ASHPD-0001 (ECAMP02) 0.1m	11/8/2017	125.3	5.31	11.190	8.94
FS-ASHPD-0001 (ECAMP02) 1.00m	11/8/2017	124.3	6.90	9.880	14.6
FS-ASHPD-0001 (ECAMP02) 3.00m	11/8/2017	123.4	6.94	9.830	14.62
FS-ASHPD-0001 (ECAMP02) 5.00m	11/8/2017	125.4	6.94	9.770	14.65
FS-ASHPD-0001 (ECAMP02) 7.00m	11/8/2017	123.7	6.94	9.740	14.69
FS-ASHPD-0001 (ECAMP02) 9.00m	11/8/2017	123.5	6.94	9.730	14.68
FS-ASHPD-0001 (ECAMP02) 11.00m	11/8/2017	124.1	6.94	9.740	14.56
FS-ASHPD-0001 (ECAMP02) 13.00m	11/8/2017	123.5	6.89	9.430	14.17
FS-ASHPD-0001 (ECAMP02) 15.00m	11/8/2017	127.1	6.69	8.570	13.8
FS-ASHPD-0001 (ECAMP02) 17.00m	11/8/2017	140.9	6.46	6.480	9.76
FS-ASHPD-0009 (ECAMP01) Microlayer	9/11/2017				
FS-ASHPD-0009 (ECAMP01) 0.1m	9/11/2017	122.0	7.21	9.090	21.95
FS-ASHPD-0009 (ECAMP01) 1.00m	9/11/2017	123.0	7.24	9.610	22

113

Table B2 (Continued)					
U.S. Geological Survey local site name	Sampling date	Specific conductance in microsiemens per centimeter at 25 degrees Celsius	pH in standard units	Dissolved oxygen in milligrams per liter	Temperature in degrees Celsius
FS-ASHPD-0009 (ECAMP01) 3.00 m	9/11/2017	123.0	7.32	9.360	21.71
FS-ASHPD-0009 (ECAMP01) 5.00 m	9/11/2017	122.0	7.34	9.380	21.3
FS-ASHPD-0010 Microlayer	9/11/2017				
FS-ASHPD-0010 0.1m	9/11/2017	123.0	7.03	9.280	21.9
FS-ASHPD-0010 1.00m	9/11/2017	123.0	7.03	9.000	21.7
FS-ASHPD-0010 3.00m	9/11/2017	123.0	7.06	9.580	21.6
FS-ASHPD-0010 5.00m	9/11/2017	123.0	6.97	8.690	21.28
FS-ASHPD-0010 7.00m	9/11/2017	123.0	6.82	8.430	20.99
FS-ASHPD-0010 9.00m	9/11/2017	124.0	6.54	6.220	20.2
FS-ASHPD-0011 Microlayer	9/12/2017				
FS-ASHPD-0011 0.1m	9/12/2017	122.0	6.86	8.880	21.28
FS-ASHPD-0011 1.00m	9/12/2017	122.0	6.91	8.840	21.26
FS-ASHPD-0011 3.00m	9/12/2017	122.0	6.88	8.690	21.18
FS-ASHPD-0011 5.00m	9/12/2017	122.0	6.88	8.720	21.17
FS-ASHPD-0011 7.00m	9/12/2017	123.0	6.76	8.140	20.99
FS-ASHPD-0011 9.00m	9/12/2017	123.0	6.53	6.700	20.43
MI-JOHPD-0001 (ECJNP03) Microlayer	9/12/2017				
MI-JOHPD-0001 (ECJNP03) 0.1m	9/12/2017	107.0	7.32	9.440	22.4
MI-JOHPD-0001 (ECJNP03) 1.00m	9/12/2017	107.0	7.37	9.520	22.4
MI-JOHPD-0001 (ECJNP03) 3.00m	9/12/2017	107.0	7.38	9.440	22.4
MI-JOHPD-0001 (ECJNP03) 5.00m	9/12/2017	107.0	7.50	9.660	21.5
MI-JOHPD-0001 (ECJNP03) 7.00m	9/12/2017	107.0	7.16	9.030	21.3
MI-JOHPD-0001 (ECJNP03) 9.00m	9/12/2017	107.0	6.87	8.490	21
MI-JOHPD-0001 (ECJNP03) 11.00m	9/12/2017	108.0	6.24	2.980	18.9
MI-JOHPD-0001 (ECJNP03) 15.00	9/12/2017	124.0	6.38	0.530	10.27
MI-JOHPD-0008 Microlayer	9/12/2017				
MI-JOHPD-0008 0.1m	9/12/2017	106.0	6.95	9.050	22.3
MI-JOHPD-0008 1.00m	9/12/2017	106.0	7.02	9.110	21
MI-JOHPD-0008 3.00m	9/12/2017	106.0	7.05	9.280	21.5
MI-JOHPD-0008 5.00m	9/12/2017	107.0	7.01	9.060	21.4
MI-JOHPD-0008 7.00m	9/12/2017	106.0	6.93	9.060	21.3
MI-JOHPD-0008 9.00m	9/12/2017	106.0	6.79	8.480	21.2
ASHPD-GWOUT-L-N-LW	9/13/2017	121.6	6.99	9.530	23.7

114

Table B2 (Continued)

U.S. Geological Survey local site name	Sampling date	Specific conductance in microsiemens per centimeter at 25 degrees Celsius	pH in standard units	Dissolved oxygen in milligrams per liter	Temperature in degrees Celsius
ASHPD-GWOUT-L-N-015	9/13/2017	124.9	6.45	5.730	22.4
ASHPD-GWOUT-L-N-030	9/13/2017	124.8	6.51	5.660	22.1
ASHPD-GWOUT-L-N-050	9/13/2017	129.3	6.47	3.820	22.0
ASHPD-GWOUT-L-N-100	9/13/2017	127.6	6.35	1.620	22.4
ASHPD-GWOUT-R-N-LW	9/13/2017	122.0	6.85	8.980	22.4
ASHPD-GWOUT-R-N-015	9/13/2017	122.1	6.29	7.010	22.1
ASHPD-GWOUT-R-N-030	9/13/2017	121.7	6.38	6.530	21.5
ASHPD-GWOUT-R-N-050	9/13/2017	122.2	6.24	4.360	21.8
ASHPD-GWOUT-R-N-100	9/13/2017	122.6	6.17	2.870	22.4
ASHPD-GWOUT-R-S-015	9/13/2017	124.3	6.32	3.940	21.8
ASHPD-GWOUT-R-S-100	9/13/2017	122.9	6.23	4.510	22.3
ASHPD-KIGAM-124N-010E-LW	9/14/2017	129.7	7.03	11.430	22.4
ASHPD-KIGAM-124N-010E-015	9/14/2017	549.3	5.82	4.210	19.4
ASHPD-KIGAM-124N-010E-030	9/14/2017	550.9	5.73	4.460	17.5
ASHPD-KIGAM-124N-010E-050	9/14/2017	468.9	5.74	3.850	17.6
ASHPD-KIGAM-124N-010E-100	9/14/2017	330.9	5.85	1.910	17.0
ASHPD-KIGAM-131N-011E-LW	9/14/2017	126.7	7.02	11.550	22.3
ASHPD-KIGAM-131N-011E-015	9/14/2017	78.9	6.04	2.470	20.3
ASHPD-KIGAM-131N-011E-030	9/14/2017	82.8	5.98	1.960	19.2
ASHPD-KIGAM-131N-011E-050	9/14/2017	94.7	5.96	0.503	18.4
ASHPD-KIGAM-131N-011E-100	9/14/2017	94.3	5.95	0.420	18.4
ASHPD-GWIN-C-LW	9/11/2017	121.9	6.90	10.230	22.3
ASHPD-GWIN-C-035	9/11/2017	107.1	5.57	9.220	16.0
ASHPD-GWIN-C-100	9/11/2017	105.0	5.57	8.500	17.8
ASHPD-GWOUT-L-N-100	2/23/2018	135.4	6.65	7.15	5.3
ASHPD-GWOUT-R-N-LW	2/23/2018	129.2	6.97	13.57	5.4
ASHPD-GWOUT-R-N-100	2/23/2018	129.4	6.61	8.5	5.3
MA-FSW 239-M01-01PT	8/5/2016	624.6	5.26	1.35	19.9
MA-FSW 239-M01-02GNT	8/5/2016	742.9	5.09	1.65	15.4
MA-FSW 239-M01-04BUT	8/5/2016	676	5.08	2.82	13.3
MA-FSW 239-M01-06WT	8/5/2016	92.81	6.24	1.86	13.1
MA-FSW 239-M01-08GY	8/5/2016	85.77	5.88	0.047	12.8

Table B2 (Continued)

U.S. Geological Survey local site name	Sampling date	Specific conductance in microsiemens per centimeter at 25 degrees Celsius	pH in standard units	Dissolved oxygen in milligrams per liter	Temperature in degrees Celsius
MA-FSW 239-M01-10P	8/5/2016	83.38	5.96	2.17	12.6
MA-FSW 239-M01-12R	8/5/2016	123.1	5.86	3.51	12.1
MA-FSW 239-M01-14BK	8/5/2016	141.2	5.66	7.73	12.6
MA-FSW 300-M03-01PT	7/7/2016	152.9	5.25	1.91	14.8
MA-FSW 300-M03-03RT	7/7/2016	74.28	5.7	6.52	14.9
MA-FSW 300-M03-06WT	7/7/2016	126.8	5.88	0.285	13.6
MA-FSW 300-M03-09Y	7/7/2016	147.6	6.25	0.051	13.1
MA-FSW 300-M03-10P	7/7/2016	135.6	6.27	0.032	12.7
MA-FSW 300-M03-11GN	7/7/2016	130.1	6.25	0.048	12.5
MA-FSW 300-M03-14BK	7/7/2016	138.5	5.92	0.079	14.8
MA-FSW 300-M03-15W	7/7/2016	168.9	5.94	0.03	14.6
MA-FSW 300-M02-01PT	7/8/2016	186.4	5.88	0.157	13.3
MA-FSW 300-M02-02GNT	7/8/2016	225.1	5.98	0.121	12
MA-FSW 300-M02-03RT	7/8/2016	253.4	5.97	0.042	13
MA-FSW 300-M02-06WT	7/8/2016	168.9	5.77	6.17	12.4
MA-FSW 300-M02-08GY	7/8/2016	145.7	5.73	7.18	11.9
MA-FSW 300-M02-10P	7/8/2016	152.3	5.64	7.57	12.2
MA-FSW 300-M02-14BK	7/8/2016	163.8	5.49	7.8	12.3
MA-FSW 300-O138	7/7/2016	76.11	6.23	4.5	14.1
MA-FSW 424-M01-01PT	7/26/2016	143.5	6.02	0.029	13.8
MA-FSW 424-M01-03RT	7/26/2016	123.9	6.24	0.034	15.7
MA-FSW 424-M01-05BKT	7/26/2016	96.51	6.14	0.042	14.7
MA-FSW 424-M01-09Y	7/26/2016	99.85	5.93	6.73	15.1
MA-FSW 424-M01-13BU	7/26/2016	59.88	5.63	5.63	14.2
MA-FSW 424-M02-11GN 72-13	7/26/2016	159.7	5.96	0.025	14.3
MA-FSW 424-M02-12R 72-13	7/26/2016	162.7	5.92	0.032	13.6
MA-FSW 424-M02-14BK 72-13	7/26/2016	131.9	6.1	0.025	14.3
MA-FSW 424-M02-15W 72-13	7/26/2016	133.9	6.1	0.033	14.2
MA-FSW 564-M01-01PT	7/6/2016	122.3	5.09	3.34	13.3
MA-FSW 564-M01-02GNT	7/6/2016	72.2	5.58	5.74	12.4
MA-FSW 564-M01-04BUT	7/6/2016	174.1	5.84	6.23	13.1
MA-FSW 564-M01-05BKT	7/6/2016	283.2	5.72	7.43	13
MA-FSW 564-M01-06WT	7/6/2016	243.2	5.65	7.71	13.1

Table B2 (Continued)

U.S. Geological Survey local site name	Sampling date	Specific conductance in microsiemens per centimeter at 25 degrees Celsius	pH in standard units	Dissolved oxygen in milligrams per liter	Temperature in degrees Celsius
MA-FSW 564-M01-08GY	7/6/2016	162.7	5.66	6.54	13.4
MA-FSW 564-M01-10P	7/6/2016	164.7	5.76	7.46	13.2
MA-FSW 564-M01-12R	7/6/2016	165.9	5.79	7.57	13.2
MA-FSW 564-M01-14BK	7/6/2016	128.7	6.34	8.03	13.5
MA-FSW 621-M01-01PT	7/11/2016	146.4	5.17	5.63	11.3
MA-FSW 621-M01-02GNT	7/11/2016	133.6	5.96	0.08	11.4
MA-FSW 621-M01-03RT	7/11/2016	150.1	6.2	0.058	11.8
MA-FSW 621-M01-05BKT	7/11/2016	233.5	6	0.408	11.8
MA-FSW 621-M01-06WT	7/11/2016	105.3	6.05	2.18	11.9
MA-FSW 621-M01-07O	7/11/2016	107.7	5.97	3.3	12
MA-FSW 621-M01-09Y	7/11/2016	166.7	5.69	7.88	11.9
MA-FSW 621-M01-11GN	7/11/2016	166.1	5.65	7.78	12
MA-FSW 621-M01-13BU	7/11/2016	76.23	5.86	6.87	11.8
MA-FSW 621-M01-15W	7/11/2016	96.51	5.98	6.06	12
MA-FSW 622-M01-01PT	7/11/2016	182.9	5.39	6.62	11.6
MA-FSW 622-M01-02GNT	7/11/2016	104.2	5.85	4.65	11.8
MA-FSW 622-M01-03RT	7/11/2016	178.8	6.24	0.099	11.8
MA-FSW 622-M01-05BKT	7/11/2016	196.6	6.32	0.057	12.4
MA-FSW 622-M01-06WT	7/11/2016	153.1	6.44	0.342	12.2
MA-FSW 622-M01-07O	7/11/2016	170.9	6.31	0.144	12.5
MA-FSW 622-M01-09Y	7/11/2016	175.4	6.19	0.165	12.5
MA-FSW 622-M01-11GN	7/11/2016	163.6	5.6	7.35	12.2
MA-FSW 622-M01-13BU	7/11/2016	162.9	5.49	7.77	12.2
MA-FSW 622-M01-15W	7/11/2016	159.8	5.47	5.16	12.9
MA-FSW 744-0004	7/26/2016	208.4	5.36	2.91	16.4
MA-FSW 744-0008	7/26/2016	64.56	5.6	3.01	15.3
MA-FSW 744-0010	7/26/2016	77.97	5.54	3.68	13.6
MA-FSW 744-0011	7/26/2016	85.94	5.55	4.03	14
MA-FSW 744-0013	7/26/2016	94.9	5.51	4.36	13.1
MA-FSW 744-0017	7/26/2016	91.04	5.63	4.41	13.2
MA-FSW 744-0019	7/26/2016	63.76	5.72	3.22	13.2
MA-FSW 744-0023	7/26/2016	68.21	6.01	1.86	14
MA-FSW 744-0025	7/26/2016	81.27	5.97	1.26	13.2

Table B2 (Continued)

U.S. Geological Survey local site name	Sampling date	Specific conductance in microsiemens per centimeter at 25 degrees Celsius	pH in standard units	Dissolved oxygen in milligrams per liter	Temperature in degrees Celsius
MA-FSW 744-0026	7/26/2016	96.58	5.91	0.285	13.4
MA-FSW 744-0028	7/26/2016	115	5.98	0.099	14
MA-FSW 744-0029	7/26/2016	154.3	6.03	0.076	12.7
MA-FSW 744-0030	7/26/2016	145.5	6.05	0.088	13
Q1 MI-QUARV-00015(QR001)	8/15/2017	106.9		8.510	
Q3	8/15/2017	98.2		9.590	
Q4	8/15/2017	103.6		9.410	
Q5	8/15/2017	116.4		3.910	
Q9	8/15/2017	110.4		8.260	
Q-FC	8/15/2017	114.0		8.460	
Q-OBR	8/15/2017	100.5		9.830	
Q-TRIB	8/15/2017	66.8		8.610	
Quash_HS_Seep1	8/16/2017	74.8		5.004	
Quash_HS_Seep2	8/16/2017	60.6		9.318	
QB010	8/17/2017	470.3		3.567	
QB018	8/17/2017	266.3		6.087	
QB020	8/17/2017	80.0		9.763	
QB026	8/17/2017	59.6		0.422	
QB039	8/18/2017	135.0		7.675	
DD004	8/17/2017	157.6		5.592	
DD-12	8/17/2017	104.5		0.820	
Quash_OV_seep1	8/14/2017	109.8		0.043	
Quash_OV_seep2	8/14/2017	97.7		0.040	
Quash_HRTS_seep	8/14/2017	103.4		0.043	
QT008	8/17/2017	112.1		0.063	
QT018	8/17/2017	74.0		5.564	
QT030	8/17/2017	152.3		0.058	
QT034	8/17/2017	123.0		0.692	
QT039	8/17/2017	113.6		0.268	
QT082	8/18/2017	123.6		0.746	
QT101	8/17/2017	75.4		0.597	
QT122		182.7		3.779	
QT142	8/18/2017	183.7		1.097	

Table B2 (Continued)

U.S. Geological Survey local site name	Sampling date	Specific conductance in microsiemens per centimeter at 25 degrees Celsius	pH in standard units	Dissolved oxygen in milligrams per liter	Temperature in degrees Celsius
Quash-Spawn1	8/16/2017	72.5		6.853	
Quash-Spawn2	8/16/2017	51.8		5.419	
Quash-Spawn3	8/14/2017	42.6		9.054	

119

Table B3. PFAS tandem mass spectrometry parameters. The Agilent Optimizer program was used to optimize product ions, fragmentor voltages, and collision energies.

Analyte	Type	Internal Standard	Precursor Ion	Product Ion (Quantifier)	Quantifier Collision Energy (V)	Product Ion (Qualifier)	Qualifier Collision Energy (V)	Fragmentor Voltage (V)
Perfluoroalkyl Carboxylates								
PFBA	Target	[$^{13}C_4$]PFBA	213	169	2			60
PFPeA	Target	[$^{13}C_5$]PFPeA	263	219	2			60
PFHxA	Target	[$^{13}C_5$]PFHxA	313	269	2	119		70
PFHpA	Target	[$^{13}C_4$]PFHpA	363	319	2	169/119	10/18	70
PFOA	Target	[$^{13}C_8$]PFOA	413	369	2	169	10	80
PFNA	Target	[$^{13}C_9$]PFNA	463	419	2	219/169	10/14	75
PFDA	Target	[$^{13}C_6$]PFDA	513	469	6	269/219	14/14	85
PFUnDA	Target	[$^{13}C_7$]PFUnDA	563	519	6	269/169	14/22	95
PFDoDA	Target	[$^{13}C_2$]PFDoDA	613	569	6	269/169	14/26	90
PFTrDA	Target	[$^{13}C_2$]PFDoDA	663	619	6	169	26	95
PFTeDA	Target	[$^{13}C_2$]PFTeDA	713	669	6	169	25	100
Perfluoroalkane Sulfonates								
PFBS	Target	[$^{13}C_3$]PFBS	299	80	38	99	30	95
PFPeS	Target	[$^{13}C_3$]PFHxS	349	80	38	99	30	140
PFHxS	Target	[$^{13}C_3$]PFHxS	399	80	58	99	34	135
PFHpS	Target	[$^{13}C_8$]PFOS	449	80	54	99	42	180
PFOS	Target	[$^{13}C_8$]PFOS	499	80	60	99	50	200
PFNS	Target	[$^{13}C_8$]PFOS	549	80	60	99	54	175
PFDS	Target	[$^{13}C_8$]PFOS	599	80	60	99	54	175
Fluorotelomer Sulfonates								
4:2 FtS	Target	[$^{13}C_2$] 4:2 FtS	327	307	10	81	30	130
6:2 FtS	Target	[$^{13}C_2$] 6:2 FtS	427	407	18	81	34	135
8:2 FtS	Target	[$^{13}C_2$] 8:2 FtS	527	507	26	81	42	180
Perfluoroalkyl Sulfonamides								

120

Table B3 (Continued)

Analyte	Type	Internal Standard	Precursor Ion	Product Ion (Quantifier)	Quantifier Collision Energy (V)	Product Ion (Qualifier)	Qualifier Collision Energy (V)	Fragmentor Voltage (V)
FOSA	Target	[$^{13}C_8$] FOSA	498	78	38			140
Perfluoroalkyl Sulfonamidoacetic Acids								
EtFOSAA	Target	d5-N-EtFOSAA	584	419	18	526	14	95
MeFOSAA	Target	d3-N-MeFOSAA	570	419	14	483	10	95
Internal Standards								
[$^{13}C_4$] PFBA	ISTD		217	172	2			60
[$^{13}C_5$] PFPeA	ISTD		268	223	2			60
[$^{13}C_5$] PFHxA	ISTD		318	273	2			70
[$^{13}C_4$] PFHpA	ISTD		367	322	2			70
[$^{13}C_8$] PFOA	ISTD		421	376	2			75
[$^{13}C_9$] PFNA	ISTD		472	427	2			85
[$^{13}C_6$] PFDA	ISTD		519	474	2			90
[$^{13}C_7$] PFUnDA	ISTD		570	525	6			85
[$^{13}C_2$] PFDoDA	ISTD		615	570	6			95
[$^{13}C_2$] PFTeDA	ISTD		715	670	6			95
[$^{13}C_3$] PFBS	ISTD		302	99	26			95
[$^{13}C_3$] PFHxS	ISTD		402	99	38			180
[$^{13}C_8$] PFOS	ISTD		507	99	50			180
[$^{13}C_2$] 4:2 FtS	ISTD		329	81	38			95
[$^{13}C_2$] 6:2 FtS	ISTD		429	81	46			95
[$^{13}C_2$] 8:2 FtS	ISTD		529	81	46			180
[$^{13}C_8$] FOSA	ISTD		506	78	38			95
d5-N-EtFOSAA	ISTD		589	419	14			95
d3-N-MeFOSAA	ISTD		573	419	14			100

121

Table B4. Average recovery (%) and relative standard deviation (RSD %) for deionized water spiked with 7.5 ng L^{-1}, 75 ng L^{-1}, and 750 ng L^{-1}.

Analyte	7.5 ng L^{-1} Spike (n=7)		75 ng L^{-1} Spike (n=6)		750 ng L^{-1} Spike (n=6)	
	Recovery (%)	RSD (%)	Recovery (%)	RSD (%)	Recovery (%)	RSD (%)
PFBA	88.8	20.0	99.2	7.13	98.6	3.44
PFPeA	108	10.0	102	4.42	99.7	4.02
PFHxA	104	9.18	103	5.51	100	3.95
PFHpA	105	9.07	101	7.27	100	3.82
PFOA	104	9.88	100	5.72	100	3.97
PFNA	107	10.1	102	5.44	101	3.27
PFDA	102	10.2	100	5.46	99.0	5.28
PFUnDA	104	9.57	102	6.22	98.7	5.61
PFDoDA	105	10.5	101	6.90	99.4	3.93
PFTrDA	109	13.8	107	7.27	108	4.33
PFTeDA	107	8.73	102	6.37	99.8	3.79
PFBS	106	9.56	101	5.02	97.0	4.19
PFPeS	125	21.1	107	5.15	122	16.0
PFHxS Linear	120	14.7	109	7.48	107	12.1
PFHxS Branched	118	8.81	98.5	9.06	97.3	5.73
PFHpS	102	11.8	102	4.98	102	3.49
PFOS Linear	111	9.56	102	6.66	100	3.70
PFOS Branched	103	9.76	88.2	11.7	89.8	3.88
PFNS	102	8.22	97.7	9.27	95.9	4.31
PFDS	102	12.3	99.1	9.22	95.4	3.24
4:2 FtS	98.8	11.6	98.6	7.36	97.1	6.63
6:2 FtS	81.6	16.2	83.4	5.75	83.6	5.88
8:2 FtS	107	11.1	101	4.63	102	7.54
MeFOSAA	100	13.9	102	7.92	93.6	5.65
EtFOSAA	109	15.8	98.5	6.94	89.9	8.99
FOSA	91.8	15.6	84.8	18.3	91.7	5.56

122

Table B5. Average recovery (%) and relative standard deviation (RSD %) for samples spiked with 75 ng L^{-1}.

Analyte	75 ng L^{-1} Spike (n=18)	
	Recovery (%)	RSD (%)
PFBA	102	5.65
PFPeA	103	7.14
PFHxA	104	5.77
PFHpA	102	6.31
PFOA	102	6.23
PFNA	103	5.91
PFDA	101	5.66
PFUnDA	102	5.63
PFDoDA	101	6.53
PFTrDA	99.6	11.7
PFTeDA	103	5.41
PFBS	105	5.47
PFPeS	96.9	10.5
PFHxS Linear	96.3	12.4
PFHxS Branched	90.8	12.9
PFHpS	103	5.93
PFOS Linear	101	6.97
PFOS Branched	90.2	11.9
PFNS	97.6	6.60
PFDS	97.5	10.6
4:2 FtS	104	9.23
6:2 FtS	83.3	8.66
8:2 FtS	103	6.81
MeFOSAA	99.2	8.36
EtFOSAA	96.0	9.16
FOSA	85.4	13.7

123

Table B6. Average recovery (%) for oxidized deionized water and oxidized sample spikes. The native spike was added after oxidation and before solid phase extraction to prevent the oxidation process from degrading the PFAA precursors in the native spike.

| Analyte | DI Water Spikes | | | | Sample Matrix Spikes | | | |
	7.5 ng L⁻¹ Recovery (%)	75 ng L⁻¹ Recovery (%)	75 ng L⁻¹ Recovery (%)	750 ng L⁻¹ Recovery (%)	75 ng L⁻¹ Recovery (%)	75 ng L⁻¹ Recovery (%)	75 ng L⁻¹ Recovery (%)	75 ng L⁻¹ Recovery (%)
PFBA	70.4	105	103	115	108	113		97.2
PFPeA	125	125	104	118	117	104		103
PFHxA	130	121	102	113	123	106		102
PFHpA	96.5	115	97.9	117	118	102		94.7
PFOA	105	116	96.8	114	116	110		98.0
PFNA	110	118	102	114	117	110		104
PFDA	107	113	96.4	115	118	109		102
PFUnDA	106	113	98.3	114	117	108		100
PFDoDA	105	116	100	116	119	104		100
PFTrDA	94.5	120	98.4	122	125	102		105
PFTeDA	104	114	99.7	113	119	104		98.8
PFBS	94.3	109	96.1	116	112	105		97.9
PFPeS	109	106	94.2	127	100	141		94.4
PFHxS Linear	106	118	107	117	106	127		92.7
PFHxS Branched	<MQL	92.7	103	92.2	86.6	114		84.0
PFHpS	85.6	117	81.8	147	113	90.8		82.5
PFOS Linear	98.8	114	92.9	137	117	101		88.4
PFOS Branched	<MQL	94.7	57.8	105	97.6	69.9		59.5
PFNS	78.8	109	76.3	128	107	100		69.3
PFDS	90.1	113	81.4	132	117	100		85.6
4:2 FtS	114	112	98.0	112	113	108		107
6:2 FtS	82.1	89.0	82.1	108	100	86.7		91.3
8:2 FtS	102	109	91.2	125	112	103		93.1
MeFOSAA	97.9	115	94.4	107	121	104		100
EtFOSAA	92.7	118	96.9	117	114	93.4		93.7
FOSA	94.0	99.2	96.1	104	110	94.3		92.2

Table B7. Method detection limit (MDL) and method quantification limit (MQL) in ng L^{-1} for all analysis dates of unoxidized water.

Date Analyzed	1/12/2018		1/16/2018		1/25/2018		2/6/2018		2/12/2018		2/19/2018		3/7/2018		3/13/2018		3/20/2018		4/23/2018	
	MDL	MQL	MDL	MQL	MDL	MQL	MDL	MQL	MDL	MQL	MDL	MQL	MDL	MQL	MDL	MQL	MDL	MQL	MDL	MQL
PFBA	0.72	2.4	0.85	2.83	0.8	2.68	1.81	6.02	1.38	4.6	1.52	5.06	1.91	6.37	1.43	4.77	1.35	4.49	1.96	6.53
PFPeA	0.78	2.6	0.5	1.66	0.78	2.61	0.65	2.18	0.8	2.65	1.01	3.36	0.88	2.92	1.21	4.03	0.64	2.14	2.79	9.29
PFHxA	0.58	1.93	0.68	2.27	0.56	1.86	0.47	1.57	0.48	1.6	0.56	1.88	0.69	2.29	0.77	2.56	0.57	1.92	0.66	2.18
PFHpA	0.31	1.04	0.28	0.93	0.19	0.65	0.2	0.67	0.21	0.7	0.27	0.9	0.33	1.1	0.37	1.23	0.35	1.18	0.4	1.33
PFOA	0.15	0.5	0.25	0.83	0.16	0.54	0.25	0.84	0.24	0.8	0.23	0.76	0.33	1.1	0.38	1.28	0.36	1.18	0.63	2.09
PFNA	0.32	1.05	0.23	0.78	0.16	0.53	0.32	1.06	0.31	1.02	0.22	0.73	0.17	0.55	0.32	1.07	0.31	1.02	0.47	1.56
PFDA	0.37	1.25	0.19	0.63	0.24	0.82	0.23	0.77	0.23	0.78	0.3	0.98	0.31	1.03	0.21	0.69	0.23	0.76	0.22	0.72
PFUnDA	0.63	2.12	0.32	1.06	0.27	0.89	0.28	0.93	0.22	0.74	0.2	0.67	0.29	0.96	0.15	0.48	0.12	0.41	0.29	0.96
PFDoDA	0.39	1.3	0.26	0.85	0.2	0.67	0.29	0.96	0.27	0.89	0.12	0.39	0.21	0.69	0.16	0.54	0.2	0.66	0.27	0.91
PFTrDA	0.68	2.25	0.18	0.6	0.28	0.93	0.3	0.99	0.24	0.79	0.25	0.82	0.57	2.03	0.11	0.36	0.17	0.58	0.42	1.4
PFTeDA	0.47	1.56	0.46	1.53	0.95	3.16	0.99	3.29	0.61	2.03	0.69	2.28	0.73	2.43	0.2	0.66	0.25	0.82	0.48	1.61
PFBS	0.34	1.13	0.24	0.81	0.33	1.09	0.42	1.41	0.44	1.46	0.59	1.97	0.98	3.26	0.76	2.54	0.6	1.99	0.56	1.86
PFPeS	0.24	0.81	0.21	0.69	0.2	0.65	0.23	0.78	0.18	0.6	0.19	0.65	0.39	1.32	0.3	0.99	0.27	0.92	0.37	1.23
Linear PFHxS	0.32	1.06	0.41	1.35	0.32	1.07	0.37	1.23	0.34	1.13	0.36	1.18	0.41	1.36	0.39	1.31	0.35	1.18	0.68	2.25
Branched PFHxS	0.46	1.53	0.5	1.65	0.46	1.53	0.44	1.48	0.4	1.32	0.42	1.39	0.5	1.67	0.63	2.08	0.47	1.56	1.03	3.42
PFHpS	0.21	0.7	0.25	0.82	0.15	0.5	0.24	0.79	0.2	0.65	0.21	0.71	0.23	0.78	0.32	1.05	0.38	1.28	0.31	1.05
Linear PFOS	0.28	0.93	0.23	0.77	0.15	0.49	0.14	0.47	0.14	0.47	0.16	0.54	0.24	0.79	0.28	0.94	0.26	0.87	0.41	1.37
Branched PFOS	0.42	1.41	0.42	1.41	0.26	0.88	0.22	0.74	0.23	0.76	0.28	0.94	0.41	1.36	0.45	1.52	0.43	1.42	0.51	1.71
PFNS	0.29	0.96	0.5	1.68	0.23	0.78	0.18	0.61	0.27	0.91	0.27	0.9	0.16	0.52	0.49	1.63	0.22	0.75	0.41	1.38
PFDS	0.56	1.87	0.19	0.63	0.56	1.85	0.46	1.55	0.12	0.38	0.2	0.65	0.67	2.24	0.15	0.49	0.15	0.5	0.42	1.39
4:2 FtS	0.2	0.66	0.21	0.71	0.15	0.52	0.14	0.46	0.2	0.66	0.2	0.68	0.04	0.15	0.21	0.69	0.14	0.45	0.21	0.71
8:2 FtS	0.4	1.34	0.11	0.37	0.44	1.46	0.58	1.94	0.21	0.7	0.46	1.55	0.16	0.55	0.11	0.38	0.11	0.36	0.35	1.18
N-MeFOSAA	0.27	0.89	0.16	0.55	0.13	0.42	0.7	2.34	0.22	0.74	0.18	0.6	0.46	1.55	0.1	0.35	0.12	0.4	0.25	0.84
N-EtFOSAA	0.55	1.83	0.3	1.01	0.19	0.62	0.29	0.98	0.32	1.06	0.14	0.48	0.18	0.59	0.14	0.48	0.16	0.52	0.18	0.62
FOSA	1.14	3.79	0.31	1.03	0.41	1.35	0.38	1.28	0.45	1.49	0.45	1.49	0.13	0.42	0.18	0.61	0.1	0.32	0.37	1.23

Table B8. Method detection limit (MDL) and method quantification limit (MQL) in ng L^{-1} for all analysis dates for samples oxidized with the total oxidizable precursor assay.

Date Analyzed	6/12/2018		7/9/2018	
	MDL	**MQL**	**MDL**	**MQL**
PFBA	1.39	4.62	1.48	4.95
PFPeA	0.65	2.15	0.59	1.97
PFHxA	0.92	3.06	0.68	2.27
PFHpA	0.37	1.24	0.19	0.64
PFOA	0.39	1.29	0.26	0.85
PFNA	0.23	0.76	0.22	0.74
PFDA	0.43	1.44	0.29	0.96
PFUnDA	0.43	1.43	0.3	0.99
PFDoDA	0.22	0.72	0.22	0.73
PFTrDA	0.19	0.64	0.15	0.5
PFTeDA	0.2	0.67	0.3	1
PFBS	0.46	1.54	0.49	1.65
PFPeS	0.26	0.85	0.74	2.48
PFHxS Linear	0.51	1.69	0.4	1.33
PFHxS Branched	0.6	2.02	0.46	1.54
PFHpS	0.17	0.57	0.09	0.28
PFOS Linear	0.48	1.6	0.19	0.64
PFOS Branched	0.67	2.22	0.49	1.62
PFNS	0.32	1.06	0.24	0.79
PFDS	0.24	0.81	0.13	0.45
4:2 FtS	1.14	3.79	0.57	1.89
8:2 FtS	0.7	2.34	0.45	1.51
N-MeFOSAA	0.35	1.17	0.25	0.82
N-EtFOSAA	0.45	1.49	0.26	0.87
FOSA	0.98	3.28	0.26	0.87

Table B9. Perfluorinated carboxylate sample concentrations (ng L^{-1}).

U.S. Geological Survey local site name	Sampling date	Date Analyzed	PFBA	PFPeA	PFHxA	PFHpA	PFOA	PFNA	PFDA	PFUnDA	PFDoDA	PFTrDA	PFTeDA
DI H2O From Peristaltic Geopump For MLSs	9/11/2017	1/16/2018	<MDL	<MDL	<MDL	<MDL	<MDL	<MDL	<MDL	<MDL	<MDL	<MDL	<MDL
DI H2O From Grundfos Pump	9/12/2017	1/16/2018	<MDL	<MDL	<MDL	<MDL	<MDL	<MQL	<MDL	<MDL	<MDL	<MDL	<MDL
DI H2O From Keck Pump	9/12/2017	1/16/2018	<MDL	<MDL	<MDL	<MDL	<MDL	<MDL	<MDL	<MDL	<MDL	<MDL	<MDL
DI H2O From Henry Sampler	9/14/2017	1/16/2018	<MDL	<MDL	<MDL	<MDL	<MDL	<MDL	<MDL	<MDL	<MDL	<MDL	<MDL
DI H2O From Microlayer Sampling Device	9/12/2017	1/16/2018	<MDL	<MDL	<MDL	<MDL	<MDL	<MDL	<MDL	<MDL	<MDL	<MDL	<MDL
DI H2O From Boat Peristaltic Geopump	9/12/2017	1/16/2018	<MDL	<MDL	<MDL	<MDL	<MDL	<MDL	<MDL	<MDL	<MDL	<MDL	<MDL
DI H2O From Boat Peristaltic Geopump	11/8/2017	1/16/2018	<MDL	<MDL	<MDL	<MDL	<MQL	<MDL	<MDL	<MDL	<MDL	<MDL	<MDL
DI H2O From MA-FSW 631-02GNT	2/22/2018	4/23/2018	<MDL	<MDL	<MDL	<MDL	<MDL	<MDL	<MDL	<MDL	<MDL	<MDL	<MDL
DI H2O From Henry Sampler	2/22/2018	4/23/2018	<MDL	<MDL	<MDL	<MDL	<MDL	<MDL	<MDL	<MDL	<MDL	<MDL	<MDL
MA-MIW 207-0069 (00MW0582B)	7/26/2017	1/16/2018	<MDL	6.75	10.355	8.89	25.715	6.995	<MQL	<MDL	<MDL	<MDL	<MDL
MA-MIW 207-0215 (00MW0582A)	7/26/2017	1/16/2018	8.81	30.96	135.22	19.08	123.71	6.2	<MQL	<MDL	<MDL	<MDL	<MDL
MA-MIW 209-0015 (00MW0584C)	7/21/2017	1/25/2018	<MDL	<MQL	<MQL	1.3	3.3	<MQL	<MQL	<MDL	<MDL	<MDL	<MDL
MA-MIW 209-0146 (00MW0584B)	7/21/2017	1/25/2018	2.99	22.59	23.12	12.24	22.65	12.85	<MDL	<MDL	<MDL	<MDL	<MDL
MA-MIW 209-0286 (00MW0584A)	7/21/2017	1/25/2018	<MDL	<MDL	<MDL	<MDL	<MQL	<MDL	<MDL	<MDL	<MDL	<MDL	<MDL
MA-MIW 210-0026	7/25/2017	1/25/2018	<MDL	<MDL	2.53	1.23	3.78	1.5	<MDL	<MDL	<MDL	<MDL	<MDL
MA-MIW 210-0046	7/25/2017	1/25/2018	<MDL	<MDL	<MDL	<MDL	<MQL	<MQL	<MDL	<MDL	<MDL	<MDL	<MDL
MA-MIW 210-0075 (00MW0609B)	7/25/2017	1/25/2018	<MDL	<MDL	<MDL	<MQL	<MQL	<MDL	<MDL	<MDL	<MDL	<MDL	<MDL
MA-MIW 210-0145	7/25/2017	1/25/2018	<MDL	<MDL	<MDL	<MDL	<MDL	<MDL	<MDL	<MDL	<MDL	<MDL	<MDL

Table B9 (Continued)

(00MW0609A)

U.S. Geological Survey local site name	Sampling date	Date Analyzed	PFBA	PFPeA	PFHxA	PFHpA	PFOA	PFNA	PFDA	PFUnDA	PFDoDA	PFTrDA	PFTeDA
MA-MIW 221-0245 (03MW1003B)	7/28/2017	1/25/2018	<MQL	14.35	19.09	9.19	19.48	8.2	<MDL	<MDL	<MDL	<MDL	<MDL
MA-MIW 221-0325 (03MW1003A)	7/28/2017	1/25/2018	<MDL	<MDL	<MDL	<MDL	<MQL	<MDL	<MDL	<MDL	<MDL	<MDL	<MDL
MA-MIW 223-0111 (03MW1005B)	7/25/2017	1/25/2018	<MDL	<MQL	<MDL	<MQL	<MQL	<MDL	<MDL	<MDL	<MDL	<MDL	<MDL
MA-MIW 223-0148 (03MW1005A)	7/25/2017	1/25/2018	<MDL	<MDL	<MDL	<MQL	0.62	<MQL	<MDL	<MDL	<MDL	<MDL	<MDL
MA-MIW 230-0015	7/20/2017	1/25/2018	26.09	150.1 / 4	206.46	79.84	68.77	129.17	1.9	<MDL	<MDL	<MDL	<MDL
MA-MIW 230-0060	7/20/2017	1/25/2018	<MDL	12.02	14.89	9.08	17.08	25.9	<MDL	<MDL	<MDL	<MDL	<MDL
MA-MIW 230-0110	7/20/2017	1/25/2018	<MDL	9.4	13.55	8.41	14.62	26.21	<MDL	<MDL	<MDL	<MDL	<MDL
MA-MIW 230-0174 (03MW2626B)	7/19/2017	1/25/2018	<MQL	17.4	23.01	11.5	24.41	15.47	<MDL	<MDL	<MDL	<MDL	<MDL
MA-MIW 230-0294 (03MW2626A)	7/19/2017	1/25/2018	<MDL	9.42	19.31	6.57	15.24	12.02	<MDL	<MDL	<MDL	<MDL	<MDL
MA-MIW 231-0040	7/19/2017	1/25/2018	4.74	29.55	33.71	16.44	34.25	19.95	<MDL	<MDL	<MDL	<MDL	<MDL
MA-MIW 231-0070	7/19/2017	1/25/2018	<MQL	12.96 / 17.94	18.13	9.72	18.6	11.08	<MDL	<MDL	<MDL	<MDL	<MDL
MA-MIW 231-0105	7/19/2017	1/25/2018	<MQL	18.59 / 5	23.55	11.9	24.885	11.775	<MDL	<MDL	<MDL	<MDL	<MDL
MA-MIW 231-0138	7/19/2017	1/12/2018	8.92	5	23.53	11.4	21.46	10.99	<MDL	<MDL	<MDL	<MDL	<MDL
MA-MIW 232-0050	7/18/2017	1/25/2018	<MDL	<MQL	2.27	1.63	3.79	<MQL Qual	<MQL	<MDL	<MDL	<MDL	<MDL
MA-MIW 232-0080	7/18/2017	1/25/2018	<MDL	4.62	12.9	2.72	22.52	<MDL	<MDL	<MDL	<MDL	<MDL	<MDL
MA-MIW 232-0115	7/18/2017	1/25/2018	<MQL	13.85	18.4	9.05	21.44	1.18	<MDL	<MDL	<MDL	<MDL	<MDL
MA-MIW 232-0150	7/18/2017	1/25/2018	2.93	17.8	22.18	10.63	26.47	<MDL	<MDL	<MDL	<MDL	<MDL	<MDL
MA-MIW 233-0016	7/26/2017	1/25/2018	<MDL	3.45	3.27	4.83	17.29	2.26	<MDL	<MDL	<MDL	<MDL	<MDL
MA-MIW 233-0070	7/26/2017	1/25/2018	3.85	14.46	17.73	9.86	22.9	3.05	<MDL	<MDL	<MDL	<MDL	<MDL
MA-MIW 233-0174 (00MW0608B)	7/26/2017	1/25/2018	<MQL	11.70 / 5	18.02	5.74	13.855	7.875	<MQL	<MDL	<MDL	<MDL	<MDL

128

Table B9 (Continued)

U.S. Geological Survey local site name	Sampling date	Date Analyzed	PFBA	PFPeA	PFHxA	PFHpA	PFOA	PFNA	PFDA	PFUnDA	PFDoDA	PFTrDA	PFTeDA
MA-MIW 233-0245 (00MW0608A)	7/26/2017	1/25/2018	<MQL	10.12	16.14	4.97	12.84	8.5	<MDL	<MDL	<MDL	<MDL	<MDL
MA-MIW 234-0055	7/20/2017	1/25/2018	<MQL	5.42	6.33	2.87	5.16	<MQL	<MDL	<MDL	<MDL	<MDL	<MDL
MA-MIW 234-0086	7/20/2017	1/25/2018	<MQL	8.52	13.415	3.935	17.905	<MQL	<MDL	<MDL	<MDL	<MDL	<MDL
MA-MIW 234-0120	7/20/2017	1/25/2018	<MQL	14.48	23.12	6.36	25.9	<MDL	<MDL	<MDL	<MDL	<MDL	<MDL
MA-MIW 234-0150	7/20/2017	1/25/2018	<MQL	10.62	19.34	4.39	27.81	<MDL	<MDL	<MDL	<MDL	<MDL	<MDL
MA-MIW 236-0025 (MAMW0396S)	7/27/2017	1/25/2018	<MQL	6.86	6.85	4.27	8.84	13.31	<MDL	<MDL	<MDL	<MDL	<MDL
MA-MIW 236-0109 (MAMW0296I)	7/27/2017	1/25/2018	7.31	23.49	26.41	14.94	27.86	14.52	<MDL	<MDL	<MDL	<MDL	<MDL
MA-MIW 236-0189 (MAMW0196D)	7/27/2017	1/25/2018	3.61	17.35	22.48	11.23	22.86	8.92	<MDL	<MDL	<MDL	<MDL	<MDL
MA-MIW 237-0145 (03MW2620B)	7/27/2017	1/16/2018	4.85	22.66	33.28	12.92	37.22	4.17	<MDL	<MDL	<MDL	<MDL	<MDL
MA-MIW 237-0254 (03MW2620A)	7/27/2017	1/16/2018	<MQL	15.84	73.3	10.18 40.28	83.67	4.37	<MDL	<MDL	<MDL	<MDL	<MDL
MA-FSW 631-M01-01PT	9/12/2017	1/16/2018	17.995	92.71	124.12	5	72.205	22.06	<MQL	<MDL	<MDL	<MDL	<MDL
MA-FSW 631-M01-02GNT	9/12/2017	1/16/2018	23.03	29.69	43.3	22.42	71.15	10.04	<MQL	<MDL	<MDL	<MDL	<MDL
MA-FSW 631-M01-03RT	9/12/2017	1/16/2018	11.87	<MQL	<MQL	<MQL	3	1.18	<MDL	<MDL	<MDL	<MDL	<MDL
MA-FSW 631-M01-04BUT	9/12/2017	1/16/2018	<MQL	2.49	4.175	7.845	19.48	3.49	<MQL	<MDL	<MDL	<MDL	<MDL
MA-FSW 631-M01-06WT	9/12/2017	1/16/2018	<MDL	<MDL	<MDL	<MDL	0.84	<MQL	<MDL	<MDL	<MDL	<MDL	<MDL
MA-FSW 631-M01-09Y	9/12/2017	1/16/2018	<MDL	<MDL	<MDL	1.19	5.28	1.05	<MDL	<MDL	<MDL	<MDL	<MDL
MA-FSW 631-M01-12R	9/12/2017	1/16/2018	<MDL	<MDL	<MDL	<MQL	6.86	1.44	<MDL	<MDL	<MDL	<MDL	<MDL
MA-FSW 631-M01-15W	9/12/2017	1/16/2018	9.13	44.09	46.41	18.15	42.57	7	<MQL	<MDL	<MDL	<MDL	<MDL
MA-FSW 631-0256 (00MW0589A)	9/12/2017	1/25/2018	4.06	20.79	28.48	11.03	28.5	15.77	<MDL	<MDL	<MDL	<MDL	<MDL
MA-FSW 632-M01-01PT	9/11/2017	2/6/2018	<MDL	<MDL	<MQL	0.87	2.62	<MQL	<MDL	<MDL	<MDL	<MDL	<MDL
MA-FSW 632-M01-	9/11/2017	2/6/2018	<MDL	<MQL	1.67	0.87	3.2	1.2	<MDL	<MDL	<MDL	<MDL	<MDL

129

Table B9 (Continued)

U.S. Geological Survey local site name	Sampling date	Date Analyzed	PFBA	PFPeA	PFHxA	PFHpA	PFOA	PFNA	PFDA	PFUnDA	PFDoDA	PFTrDA	PFTeDA
02GNT													
MA-FSW 632-M01-03RT	9/11/2017	2/6/2018	<MDL	<MQL	<MQL	0.85	2.19	<MQL	<MQL	<MDL	<MDL	<MDL	<MDL
MA-FSW 632-M01-05BKT	9/11/2017	2/6/2018	19.43	56.01	89.25	40.08	80.14	9.47	<MQL	<MDL	<MDL	<MDL	<MDL
MA-FSW 632-M01-06WT	9/11/2017	2/6/2018	<MQL	8.97	10.69	7.22	19.41	3.6	<MQL	<MDL	<MDL	<MDL	<MDL
MA-FSW 632-M01-07O	9/11/2017	2/6/2018	<MDL	<MDL	<MDL	0.86	4.77	1.29	<MDL	<MDL	<MDL	<MDL	<MDL
MA-FSW 632-M01-11GN	9/11/2017	2/6/2018	<MQL	15.1	20.15	9.87	20.95	3.71	<MDL	<MDL	<MDL	<MDL	<MDL
MA-FSW 632-M01-15W	9/11/2017	2/6/2018	6.59	24.665	34.69	14.005	36.3	11.555	<MDL	<MDL	<MDL	<MDL	<MDL
MA-FSW 632-0195 (00MW0606B)	9/11/2017	1/16/2018	4.28	19.65	28.37	12.33	33.05	4.64	<MQL	<MDL	<MDL	<MDL	<MDL
MA-FSW 632-0325 (00MW0606A)	9/11/2017	1/16/2018	<MDL	3.67	5.56	2.91	8.74	2.03	<MDL	<MDL	<MDL	<MDL	<MDL
MA-FSW 665-0040	9/12/2017	1/16/2018	<MDL	<MDL	<MDL	<MDL	<MQL	<MQL	<MDL	<MDL	<MDL	<MDL	<MDL
MA-FSW 665-0089	9/12/2017	1/16/2018	<MDL	2.965	3.635	3.545	14.85	2.33	<MDL	<MDL	<MDL	<MDL	<MDL
MA-FSW 665-0139	9/12/2017	1/16/2018	<MDL	2.74	2.43	<MQL Qual	7.38	1.94	<MDL	<MDL	<MDL	<MDL	<MDL
MA-FSW 665-0264 (03MW1014B)	9/12/2017	1/16/2018	5.4	26.28	32.62	13.58	29.38	26.02	<MDL	<MDL	<MDL	<MDL	<MDL
MA-FSW 665-0295 (03MW1014A)	9/12/2017	1/16/2018	<MQL	15.84	31.79	8.57	20.07	10.92	<MDL	<MDL	<MDL	<MDL	<MDL
MA-FSW 722-M01-01PT	9/13/2017	2/12/2018	<MDL	<MDL	<MDL	<MQL	2.465	1.75	<MDL	<MQL	<MDL	<MDL	<MDL
MA-FSW 722-M01-02GNT	9/13/2017	2/12/2018	<MQL	<MDL	1.69	2.08	16.35	6.65	<MQL	<MQL	<MDL	<MDL	<MDL
MA-FSW 722-M01-06WT	9/13/2017	2/12/2018	<MDL	<MQL	<MQL	<MQL Qual	5.45	1.51	<MDL	<MDL	<MDL	<MDL	<MDL
MA-FSW 722-M01-08GY	9/13/2017	2/12/2018	<MQL	12.07	16.84	5.75	15.58	2.93	<MDL	<MQL	<MDL	<MDL	<MDL
MA-FSW 722-M01-09Y	9/13/2017	2/12/2018	<MDL	<MQL	1.61	1.08	3.84	1.26	<MDL	<MDL	<MDL	<MDL	<MDL
MA-FSW 722-M01-11GN	9/14/2017	2/12/2018	<MDL	<MDL	<MQL	1.72	5.53	1.44	<MDL	<MDL	<MDL	<MDL	<MDL

Table B9 (Continued)

U.S. Geological Survey local site name	Sampling date	Date Analyzed	PFBA	PFPeA	PFHxA	PFHpA	PFOA	PFNA	PFDA	PFUnDA	PFDoDA	PFTrDA	PFTeDA
MA-FSW 722-M01-12R	9/14/2017	2/12/2018	<MDL	<MDL	<MQL	3.43	14.07	1.84	<MDL	<MDL	<MDL	<MDL	<MDL
MA-FSW 722-M01-14BK	9/14/2017	2/12/2018	<MDL	4.27	6.84	4.72	16.26	3.01	<MDL	<MDL	<MDL	<MDL	<MDL
MA-FSW 722-M01-15W	9/14/2017	2/12/2018	9.1	37.87	39.25	16.98	29.22	4.63	<MDL	<MDL	<MDL	<MDL	<MDL
MA-FSW 722-M02-01PT	9/13/2017	2/12/2018	<MDL	5.26	4.98	4.41	13.73	3.9	<MQL	<MDL	<MDL	<MDL	<MDL
MA-FSW 722-M02-03RT	9/13/2017	2/12/2018	<MDL	<MDL	<MQL	<MQL Qual	2.83	1.29	<MDL	<MQL	<MDL	<MDL	<MDL
MA-FSW 722-M02-05BKT	9/13/2017	2/12/2018	<MDL	<MQL	3.81	3.98	16.76	3.56	<MQL	<MQL	<MDL	<MDL	<MDL
MA-FSW 722-M02-08GY	9/13/2017	2/12/2018	<MDL	<MQL	<MQL	<MQL	1.6	<MQL	<MDL	<MDL	<MDL	<MDL	<MDL
MA-FSW 722-M02-10P	9/13/2017	2/12/2018	<MDL	<MDL	<MDL	<MQL	1.35	<MQL	<MDL	<MDL	<MDL	<MDL	<MDL
MA-FSW 722-M02-12R	9/13/2017	2/12/2018	<MDL	8.87	11.545	5.865	16.545	2.98	<MQL	<MQL	<MDL	<MDL	<MDL
MA-FSW 722-M02-15W	9/13/2017 2/23/2018	2/12/2018	<MDL	5.775 124.1	3.705	1.625	8.385	2.595	<MDL	<MDL	<MDL	<MDL	<MDL
MA-FSW 722-M01-02GNT		4/23/2018	14.03	4	134.9	49.01	242.95	30.71	<MQL	<MDL	<MDL	<MDL	<MDL
MA-FSW 722-M01-06WT	2/23/2018 2/23/2018	4/23/2018	9.315	<MQL	5.205	5.035	40.385	5.405	<MDL	<MDL	<MDL	<MDL	<MDL
MA-FSW 722-M01-08GY		4/23/2018	10.69	63.63	93.18	49.67	135.04	13.6	<MQL	<MDL	<MDL	<MDL	<MDL
MA-FSW 722-M01-09Y	2/23/2018 2/23/2018	4/23/2018	9.36	55.91	83.02	46.35	129.49	13.33	<MQL	<MDL	<MDL	<MDL	<MDL
MA-FSW 722-M01-11GN		4/23/2018	19.36	89.23	136.93	68.67	175.73	15.58	<MQL	<MDL	<MDL	<MDL	<MDL
MA-FSW 722-M01-12R	2/23/2018	4/23/2018	11.2	59.42	89.7	47.15 64.87	123.73	10.79	<MQL	<MDL	<MDL	<MDL	<MDL
MA-FSW 722-M02-01PT	2/23/2018 2/23/2018	4/23/2018	40.89	79.34 100.5	123.69	5	140.47	8.435	<MQL	<MDL	<MDL	<MDL	<MDL
MA-FSW 722-M02-05BKT		4/23/2018	6.94	3	131.41	57.29 39.54	203	18.64	<MQL	<MQL	<MDL	<MDL	<MDL
MA-FSW 722-M02-08GY	2/23/2018	4/23/2018	9.97	25.28	35.78	5	77.645	20.55	<MQL	<MDL	<MDL	<MDL	<MDL
MA-FSW 722-M02-15W	2/23/2018	4/23/2018	<MDL	<MDL	<MDL	<MQL	2.81	<MQL	<MDL	<MDL	<MDL	<MDL	<MDL
FS-ASHPD-0001 (ECAMP02) Microlayer	9/11/2017	2/12/2018	<MQL	15.48	24.01	11.94	32.79	3.27	<MDL	<MQL	<MDL	<MDL	<MQL

Table B9 (Continued)

U.S. Geological Survey local site name	Sampling date	Date Analyzed	PFBA	PFPeA	PFHxA	PFHpA	PFOA	PFNA	PFDA	PFUnDA	PFDoDA	PFTrDA	PFTeDA
FS-ASHPD-0001 (ECAMP02) 0.1m	9/11/2017	2/12/2018	<MQL	14.99	23.7	11.79	30.54	2.91	<MDL	<MDL	<MDL	<MDL	<MDL
FS-ASHPD-0001 (ECAMP02) 1.00m	9/11/2017	2/12/2018	<MQL	15.3	23.975	11.52	30.975	2.875	<MDL	<MDL	<MDL	<MDL	<MDL
FS-ASHPD-0001 (ECAMP02) 3.00m	9/11/2017	2/12/2018	<MQL	14.82	23.48	11.565	30.86	2.735	<MDL	<MDL	<MDL	<MDL	<MDL
FS-ASHPD-0001 (ECAMP02) 5.00m	9/11/2017	2/12/2018	<MQL	15.14	23.37	11.42	30.93	2.87	<MDL	<MQL	<MQL	<MDL	<MDL
FS-ASHPD-0001 (ECAMP02) 7.00m	9/11/2017	2/12/2018	<MQL	15	24.26	11.62	31.25	2.9	<MDL	<MDL	<MDL	<MDL	<MDL
FS-ASHPD-0001 (ECAMP02) 9.00m	9/11/2017	2/12/2018	<MQL	15.21	23.17	11.87	30.2	2.81	<MDL	<MDL	<MDL	<MDL	<MDL
FS-ASHPD-0001 (ECAMP02) 11.00m	9/11/2017	2/12/2018	<MQL	13.77	21.73	10.04	24.3	3.05	<MDL	<MQL	<MQL	<MDL	<MDL
FS-ASHPD-0001 (ECAMP02) 13.00m	9/11/2017	2/12/2018	<MQL	13.665	20.2	9.51	22.915	2.705	<MDL	<MDL	<MDL	<MDL	<MDL
FS-ASHPD-0001 (ECAMP02) 15.00m	9/11/2017	2/12/2018	<MQL	13.91	19.82	9.69	22.93	2.87	<MDL	<MQL	<MQL	<MDL	<MDL
FS-ASHPD-0001 (ECAMP02) 17.00m	9/11/2017	2/12/2018	<MQL	13.28	20.2	9.99	22.51	2.92	<MDL	<MQL	<MDL	<MDL	<MDL
FS-ASHPD-0001 (ECAMP02) Microlayer	11/8/2017	2/12/2018	<MQL	14.78	23	11.12	31.5	3.195	<MQL	<MQL	<MQL	<MDL	<MDL
FS-ASHPD-0001 (ECAMP02) 0.1m	11/8/2017	2/12/2018	<MQL	14.87	23.04	11.87	31.44	3.05	<MDL	<MDL	<MDL	<MDL	<MDL
FS-ASHPD-0001 (ECAMP02) 1.00m	11/8/2017	2/12/2018	5.58	15.12	23.67	11.67	31.36	2.97	<MDL	<MDL	<MDL	<MDL	<MDL
FS-ASHPD-0001 (ECAMP02) 3.00m	11/8/2017	2/12/2018	<MQL	15.21	23.22	11.16	30.86	2.91	<MDL	<MDL	<MDL	<MDL	<MDL
FS-ASHPD-0001 (ECAMP02) 5.00m	11/8/2017	2/12/2018	<MQL	14.69	23.93	11.42	30.78	3.13	<MDL	<MQL	<MDL	<MDL	<MDL
FS-ASHPD-0001 (ECAMP02) 7.00m	11/8/2017	2/19/2018	<MQL	14.73	21.87	10.63	28.98	2.44	<MDL	<MQL	<MDL	<MDL	<MDL
FS-ASHPD-0001 (ECAMP02) 9.00m	11/8/2017	2/19/2018	<MQL	14.42	21.705	11.08	29.86	2.74	<MDL	<MQL	<MQL	<MDL	<MDL
FS-ASHPD-0001	11/8/2017	2/19/2018	<MQL	14.64	22.29	11.16	29.91	2.77	<MDL	<MDL	<MDL	<MDL	<MDL

Table B9 (Continued)

U.S. Geological Survey local site name	Sampling date	Date Analyzed	PFBA	PFPeA	PFHxA	PFHpA	PFOA	PFNA	PFDA	PFUnDA	PFDoDA	PFTrDA	PFTeDA
(ECAMP02) 11.00m FS-ASHPD-0001													
(ECAMP02) 13.00m FS-ASHPD-0001	11/8/2017	2/19/2018	5.78	15.54	23.38	11.54 / 10.84	31.1	2.83	<MDL	<MDL	<MDL	<MDL	<MDL
(ECAMP02) 15.00m FS-ASHPD-0001	11/8/2017	2/19/2018	<MQL	14.27	21.59	5	28.56	2.53	<MDL	<MDL	<MDL	<MDL	<MDL
(ECAMP02) 17.00m FS-ASHPD-0009	11/8/2017	2/19/2018	<MQL	13.93	20.55	9.64	23.91	2.43	<MDL	<MDL	<MDL	<MDL	<MDL
(ECAMP01) Microlayer FS-ASHPD-0009	9/11/2017	2/12/2018	5.99	15.08	23.42	11.37	31.76	3.9	<MQL	0.8	<MDL	<MDL	<MDL
(ECAMP01) 0.1m FS-ASHPD-0009	9/11/2017	2/12/2018	5.35	15.13 / 14.86	22.9	11.55 / 11.21	30.19	2.83	<MDL	<MDL	<MDL	<MDL	<MDL
(ECAMP01) 1.00m FS-ASHPD-0009	9/11/2017	2/12/2018	5.33	5	23.005	5	30.055	2.94	<MDL	<MDL	<MDL	<MDL	<MDL
(ECAMP01) 3.00 m FS-ASHPD-0009	9/11/2017	2/12/2018	<MQL	14.78	22.84	10.64	30.96	2.7	<MDL	<MDL	<MDL	<MDL	<MDL
(ECAMP01) 5.00 m FS-ASHPD-0009	9/11/2017	2/12/2018	4.64	15.01	22.22	11.04	30.08	2.92	<MDL	<MDL	<MDL	<MDL	<MDL
FS-ASHPD-0010 Microlayer	9/11/2017	2/19/2018	<MQL	13.78	21.17	11.41	28.28	2.65	<MDL	<MDL	<MDL	<MDL	<MDL
FS-ASHPD-0010 0.1m	9/11/2017	2/19/2018	<MQL	14.02 / 13.95	20.39	10.49	27.53	2.56	<MDL	<MDL	<MDL	<MDL	<MDL
FS-ASHPD-0010 1.00m	9/11/2017	2/19/2018	<MQL	5	20.29	10.65	27.375	2.445	<MQL	<MQL	<MQL	<MDL	<MDL
FS-ASHPD-0010 3.00m	9/11/2017	2/19/2018	<MQL	13.11	19.71	10.41	26.81	2.55	<MDL	<MDL	<MDL	<MDL	<MDL
FS-ASHPD-0010 5.00m	9/11/2017	2/19/2018	<MQL	13.31	20	10.2	26.9	2.31	<MDL	<MQL	<MQL	<MDL	<MDL
FS-ASHPD-0010 7.00m	9/11/2017	2/19/2018	<MQL	15.26 / 14.46	22.2	11.66 / 11.11	29.41	2.68	<MDL	<MQL	<MQL	<MDL	<MDL
FS-ASHPD-0010 9.00m	9/11/2017	2/19/2018	<MQL	5	22.425	5	28.68	2.77	<MDL	<MDL	<MDL	<MDL	<MDL
FS-ASHPD-0011 Microlayer	9/12/2017	2/12/2018	6.77	16.58	25.82	12.62	33.45	2.88	<MDL	<MDL	<MDL	<MDL	<MDL
FS-ASHPD-0011 0.1m	9/12/2017	2/12/2018	5.89	16.9	24.58	11.98	32.21	3.02	<MDL	<MDL	<MDL	<MDL	<MDL
FS-ASHPD-0011 1.00m	9/12/2017	2/12/2018	5.84	15.84	24.6	12.11	31.26	2.91	<MDL	<MDL	<MDL	<MDL	<MDL
FS-ASHPD-0011 3.00m	9/12/2017	2/12/2018	5.355	15.81	24.61	11.76	32.53	3.02	<MDL	<MQL	<MDL	<MDL	<MDL
FS-ASHPD-0011 5.00m	9/12/2017	2/12/2018	5.06	15.76	25.3	11.8	32.66	3	<MDL	<MDL	<MDL	<MDL	<MDL
FS-ASHPD-0011 7.00m	9/12/2017	2/12/2018	5.01	16.07	25.7	11.45	32.16	2.82	<MDL	<MDL	<MDL	<MDL	<MDL

133

Table B9 (Continued)

U.S. Geological Survey local site name	Sampling date	Date Analyzed	PFBA	PFPeA	PFHxA	PFHpA	PFOA	PFNA	PFDA	PFUnDA	PFDoDA	PFTrDA	PFTeDA
FS-ASHPD-0011 9.00m MI-JOHPD-0001	9/12/2017	2/12/2018	4.91	15.29	23.39	11.04	31.68	2.92	<MDL	<MQL	<MDL	<MDL	<MDL
(ECJNP03) Microlayer MI-JOHPD-0001	9/12/2017	2/19/2018	<MQL	12.47	17.47	8.66	15.81	37.57	<MQL	<MQL / <MQL Qual	<MQL	<MDL	<MDL
(ECJNP03) 0.1m MI-JOHPD-0001	9/12/2017	2/19/2018	<MQL	12.38	16.665	8.45	14.825	20.87	<MDL	<MDL	<MDL	<MDL	<MDL
(ECJNP03) 1.00m MI-JOHPD-0001	9/12/2017	2/19/2018	<MQL	12.06	15.29	8.57	14.82	20.39	<MDL	<MDL	<MDL	<MDL	<MDL
(ECJNP03) 3.00m MI-JOHPD-0001	9/12/2017	2/19/2018	<MQL	12.67	15.67	8.55	15.06	20.28	<MDL	<MDL	<MDL	<MDL	<MDL
(ECJNP03) 5.00m MI-JOHPD-0001	9/12/2017	2/19/2018	<MQL	12.36	16.34	8.55	15.19	19.84	<MDL	<MDL	<MDL	<MDL	<MDL
(ECJNP03) 7.00m MI-JOHPD-0001	9/12/2017	2/19/2018	<MQL	12.05	15.17	8.56	14.33	19.91	<MDL	<MDL	<MDL	<MDL	<MDL
(ECJNP03) 9.00m MI-JOHPD-0001	9/12/2017	2/19/2018	<MQL	12.2	15.63	8.22	14.39	19.66	<MDL	<MDL	<MDL	<MDL	<MDL
(ECJNP03) 11.00m MI-JOHPD-0001	9/12/2017	2/19/2018	<MQL	11.87	14.64	8.39	14.65	21	<MDL	<MDL	<MDL	<MDL	<MDL
(ECJNP03) 15.00 MI-JOHPD-0008	9/12/2017	2/19/2018	<MQL	12.49	15.44	8.67	14.91	20.06	<MDL	<MDL	<MDL	<MDL	<MDL
Microlayer	9/12/2017	2/19/2018	<MQL	12.27 / 12.63	15.43	8.69	14.82	21.68	<MDL	<MDL	<MDL	<MDL	<MDL
MI-JOHPD-0008 0.1m	9/12/2017	2/19/2018	<MQL	5	16.285	8.315	14.56	19.135	<MDL	<MDL	<MDL	<MDL	<MDL
MI-JOHPD-0008 1.00m	9/12/2017	2/19/2018	<MQL	12.49	16.13	8.76	14.59	19.53	<MDL	<MDL	<MDL	<MDL	<MDL
MI-JOHPD-0008 3.00m	9/12/2017	2/19/2018	<MQL	13.24	16.33	8.83	14.85	19.52	<MDL	<MDL	<MDL	<MDL	<MDL
MI-JOHPD-0008 5.00m	9/12/2017	2/19/2018	<MQL	12.18	15.38	8.565	14.2	18.34	<MDL	<MDL	<MDL	<MDL	<MDL
MI-JOHPD-0008 7.00m	9/12/2017	2/19/2018	<MQL	13.1	15.93	8.28	14.45	19.64	<MDL	<MDL	<MDL	<MDL	<MDL
MI-JOHPD-0008 9.00m	9/12/2017	2/19/2018	<MQL	12.13	15.17	8.07	14.145	18.455	<MDL	<MDL	<MDL	<MDL	<MDL
ASHPD-GWOUT-L-N-LW	9/13/2017	3/7/2018	<MQL	15.81	24.68 / 35.262	12.97 / 18.18	33.69	3.16	<MDL	<MQL	<MDL	<MDL	<MDL
ASHPD-GWOUT-L-N-015	9/13/2017	3/7/2018	10.58	24.68	5	25	43.285	4.065	<MDL	<MQL	<MDL	<MDL	<MDL
ASHPD-GWOUT-L-N-030	9/13/2017	3/7/2018	12.24	15.71	22.67	13.2	39.37	4.52	<MDL	<MQL	<MDL	<MDL	<MDL

134

U.S. Geological Survey local site name	Sampling date	Date Analyzed	PFBA	PFPeA	PFHxA	PFHpA	PFOA	PFNA	PFDA	PFUnDA	PFDoDA	PFTrDA	PFTeDA
ASHPD-GWOUT-L-N-050	9/13/2017	3/7/2018	<MQL	<MQL	2.72	2.52	12.95	2.48	<MDL	<MQL	<MDL	<MDL	<MDL
ASHPD-GWOUT-L-N-100	9/13/2017	3/7/2018	<MDL	<MQL	<MQL	<MQL	1.77	<MQL Qual	<MDL	<MDL	<MDL	<MDL	<MDL
ASHPD-GWOUT-R-N-LW	9/13/2017	3/13/2018	<MQL	16.03	24.7	12.57	32.56	3	<MDL	<MQL	<MDL	<MDL	<MDL
ASHPD-GWOUT-R-N-015	9/13/2017	3/13/2018	5.48	22.69	32.35	15.25	38.82	4.03	<MQL	0.93	<MDL	<MDL	<MDL
ASHPD-GWOUT-R-N-030	9/13/2017	3/13/2018	25.84	77.57 / 20.08	99.95	43.16 / 13.72	92.5	7.01	<MDL	0.61	<MDL	<MDL	<MDL
ASHPD-GWOUT-R-N-050	9/13/2017	3/13/2018	8.75	5	23.91	5	35.68	3.26	<MDL	<MQL	<MDL	<MDL	<MDL
ASHPD-GWOUT-R-N-100	9/13/2017	3/13/2018	<MDL	<MDL	<MDL	<MDL	<MQL	<MDL	<MDL	<MQL	<MDL	<MDL	<MDL
ASHPD-GWOUT-R-S-015	9/13/2017	3/7/2018	8.77	22.15	33.2	17.11	41.48	5.46	<MQL	2.01	<MDL	<MDL	<MDL
ASHPD-GWOUT-R-S-100	9/13/2017	3/7/2018	6.63	15.74	33.87	20.9	44.03	5.03	<MQL	<MQL	<MDL	<MDL	<MDL
ASHPD-KIGAM-124N-010E-LW	9/14/2017	3/13/2018	5.14	24.52	42.19	19.63	63.77	6	<MQL	5.32	<MDL	<MDL	<MDL
ASHPD-KIGAM-124N-010E-015	9/14/2017	3/13/2018	10.34	28.37	32.78	21.74	50.21	25.86	1.95	69.66 / 163.1	<MDL	<MDL	<MDL
ASHPD-KIGAM-124N-010E-030	9/14/2017	3/13/2018	9	23.09	26.38	17.81	41.2	29.32	1.78	5 / 182.8	<MDL	<MDL	<MDL
ASHPD-KIGAM-124N-010E-050	9/14/2017	3/13/2018	12.43	27.09 / 42.39	31.31	20.59 / 37.21	49.73	36.14	2.26	7 / 243.3	<MDL	<MDL	<MDL
ASHPD-KIGAM-124N-010E-100	9/14/2017	3/7/2018	19.8	5	51.745	5	83.81	68.965	2.945	75	<MDL	<MDL	<MDL
ASHPD-KIGAM-131N-011E-LW	9/14/2017	3/7/2018	11.34	28.27 / 20.82	48.2	24.74 / 22.76	86.8	7.4	<MQL	10.7	<MDL	<MDL	<MDL
ASHPD-KIGAM-131N-011E-015	9/14/2017	3/7/2018	10.205	5	22.31	5	54.98	21.745	2.815	96	<MDL	<MDL	<MDL
ASHPD-KIGAM-131N-011E-030	9/14/2017	3/7/2018	8.91	20.93	23.52	23.16	52.36	22.95	2.61	82.33	<MDL	<MDL	<MDL
ASHPD-KIGAM-131N-011E-050	9/14/2017	3/7/2018	10.37	25.67	26.7	24.17	58.98	30.74	2.7	120.6	<MDL	<MDL	<MDL

U.S. Geological Survey local site name	Sampling date	Date Analyzed	PFBA	PFPeA	PFHxA	PFHpA	PFOA	PFNA	PFDA	PFUnDA	PFDoDA	PFTrDA	PFTeDA
011E-050 ASHPD-KIGAM-131N-011E-100	9/14/2017	3/7/2018	11.745	25.98	26.695	23.91	57.67	33.785	3.675	116.29 / 45	<MDL	<MDL	<MDL
ASHPD-GWIN-C-LW	9/11/2017	2/19/2018	<MQL	13.92	20.92	11.18	27.82	2.52	<MDL	<MDL	<MDL	<MDL	<MDL
ASHPD-GWIN-C-035	9/11/2017	2/19/2018	<MQL	6.82	5.66	6.84	7.61	<MQL	<MDL	<MDL	<MDL	<MDL	<MDL
ASHPD-GWIN-C-100	9/11/2017	2/19/2018	<MQL	4.28	3.72	3.63	4.57	<MQL	<MDL	<MDL	<MDL	<MDL	<MDL
ASHPD-GWOUT-L-N-100	9/11/2017 2/23/2018	4/23/2018	6.59	<MDL	2.54	1.66	3.68	<MQL	<MDL	<MDL	<MDL	<MDL	<MDL
ASHPD-GWOUT-R-N-LW	2/23/2018	4/23/2018	<MQL	13.68	24.81	12.04	36.59	3.24	<MDL	<MDL	<MDL	<MDL	<MDL
ASHPD-GWOUT-R-N-100	2/23/2018	4/23/2018	<MDL	<MQL	2.595	1.64	6.73	<MQL	<MDL	<MQL	<MDL	<MDL	<MDL
MA-FSW 239-M01-01PT	8/5/2016	3/13/2018	<MDL	<MDL	<MDL	<MDL	<MQL	<MDL	<MDL	<MQL	<MDL	<MDL	<MDL
MA-FSW 239-M01-02GNT	8/5/2016	3/13/2018	<MDL	<MDL	<MDL	<MQL	4.59	4.24	<MDL	<MDL	<MDL	<MDL	<MDL
MA-FSW 239-M01-04BUT	8/5/2016	3/13/2018	<MDL	5.45	3.19	3.4	7.93	6.51	<MQL	<MDL	<MDL	<MDL	<MDL
MA-FSW 239-M01-06WT	8/5/2016	3/13/2018	15.19	44.93	40.76	36.05	85.98	43.63	3.68	4.18	<MDL	<MDL	<MDL
MA-FSW 239-M01-08GY	8/5/2016	3/13/2018	<MDL	8.825 / 26.66	8.005	4.94	16.54	5.81	<MQL	2.645	<MDL	<MDL	<MDL
MA-FSW 239-M01-10P	8/5/2016	3/13/2018	7.82	5	20.93	5.395	3.775	1.185	<MDL	<MQL	<MDL	<MDL	<MDL
MA-FSW 239-M01-12R	8/5/2016	3/13/2018	<MDL	<MDL	<MQL	<MQL	<MQL	<MDL	<MDL	<MDL	<MDL	<MDL	<MDL
MA-FSW 239-M01-14BK	8/5/2016	3/13/2018	<MDL	<MDL	<MDL	<MDL	<MQL	<MDL	<MDL	<MDL	<MDL	<MDL	<MDL
MA-FSW 300-M03-01PT	7/7/2016	3/13/2018	11.22	39.11	72.75	27.61	72.8	2.09	<MQL	<MQL	<MDL	<MDL	<MDL
MA-FSW 300-M03-03RT	7/7/2016	3/13/2018	<MQL	8.3	11.77	11.33	42.45	13.88	<MQL	<MDL	<MDL	<MDL	<MDL
MA-FSW 300-M03-06WT	7/7/2016	3/13/2018	12.25	41.92 / 41.97	78.21	54.63	130.78 / 156.13	72.46	0.86	1.27	<MDL	<MDL	<MDL
MA-FSW 300-M03-09Y	7/7/2016	3/13/2018	13.895	5	107.47	53.37	5	12.165	<MQL	0.525	<MDL	<MDL	<MDL

136

Table B9 (Continued)

U.S. Geological Survey local site name	Sampling date	Date Analyzed	PFBA	PFPeA	PFHxA	PFHpA	PFOA	PFNA	PFDA	PFUnDA	PFDoDA	PFTrDA	PFTeDA
MA-FSW 300-M03-10P	7/7/2016	3/13/2018	11.615	38.86	71.88	28.54	75.335	2.2	<MQL	<MQL	<MDL	<MDL	<MDL
MA-FSW 300-M03-11GN	7/7/2016	3/13/2018	11.79	5	48.93	14.35	27.93	<MQL	<MQL	<MDL	<MDL	<MDL	<MDL
MA-FSW 300-M03-14BK	7/7/2016	3/13/2018	18.18	34.89	91.08	23.59	132.64	<MQL	<MQL	<MDL	<MDL	<MDL	<MDL
MA-FSW 300-M03-15W	7/7/2016	3/13/2018	15.81	58	80.17	21.74	127.58	1.09	<MQL	<MDL	<MDL	<MDL	<MDL
MA-FSW 300-M02-01PT	7/8/2016	3/13/2018	19.2	57.23	103.52	28.29	149.85	1.21	<MQL	<MDL	<MDL	<MDL	<MDL
MA-FSW 300-M02-02GNT	7/8/2016	3/13/2018	19.45	71.83	75.51	21.9	114.86	1.35	<MQL	<MDL	<MDL	<MDL	<MDL
MA-FSW 300-M02-03RT	7/8/2016	4/23/2018	19.76	63.56	50.62	16.53	77.47	<MQL	<MDL	<MDL	<MDL	<MDL	<MDL
MA-FSW 300-M02-06WT	7/8/2016	3/13/2018	7.18	41.68	53.12	23.01	58.8	2.68	<MDL	<MDL	<MDL	<MDL	<MDL
MA-FSW 300-M02-08GY	7/8/2016	3/13/2018	<MDL	27.03	7.62	2.76	7.43	<MDL	<MDL	<MDL	<MDL	<MDL	<MDL
MA-FSW 300-M02-10P	7/8/2016	3/13/2018	<MDL	6.2	<MQL	1.23	<MQL	<MDL	<MDL	<MDL	<MDL	<MDL	<MDL
MA-FSW 300-M02-14BK	7/8/2016	3/13/2018	<MDL	<MQL	<MDL	<MDL	<MDL	<MDL	<MDL	<MDL	<MDL	<MDL	<MDL
MA-FSW 300-0138	7/7/2016	3/7/2018	<MDL	<MDL	<MDL	<MDL	<MDL	<MDL	<MDL	<MDL	<MDL	<MDL	<MDL
MA-FSW 424-M01-01PT	7/26/2016	4/23/2018	38.77	106.7	210.86	70.43	273.34	15.93	<MDL	2.39	<MDL	<MDL	<MDL
MA-FSW 424-M01-03RT	7/26/2016	4/23/2018	24.62	2	63.12	29.54	38.54	<MQL	<MDL	<MDL	<MDL	<MDL	<MDL
MA-FSW 424-M01-05BKT	7/26/2016	4/23/2018	<MQL	74.42	4.68	<MQL	<MQL	<MQL	<MDL	<MDL	<MDL	<MDL	<MDL
MA-FSW 424-M01-09Y	7/26/2016	4/23/2018	<MQL	<MDL	<MQL	<MQL	<MQL	<MQL	<MDL	<MDL	<MDL	<MDL	<MDL
MA-FSW 424-M01-13BU	7/26/2016	4/23/2018	<MDL	284.5	<MDL	206.2	<MDL	<MDL	<MDL	<MDL	<MDL	<MDL	<MDL
MA-FSW 424-M02-11GN 72-13	7/26/2016	4/23/2018	94.035	55	425	25	946.08	68.21	3.745	31.19	<MDL	<MDL	<MDL
	7/26/2016	4/23/2018	159.2	480.9	752.15	316.7	2277.1	40.4	2.31	5	<MDL	<MDL	<MDL
MA-FSW 424-M02-12R 72-13	7/26/2016	4/23/2018	94.83	7	524.41	7	8	18.23	<MQL	17.82	<MDL	<MDL	<MDL
MA-FSW 424-M02-	7/26/2016	4/23/2018		259.4		182.8	864.8			6.65	<MDL	<MDL	<MDL

137

Table B9 (Continued)

U.S. Geological Survey local site name	Sampling date	Date Analyzed	PFBA	PFPeA	PFHxA	PFHpA	PFOA	PFNA	PFDA	PFUnDA	PFDoDA	PFTrDA	PFTeDA
14BK 72-13				2	2	1							
MA-FSW 424-M02-15W 72-13	7/26/2016	4/23/2018	19.64	54	90.74	39.03	114.52	6.49	<MQL	3.37	<MDL	<MDL	<MDL
MA-FSW 564-M01-01PT	7/6/2016	3/13/2018	<MDL	<MDL	<MDL	<MDL	<MDL	<MDL	<MDL	<MDL	<MDL	<MDL	<MDL
MA-FSW 564-M01-02GNT	7/6/2016	3/13/2018	6.71	7.545	7.97	8.99	47.815	2.505	<MDL	<MQL	<MDL	<MDL	<MDL
MA-FSW 564-M01-04BUT	7/6/2016	3/7/2018	12.17	39.68	35.69	19.23 17.04	23.97	2.8	<MDL	<MDL	<MDL	<MDL	<MDL
MA-FSW 564-M01-05BKT	7/6/2016	3/7/2018	9.815	40.71	30.46	5	21.9	1.48	<MDL	<MDL	<MDL	<MDL	<MDL
MA-FSW 564-M01-06WT	7/6/2016	3/7/2018	6.86	21.87	17.11	8.52	9.91	<MQL	<MDL	<MDL	<MDL	<MDL	<MDL
MA-FSW 564-M01-08GY	7/6/2016	3/7/2018	<MQL	8.67	6.01	3.28	3.13	<MQL	<MDL	<MDL	<MDL	<MDL	<MDL
MA-FSW 564-M01-10P	7/6/2016	3/7/2018	<MQL	3.02	<MQL	<MQL	<MQL	<MQL	<MDL	<MDL	<MDL	<MDL	<MDL
MA-FSW 564-M01-12R	7/6/2016	3/7/2018	<MDL	3.27	2.91	<MQL	2.76	<MQL	<MDL	<MDL	<MDL	<MDL	<MDL
MA-FSW 564-M01-14BK	7/6/2016	3/7/2018	<MDL	<MDL	<MDL	<MDL	<MQL	<MDL	<MDL	<MDL	<MDL	<MDL	<MDL
MA-FSW 621-M01-01PT	7/11/2016	3/13/2018	<MDL	<MQL 55.92	<MQL	2.79	5.89	7.12	<MDL	<MDL	<MDL	<MDL	<MDL
MA-FSW 621-M01-02GNT	7/11/2016	3/13/2018	15.955	5	58.6	54.62	91.095	35.685	1.21	<MQL	<MDL	<MDL	<MDL
MA-FSW 621-M01-03RT	7/11/2016	4/23/2018	7.27	26.39	28.29	25.03	55.09	14.68	<MDL	<MDL	<MDL	<MDL	<MDL
MA-FSW 621-M01-05BKT	7/11/2016	3/13/2018	5.18	18.94	14.73	7.89	6.34	1.58	<MDL	<MDL	<MDL	<MDL	<MDL
MA-FSW 621-M01-06WT	7/11/2016	4/23/2018	<MQL	<MQL	5.96	2.92	2.63	<MQL	<MDL	<MDL	<MDL	<MDL	<MDL
MA-FSW 621-M01-07O	7/11/2016	3/13/2018	<MQL	5.85	4.24	1.89	<MQL	<MQL	<MDL	<MDL	<MDL	<MDL	<MDL
MA-FSW 621-M01-09Y	7/11/2016	3/13/2018	<MQL	<MDL	<MQL	<MQL	<MQL	<MDL	<MDL	<MDL	<MDL	<MDL	<MDL
MA-FSW 621-M01-11GN	7/11/2016	3/13/2018	<MDL	<MDL	<MDL	<MDL	<MQL	<MDL	<MDL	<MDL	<MDL	<MDL	<MDL
MA-FSW 621-M01-13BU	7/11/2016	3/13/2018	<MDL	<MDL	<MQL	<MDL	<MDL	<MDL	<MDL	<MDL	<MDL	<MDL	<MDL

Table B9 (Continued)

U.S. Geological Survey local site name	Sampling date	Date Analyzed	PFBA	PFPeA	PFHxA	PFHpA	PFOA	PFNA	PFDA	PFUnDA	PFDoDA	PFTrDA	PFTeDA
MA-FSW 621-M01-15W	7/11/2016	3/13/2018	<MDL	<MDL	<MQL	<MDL	<MDL	<MDL	<MDL	<MDL	<MDL	<MDL	<MDL
MA-FSW 622-M01-01PT	7/11/2016	3/20/2018	<MDL	<MDL	<MDL	<MDL	<MQL	<MDL	<MDL	<MDL	<MDL	<MDL	<MDL
MA-FSW 622-M01-02GNT	7/11/2016	3/20/2018	12.7	24.62	20.41	15.42	45.65	14.51	1.94	2.66	<MDL	<MDL	<MDL
MA-FSW 622-M01-03RT	7/11/2016	4/23/2018	11.71	29.45	24.26	12.29	14.24	2.79	<MDL	<MQL	<MDL	<MDL	<MDL
MA-FSW 622-M01-05BKT	7/11/2016	3/20/2018	7.1	12.28	9.28	4.05	5.75	<MQL	<MDL	<MDL	<MDL	<MDL	<MDL
MA-FSW 622-M01-06WT	7/11/2016	4/23/2018	<MQL	9.91	5.88	2.19	3.73	<MDL	<MDL	<MDL	<MDL	<MDL	<MDL
MA-FSW 622-M01-07O	7/11/2016	3/20/2018	5.135	10.23	6.75	2.74	4.395	<MQL	<MDL	<MDL	<MDL	<MDL	<MDL
MA-FSW 622-M01-09Y	7/11/2016	3/20/2018	5.15	6.09	3.265	1.36	2.185	<MDL	<MDL	<MDL	<MDL	<MDL	<MDL
MA-FSW 622-M01-11GN	7/11/2016	3/20/2018	6.79	2.86	3.7	<MQL	1.52	<MDL	<MDL	<MDL	<MDL	<MDL	<MDL
MA-FSW 622-M01-13BU	7/11/2016	3/20/2018	<MDL	3.04	2.16	<MQL	<MQL	<MDL	<MDL	<MDL	<MDL	<MDL	<MDL
MA-FSW 622-M01-15W	7/11/2016	3/20/2018	<MQL	3.9	5.01	1.26	4.43	<MDL	<MDL	<MDL	<MDL	<MDL	<MDL
MA-FSW 744-0004	7/26/2016	3/20/2018	<MQL	2.97	3.64	4.1	9.2	13.96	<MQL	<MDL	<MDL	<MDL	<MDL
MA-FSW 744-0008	7/26/2016	3/20/2018	4.93	9.51	11.22	12.23	31.26	16.46	1.73	<MQL	<MDL	<MDL	<MDL
MA-FSW 744-0010	7/26/2016	3/20/2018	<MQL	9.76	10.83	11.78	29.96	15.75	1.77	<MQL	<MDL	<MDL	<MDL
MA-FSW 744-0011	7/26/2016	3/20/2018	4.86	9.11	9.27	10.86	29.08	18.52	1.91	Qual	<MDL	<MDL	<MDL
MA-FSW 744-0013	7/26/2016	3/20/2018	4.69	8.44	8.27	9.07	25.63	18.85	1.97	1.41	<MDL	<MDL	0.9
MA-FSW 744-0017	7/26/2016	3/20/2018	4.82	9.8	7.535	8.915	22.56	17.105	3.09	3.69	<MDL	<MDL	<MQL
MA-FSW 744-0019	7/26/2016	3/20/2018	12.01	34.05	27.51	25.95	71.73	54.51	5.94	18.06	<MDL	<MDL	<MDL
MA-FSW 744-0023	7/26/2016	3/20/2018	32.57	69.94	58.67	55.86	163.55	124.18	10.15	28.08	<MDL	<MDL	<MDL
MA-FSW 744-0025	7/26/2016	3/21/2018	24.215	65.15	60.28	54.85	156.52	100.085	7.22	25.36	<MDL	<MDL	<MQL
MA-FSW 744-0026	7/26/2016	4/23/2018	24.8	77.59	73.62	69.33	188.73	129.13	6.78	26.43	<MDL	<MDL	<MDL
MA-FSW 744-0028	7/26/2016	4/23/2018	28.81	84.05	111.1	68.55	228.12	82.55	4.165	17.34	<MDL	<MDL	<MDL
MA-FSW 744-0029	7/26/2016	4/23/2018	76.62	204.68	476.11	154.03	840.19	20.57	<MDL	<MQL	<MDL	<MDL	<MDL

139

Table B9 (Continued)

U.S. Geological Survey local site name	Sampling date	Date Analyzed	PFBA	PFPeA	PFHxA	PFHpA	PFOA	PFNA	PFDA	PFUnDA	PFDoDA	PFTrDA	PFTeDA
MA-FSW 744-0030 Q1 MI-QUARV-00015(QR001)	7/26/2016	4/23/2018	76.08	193.64	469.32	147.45	790.12	16.12	<MDL	<MQL	<MDL	<MDL	<MDL
Q3	8/15/2017	2/6/2018	<MQL	14.01	16.86	9.04	15.86	22.45	<MDL	<MDL	<MDL	<MDL	<MDL
Q4	8/15/2017	2/6/2018	<MQL	20.32	22.3	12.55	19.01	7.46	<MQL	<MDL	<MDL	<MDL	<MDL
Q5	8/15/2017	2/6/2018	<MQL	16.84	19.05	13.51	16.26	6.18	<MDL	<MDL	<MDL	<MDL	<MDL
Q9	8/15/2017	2/6/2018	8.67	14.95	18.16	9.9	14.91	5.18	<MDL	<MDL	<MDL	<MDL	<MDL
Q-FC	8/15/2017	2/6/2018	14.77	10.18	12.41	8.5	11.32	3.57	<MDL	<MDL	<MDL	<MDL	<MDL
Q-OBR	8/15/2017	2/6/2018	<MQL	13	15.89	9.49	14.18	4.35	<MDL	<MDL	<MDL	<MDL	<MDL
Q-TRIB	8/15/2017	2/6/2018	<MQL	17.21	19.58	12.98	17	6.68	<MDL	<MDL	<MDL	<MDL	<MDL
		2/6/2018	6.51	18.22	17.625	9.215	10.19	2.01	<MDL	<MDL	<MDL	<MDL	<MDL
Quash_HS_Seep1	8/16/2017	2/6/2018	<MDL	<MDL	<MDL	<MQL	<MQL	<MDL	<MDL	<MDL	<MDL	<MDL	<MDL
Quash_HS_Seep2	8/16/2017	2/6/2018	<MDL	<MDL	<MDL	<MQL	<MQL	<MDL	<MDL	<MDL	<MDL	<MDL	<MDL
QB010	8/17/2017	2/6/2018	<MQL	17.16	14.58	7.97	20.45	1.21	<MDL	<MDL	<MDL	<MDL	<MDL
QB018	8/17/2017	2/6/2018	<MDL	6.15	3.92	1.28	1.14	<MDL	<MDL	<MDL	<MDL	<MDL	<MDL
QB020	8/17/2017	2/6/2018	<MQL	10.92	19.97	5.14	29.32	<MDL	<MDL	<MDL	<MDL	<MDL	<MDL
QB026	8/17/2017	2/6/2018	<MQL	15.08	18.36	9.09	18.23	3.98	<MDL	<MDL	<MDL	<MDL	<MDL
QB039	8/18/2017	2/6/2018	8.59	31.12	42.86	23.42	56.34	63.54	<MDL	<MDL	<MDL	<MDL	<MDL
DD004	8/17/2017	2/6/2018	<MDL	5.25	5.98	2.14	4.77	<MQL	<MDL	<MDL	<MDL	<MDL	<MDL
DD-12	8/17/2017	2/6/2018	<MQL	16.86	21.795	11.26	19.97	11.15	<MDL	<MDL	<MDL	<MDL	<MDL
Quash_OV_seep1	8/14/2017	2/6/2018	<MQL	13.04	21.8	5.66	25.77	<MDL	<MDL	<MDL	<MDL	<MDL	<MDL
Quash_OV_seep2	8/14/2017	2/12/2018	<MDL	<MDL	1.96	<MQL	1.6	<MDL	<MDL	<MDL	<MDL	<MDL	<MDL
Quash_HRTS_seep	8/14/2017	2/6/2018	<MDL	8.36	17.23	3.86	20.96	<MDL	<MDL	<MDL	<MDL	<MDL	<MDL
QT008	8/17/2017	2/6/2018	<MQL	15.15	25.51	7.61	28.4	<MDL	<MDL	<MDL	<MDL	<MDL	<MDL
QT018	8/17/2017	2/6/2018	<MDL	<MQL	2.83	1.68	3.32	<MQL	<MDL	<MDL	<MDL	<MDL	<MDL
QT030	8/17/2017	2/6/2018	<MQL	3.35	7.29	1.32	10.3	<MDL	<MDL	<MDL	<MDL	<MDL	<MDL
QT034	8/17/2017	2/6/2018	<MDL	<MDL	<MDL	<MQL	2.54	<MDL	<MDL	<MDL	<MDL	<MDL	<MDL
QT039	8/17/2017	2/6/2018	<MQL	18.26	25.125	8.25	19.85	<MDL	<MDL	<MDL	<MDL	<MDL	<MDL
QT082	8/18/2017	2/6/2018	<MDL	<MQL	<MQL	0.84	3.66	1.53	<MDL	<MDL	<MDL	<MDL	<MDL
QT101	8/17/2017	2/6/2018	<MDL	4.13	5.71	1.85	3.33	1.21	<MDL	<MDL	<MDL	<MDL	<MDL
QT122		2/6/2018	<MDL	11.26	12.46	5.17	8.06	<MQL	<MDL	<MDL	<MDL	<MDL	<MDL
QT142	8/18/2017	2/6/2018	23.7	95.26	102.99	46.18	96.81	10.89	<MDL	<MDL	<MDL	<MDL	<MDL

140

Table B9 (Continued)

U.S. Geological Survey local site name	Sampling date	Date Analyzed	PFBA	PFPeA	PFHxA	PFHpA	PFOA	PFNA	PFDA	PFUnDA	PFDoDA	PFTrDA	PFTeDA
Quash-Spawn1	8/16/2017	2/12/2018	<MQL	20.79	14.38	5.8	15.48	<MDL	<MDL	<MDL	<MDL	<MDL	<MDL
Quash-Spawn2	8/16/2017	2/12/2018	<MDL	<MDL	<MDL	<MDL	<MDL	<MDL	<MDL	<MDL	<MDL	<MDL	<MDL
Quash-Spawn3	8/14/2017	2/12/2018	<MDL	<MDL	<MDL	<MDL	<MDL	<MDL	<MDL	<MDL	<MDL	<MDL	<MDL

Table B10. Perfluorinated sulfonate sample concentrations (ng L^{-1}).

U.S. Geological Survey local site name	Sampling Date	Date Analyzed	PFBS	PFPeS	PFHxS Linear	PFHxS Branched	PFHpS	PFOS Linear	PFOS Branched	PFNS	PFDS
DI H2O From Peristaltic Geopump For MLSs	9/11/2017	1/16/2018									<MDL
DI H2O From Grundfos Pump	9/12/2017	1/16/2018	<MQL	<MDL	<MDL	<MDL	<MQL	<MDL	<MQL	<MDL	<MDL
DI H2O From Keck Pump	9/12/2017	1/16/2018	<MQL	<MDL	<MDL	<MDL	<MDL	<MDL	<MDL	<MDL	<MDL
DI H2O From Henry	9/14/2017	1/16/2018	<MQL	<MDL	<MDL	<MDL	<MDL	<MDL	<MDL	<MDL	<MDL
DI H2O From Microlayer Sampler	9/12/2017	1/16/2018	<MQL	<MDL	<MDL	<MDL	<MDL	<MDL	<MDL	<MDL	<MDL
DI H2O From Microlayer Sampling Device	9/12/2017	1/16/2018	<MQL	<MDL	<MDL	<MDL	<MDL	<MDL	<MDL	<MDL	<MDL
DI H2O From Boat Peristaltic Geopump	9/12/2017	1/16/2018	<MQL	<MDL	<MDL	<MDL	<MDL	<MDL	<MDL	<MDL	<MDL
DI H2O From Boat Peristaltic Geopump	11/8/2017	1/16/2018	<MQL	<MDL	<MDL	<MDL	<MDL	<MDL	<MDL	<MDL	<MDL
DI H2O From MA-FSW 631-02GNT	2/22/2018	4/23/2018	<MDL	<MDL	<MDL	<MDL	<MDL	<MDL	<MDL	<MDL	<MDL
DI H2O From Henry Sampler	2/22/2018	4/23/2018	<MDL	<MQL	<MDL	<MDL	<MDL	<MDL	<MDL	<MDL	<MDL
MA-MIW 207-0069 (00MW0582B)	7/26/2017	1/16/2018	1.73	Qual	18.665	4.105	1.21	81.325	14.61	<MDL	<MDL
MA-MIW 207-0215 (00MW0582A)	7/26/2017	1/16/2018	24.7	19.29	87.55	19.86	1.98	44.46	14.75	<MDL	<MDL
MA-MIW 209-0015 (00MW0584C)	7/21/2017	1/25/2018	1.35	<MQL	<MQL	<MDL	<MQL	1.38	1.17	<MDL	<MDL
MA-MIW 209-0146 (00MW0584B)	7/21/2017	1/25/2018	5.19	5.56	44.91	8.03	1.85	19.91	18.18	<MDL	<MDL
MA-MIW 209-0286 (00MW0584A)	7/21/2017	1/25/2018	<MDL	<MDL	1.42	<MDL	<MDL	<MQL	<MQL	<MDL	<MDL
MA-MIW 210-0026	7/25/2017	1/25/2018	2.58	2.64	34.95	5.64	<MQL	21.89	8.17	<MDL	<MDL
MA-MIW 210-0046	7/25/2017	1/25/2018	<MDL	<MDL	<MDL	<MDL	<MDL	0.97	<MQL	<MDL	<MDL
MA-MIW 210-0075 (00MW0609B)	7/25/2017	1/25/2018	<MQL	<MDL	<MDL	<MDL	<MDL	<MDL	<MDL	<MDL	<MDL
MA-MIW 210-0145 (00MW0609A)	7/25/2017	1/25/2018	<MQL	<MDL	<MDL	<MDL	<MDL	<MDL	<MDL	<MDL	<MDL
MA-MIW 221-0245 (03MW1003B)	7/28/2017	1/25/2018	4.05	5.35	41.36	8.21	1.63	23.16	12.28	<MDL	<MDL

Table B10 (Continued)

U.S. Geological Survey local site name	Sampling Date	Date Analyzed	PFBS	PFPeS	PFHxS Linear	PFHxS Branched	PFHpS	PFOS Linear	PFOS Branched	PFNS	PFDS
MA-MIW 221-0325 (03MW1003A)	7/28/2017	1/25/2018	<MQL	<MDL	<MDL	<MDL	<MDL	<MDL	<MDL	<MDL	<MDL
MA-MIW 223-0111 (03MW1005B)	7/25/2017	1/25/2018	1.87	2.8	14.59	3.37	<MDL	<MDL	<MDL	<MDL	<MDL
MA-MIW 223-0148 (03MW1005A)	7/25/2017	1/25/2018	1.76	2.91	11.8	3.18	<MDL	1.3	<MQL	<MDL	<MDL
MA-MIW 230-0015	7/20/2017	1/25/2018	3.19	3.99	40.63	10.74	2.39	415.03	59.06	<MDL	<MDL
MA-MIW 230-0060	7/20/2017	1/25/2018	4.92	5.91	45.21	9.23	1.8	39	19.57	<MDL	<MDL
MA-MIW 230-0110	7/20/2017	1/25/2018	4.68	5.11	41.7	8.54	1.34	51.63	18.3	<MDL	<MDL
MA-MIW 230-0174 (03MW2626B)	7/19/2017	1/25/2018	5.33	5.73	46.03	9.25	1.81	31.92	18.1	<MDL	<MDL
MA-MIW 230-0294 (03MW2626A)	7/19/2017	1/25/2018	5.78	5.36	33.69	7.37	1.11	39.74	14.14	<MDL	<MDL
MA-MIW 231-0040	7/19/2017	1/25/2018	5.95	5.07	43.72	8.13	1.9	99.38	39.17	<MDL	<MDL
MA-MIW 231-0070	7/19/2017	1/25/2018	6.24	5.41	42.43	8.69	1.42	29.32	15.48	<MDL	<MDL
MA-MIW 231-0105	7/19/2017	1/25/2018	4.955	6.28	49.325	9.255	1.735	34.68	16.685	<MDL	<MDL
MA-MIW 231-0138	7/19/2017	1/12/2018	4.985	5.97	42.945	9.53	1.46	31.435	17.395	<MDL	<MDL
MA-MIW 232-0050	7/18/2017	1/25/2018	1.82	<MQL	2.96	<MQL	<MQL	2.02	2.92	<MDL	<MDL
MA-MIW 232-0080	7/18/2017	1/25/2018	5.41	5.21	29.65	6.91	<MQL	0.61	4.05	<MDL	<MDL
MA-MIW 232-0115	7/18/2017	1/25/2018	4.55	5.1	37.54	7.85	2.1	32.47	25.49	<MDL	<MDL
MA-MIW 232-0150	7/18/2017	1/25/2018	4.65	4.78	38.03	7.21	2.28	44.82	28.63	<MDL	<MDL
MA-MIW 233-0016	7/26/2017	1/25/2018	2.98	2.28	29.11	2.81	<MQL <MQL	16.22	4.11	<MDL	<MDL
MA-MIW 233-0070	7/26/2017	1/25/2018	4.9	6.77	51.77	10.64	Qual	29.13	13.82	<MDL	<MDL
MA-MIW 233-0174 (00MW0608B)	7/26/2017	1/25/2018	5.085	5.93	26.945	6.195	1.24	6.95	8.63	<MDL	<MDL
MA-MIW 233-0245 (00MW0608A)	7/26/2017	1/25/2018	<MDL	4.03	21.99	4.8	1.26	11.8	9.1	<MDL	<MDL
MA-MIW 234-0055	7/20/2017	1/25/2018	1.36	0.67	3.16	<MQL	<MDL	<MQL	<MQL	<MDL	<MDL
MA-MIW 234-0086	7/20/2017	1/25/2018	5.015	5.385	28.63	6.745	0.93 <MQL	4.36	5.095	<MDL	<MDL
MA-MIW 234-0120	7/20/2017	1/25/2018	8.12	9.2	52.57	10.58	Qual	2.71	5.52	<MDL	<MDL
MA-MIW 234-0150	7/20/2017	1/25/2018	8.61	9.21	48.91	11.04	1.12	2.04	5.02	<MDL	<MDL

143

Table B10 (Continued)

U.S. Geological Survey local site name	Sampling Date	Date Analyzed	PFBS	PFPeS	PFHxS Linear	PFHxS Branched	PFHpS	PFOS Linear	PFOS Branched	PFNS	PFDS
MA-MIW 236-0025 (MAMW0396S)	7/27/2017	1/25/2018	3.43	1.64	17.13	3.12	<MQL Qual	20.01	7.22	<MDL	<MDL
MA-MIW 236-0109 (MAMW0296I)	7/27/2017	1/25/2018	5.25	4.62	42.07	7.23	2.34	46.94	24.72	<MDL	<MDL
MA-MIW 236-0189 (MAMW0196D)	7/27/2017	1/25/2018	5.2	6.43	46.39	9.07	<MQL Qual	26.27	17.27	<MDL	<MDL
MA-MIW 237-0145 (03MW2620B)	7/27/2017	1/16/2018	6.71	7.34	50.47	10.68	1.6	26.68	16.71	<MDL	<MDL
MA-MIW 237-0254 (03MW2620A)	7/27/2017	1/16/2018	15.28	10.12	46.77	9.17	1.27	12.62	8.55	<MDL	<MDL
MA-FSW 631-M01-01PT	9/12/2017	1/16/2018	6.69	8.62	66.985	14.295	1.985	256.01	21.3	<MDL	<MDL
MA-FSW 631-M01-02GNT	9/12/2017	1/16/2018	4.97	4.5	45.29	8.39	4.51	97.47	70.58	<MDL	<MDL
MA-FSW 631-M01-03RT	9/12/2017	1/16/2018	9	10.61	92.52	20.96	6	27.05	121.92	<MDL	<MDL
MA-FSW 631-M01-04BUT	9/12/2017	1/16/2018	8.9	11.055	80	17.13	2.725	65.305	44.97	<MDL	<MDL
MA-FSW 631-M01-06WT	9/12/2017	1/16/2018	8.24	5.16	48.3	3.85	2.16	19.23	16.75	<MDL	<MDL
MA-FSW 631-M01-09Y	9/12/2017	1/16/2018	6.05	8.58	64.28	22.72	1.98	23.61	23.8	<MDL	<MDL
MA-FSW 631-M01-12R	9/12/2017	1/16/2018	6.06	6.29	44.96	10.38	1.44	25.87	15.3	<MDL	<MDL
MA-FSW 631-M01-15W	9/12/2017	1/16/2018	4.96	6.04	50	10.14	2.06	48.03	23.81	<MDL	<MDL
MA-FSW 631-0256 (00MW0589A)	9/12/2017	1/25/2018	5.01	9.26	48.99	9.74	2.09	24.61	15.85	<MDL	<MDL
MA-FSW 632-M01-01PT	9/11/2017	2/6/2018	1.76	1.24	8.57	3.54	<MQL Qual	2.07	13.55	<MDL	<MDL
MA-FSW 632-M01-02GNT	9/11/2017	2/6/2018	14.99	2.53	99.53	3.07	1.28	16.73	2.82	<MDL	<MDL
MA-FSW 632-M01-03RT	9/11/2017	2/6/2018	<MQL	<MQL	5.97	<MQL	<MQL	32.71	5.84	<MDL	<MDL
MA-FSW 632-M01-05BKT	9/11/2017	2/6/2018	7.6	12.55	77.63	18.91	2.62	51.01	27.44	<MDL	<MDL
MA-FSW 632-M01-06WT	9/11/2017	2/6/2018	4.39	3.7	38.33	6.18	1.13	34.31	12.78	<MDL	<MDL
MA-FSW 632-M01-07O	9/11/2017	2/6/2018	14.72	21.17	114.96	21.42	1.4	23.15	11.7	<MDL	<MDL
MA-FSW 632-M01-11GN	9/11/2017	2/6/2018	4.51	6.31	44.67	8.03	1.47	32.57	14.37	<MDL	<MDL
MA-FSW 632-M01-15W	9/11/2017	1/16/2018	8.085	9.295	60.54	11.87	1.555	24.975	15.16	<MDL	<MDL
MA-FSW 632-0195 (00MW0606B)	9/11/2017	1/16/2018	5.04	6.62	46.62	8.93	1.77	31.35	16.19	<MDL	<MDL
MA-FSW 632-0325 (00MW0606A)	9/11/2017	1/16/2018	<MDL	1.65	9.63	2	<MQL	5.5	5.67	<MDL	<MDL
MA-FSW 665-0040	9/12/2017	1/16/2018	3.18	<MQL	9.41	<MDL	<MQL	24.09	3.88	<MDL	<MDL
MA-FSW 665-0089	9/12/2017	1/16/2018	13.33	17.335	73.22	38.755	2.325	34.965	22.18	<MDL	<MDL

U.S. Geological Survey local site name	Sampling Date	Date Analyzed	PFBS	PFPeS	PFHxS Linear	PFHxS Branched	PFHpS	PFOS Linear	PFOS Branched	PFNS	PFDS
MA-FSW 665-0139	9/12/2017	1/16/2018	6.42	6.14	47.07	8.23	1.29	25.17	11.86	<MDL	<MDL
MA-FSW 665-0264 (03MW1014B)	9/12/2017	1/16/2018	8.12	7.62	47.68	9.68	2.65	32.24	24.4	<MDL	<MDL
MA-FSW 665-0295 (03MW1014A)	9/12/2017	1/16/2018	<MDL	5.03	29.56	6.38	1.54	19.13	12.91	<MDL	<MDL
MA-FSW 722-M01-01PT	9/13/2017	2/12/2018	5.77	3.065	47.985	2.49	1.225	40.655	11.495	<MDL	<MDL
MA-FSW 722-M01-02GNT	9/13/2017	2/12/2018	4.54	3.97	32.24	5.94	1.25	32.14	11.03	<MDL	<MDL
MA-FSW 722-M01-06WT	9/13/2017	2/12/2018	5.78	5.24	52.14	7.04	1.17	46.3	11.71	<MDL	<MDL
MA-FSW 722-M01-08GY	9/13/2017	2/12/2018	13.57	17.34	121.7	23.44	1.61	31.79	13.79	<MDL	<MDL
MA-FSW 722-M01-09Y	9/13/2017	2/12/2018	4.665	4.975	49.82	6.9	0.815	24.4	11.96	<MDL	<MDL
MA-FSW 722-M01-11GN	9/14/2017	2/12/2018	5.14	7.33	56.21	11.08	1.3	14.74	16.03	<MDL	<MDL
MA-FSW 722-M01-12R	9/14/2017	2/12/2018	5.66	6.78	54.89	11.19	1.71	11.84	13.38	<MDL	<MDL
MA-FSW 722-M01-14BK	9/14/2017	2/12/2018	6.16	7.55	54.57	13.06	1.27	30.05	14.93	<MDL	<MDL
MA-FSW 722-M01-15W	9/14/2017	2/12/2018	4.7	6.27	53.88	9.45	1.31	34.2	14.8	<MDL	<MDL
MA-FSW 722-M02-01PT	9/13/2017	2/12/2018	3.67	<MQL	8.88	<MQL	<MQL	63.34	8.79	<MDL	<MDL
MA-FSW 722-M02-03RT	9/13/2017	2/12/2018	4.64	7.33	55.89	8.06	1.66	39.09	13.17	<MDL	<MDL
MA-FSW 722-M02-05BKT	9/13/2017	2/12/2018	6.31	4.81	39.63	6.61	1.18	27.42	10.31	<MDL	<MDL
MA-FSW 722-M02-08GY	9/13/2017	2/12/2018	6.18	8.37	60.54	11.63	1.91	39.25	13.4	<MDL	<MDL
MA-FSW 722-M02-10P	9/13/2017	2/12/2018	4.52	6.95	41.37	7.34	1.15	28.32	8.43	<MDL	<MDL
MA-FSW 722-M02-12R	9/13/2017	2/12/2018	4.19	6.08	48.585	11.945	1.38	60.43	13.315	<MDL	<MDL
MA-FSW 722-M02-15W	9/13/2017	2/12/2018	7.275	11.245	66.085	23.89	2.565	62.795	25.38	<MDL	<MDL
MA-FSW 722-M01-02GNT	2/23/2018	4/23/2018	4.49	8.7	85.12	15.68	2.61	47.83	28.62	<MDL	<MDL
MA-FSW 722-M01-06WT	2/23/2018	4/23/2018	3.73	6.285	61.97	12.74	2.325	21.835	25.4	<MDL	<MDL
MA-FSW 722-M01-08GY	2/23/2018	4/23/2018	4.54	6.84	69.17	12.63	2.43	39.1	24.36	<MDL	<MDL
MA-FSW 722-M01-09Y	2/23/2018	4/23/2018	4.26	6.39	70.56	13.06	2.39	38.5	22.25	<MDL	<MDL
MA-FSW 722-M01-11GN	2/23/2018	4/23/2018	5.12	7.65	86.71	15.31	2.73	35.35	24.3	<MDL	<MDL
MA-FSW 722-M01-12R	2/23/2018	4/23/2018	4.6	6.54	60.99	11.53	1.9	25.68	21.67	<MDL	<MDL
MA-FSW 722-M02-01PT	2/23/2018	4/23/2018	4.355	4.3	38.07	11.84	3.13	39.455	91.14	<MDL	<MDL
MA-FSW 722-M02-05BKT	2/23/2018	4/23/2018	3.78	7.33	83.07	14.1	2.82	25.85	25.61	<MDL	<MDL
MA-FSW 722-M02-08GY	2/23/2018	4/23/2018	3.93	7.015	77.305	13.645	2.645	28.135	23.95	<MDL	<MDL
MA-FSW 722-M02-15W	2/23/2018	4/23/2018	4.89	18.3	99.92	49.37	3.57	17.89	38.7	<MDL	<MDL
FS-ASHPD-0001	9/11/2017	2/12/2018	4.3	6.68	69.65	11.99	2.07	54.28	22.04	<MDL	<MDL

Table B10 (Continued)

U.S. Geological Survey local site name	Sampling Date	Date Analyzed	PFBS	PFPeS	PFHxS Linear	PFHxS Branched	PFHpS	PFOS Linear	PFOS Branched	PFNS	PFDS
(ECAMP02) Microlayer FS-ASHPD-0001	9/11/2017	2/12/2018									
(ECAMP02) 0.1m FS-ASHPD-0001	9/11/2017		4.57	6.36	65	11.93	1.95	36.26	17.84	<MDL	<MDL
(ECAMP02) 1.00m FS-ASHPD-0001	9/11/2017	2/12/2018	4.43	6.95	69.435	11.695	1.92	36.455	17.61	<MDL	<MDL
(ECAMP02) 3.00m FS-ASHPD-0001	9/11/2017	2/12/2018	4.555	6.695	67.93	11.465	2.02	34.675	16.93	<MDL	<MDL
(ECAMP02) 5.00m FS-ASHPD-0001	9/11/2017	2/12/2018	4.8	7.06	70.07	12.48	2.31	37.99	19.31	<MDL	<MDL
(ECAMP02) 7.00m FS-ASHPD-0001	9/11/2017	2/12/2018	4.75	6.85	66.15	11.91	2.33	33.29	16.05	<MDL	<MDL
(ECAMP02) 9.00m FS-ASHPD-0001	9/11/2017	2/12/2018	4.24	6.36	65.45	11.26	2.31	35.9	17.52	<MDL	<MDL
(ECAMP02) 11.00m FS-ASHPD-0001	9/11/2017	2/12/2018	4.03	5.09	53.97	9.79	1.55	32.31	14.37	<MDL	<MDL
(ECAMP02) 13.00m FS-ASHPD-0001	9/11/2017	2/12/2018	4.21	5.78	53.505	9.33	1.7	25.93	14.525	<MDL	<MDL
(ECAMP02) 15.00m FS-ASHPD-0001	9/11/2017	2/12/2018	4.12	5.44	54.18	9.51	1.7	29.24	13.99	<MDL	<MDL
(ECAMP02) 17.00m FS-ASHPD-0001	9/11/2017	2/12/2018	3.65	5.3	50.24	8.78	1.36	28.33	13.61	<MDL	<MDL
(ECAMP02) Microlayer FS-ASHPD-0001	11/8/2017	2/12/2018	4.34	7.945	69.8	12.52	1.93	49.99	22.07	<MDL	<MQL
(ECAMP02) 0.1m FS-ASHPD-0001	11/8/2017	2/12/2018	4.69	7.09	69.87	11.57	2.19	36.41	17.97	<MDL	<MDL
(ECAMP02) 1.00m FS-ASHPD-0001	11/8/2017	2/12/2018	4.65	7.23	70.63	11.48	2.1	34.49	16.99	<MDL	<MDL
(ECAMP02) 3.00m FS-ASHPD-0001	11/8/2017	2/12/2018	4.16	6.74	67.44	11.65	1.84	36.25	17.59	<MDL	<MDL
(ECAMP02) 5.00m FS-ASHPD-0001	11/8/2017	2/12/2018	4.76	6.91	65.92	11.23	1.88	34.51	16.43	<MDL	<MDL
(ECAMP02) 7.00m FS-ASHPD-0001	11/8/2017	2/19/2018	4.56	5.87	58.96	11.24	1.77	32.05	16.43	<MDL	<MDL
(ECAMP02) 9.00m FS-ASHPD-0001	11/8/2017	2/19/2018	4.19	6.14	61.485	11.555	2.04	33.14	16.92	<MDL	<MDL
(ECAMP02) 11.00m FS-ASHPD-0001	11/8/2017	2/19/2018	4.44	6.55	62.96	11.33	2.32	34.7	17.47	<MDL	<MDL

Table B10 (Continued)

U.S. Geological Survey local site name	Sampling Date	Date Analyzed	PFBS	PFPeS	PFHxS Linear	PFHxS Branched	PFHpS	PFOS Linear	PFOS Branched	PFNS	PFDS
FS-ASHPD-0001 (ECAMP02) 13.00m	11/8/2017	2/19/2018	4.54	5.95	62.36	11.66	2.21	34.38	17.71	<MDL	<MDL
FS-ASHPD-0001 (ECAMP02) 15.00m	11/8/2017	2/19/2018	4.695	6.35	63.275	11.605	1.875	33.065	15.78	<MDL	<MDL
FS-ASHPD-0001 (ECAMP02) 17.00m	11/8/2017	2/19/2018	4.24	5.18	52.7	9.53	1.83	28.56	14.18	<MDL	<MDL
FS-ASHPD-0009 (ECAMP01) Microlayer	9/11/2017	2/12/2018	4.96	6.38	64.58	11.35	1.95	66.82	25.64	<MDL	<MDL
FS-ASHPD-0009 (ECAMP01) 0.1m	9/11/2017	2/12/2018	4.34	6.33	62.89	10.5	1.84	34.83	16.79	<MDL	<MDL
FS-ASHPD-0009 (ECAMP01) 1.00m	9/11/2017	2/12/2018	4.34	6.495	62.725	10.585	2.065	34.955	16.67	<MDL	<MDL
FS-ASHPD-0009 (ECAMP01) 3.00 m	9/11/2017	2/12/2018	4.45	6.17	61.19	10.4	1.72	35.53	16.4	<MDL	<MDL
FS-ASHPD-0009 (ECAMP01) 5.00 m	9/11/2017	2/12/2018	4.29	5.94	63.4	11.27	1.79	34.49	16.95	<MDL	<MDL
FS-ASHPD-0010 Microlayer	9/11/2017	2/19/2018	4.2	5.8	59.92	10.61	2	35.01	17.28	<MDL	<MDL
FS-ASHPD-0010 0.1m	9/11/2017	2/19/2018	4.37	6.11	62.02	11.12	1.87	31.6	16.2	<MDL	<MDL
FS-ASHPD-0010 1.00m	9/11/2017	2/19/2018	4.07	5.77	58.235	10.6	1.835	30.325	15.915	<MDL	<MDL
FS-ASHPD-0010 3.00m	9/11/2017	2/19/2018	4.15	5.45	58.12	10.38	1.83	30.1	15.35	<MDL	<MDL
FS-ASHPD-0010 5.00m	9/11/2017	2/19/2018	4	5.91	57.28	11.02	1.74	29.43	14.8	<MDL	<MDL
FS-ASHPD-0010 7.00m	9/11/2017	2/19/2018	4.63	6.56	67.17	12.23	2.01	33.63	16.26	<MDL	<MDL
FS-ASHPD-0010 9.00m	9/11/2017	2/19/2018	4.345	6.74	64.945	12.03	1.84	36.105	16.23	<MDL	<MDL
FS-ASHPD-0011 Microlayer	9/12/2017	2/12/2018	5.01	6.76	69.82	12.25	1.84	33.47	15.86	<MDL	<MDL
FS-ASHPD-0011 0.1m	9/12/2017	2/12/2018	4.86	7.28	70.76	12.19	1.96	36.63	17.34	<MDL	<MDL
FS-ASHPD-0011 1.00m	9/12/2017	2/12/2018	4.9	6.46	66.72	11.95	2.37	35.76	17.71	<MDL	<MDL
FS-ASHPD-0011 3.00m	9/12/2017	2/12/2018	4.81	6.545	66.225	11.2	1.79	37.935	17.74	<MDL	<MDL
FS-ASHPD-0011 5.00m	9/12/2017	2/12/2018	4.79	6.7	66.89	11.9	2.05	37.47	17.84	<MDL	<MDL
FS-ASHPD-0011 7.00m	9/12/2017	2/12/2018	4.7	6.58	69.73	12.2	1.82	34.65	17.81	<MDL	<MDL
FS-ASHPD-0011 9.00m	9/12/2017	2/12/2018	4.91	6.44	65.03	11.35	1.87	37.13	16.31	<MDL	<MDL
MI-JOHPD-0001 (ECJNP03) Microlayer	9/12/2017	2/19/2018	3.87	3.66	36.43	6.79	2.08	162.75	47.81	<MDL	<MDL
MI-JOHPD-0001 (ECJNP03) 0.1m	9/12/2017	2/19/2018	4.015	4.025	38.565	7.42	1.59	38.935	18.17	<MDL	<MDL
MI-JOHPD-0001 (ECJNP03) 1.00m	9/12/2017	2/19/2018	3.93	3.98	38	7.57	1.57	40.05	18.81	<MDL	<MDL

Table B10 (Continued)

U.S. Geological Survey local site name	Sampling Date	Date Analyzed	PFBS	PFPeS	PFHxS Linear	PFHxS Branched	PFHpS	PFOS Linear	PFOS Branched	PFNS	PFDS
MI-JOHPD-0001 (ECJNP03) 3.00m	9/12/2017	2/19/2018	4.39	4.22	37.38	7.57	1.68	38.4	18.99	<MDL	<MDL
MI-JOHPD-0001 (ECJNP03) 5.00m	9/12/2017	2/19/2018	4.09	3.78	35.87	7.1	1.62	39.38	18.75	<MDL	<MDL
MI-JOHPD-0001 (ECJNP03) 7.00m	9/12/2017	2/19/2018	3.8	3.69	37.35	6.53	1.37	36.2	18.02	<MDL	<MDL
MI-JOHPD-0001 (ECJNP03) 9.00m	9/12/2017	2/19/2018	4	3.96	38.87	7.78	1.52	37.21	18.61	<MDL	<MDL
MI-JOHPD-0001 (ECJNP03) 11.00m	9/12/2017	2/19/2018	3.72	3.98	38.05	6.51	<MQL Qual	37.1	17.61	<MDL	<MDL
MI-JOHPD-0001 (ECJNP03) 15.00	9/12/2017	2/19/2018	3.71	3.77	36.2	6.91	<MQL Qual	37.93	17	<MDL	<MDL
MI-JOHPD-0008 Microlayer	9/12/2017	2/19/2018	3.99	3.73	36.62	7.09	1.35	54.49	21.29	<MDL	<MDL
MI-JOHPD-0008 0.1m	9/12/2017	2/19/2018	3.595	3.865	36.72	6.94	1.485	36.305	17.685	<MDL	<MDL
MI-JOHPD-0008 1.00m	9/12/2017	2/19/2018	3.79	4.06	38.43	7.24	<MQL Qual	34.84	16.55	<MDL	<MDL
MI-JOHPD-0008 3.00m	9/12/2017	2/19/2018	4.2	4	38.16	7.23	1.62	37.38	17.97	<MDL	<MDL
MI-JOHPD-0008 5.00m	9/12/2017	2/19/2018	3.56	3.695	37.115	6.855	1.48	34.81	17.47	<MDL	<MDL
MI-JOHPD-0008 7.00m	9/12/2017	2/19/2018	3.65	3.79	36.79	6.86	1.32	35.93	17.65	<MDL	<MDL
MI-JOHPD-0008 9.00m	9/12/2017	2/19/2018	3.875	4.06	36.22	6.61	1.375	35.81	16.88	<MDL	<MDL
ASHPD-GWOUT-L-N-LW	9/13/2017	3/7/2018	4.69	6.94	62.33	11.55	2.23	42.48	19.41	<MDL	<MDL
ASHPD-GWOUT-L-N-015	9/13/2017	3/7/2018	6.465	8.2575	68.8775	13.635	2.115	47.005	20.265	<MDL	<MDL
ASHPD-GWOUT-L-N-030	9/13/2017	3/7/2018	5.78	<MQL Qual	70.79	13.64	2.2	47.11	20.59	<MDL	<MDL
ASHPD-GWOUT-L-N-050	9/13/2017	3/7/2018	6.74	8.94	75.91	15.01	2.31	33.06	21.78	<MDL	<MDL
ASHPD-GWOUT-L-N-100	9/13/2017	3/13/2018	7.845	7.575	64.29	11.235	1.795	26.875	16.83	<MDL	<MDL
ASHPD-GWOUT-R-N-LW	9/13/2017	3/13/2018	4.78	6.2	56.6	10.15	1.81	36.88	16.02	<MDL	<MDL
ASHPD-GWOUT-R-N-015	9/13/2017	3/13/2018	5.98	6.73	61.34	11.05	<MQL Qual	42.74	15.11	<MDL	<MDL
ASHPD-GWOUT-R-N-030	9/13/2017	3/13/2018	5.23	6.39	60.72	12.44	<MQL Qual	40.7	15.43	<MDL	<MDL
ASHPD-GWOUT-R-N-050	9/13/2017	3/13/2018	6.11	8.515	70.04	13.42	2.1	35.445	16.155	<MDL	<MDL
ASHPD-GWOUT-R-N-100	9/13/2017	3/13/2018	7.83	7.46	65.77	8.99	1.48	34.49	14.47	<MDL	<MDL
ASHPD-GWOUT-R-S-015	9/13/2017	3/7/2018	6.63	9.57	75.19	14.28	2.2	96.4	28.7	<MDL	<MDL

Table B10 (Continued)

U.S. Geological Survey local site name	Sampling Date	Date Analyzed	PFBS	PFPeS	PFHxS Linear	PFHxS Branched	PFHpS	PFOS Linear	PFOS Branched	PFNS	PFDS
ASHPD-GWOUT-R-S-100	9/13/2017	3/7/2018	7.21	11.12	90	18.68	2.74	47.46	27.63	<MDL	<MDL
ASHPD-KIGAM-124N-010E-LW	9/14/2017	3/13/2018	7.79	9.27	99.43	16.77	5.05	106.49	52.88	<MDL	<MDL
ASHPD-KIGAM-124N-010E-015	9/14/2017	3/13/2018	4.43	3.75	29.86	5.95	2.3	203.86	33.04	<MQL	<MDL
ASHPD-KIGAM-124N-010E-030	9/14/2017	3/13/2018	3.04	2.85	23.36	4.07	2.11	183.69	31.35	<MQL	<MDL
ASHPD-KIGAM-124N-010E-050	9/14/2017	3/13/2018	3.5	3.62	30.71	5.69	2.22	197.07	38.98	<MQL	<MDL
ASHPD-KIGAM-124N-010E-100	9/14/2017		6.71	7.595	69.37	10.945	4.64	246.45	69.405	<MQL Qual	<MDL
ASHPD-KIGAM-131N-011E-LW	9/14/2017	3/7/2018	8.91	14.52	150.04	25.81	6.28	122.45	62.1	<MDL	<MDL
ASHPD-KIGAM-131N-011E-015	9/14/2017	3/7/2018	<MQL	2.795	25.34	5.04	2.38	142.23	39.455	<MQL	<MDL
ASHPD-KIGAM-131N-011E-030	9/14/2017		<MQL	2.62	27.03	5.36	2.39	138.49	37.59	<MQL	<MDL
ASHPD-KIGAM-131N-011E-050	9/14/2017	3/7/2018	<MQL	3.9	39.8	6.4	3.18	145.95	41.23	<MQL	<MDL
ASHPD-KIGAM-131N-011E-100	9/14/2017		<MQL	3.745	38.66	6.4	3.54	143.645	44.33	<MQL	<MDL
ASHPD-GWIN-C-LW	9/11/2017	2/19/2018	4.23	5.92	58.37	10.24	1.92	32.4	16.32	<MDL	<MDL
ASHPD-GWIN-C-035	9/11/2017	2/19/2018	<MQL	0.98	8.64	1.47	<MQL	6.61	3.97	<MDL	<MDL
ASHPD-GWIN-C-100	9/11/2017	2/19/2018	<MDL	<MQL Qual	6.1	<MQL	<MQL Qual	8.87	3.31	<MDL	<MDL
ASHPD-GWOUT-L-N-100	2/23/2018	4/23/2018	3.47	4.41	47.44	7.82	<MQL	30.45	11.82	<MDL	<MDL
ASHPD-GWOUT-R-N-LW	2/23/2018	4/23/2018	4.15	6.69	69.38	12.83	2.41	46.54	19.86	<MDL	<MDL
ASHPD-GWOUT-R-N-100	2/23/2018	4/23/2018	2.56	3.125	34.135	5.995	<MQL Qual	27.87	8.765	<MDL	<MDL
MA-FSW 239-M01-01PT	8/5/2016	3/13/2018	<MQL	<MQL	3.77	<MDL	<MDL	1.88	<MQL	<MDL	<MDL
MA-FSW 239-M01-02GNT	8/5/2016	3/13/2018	<MDL	<MQL	1.94	<MDL	<MDL	9.37	2.03	<MDL	<MDL
MA-FSW 239-M01-04BUT	8/5/2016	3/13/2018	<MDL	<MDL	2.59	<MDL	<MDL	10.68	2.34	<MDL	<MDL
MA-FSW 239-M01-06WT	8/5/2016	3/13/2018	<MQL	2.02	25.68	3.34	1.71	171.15	30.69	<MDL	<MDL
MA-FSW 239-M01-08GY	8/5/2016	3/13/2018	<MQL	1.23	20.775	2.83	<MQL	39.965	10.44	<MDL	<MDL
MA-FSW 239-M01-10P	8/5/2016	3/13/2018	3.575	7.7	42.17	8.26	<MQL	11.86	1.81	<MDL	<MDL

Table B10 (Continued)

U.S. Geological Survey local site name	Sampling Date	Date Analyzed	PFBS	PFPeS	PFHxS Linear	PFHxS Branched	PFHpS	PFOS Linear	PFOS Branched	PFNS	PFDS
MA-FSW 239-M01-12R	8/5/2016	3/13/2018	<MDL	<MDL	<MQL	<MDL	<MDL	1	<MDL	<MDL	<MDL
MA-FSW 239-M01-14BK	8/5/2016	3/13/2018	<MDL	<MDL	<MDL	<MDL	<MDL	3.09	<MDL	<MDL	<MDL
MA-FSW 300-M03-01PT	7/7/2016	3/13/2018	7.46	10.94	679.33	79.85	7.21	297.42	34.19	<MQL	<MDL
MA-FSW 300-M03-03RT	7/7/2016	3/13/2018	<MQL	1.6	35.02	5.11	1.75	15.55	11.09	<MDL	<MDL
MA-FSW 300-M03-06WT	7/7/2016	3/13/2018	9.71	14.66	836.81	126.6	7.43	99.39	42.76	<MDL	<MDL
	7/7/2016							244.59			
MA-FSW 300-M03-09Y	7/7/2016	3/13/2018	12.825	20.315	1300	207.705	12.165	5	56.73	<MQL	<MDL
	7/7/2016							302.92			
MA-FSW 300-M03-10P	7/7/2016	3/13/2018	7.255	10.975	723.32	84.5	7.595	5	35.69	<MDL	<MDL
MA-FSW 300-M03-11GN	7/7/2016	3/13/2018	4.71	6.88	256.77	30.83	4.46	315.32	20.71	<MDL	<MDL
MA-FSW 300-M03-14BK	7/7/2016	3/13/2018	7.6	9.93	228.8	22.48	5.63	432.94	49.41	<MDL	<MDL
MA-FSW 300-M03-15W	7/8/2016	3/13/2018	7.44	8.44	187.97	18.24	6.32	445.72	59.53	<MDL	<MDL
MA-FSW 300-M02-01PT	7/8/2016	3/13/2018	8.73	10.19	255.23	24.91	7.32	573.21	69.05	<MDL	<MDL
MA-FSW 300-M02-02GNT	7/8/2016	3/13/2018	7.37	7.74	190.16	18.35	6.33	579.3	69.23	<MDL	<MDL
MA-FSW 300-M02-03RT	7/8/2016	4/23/2018	4.63	6.17	135.81	14.61	4.61	519.86	55.83	<MQL	<MDL
MA-FSW 300-M02-06WT	7/8/2016	3/13/2018	4.13	8.3	102.67	12.64	1.83	169.71	22.07	<MDL	<MDL
MA-FSW 300-M02-08GY	7/8/2016	3/13/2018	<MQL	1.16	23.78	<MQL	<MDL	31.39	3.08	<MDL	<MDL
MA-FSW 300-M02-10P	7/8/2016	3/13/2018	<MDL	<MDL	3.33	<MDL	<MDL	8.84	<MDL	<MDL	<MDL
MA-FSW 300-M02-14BK	7/8/2016	3/13/2018	<MDL	<MDL	<MDL	<MDL	<MDL	<MQL	<MDL	<MDL	<MDL
MA-FSW 300-0138	7/7/2016	3/7/2018	<MDL	<MDL	<MDL	<MDL	<MDL	<MQL	<MDL	<MDL	<MDL
MA-FSW 424-M01-01PT	7/26/2016	4/23/2018	27.03	59.5	941.86	128.9	19.43	25.26	126.64	<MDL	<MDL
MA-FSW 424-M01-03RT	7/26/2016	4/23/2018	5.43	6.11	91.16	13.91	<MQL	6.23	20.65	<MDL	<MDL
MA-FSW 424-M01-05BKT	7/26/2016	4/23/2018	<MQL	<MQL	6.37	<MDL	<MDL	1.73	<MQL	<MDL	<MDL
MA-FSW 424-M01-09Y	7/26/2016	4/23/2018	<MDL	<MQL	7.955	<MQL	<MDL	<MQL	<MQL	<MDL	<MDL
MA-FSW 424-M01-13BU	7/26/2016	4/23/2018	<MDL	<MDL	<MDL	<MDL	<MQL	<MQL	<MDL	<MDL	<MDL
MA-FSW 424-M02-11GN 72-13	7/26/2016	4/23/2018	55.19	161.83	2500	373.57	86.41	317.42	265.075	<MQL	<MDL
								5			
MA-FSW 424-M02-12R 72-13	7/26/2016	4/23/2018	84.58	256.68	2770	522.33	278.53	850.55	685.45	2.15	<MDL
MA-FSW 424-M02-14BK 72-13	7/26/2016	4/23/2018	62.45	167.46	1800	332.44	74.81	155.1	376.9	<MDL	<MDL
MA-FSW 424-M02-15W 72-13	7/26/2016	4/23/2018	16.38	25.45	439.16	57.94	18.07	57.92	226.58	<MDL	<MDL
MA-FSW 564-M01-01PT	7/6/2016	3/13/2018	<MDL	<MDL	<MDL	<MDL	<MDL	<MQL	<MDL	<MDL	<MDL
MA-FSW 564-M01-02GNT	7/6/2016	3/13/2018	<MQL	<MQL	10.83	<MQL	1.655	15.26	10.655	<MDL	<MDL

Table B10 (Continued)

U.S. Geological Survey local site name	Sampling Date	Date Analyzed	PFBS	PFPeS	PFHxS Linear	PFHxS Branched	PFHpS	PFOS Linear	PFOS Branched	PFNS	PFDS
MA-FSW 564-M01-04BUT	7/6/2016	3/7/2018	4.42	5.98	91.42	13.49	4.32	165.59	43.98	<MDL	<MDL
		3/7/2018		Qual				115.72	51		
MA-FSW 564-M01-05BKT	7/6/2016	3/7/2018	4.955	5.97	55.485	8.93	4.26	5	16.53	<MDL	<MDL
MA-FSW 564-M01-06WT	7/6/2016	3/7/2018	3.72	4.21	31.64	5.23	1.23	33.61	1.74	<MDL	<MDL
MA-FSW 564-M01-08GY	7/6/2016	3/7/2018	<MDL	<MDL	2.72	<MDL	<MQL	11.53	<MQL	<MDL	<MDL
MA-FSW 564-M01-10P	7/6/2016	3/7/2018	<MDL	<MDL	<MQL	<MDL	<MDL	6.49	<MQL	<MDL	<MDL
MA-FSW 564-M01-12R	7/6/2016	3/7/2018	<MDL	<MDL	3.94	<MQL	<MDL	13.01	<MQL	<MDL	<MDL
MA-FSW 564-M01-14BK	7/6/2016	3/7/2018	<MDL	<MDL	1.575	<MDL	<MDL	<MQL	<MQL	<MDL	<MDL
MA-FSW 621-M01-01PT	7/11/2016	3/13/2018	<MDL	<MQL	3.28	<MDL	<MDL	11.81	1.58	<MDL	<MDL
MA-FSW 621-M01-02GNT	7/11/2016	3/13/2018	8.35	12.435	136.35	19.46	3.865	56.325	15.725	<MQL	<MDL
MA-FSW 621-M01-03RT	7/11/2016	4/23/2018	5.26	9.26	147.44	18.21	3.08	45.81	11.76	<MDL	<MDL
MA-FSW 621-M01-05BKT	7/11/2016	3/13/2018	2.63	1.81	27.28	2.42	<MQL	64.12	6.82	<MDL	<MDL
MA-FSW 621-M01-06WT	7/11/2016	4/23/2018	<MDL	<MQL	10.67	<MQL	<MDL	37.65	1.96	<MDL	<MDL
MA-FSW 621-M01-07O	7/11/2016	3/13/2018	<MDL	<MQL	5.88	<MDL	<MDL	19.83	<MQL	<MDL	<MDL
MA-FSW 621-M01-09Y	7/11/2016	3/13/2018	<MDL	<MDL	<MQL	<MDL	<MDL	<MQL	<MDL	<MDL	<MDL
MA-FSW 621-M01-11GN	7/11/2016	3/13/2018	<MDL	<MDL	<MQL	<MDL	<MDL	<MQL	<MDL	<MDL	<MDL
MA-FSW 621-M01-13BU	7/11/2016	3/13/2018	<MDL	<MDL	<MDL	<MDL	<MDL	<MQL	<MDL	<MDL	<MDL
MA-FSW 621-M01-15W	7/11/2016	3/13/2018	<MDL	<MDL	<MDL	<MDL	<MDL	<MQL	<MDL	<MDL	<MDL
MA-FSW 622-M01-01PT	7/11/2016	3/20/2018	<MDL	<MDL	1.97	<MDL	<MDL	<MQL	<MQL	<MDL	<MDL
								Qual			
MA-FSW 622-M01-02GNT	7/11/2016	3/20/2018	2.55	2.29	41.44	5.05	1.44	54.09	12.25	<MDL	<MDL
MA-FSW 622-M01-03RT	7/11/2016	4/23/2018	5.76	7.48	108.62	14.2	1.29	84.38	9.36	<MDL	<MDL
MA-FSW 622-M01-05BKT	7/11/2016	3/20/2018	<MQL	2.11	19.07	2.04	<MQL	68.74	8.99	<MDL	<MDL
MA-FSW 622-M01-06WT	7/11/2016	4/23/2018	<MDL	<MDL	12.08	<MDL	<MQL	49.67	3.44	<MDL	<MDL
MA-FSW 622-M01-07O	7/11/2016	3/20/2018	<MDL	<MQL	9.94	<MQL	<MDL	41.855	2.705	<MDL	<MDL
MA-FSW 622-M01-09Y	7/11/2016	3/20/2018	<MDL	<MDL	4.7	<MDL	<MDL	20.725	1.62	<MDL	<MDL
MA-FSW 622-M01-11GN	7/11/2016	3/20/2018	<MDL	<MDL	2.45	<MDL	<MDL	8.75	<MQL	<MDL	<MDL
MA-FSW 622-M01-13BU	7/11/2016	3/20/2018	<MDL	<MDL	1.48	<MDL	<MDL	2.66	<MDL	<MDL	<MDL
MA-FSW 622-M01-15W	7/11/2016	3/20/2018	<MDL	<MQL	6.8	<MQL	<MQL	3.94	<MQL	<MDL	<MDL
MA-FSW 744-0004	7/26/2016	3/20/2018	<MQL	<MQL	2.77	<MDL	<MQL	27.48	6.43	<MDL	<MDL
MA-FSW 744-0008	7/26/2016	3/20/2018	<MQL	<MQL	6.53	<MQL	<MQL	111.71	13.53	<MDL	<MDL
MA-FSW 744-0010	7/26/2016	3/20/2018	<MQL	<MQL	5.65	<MQL	<MQL	86.68	13.2	<MDL	<MDL
MA-FSW 744-0011	7/26/2016	3/20/2018	<MQL	<MQL	5.81	<MQL	<MQL	79.31	12.42	<MDL	<MDL

Table B10 (Continued)

U.S. Geological Survey local site name	Sampling Date	Date Analyzed	PFBS	PFPeS	PFHxS Linear	PFHxS Branched	PFHpS	PFOS Linear	PFOS Branched	PFNS	PFDS
MA-FSW 744-0013	7/26/2016	3/20/2018	<MQL	<MQL	6.49	<MQL	<MDL	63.1	10.46	<MDL	<MDL
MA-FSW 744-0017	7/26/2016	3/20/2018	<MQL	0.96	8.395	1.59	<MQL	77.82	11.055	<MQL	<MDL
	7/26/2016	3/20/2018								<MQL	
MA-FSW 744-0019	7/26/2016	3/20/2018	<MQL	1.85	24.36	4.15	2.29	159.26	33.04	Qual	<MDL
MA-FSW 744-0023	7/26/2016	3/21/2018	2.6	4.07	56.61	8.85	5.14	220.54	69.3	<MQL	<MDL
								180.22		Qual	
MA-FSW 744-0025	7/26/2016	4/23/2018	3.47	6.73	115.28	17.445	7.36	5	87.1	2.075	<MDL
MA-FSW 744-0026	7/26/2016	4/23/2018	4.6	9.87	170.27	25.06	11.56	169.23	145.67	2.46	<MDL
MA-FSW 744-0028	7/26/2016	4/23/2018	10.665	25.14	425.6	61.775	22.025	129.5	199.855	1.49	<MDL
MA-FSW 744-0029	7/26/2016	4/23/2018	43.07	115.9	2027.25	314.99	76.02	60.63	622.02	<MDL	<MDL
MA-FSW 744-0030	7/26/2016	4/23/2018	49	124.32	2077.27	315.72	71.08	53.08	537.07	<MDL	<MDL
Q1 MI-QUARV-00015(QR001)	8/15/2017	2/6/2018	4.2	3.8	37.17	7.02	1.5	46.65	20.31	<MDL	<MDL
Q3	8/15/2017	2/6/2018	5.25	5.98	70.02	13.02	3.04	78.33	36.01	<MDL	<MDL
Q4	8/15/2017	2/6/2018	5.07	4.74	52.69	10.31	2.22	56.53	26.92	<MDL	<MDL
Q5	8/15/2017	2/6/2018	4.74	4.59	50.57	9.64	2.01	45.84	22.81	<MDL	<MDL
Q9	8/15/2017	2/6/2018	4.34	3.21	33.36	7.01	<MQL Qual	28.21	14.59	<MDL	<MDL
Q-FC	8/15/2017	2/6/2018	4.74	4.27	42.98	8.72	1.81	39.41	20.8	<MDL	<MDL
Q-OBR	8/15/2017	2/6/2018	4.13	4.92	55.86	10.41	2.35	58.75	27.81	<MDL	<MDL
Q-TRIB	8/15/2017	2/6/2018	3.695	4.655	42.495	8.12	2.13	49.615	24.28	<MDL	<MDL
Quash_HS_Seep1	8/16/2017	2/6/2018	<MQL	<MDL	1.7	<MDL	<MDL	<MDL	<MQL	<MDL	<MDL
Quash_HS_Seep2	8/16/2017	2/6/2018	<MDL	<MDL	<MDL	<MDL	<MDL	<MQL	<MQL	<MDL	<MDL
QB010	8/17/2017	2/6/2018	3.62	<MQL	3.25	<MQL	<MDL	1.27	<MQL	<MDL	<MDL
QB018	8/17/2017	2/6/2018	<MQL	0.86	4.69	<MQL	<MDL	<MQL	<MQL	<MDL	<MDL
QB020	8/17/2017	2/6/2018	7.73	7.37	41.96	8.43	0.98	2.38	4.03	<MDL	<MDL
QB026	8/17/2017	2/6/2018	5.34	5	43.16	7.22	1.44	29.6	15.2	<MDL	<MDL
QB039	8/18/2017	2/6/2018	7.02	11.41	149.22	27.27	7.13	135.57	61.6	<MDL	<MDL
DD004	8/17/2017	2/6/2018	1.7	1.53	25.71	4.49	<MQL Qual	28.5	10.17	<MDL	<MDL
DD-12	8/14/2017	2/6/2018	6.57	6.035	46.04	8.86	1.6	30.505	17.645	<MDL	<MDL
Quash_OV_seep1	8/14/2017	2/6/2018	8.5	9	51.02	9.71	1.6	5.99	7.21	<MDL	<MDL
Quash_OV_seep2	8/14/2017	2/12/2018	1.7	1.23	10.5	2.05	<MDL	<MDL	0.83	<MDL	<MDL
Quash_HRTS_seep	8/14/2017	2/6/2018	7.32	7.57	44.05	9.78	0.94	<MQL	4.41	<MDL	<MDL

Table B10 (Continued)

U.S. Geological Survey local site name	Sampling Date	Date Analyzed	PFBS	PFPeS	PFHxS Linear	PFHxS Branched	PFHpS	PFOS Linear	PFOS Branched	PFNS	PFDS
QT008	8/17/2017	2/6/2018	8.97	12.02	68.88	13.32	1.88	3.97	11.33	<MDL	<MDL
QT018	8/17/2017	2/6/2018	<MQL	<MQL	3.99	<MQL	<MDL	0.53	<MQL	<MDL	<MDL
QT030	8/17/2017	2/6/2018	3.62	2.18	15.9	3.66	<MQL	<MQL	1.75	<MDL	<MDL
QT034	8/17/2017	2/6/2018	16.06	5.65	42.57	5.41	<MDL	<MQL	<MQL Qual	<MDL	<MDL
QT039	8/17/2017	2/6/2018	6	7.15	49.88	9.86	1.915	6.25	12.05	<MDL	<MDL
QT082	8/18/2017	2/6/2018	1.55	<MDL	2.17	<MDL	<MDL	8.44	2.66	<MDL	<MDL
QT101	8/17/2017	2/6/2018	<MQL	<MDL	1.55	<MDL	<MDL	3.22	<MQL	<MDL	<MDL
QT122	8/18/2017	2/6/2018	3.21	3.82	45.71	8.91	1.4	30.93	15.76	<MDL	<MDL
QT142	8/16/2017	2/6/2018	22.92	32.12	368.99	60.48	27.15	763.75	237.74	<MDL	<MDL
Quash-Spawn1	8/16/2017	2/12/2018	<MQL	<MQL	2.91	<MDL	<MQL	0.55	<MQL	<MDL	<MDL
Quash-Spawn2	8/16/2017	2/12/2018	<MDL	<MQL	<MQL	<MDL	<MDL	<MDL	<MQL	<MDL	<MDL
Quash-Spawn3	8/14/2017	2/12/2018	<MDL	<MDL	<MDL	<MDL	<MDL	<MDL	<MDL	<MDL	<MDL

Table B11. Precursor sample concentrations (ng L^{-1}) measured with LC-MS/MS.

U.S. Geological Survey local site name	Sampling Date	Date Analyzed	4:2 FtS	8:2 FtS	N-MeFOSAA	N-EtFOSAA	FOSA
DI H2O From Peristaltic Geopump For MLSs	9/11/2017	1/16/2018	<MDL	<MDL	<MQL	<MQL	<MDL
DI H2O From Grundfos Pump	9/12/2017	1/16/2018	<MDL	<MDL	<MDL	<MDL	<MDL
DI H2O From Keck Pump	9/12/2017	1/16/2018	<MDL	<MDL	<MDL	<MDL	<MDL
DI H2O From Henry Sampler	9/14/2017	1/16/2018	<MDL	<MDL	<MDL	<MDL	<MDL
DI H2O From Microlayer Sampling Device	9/12/2017	1/16/2018	<MDL	<MDL	<MDL	<MDL	<MDL
DI H2O From Boat Peristaltic Geopump	9/12/2017	1/16/2018	<MDL	<MDL	<MDL	<MDL	<MDL
DI H2O From Boat Peristaltic Geopump	11/8/2017	1/16/2018	<MDL	<MDL	<MDL	<MDL	<MDL
DI H2O From MA-FSW 631-02GNT	2/22/2018	4/23/2018	<MDL	<MDL	<MDL	<MDL	<MDL
DI H2O From Henry Sampler	2/22/2018	4/23/2018	<MDL	<MDL	<MDL	<MDL	<MDL
MA-MIW 207-0069 (00MW0582B)	7/26/2017	1/16/2018	<MDL	<MDL	<MDL	<MDL	<MDL
MA-MIW 207-0215 (00MW0582A)	7/26/2017	1/16/2018	<MQL	<MDL	<MDL	1.2	<MDL
MA-MIW 209-0015 (00MW0584C)	7/21/2017	1/25/2018	<MDL	<MDL	<MDL	<MDL	<MDL
MA-MIW 209-0146 (00MW0584B)	7/21/2017	1/25/2018	<MQL	<MDL	<MDL	<MDL	<MDL
MA-MIW 209-0286 (00MW0584A)	7/21/2017	1/25/2018	<MDL	<MDL	<MDL	<MDL	<MDL
MA-MIW 210-0026	7/25/2017	1/25/2018	<MDL	<MDL	<MDL	<MDL	<MDL
MA-MIW 210-0046	7/25/2017	1/25/2018	<MDL	<MDL	<MDL	<MDL	<MDL
MA-MIW 210-0075 (00MW0609B)	7/25/2017	1/25/2018	<MDL	<MDL	<MDL	<MDL	<MDL
MA-MIW 210-0145 (00MW0609A)	7/25/2017	1/25/2018	<MDL	<MDL	<MDL	<MDL	<MDL
MA-MIW 221-0245 (03MW1003B)	7/28/2017	1/25/2018	<MDL	<MDL	<MDL	<MDL	<MDL
MA-MIW 221-0325 (03MW1003A)	7/28/2017	1/25/2018	<MDL	<MDL	<MDL	<MDL	<MDL
MA-MIW 223-0111 (03MW1005B)	7/25/2017	1/25/2018	<MDL	<MDL	<MDL	<MDL	<MDL
MA-MIW 223-0148 (03MW1005A)	7/25/2017	1/25/2018	<MDL	<MDL	<MQL	<MDL	<MDL
MA-MIW 230-0015	7/20/2017	1/25/2018	<MDL	<MDL	<MDL	<MDL	<MDL
MA-MIW 230-0060	7/20/2017	1/25/2018	<MDL	<MDL	<MDL	<MDL	<MDL
MA-MIW 230-0110	7/20/2017	1/25/2018	<MQL	<MDL	<MDL	<MDL	<MDL
MA-MIW 230-0174 (03MW2626B)	7/19/2017	1/25/2018	<MDL	<MDL	<MDL	<MDL	<MDL
MA-MIW 230-0294 (03MW2626A)	7/19/2017	1/25/2018	<MDL	<MDL	<MDL	<MDL	<MDL
MA-MIW 231-0040	7/19/2017	1/25/2018	<MDL	<MDL	<MDL	<MDL	<MDL

Table B11 (Continued)

U.S. Geological Survey local site name	Sampling Date	Date Analyzed	4:2 FtS	8:2 FtS	N-MeFOSAA	N-EtFOSAA	FOSA
MA-MIW 231-0070	7/19/2017	1/25/2018	<MDL	<MDL	<MDL	<MDL	<MDL
MA-MIW 231-0105	7/19/2017	1/25/2018	<MDL	<MDL	<MDL	<MDL	<MDL
MA-MIW 231-0138	7/19/2017	1/12/2018	<MDL	<MDL	<MDL	<MDL	<MDL
MA-MIW 232-0050	7/18/2017	1/25/2018	<MDL	<MDL	<MDL	<MDL	<MDL
MA-MIW 232-0080	7/18/2017	1/25/2018	<MDL	<MDL	<MQL	<MDL	<MDL
MA-MIW 232-0115	7/18/2017	1/25/2018	<MQL	<MDL	<MDL	<MDL	<MDL
MA-MIW 232-0150	7/18/2017	1/25/2018	<MDL	<MDL	<MDL	<MDL	<MDL
MA-MIW 233-0016	7/26/2017	1/25/2018	<MDL	<MDL	<MDL	<MDL	<MDL
MA-MIW 233-0070	7/26/2017	1/25/2018	<MDL	<MDL	<MDL	<MDL	<MDL
MA-MIW 233-0174 (00MW0608B)	7/26/2017	1/25/2018	<MDL	<MDL	<MDL	<MQL	<MDL
MA-MIW 233-0245 (00MW0608A)	7/26/2017	1/25/2018	<MDL	<MDL	<MDL	<MQL	<MDL
MA-MIW 234-0055	7/20/2017	1/25/2018	<MQL	<MDL	<MDL	<MDL	<MDL
MA-MIW 234-0086	7/20/2017	1/25/2018	<MDL	<MDL	<MDL	<MDL	<MDL
MA-MIW 234-0120	7/20/2017	1/25/2018	<MDL	<MDL	<MDL	<MDL	<MDL
MA-MIW 234-0150	7/20/2017	1/25/2018	<MDL	<MDL	<MDL	<MDL	<MDL
MA-MIW 236-0025 (MAMW0396S)	7/27/2017	1/25/2018	0.6	<MDL	<MDL	<MDL	<MDL
MA-MIW 236-0109 (MAMW0296I)	7/27/2017	1/25/2018	<MDL	<MDL	<MDL	<MDL	<MDL
MA-MIW 236-0189 (MAMW0196D)	7/27/2017	1/25/2018	<MDL	<MDL	<MDL	<MDL	<MDL
MA-MIW 237-0145 (03MW2620B)	7/27/2017	1/16/2018	<MDL	<MDL	<MDL	<MDL	<MDL
MA-MIW 237-0254 (03MW2620A)	7/27/2017	1/16/2018	<MDL	<MDL	<MDL	1.39	<MDL
MA-FSW 631-M01-01PT	9/12/2017	1/16/2018	<MDL	<MDL	<MQL	<MDL	<MDL
MA-FSW 631-M01-02GNT	9/12/2017	1/16/2018	<MDL	<MDL	<MDL	<MDL	<MDL
MA-FSW 631-M01-03RT	9/12/2017	1/16/2018	<MDL	<MDL	<MDL	<MDL	<MDL
MA-FSW 631-M01-04BUT	9/12/2017	1/16/2018	<MDL	<MDL	<MDL	<MDL	<MDL
MA-FSW 631-M01-06WT	9/12/2017	1/16/2018	<MDL	<MDL	<MDL	<MDL	<MDL
MA-FSW 631-M01-09Y	9/12/2017	1/16/2018	<MDL	<MDL	<MDL	<MDL	<MDL
MA-FSW 631-M01-12R	9/12/2017	1/16/2018	<MDL	<MDL	<MDL	<MDL	<MDL
MA-FSW 631-M01-15W	9/12/2017	1/16/2018	<MDL	<MDL	<MDL	<MDL	<MDL
MA-FSW 631-0256 (00MW0589A)	9/12/2017	1/25/2018	<MDL	<MDL	<MQL	4.24	<MDL
MA-FSW 632-M01-01PT	9/11/2017	2/6/2018	<MDL	<MDL	<MDL	<MDL	<MDL
MA-FSW 632-M01-02GNT	9/11/2017	2/6/2018	<MDL	<MDL	<MDL	<MDL	<MDL

Table B11 (Continued)

U.S. Geological Survey local site name	Sampling Date	Date Analyzed	4:2 FtS	8:2 FtS	N-MeFOSAA	N-EtFOSAA	FOSA
MA-FSW 632-M01-03RT	9/11/2017	2/6/2018	<MDL	<MDL	<MDL	<MDL	<MDL
MA-FSW 632-M01-05BKT	9/11/2017	2/6/2018	<MQL	<MDL	<MDL	<MDL	<MDL
MA-FSW 632-M01-06WT	9/11/2017	2/6/2018	<MDL	<MDL	<MDL	<MDL	<MDL
MA-FSW 632-M01-07O	9/11/2017	2/6/2018	<MDL	<MDL	<MDL	<MDL	<MDL
MA-FSW 632-M01-11GN	9/11/2017	2/6/2018	<MDL	<MDL	<MDL	<MDL	<MDL
MA-FSW 632-M01-15W	9/11/2017	2/6/2018	<MQL	<MDL	<MDL	<MDL	<MDL
MA-FSW 632-0195 (00MW0606B)	9/11/2017	1/16/2018	<MDL	<MDL	<MDL	<MQL Qual	<MDL
MA-FSW 632-0325 (00MW0606A)	9/11/2017	1/16/2018	<MDL	<MDL	<MDL	<MDL	<MDL
MA-FSW 665-0040	9/12/2017	1/16/2018	<MDL	<MDL	<MDL	<MDL	<MDL
MA-FSW 665-0089	9/12/2017	1/16/2018	<MDL	<MDL	<MDL	<MDL	<MDL
MA-FSW 665-0139	9/12/2017	1/16/2018	<MDL	<MDL	<MDL	<MDL	<MDL
MA-FSW 665-0264 (03MW1014B)	9/12/2017	1/16/2018	<MDL	<MDL	<MDL	<MDL	<MDL
MA-FSW 665-0295 (03MW1014A)	9/12/2017	1/16/2018	<MDL	<MDL	<MDL	3.89	<MDL
MA-FSW 722-M01-01PT	9/13/2017	2/12/2018	<MDL	<MDL	<MDL	<MDL	<MDL
MA-FSW 722-M01-02GNT	9/13/2017	2/12/2018	<MDL	<MDL	<MDL	<MDL	<MDL
MA-FSW 722-M01-06WT	9/13/2017	2/12/2018	<MDL	<MDL	<MDL	<MDL	<MDL
MA-FSW 722-M01-08GY	9/13/2017	2/12/2018	<MDL	<MDL	<MDL	<MDL	<MDL
MA-FSW 722-M01-09Y	9/13/2017	2/12/2018	<MDL	<MDL	<MDL	<MDL	<MDL
MA-FSW 722-M01-11GN	9/14/2017	2/12/2018	<MDL	<MDL	<MDL	<MDL	<MDL
MA-FSW 722-M01-12R	9/14/2017	2/12/2018	<MDL	<MDL	<MDL	<MDL	<MDL
MA-FSW 722-M01-14BK	9/14/2017	2/12/2018	<MDL	<MDL	<MDL	<MDL	<MDL
MA-FSW 722-M01-15W	9/14/2017	2/12/2018	<MDL	<MDL	<MDL	<MDL	<MDL
MA-FSW 722-M02-01PT	9/13/2017	2/12/2018	<MDL	<MDL	<MDL	<MDL	<MDL
MA-FSW 722-M02-03RT	9/13/2017	2/12/2018	<MDL	<MDL	<MDL	<MDL	<MDL
MA-FSW 722-M02-05BKT	9/13/2017	2/12/2018	<MDL	<MDL	<MDL	<MDL	<MDL
MA-FSW 722-M02-08GY	9/13/2017	2/12/2018	<MDL	<MDL	<MDL	<MDL	<MDL
MA-FSW 722-M02-10P	9/13/2017	2/12/2018	<MDL	<MDL	<MDL	<MDL	<MDL
MA-FSW 722-M02-12R	9/13/2017	2/12/2018	<MDL	<MDL	<MDL	<MDL	<MDL
MA-FSW 722-M02-15W	9/13/2017	2/12/2018	<MDL	<MDL	<MDL	<MDL	<MDL
MA-FSW 722-M01-02GNT	2/23/2018	4/23/2018	<MDL	<MDL	<MDL	<MDL	<MDL
MA-FSW 722-M01-06WT	2/23/2018	4/23/2018	<MDL	<MDL	<MDL	<MDL	<MDL
MA-FSW 722-M01-08GY	2/23/2018	4/23/2018	<MDL	<MDL	<MDL	<MDL	<MDL
MA-FSW 722-M01-09Y	2/23/2018	4/23/2018	<MDL	<MDL	<MDL	<MQL	<MDL

Table B11 (Continued)

U.S. Geological Survey local site name	Sampling Date	Date Analyzed	4:2 FtS	8:2 FtS	N-MeFOSAA	N-EtFOSAA	FOSA
MA-FSW 722-M01-11GN	2/23/2018	4/23/2018	<MDL	<MDL	<MDL	<MDL	<MDL
MA-FSW 722-M01-12R	2/23/2018	4/23/2018	<MDL	<MDL	<MDL	<MDL	<MDL
MA-FSW 722-M02-01PT	2/23/2018	4/23/2018	<MDL	<MDL	<MDL	<MQL	<MDL
MA-FSW 722-M02-05BKT	2/23/2018	4/23/2018	<MDL	<MDL	<MDL	<MDL	<MDL
MA-FSW 722-M02-08GY	2/23/2018	4/23/2018	<MDL	<MDL	<MDL	<MDL	<MDL
MA-FSW 722-M02-15W	2/23/2018	4/23/2018	<MDL	<MDL	<MDL	<MDL	<MDL
FS-ASHPD-0001 (ECAMP02) Microlayer	9/11/2017	2/12/2018	<MDL	<MDL	<MDL	<MDL	2.44
FS-ASHPD-0001 (ECAMP02) 0.1m	9/11/2017	2/12/2018	<MDL	<MDL	<MDL	<MDL	<MDL
FS-ASHPD-0001 (ECAMP02) 1.00m	9/11/2017	2/12/2018	<MDL	<MDL	<MDL	<MDL	<MDL
FS-ASHPD-0001 (ECAMP02) 3.00m	9/11/2017	2/12/2018	<MDL	<MDL	<MDL	<MDL	<MDL
FS-ASHPD-0001 (ECAMP02) 5.00m	9/11/2017	2/12/2018	<MDL	<MDL	<MDL	<MDL	<MDL
FS-ASHPD-0001 (ECAMP02) 7.00m	9/11/2017	2/12/2018	<MDL	<MDL	<MDL	<MDL	<MDL
FS-ASHPD-0001 (ECAMP02) 9.00m	9/11/2017	2/12/2018	<MDL	<MDL	<MDL	<MDL	<MDL
FS-ASHPD-0001 (ECAMP02) 11.00m	9/11/2017	2/12/2018	<MDL	<MDL	<MDL	<MDL	<MDL
FS-ASHPD-0001 (ECAMP02) 13.00m	9/11/2017	2/12/2018	<MDL	<MDL	<MDL	<MDL	<MDL
FS-ASHPD-0001 (ECAMP02) 15.00m	9/11/2017	2/12/2018	<MDL	<MDL	<MDL	<MDL	<MDL
FS-ASHPD-0001 (ECAMP02) 17.00m	9/11/2017	2/12/2018	<MDL	<MDL	<MDL	<MDL	<MDL
FS-ASHPD-0001 (ECAMP02) Microlayer	11/8/2017	2/12/2018	<MDL	<MDL	<MDL	<MDL	<MDL
FS-ASHPD-0001 (ECAMP02) 0.1m	11/8/2017	2/12/2018	<MDL	<MDL	<MDL	<MDL	<MDL
FS-ASHPD-0001 (ECAMP02) 1.00m	11/8/2017	2/12/2018	<MDL	<MDL	<MDL	<MDL	<MDL
FS-ASHPD-0001 (ECAMP02) 3.00m	11/8/2017	2/12/2018	<MDL	<MDL	<MDL	<MDL	<MDL
FS-ASHPD-0001 (ECAMP02) 5.00m	11/8/2017	2/12/2018	<MDL	<MDL	<MDL	<MDL	<MDL
FS-ASHPD-0001 (ECAMP02) 7.00m	11/8/2017	2/19/2018	<MDL	<MDL	<MDL	<MQL	<MDL
FS-ASHPD-0001 (ECAMP02) 9.00m	11/8/2017	2/19/2018	<MDL	<MDL	<MDL	<MDL	<MDL
FS-ASHPD-0001 (ECAMP02) 11.00m	11/8/2017	2/19/2018	<MDL	<MDL	<MDL	<MDL	<MDL
FS-ASHPD-0001 (ECAMP02) 13.00m	11/8/2017	2/19/2018	<MDL	<MDL	<MDL	<MDL	<MDL
FS-ASHPD-0001 (ECAMP02) 15.00m	11/8/2017	2/12/2018	<MDL	<MDL	<MDL	<MDL	<MDL
FS-ASHPD-0001 (ECAMP02) 17.00m	11/8/2017	2/12/2018	<MDL	<MDL	<MDL	<MQL	<MDL
FS-ASHPD-0009 (ECAMP01) Microlayer	9/11/2017	2/12/2018	<MDL	<MDL	<MDL	<MDL	<MDL
FS-ASHPD-0009 (ECAMP01) 0.1m	9/11/2017	2/12/2018	<MDL	<MDL	<MDL	<MDL	<MDL
FS-ASHPD-0009 (ECAMP01) 1.00m	9/11/2017	2/12/2018	<MDL	<MDL	<MDL	<MDL	<MDL
FS-ASHPD-0009 (ECAMP01) 3.00 m	9/11/2017	2/12/2018	<MDL	<MDL	<MDL	<MDL	<MDL
FS-ASHPD-0009 (ECAMP01) 5.00 m	9/11/2017	2/12/2018	<MDL	<MDL	<MDL	<MDL	<MDL

Table B11 (Continued)

U.S. Geological Survey local site name	Sampling Date	Date Analyzed	4:2 FtS	8:2 FtS	N-MeFOSAA	N-EtFOSAA	FOSA
FS-ASHPD-0010 Microlayer	9/11/2017	2/19/2018	<MDL	<MDL	<MDL	<MDL	<MDL
FS-ASHPD-0010 0.1m	9/11/2017	2/19/2018	<MDL	<MDL	<MDL	<MDL	<MDL
FS-ASHPD-0010 1.00m	9/11/2017	2/19/2018	<MDL	<MDL	<MDL	<MDL	<MDL
FS-ASHPD-0010 3.00m	9/11/2017	2/19/2018	<MDL	<MDL	<MDL	<MDL	<MDL
FS-ASHPD-0010 5.00m	9/11/2017	2/19/2018	<MDL	<MDL	<MDL	<MDL	<MDL
FS-ASHPD-0010 7.00m	9/11/2017	2/19/2018	<MDL	<MDL	<MDL	<MDL	<MDL
FS-ASHPD-0010 9.00m	9/11/2017	2/19/2018	<MDL	<MDL	<MDL	<MDL	<MDL
FS-ASHPD-0011 Microlayer	9/12/2017	2/12/2018	<MDL	<MDL	<MDL	<MDL	<MDL
FS-ASHPD-0011 0.1m	9/12/2017	2/12/2018	<MDL	<MDL	<MDL	<MDL	<MDL
FS-ASHPD-0011 1.00m	9/12/2017	2/12/2018	<MDL	<MDL	<MDL	<MDL	<MDL
FS-ASHPD-0011 3.00m	9/12/2017	2/12/2018	<MDL	<MDL	<MDL	<MDL	<MDL
FS-ASHPD-0011 5.00m	9/12/2017	2/12/2018	<MDL	<MDL	<MDL	<MDL	<MDL
FS-ASHPD-0011 7.00m	9/12/2017	2/12/2018	<MDL	<MDL	<MDL	<MDL	<MDL
FS-ASHPD-0011 9.00m	9/12/2017	2/12/2018	<MDL	<MDL	<MDL	<MDL	<MDL
MI-JOHPD-0001 (ECJNP03) Microlayer	9/12/2017	2/19/2018	<MDL	<MDL	<MDL	<MDL	<MDL
MI-JOHPD-0001 (ECJNP03) 0.1m	9/12/2017	2/19/2018	<MDL	<MDL	<MDL	<MDL	<MDL
MI-JOHPD-0001 (ECJNP03) 1.00m	9/12/2017	2/19/2018	<MDL	<MDL	<MDL	<MDL	<MDL
MI-JOHPD-0001 (ECJNP03) 3.00m	9/12/2017	2/19/2018	<MDL	<MDL	<MDL	<MDL	<MDL
MI-JOHPD-0001 (ECJNP03) 5.00m	9/12/2017	2/19/2018	<MDL	<MDL	<MDL	<MDL	<MDL
MI-JOHPD-0001 (ECJNP03) 7.00m	9/12/2017	2/19/2018	<MDL	<MDL	<MDL	<MDL	<MDL
MI-JOHPD-0001 (ECJNP03) 9.00m	9/12/2017	2/19/2018	<MDL	<MDL	<MDL	<MDL	<MDL
MI-JOHPD-0001 (ECJNP03) 11.00m	9/12/2017	2/19/2018	<MDL	<MDL	<MDL	<MDL	<MDL
MI-JOHPD-0001 (ECJNP03) 15.00	9/12/2017	2/19/2018	<MDL	<MDL	<MDL	<MDL	<MDL
MI-JOHPD-0008 Microlayer	9/12/2017	2/19/2018	<MDL	<MDL	<MDL	<MDL	<MDL
MI-JOHPD-0008 0.1m	9/12/2017	2/19/2018	<MDL	<MDL	<MDL	<MDL	<MDL
MI-JOHPD-0008 1.00m	9/12/2017	2/19/2018	<MDL	<MDL	<MDL	<MDL	<MDL
MI-JOHPD-0008 3.00m	9/12/2017	2/19/2018	<MDL	<MDL	<MDL	<MDL	<MDL
MI-JOHPD-0008 5.00m	9/12/2017	2/19/2018	<MDL	<MDL	<MDL	<MDL	<MDL
MI-JOHPD-0008 7.00m	9/12/2017	2/19/2018	<MDL	<MDL	<MDL	<MDL	<MDL
MI-JOHPD-0008 9.00m	9/12/2017	2/19/2018	<MDL	<MDL	<MDL	<MDL	<MDL
ASHPD-GWOUT-L-N-LW	9/13/2017	3/7/2018	<MQL	<MDL	<MDL	<MDL	<MDL
ASHPD-GWOUT-L-N-015	9/13/2017	3/7/2018	<MQL	<MDL	<MDL	<MQL	<MDL
ASHPD-GWOUT-L-N-030	9/13/2017	3/7/2018		0.2	<MDL	<MDL	<MDL
ASHPD-GWOUT-L-N-050	9/13/2017	3/7/2018	<MQL	<MDL	<MDL	<MDL	<MDL

Table B11 (Continued)

U.S. Geological Survey local site name	Sampling Date	Date Analyzed	4:2 FtS	8:2 FtS	N-MeFOSAA	N-EtFOSAA	FOSA
ASHPD-GWOUT-L-N-100	9/13/2017	3/7/2018	<MQL	<MDL	<MDL	<MDL	<MDL
ASHPD-GWOUT-R-N-LW	9/13/2017	3/13/2018	<MDL	<MDL	<MDL	<MDL	<MDL
ASHPD-GWOUT-R-N-015	9/13/2017	3/13/2018	<MDL	<MDL	<MDL	<MDL	<MDL
ASHPD-GWOUT-R-N-030	9/13/2017	3/13/2018	<MDL	<MDL	<MDL	<MDL	<MDL
ASHPD-GWOUT-R-N-050	9/13/2017	3/13/2018	<MDL	<MDL	<MDL	<MDL	<MDL
ASHPD-GWOUT-R-N-100	9/13/2017	3/13/2018	<MDL	<MDL	<MDL	<MDL	<MDL
ASHPD-GWOUT-R-S-015	9/13/2017	3/7/2018	<MQL	<MDL	<MDL	<MDL	<MQL
ASHPD-GWOUT-R-S-100	9/13/2017	3/7/2018	<MQL	<MDL	<MDL	<MDL	<MDL
ASHPD-KIGAM-124N-010E-LW	9/14/2017	3/13/2018	<MDL	<MDL	<MDL	<MQL	<MDL
ASHPD-KIGAM-124N-010E-015	9/14/2017	3/13/2018	<MDL	7.72	1.67	2.03	2.01
ASHPD-KIGAM-124N-010E-030	9/14/2017	3/13/2018	<MDL	4.35	0.57	2.22	3.19
ASHPD-KIGAM-124N-010E-050	9/14/2017	3/13/2018	<MDL	4.92	0.62	3.05	2.51
ASHPD-KIGAM-124N-010E-100	9/14/2017	3/7/2018	<MQL	12.915	<MQL	1.985	<MQL
ASHPD-KIGAM-131N-011E-LW	9/14/2017	3/7/2018	<MQL Qual	<MDL	<MDL	<MQL	<MDL
ASHPD-KIGAM-131N-011E-015	9/14/2017	3/7/2018	<MDL	<MQL	<MDL	<MQL	<MQL
ASHPD-KIGAM-131N-011E-030	9/14/2017	3/7/2018	<MQL	<MDL	<MDL	<MQL	<MDL
ASHPD-KIGAM-131N-011E-050	9/14/2017	3/7/2018	<MQL	0.88	<MQL	<MQL	<MDL
ASHPD-KIGAM-131N-011E-100	9/14/2017	3/7/2018	<MQL	1.14	<MDL	<MQL Qual	0.47
ASHPD-GWIN-C-LW	9/11/2017	2/19/2018	<MDL	<MDL	<MDL	<MDL	<MDL
ASHPD-GWIN-C-035	9/11/2017	2/19/2018	<MDL	<MDL	<MDL	<MDL	<MDL
ASHPD-GWIN-C-100	9/11/2017	2/19/2018	<MDL	<MDL	<MDL	<MDL	<MDL
ASHPD-GWOUT-L-N-100	2/23/2018	4/23/2018	<MDL	<MDL	<MDL	<MDL	<MDL
ASHPD-GWOUT-R-N-LW	2/23/2018	4/23/2018	<MQL	<MDL	<MDL	<MDL	<MDL
ASHPD-GWOUT-R-N-100	2/23/2018	4/23/2018	<MDL	<MDL	<MDL	<MDL	<MDL
MA-FSW 239-M01-01PT	8/5/2016	3/13/2018	<MDL	<MDL	<MDL	<MDL	<MDL
MA-FSW 239-M01-02GNT	8/5/2016	3/13/2018	<MDL	<MDL	<MDL	<MDL	<MDL
MA-FSW 239-M01-04BUT	8/5/2016	3/13/2018	<MDL	<MDL	<MDL	<MDL	<MDL
MA-FSW 239-M01-06WT	8/5/2016	3/13/2018	<MQL	<MQL	<MDL	<MDL	<MQL
MA-FSW 239-M01-08GY	8/5/2016	3/13/2018	<MDL	<MDL	<MQL	<MQL	<MDL
MA-FSW 239-M01-10P	8/5/2016	3/13/2018	<MDL	<MDL	<MDL	<MDL	<MDL
MA-FSW 239-M01-12R	8/5/2016	3/13/2018	<MDL	<MDL	<MDL	<MDL	<MDL
MA-FSW 239-M01-14BK	8/5/2016	3/13/2018	<MDL	<MDL	<MDL	<MDL	<MDL
MA-FSW 300-M03-01PT	7/7/2016	3/13/2018	<MDL	<MQL	0.81	1.91	0.64

Table B11 (Continued)

U.S. Geological Survey local site name	Sampling Date	Date Analyzed	4:2 FtS	8:2 FtS	N-MeFOSAA	N-EtFOSAA	N-EtFOSAA	FOSA
MA-FSW 300-M03-03RT	7/7/2016	3/13/2018	<MDL	<MDL	<MDL	<MDL	<MDL	<MDL
MA-FSW 300-M03-06WT	7/7/2016	3/13/2018	<MDL	<MDL	<MDL	<MDL	<MDL	<MQL
MA-FSW 300-M03-09Y	7/7/2016	3/13/2018	<MDL	<MQL	1.005	<MDL	3.69	0.715
MA-FSW 300-M03-10P	7/7/2016	3/13/2018	<MDL	<MQL	0.555	<MDL	2.39	<MQL
MA-FSW 300-M03-11GN	7/7/2016	3/13/2018	<MDL	<MQL	0.52	<MDL	1.34	<MQL
MA-FSW 300-M03-14BK	7/7/2016	3/13/2018	<MDL	1.31	<MDL	<MDL	0.65	<MQL
MA-FSW 300-M03-15W	7/7/2016	3/13/2018	<MQL	1.78	<MQL	<MQL	<MDL	<MDL
MA-FSW 300-M02-01PT	7/8/2016	3/13/2018	<MQL	<MQL Qual	<MQL	<MQL	<MDL	<MDL
MA-FSW 300-M02-02GNT	7/8/2016	3/13/2018	<MQL	3.11	<MDL	<MDL	<MDL	<MDL
MA-FSW 300-M02-03RT	7/8/2016	4/23/2018	<MQL	2.25	<MDL	<MDL	<MDL	<MDL
MA-FSW 300-M02-06WT	7/8/2016	3/13/2018	<MDL	<MDL	<MDL	<MDL	<MDL	<MDL
MA-FSW 300-M02-08GY	7/8/2016	3/13/2018	<MDL	<MQL	<MDL	<MDL	<MDL	<MDL
MA-FSW 300-M02-10P	7/8/2016	3/13/2018	<MDL	<MDL	<MDL	<MDL	<MDL	<MDL
MA-FSW 300-M02-14BK	7/8/2016	3/13/2018	<MDL	<MDL	<MDL	<MDL	<MDL	<MDL
MA-FSW 300-0138	7/7/2016	3/7/2018	<MDL	<MDL	<MDL	<MDL	<MDL	<MDL
MA-FSW 424-M01-01PT	7/26/2016	4/23/2018	<MQL	<MQL	<MQL	<MQL	1.34	<MQL
MA-FSW 424-M01-03RT	7/26/2016	4/23/2018	<MQL	<MDL	<MDL	<MQL	<MDL	<MDL
MA-FSW 424-M01-05BKT	7/26/2016	4/23/2018	<MDL	<MDL	<MDL	<MQL	<MDL	<MDL
MA-FSW 424-M01-09Y	7/26/2016	4/23/2018	<MDL	<MDL	<MDL	<MDL	<MDL	<MDL
MA-FSW 424-M01-13BU	7/26/2016	4/23/2018	<MDL	<MDL	<MDL	<MDL	<MDL	<MDL
MA-FSW 424-M02-11GN 72-13	7/26/2016	4/23/2018	<MQL	2.36	1.17	<MQL	4.6	2.055
MA-FSW 424-M02-12R 72-13	7/26/2016	4/23/2018	<MQL	<MQL	1.04	<MDL	5.82	1.96
MA-FSW 424-M02-14BK 72-13	7/26/2016	4/23/2018	<MQL	1.5	<MQL	<MQL	2.69	<MQL
MA-FSW 424-M02-15W 72-13	7/26/2016	4/23/2018	<MQL	<MQL	<MQL	<MQL	1.69	<MQL
MA-FSW 564-M01-01PT	7/6/2016	3/13/2018	<MDL	<MQL	<MDL	<MDL	<MDL	<MDL
MA-FSW 564-M01-02GNT	7/6/2016	3/13/2018	<MDL	<MDL	<MQL	<MDL	<MDL	<MDL
MA-FSW 564-M01-04BUT	7/6/2016	3/7/2018	<MQL	<MDL	<MDL	<MQL	<MDL	<MQL
MA-FSW 564-M01-05BKT	7/6/2016	3/7/2018	<MQL	<MDL	<MQL	<MDL	<MDL	<MDL
MA-FSW 564-M01-06WT	7/6/2016	3/7/2018	<MDL	<MDL	<MDL	<MDL	<MDL	<MQL
MA-FSW 564-M01-08GY	7/6/2016	3/7/2018	<MDL	<MDL	<MDL	<MDL	<MDL	<MDL
MA-FSW 564-M01-10P	7/6/2016	3/7/2018	<MDL	<MDL	<MDL	<MDL	<MDL	<MDL
MA-FSW 564-M01-12R	7/6/2016	3/7/2018	<MDL	<MDL	<MDL	<MDL	<MDL	<MDL
MA-FSW 564-M01-14BK	7/6/2016	3/7/2018	<MDL	<MDL	<MQL	<MQL	<MDL	<MDL
MA-FSW 621-M01-01PT	7/11/2016	3/13/2018	<MDL	<MDL	<MDL	<MDL	<MDL	<MDL

Table B11 (Continued)

U.S. Geological Survey local site name	Sampling Date	Date Analyzed	4:2 FtS	8:2 FtS	N-MeFOSAA	N-EtFOSAA	FOSA
MA-FSW 621-M01-02GNT	7/11/2016	3/13/2018	<MDL	0.73	<MQL	<MDL	0.72
MA-FSW 621-M01-03RT	7/11/2016	4/23/2018	<MDL	<MDL	<MDL	<MQL	<MDL
MA-FSW 621-M01-05BKT	7/11/2016	3/13/2018	<MDL	<MDL	<MQL	<MQL	<MDL
MA-FSW 621-M01-06WT	7/11/2016	4/23/2018	<MDL	<MDL	<MDL	<MDL	<MDL
MA-FSW 621-M01-07O	7/11/2016	3/13/2018	<MDL	<MDL	<MQL	<MDL	<MDL
MA-FSW 621-M01-09Y	7/11/2016	3/13/2018	<MDL	<MDL	<MDL	<MDL	<MDL
MA-FSW 621-M01-11GN	7/11/2016	3/13/2018	<MDL	<MDL	<MDL	<MDL	<MDL
MA-FSW 621-M01-13BU	7/11/2016	3/13/2018	<MDL	<MDL	<MDL	<MDL	<MDL
MA-FSW 621-M01-15W	7/11/2016	3/13/2018	<MDL	<MDL	<MDL	<MDL	<MDL
MA-FSW 622-M01-01PT	7/11/2016	3/20/2018	<MDL	<MDL	<MDL	<MDL	<MDL
MA-FSW 622-M01-02GNT	7/11/2016	3/20/2018	<MDL	<MDL	<MQL	<MDL	<MDL
MA-FSW 622-M01-03RT	7/11/2016	4/23/2018	<MDL	<MDL	<MDL	<MQL	<MDL
MA-FSW 622-M01-05BKT	7/11/2016	3/20/2018	<MDL	<MDL	<MDL	<MDL	<MDL
MA-FSW 622-M01-06WT	7/11/2016	4/23/2018	<MQL	<MDL	<MDL	<MDL	<MDL
MA-FSW 622-M01-07O	7/11/2016	3/20/2018	0.55	<MDL	<MDL	<MDL	<MDL
MA-FSW 622-M01-09Y	7/11/2016	3/20/2018	<MDL	<MDL	<MDL	<MDL	<MDL
MA-FSW 622-M01-11GN	7/11/2016	3/20/2018	<MDL	<MDL	<MDL	<MDL	<MDL
MA-FSW 622-M01-13BU	7/11/2016	3/20/2018	<MDL	<MDL	<MDL	<MDL	<MDL
MA-FSW 622-M01-15W	7/11/2016	3/20/2018	<MDL	<MDL	<MDL	<MDL	<MDL
MA-FSW 744-0004	7/26/2016	3/20/2018	<MDL	<MDL	<MDL	<MDL	<MDL
MA-FSW 744-0008	7/26/2016	3/20/2018	<MDL	<MDL	<MDL	<MDL	<MDL
MA-FSW 744-0010	7/26/2016	3/20/2018	<MDL	<MDL	<MDL	<MDL	<MDL
MA-FSW 744-0011	7/26/2016	3/20/2018	<MDL	<MDL	<MDL	<MDL	<MDL
MA-FSW 744-0013	7/26/2016	3/20/2018	<MDL	<MDL	<MDL	<MDL	<MDL
MA-FSW 744-0017	7/26/2016	3/20/2018	<MDL	0.9	<MDL	<MDL	<MDL
MA-FSW 744-0019	7/26/2016	3/20/2018	<MDL	5.79	<MQL	<MDL	1.83
MA-FSW 744-0023	7/26/2016	3/20/2018	<MDL	6.51	0.7	1.18	2.37
MA-FSW 744-0025	7/26/2016	3/21/2018	<MDL	<MDL	1.01	0.845	2.52
MA-FSW 744-0026	7/26/2016	4/23/2018	<MDL	<MDL	1.33	0.79	2.99
MA-FSW 744-0028	7/26/2016	4/23/2018	<MDL	<MQL	1.375	1.765	2.11
MA-FSW 744-0029	7/26/2016	4/23/2018	<MDL	<MDL	<MDL	3.58	<MDL
MA-FSW 744-0030	7/26/2016	4/23/2018	<MDL	<MDL	<MQL	<MQL	<MDL
Q1 MI-QUARV-00015(QR001)	8/15/2017	2/6/2018	<MQL	<MDL	<MDL	<MDL	<MDL
Q3	8/15/2017	2/6/2018	<MQL	<MDL	<MDL	<MDL	<MQL

Table B11 (Continued)

U.S. Geological Survey local site name	Sampling Date	Date Analyzed	4:2 FtS	8:2 FtS	N-MeFOSAA	N-EtFOSAA	FOSA
Q4	8/15/2017	2/6/2018	<MQL	<MDL	<MDL	<MDL	<MDL
Q5	8/15/2017	2/6/2018	<MQL	<MDL	<MDL	<MDL	<MDL
Q9	8/15/2017	2/6/2018	<MQL	<MDL	<MDL	<MDL	<MDL
Q-FC	8/15/2017	2/6/2018	<MQL	<MDL	<MDL	<MDL	<MDL
Q-OBR	8/15/2017	2/6/2018	<MQL	<MDL	<MDL	<MDL	<MDL
Q-TRIB	8/15/2017	2/6/2018	0.66	<MDL	<MDL	<MDL	<MQL
Quash_HS_Seep1	8/16/2017	2/6/2018	<MQL Qual	<MDL	<MDL	<MDL	<MDL
Quash_HS_Seep2	8/16/2017	2/6/2018	<MQL	<MDL	<MDL	<MDL	<MDL
QB010	8/17/2017	2/6/2018	<MQL Qual	<MDL	<MDL	<MDL	<MDL
QB018	8/17/2017	2/6/2018	<MQL Qual	<MDL	<MDL	<MDL	<MDL
QB020	8/17/2017	2/6/2018	<MQL	<MDL	<MDL	<MDL	<MDL
QB026	8/17/2017	2/6/2018	<MDL	<MDL	<MDL	<MDL	<MDL
QB039	8/18/2017	2/6/2018	<MQL	3.01	<MDL	<MDL	<MDL
DD004	8/17/2017	2/6/2018	<MDL	<MDL	<MDL	<MDL	<MDL
DD-12	8/17/2017	2/6/2018	<MDL	<MDL	<MDL	<MDL	<MDL
Quash_OV_seep1	8/14/2017	2/6/2018	<MDL	<MDL	<MDL	<MDL	<MDL
Quash_OV_seep2	8/14/2017	2/12/2018	<MDL	<MDL	<MDL	<MDL	<MDL
Quash_HRTS_seep	8/14/2017	2/6/2018	<MDL	<MDL	<MDL	<MDL	<MDL
QT008	8/17/2017	2/6/2018	<MDL	<MDL	<MDL	<MDL	<MDL
QT018	8/17/2017	2/6/2018	<MQL Qual	<MDL	<MDL	<MDL	<MDL
QT030	8/17/2017	2/6/2018	<MQL	<MDL	<MDL	<MDL	<MDL
QT034	8/17/2017	2/6/2018	<MQL	<MDL	<MDL	<MDL	<MDL
QT039	8/17/2017	2/6/2018	<MQL	<MDL	<MDL	<MDL	<MDL
QT082	8/18/2017	2/6/2018	<MQL Qual	<MDL	<MDL	<MDL	<MDL
QT101	8/17/2017	2/6/2018	<MDL	<MDL	<MDL	<MDL	<MDL
QT122		2/6/2018	<MDL	<MDL	<MDL	<MDL	<MDL
QT142	8/18/2017	2/6/2018	1.04	7.52	<MDL	<MDL	<MDL
Quash-Spawn1	8/16/2017	2/12/2018	<MDL	<MDL	<MDL	<MDL	<MDL
Quash-Spawn2	8/16/2017	2/12/2018	<MDL	<MDL	<MDL	<MDL	<MDL
Quash-Spawn3	8/14/2017	2/12/2018	<MDL	<MDL	<MDL	<MDL	<MDL

Table B12. Increase in perfluorinated carboxylates from the total oxidizable precursor assay (post-oxidation minus pre-oxidation concentrations. Samples for which there was no increase are set to zero. Samples with a concentration after oxidation and below the method detection limit (MDL) before oxidation were set to the concentration post-oxidation. Samples with a concentration after oxidation and below the method quantitation limit (MQL) before oxidation were set to the concentration post-oxidation minus the MQL*sqrt(2)/2.

U.S. Geological Survey local site name	Sampling Date	Date Analyzed	PFBA	PFPeA	PFHxA	PFHpA	PFOA	PFNA	PFDA	PFUnDA
MA-MIW 210-0026	7/25/2017	07/09/2018	0.0	17.7	33.1	0.0	0.0	0.0	0.0	0.0
MA-MIW 210-0145 (00MW0609A)	7/25/2017	07/09/2018	0.0	0.0	0.0	0.0	0.0	0.0	0.0	0.0
MA-FSW 631-M01-01PT	9/12/2017	06/12/2018	105.7	37.8	87.4	3.2	7.5	1.4	0.0	0.0
MA-FSW 631-M01-02GNT	9/12/2017	06/12/2018	53.8	20.8	56.2	0.0	8.9	0.2	0.0	0.0
MA-FSW 631-M01-03RT	9/12/2017	06/12/2018	46.4	18.1	64.1	0.0	1.8	0.0	0.0	0.0
MA-FSW 631-M01-04BUT	9/12/2017	06/12/2018	69.9	15.0	55.5	0.0	0.9	0.0	0.0	0.0
MA-FSW 631-M01-06WT	9/12/2017	06/12/2018	27.9	16.0	45.4	0.0	1.6	0.0	0.0	0.0
MA-FSW 631-M01-09Y	9/12/2017	06/12/2018	39.9	14.7	42.3	0.0	6.7	0.3	0.0	0.0
MA-FSW 631-M01-12R	9/12/2017	06/12/2018	30.0	13.3	46.4	0.0	2.2	0.0	0.0	0.0
MA-FSW 631-M01-15W	9/12/2017	06/12/2018	58.3	17.0	73.2	0.0	2.3	0.0	0.0	0.0
MA-FSW 632-M01-01PT	9/11/2017	07/09/2018	0.0	11.4	10.3	0.0	0.6	0.0	0.0	0.0
MA-FSW 632-M01-05BKT	9/11/2017	07/09/2018	33.6	16.7	46.8	0.0	0.0	0.6	0.0	0.0
MA-FSW 632-M01-07O	9/11/2017	07/09/2018	0.0	18.7	42.2	0.0	1.0	0.0	0.0	0.0
MA-FSW 632-0325 (00MW0606A)	9/11/2017	07/09/2018	0.0	4.9	16.2	0.0	0.9	0.0	0.0	0.0
MA-FSW 722-M01-01PT	9/13/2017	07/09/2018	0.0	16.4	38.6	0.0	1.3	0.4	0.0	0.0
MA-FSW 722-M01-06WT	9/13/2017	07/09/2018	0.0	14.2	30.6	0.0	0.8	0.0	0.0	0.0
MA-FSW 722-M01-08GY	9/13/2017	07/09/2018	40.0	20.7	52.9	0.0	3.0	0.2	0.0	0.0
MA-FSW 722-M01-11GN	9/14/2017	07/09/2018	0.0	17.0	36.3	0.0	1.2	0.0	0.0	0.0
MA-FSW 722-M01-15W	9/14/2017	07/09/2018	19.8	28.9	46.6	0.0	5.3	1.0	0.0	0.0
MA-FSW 722-M02-01PT	9/13/2017	07/09/2018	0.0	12.7	33.1	0.0	0.0	0.0	0.0	0.0
MA-FSW 722-M02-03RT	9/13/2017	07/09/2018	0.0	17.8	34.8	0.5	1.2	0.2	0.0	0.0
MA-FSW 722-M02-05BKT	9/13/2017	07/09/2018	23.7	17.0	34.9	0.2	1.0	0.4	0.0	0.0
FS-ASHPD-0001 (ECAMP02) Microlayer	9/11/2017	06/12/2018	47.5	32.7	91.4	7.5	13.5	0.3	0.0	0.0
FS-ASHPD-0001 (ECAMP02) 0.1m	9/11/2017	06/12/2018	47.4	33.9	85.3	6.5	20.4	1.2	0.0	0.0
FS-ASHPD-0001 (ECAMP02) 1.00m	9/11/2017	06/12/2018	43.7	33.2	83.1	8.4	16.0	0.7	0.0	0.0
FS-ASHPD-0001 (ECAMP02) 3.00m	9/11/2017	06/12/2018	49.7	36.5	86.9	7.4	19.8	1.4	0.0	0.0
FS-ASHPD-0001 (ECAMP02) 5.00m	9/11/2017	06/12/2018	34.7	37.1	91.8	9.9	16.6	1.5	0.0	0.0
FS-ASHPD-0001 (ECAMP02) 9.00m	9/11/2017	06/12/2018	50.7	32.4	83.4	4.8	20.6	1.2	0.0	0.0
FS-ASHPD-0001 (ECAMP02) 13.00m	9/11/2017	06/12/2018	24.5	32.5	82.5	9.4	15.9	2.2	0.0	0.0

Table B12 (Continued)

U.S. Geological Survey local site name	Sampling Date	Date Analyzed	PFBA	PFPeA	PFHxA	PFHpA	PFOA	PFNA	PFDA	PFUnDA
FS-ASHPD-0001 (ECAMP02) 17.00m	9/11/2017	06/12/2018	30.2	33.5	76.1	5.8	15.4	0.7	0.0	0.0
ASHPD-GWOUT-L-N-LW	9/13/2017	06/12/2018	36.1	30.2	83.3	4.3	7.2	0.0	0.0	0.0
ASHPD-GWOUT-L-N-015	9/13/2017	06/12/2018	7.9	19.2	69.4	2.7	9.3	0.4	0.0	0.0
ASHPD-GWOUT-L-N-030	9/13/2017	06/12/2018	13.3	11.2	54.2	1.2	3.8	0.5	0.0	0.0
ASHPD-GWOUT-L-N-050	9/13/2017	06/12/2018	8.9	13.6	50.2	0.0	4.5	0.8	0.0	0.0
ASHPD-GWOUT-L-N-100	9/13/2017	06/12/2018	0.0	8.5	45.7	0.0	2.1	0.0	0.0	0.0
ASHPD-GWOUT-R-N-LW	9/13/2017	07/09/2018	54.5	31.0	75.2	1.6	5.1	1.0	0.0	0.0
ASHPD-GWOUT-R-N-015	9/13/2017	07/09/2018	23.8	21.6	49.5	1.0	0.0	1.2	0.0	0.0
ASHPD-GWOUT-R-N-030	9/13/2017	06/12/2018	1.5	42.7	83.0	4.8	16.5	0.8	0.0	0.0
ASHPD-GWOUT-R-N-050	9/13/2017	06/12/2018	18.2	22.2	63.9	5.4	10.0	1.0	0.0	0.0
ASHPD-GWOUT-R-N-100	9/13/2017	06/12/2018	29.1	29.9	61.2	0.0	2.5	0.0	0.0	0.0
ASHPD-KIGAM-124N-010E-LW	9/14/2017	07/09/2018	131.6	60.6	153.9	7.6	14.5	3.8	0.0	1.0
ASHPD-KIGAM-124N-010E-015	9/14/2017	07/09/2018	58.1	71.2	195.9	16.5	35.1	14.4	0.8	36.4
ASHPD-KIGAM-124N-010E-030	9/14/2017	07/09/2018	87.4	57.1	169.0	8.0	23.4	19.3	0.7	75.1
ASHPD-KIGAM-124N-010E-050	9/14/2017	07/09/2018	50.6	71.3	177.0	11.8	21.0	8.2	0.0	20.1
ASHPD-KIGAM-124N-010E-100	9/14/2017	07/09/2018	48.1	70.3	204.9	0.6	16.4	0.0	0.0	38.0
ASHPD-KIGAM-131N-011E-LW	9/14/2017	07/09/2018	57.7	47.7	136.2	0.6	0.0	0.0	0.0	0.0
ASHPD-KIGAM-131N-011E-015	9/14/2017	07/09/2018	8.1	37.5	99.7	0.0	2.7	1.0	0.1	0.0
ASHPD-KIGAM-131N-011E-030	9/14/2017	07/09/2018	14.9	42.5	97.3	2.0	5.8	0.0	0.0	0.0
ASHPD-KIGAM-131N-011E-050	9/14/2017	07/09/2018	26.6	36.3	100.8	0.3	0.5	0.0	0.0	0.0
ASHPD-KIGAM-131N-011E-100	9/14/2017	07/09/2018	15.0	37.0	107.0	0.0	1.5	0.0	0.0	0.0
ASHPD-GWOUT-L-N-100	2/23/2018	07/09/2018	0.0	21.1	35.6	0.0	0.0	0.0	0.0	0.0
ASHPD-GWOUT-R-N-LW	2/23/2018	07/09/2018	17.2	30.6	55.7	0.0	0.0	0.0	0.0	0.0
ASHPD-GWOUT-R-N-100	2/23/2018	07/09/2018	0.0	1.8	33.8	0.5	0.0	0.0	0.0	0.0

Table B13. Sediment/water distribution coefficients (K_d) for upwelling (GWIN) and downwelling (GWOUT) sites in Ashumet Pond.*

Sample Location*	PFBA	PFPeA	PFHxA	PFHpA	PFOA	PFNA	PFDA	PFUA	PFBS	PFPeS	PFHxS	PFHpS	PFOS
GWOUT-R-N Surface		15.9	14.3	30.3	105.2	403.9			0.76	0.88	0.76	3.51	14.7
GWOUT-R-N 15cm	26.5	34.6	32.1	27.0	23.2	33.1		251	1.14	1.19	1.33		15.6
GWOUT-R-N 30cm	6.06	11.8	13.8	12.9	11.7	14.5		416	1.48	1.67	1.66		17.7
GWOUT-L-N Surface		16.1	12.2	11.2	17.3	43.0			0.72	1.00	0.83	3.54	13.2
GWOUT-L-N 15cm	23.6	32.6	37.7	36.5	38.5	53.5			1.49	2.53	2.68	7.07	18.6
GWOUT-L-N 30cm	18.3	22.9	26.4	24.4	26.9	33.2			2.84		2.47	4.75	11.5
GWIN-131N Surface		1.54	0.75	0.85	0.95	13.6		366	0.26	0.41	0.11	1.70	4.94
GWIN-131N 15 cm		0.35	1.44	0.27	0.32	1.82	2.71	13.1		0.61	0.63	1.83	1.31
GWIN-131N 30 cm	1.53	0.30	2.62	0.28	0.32	1.28	2.20	14.4		0.65	0.45	1.29	1.26
GWIN-124N Surface	2.24	1.11	1.54	0.91	1.03	30.0		823	0.83	0.85	0.28	2.53	9.06
GWIN-124N 15 cm		0.37	1.52	0.35	0.46	2.79	3.48	30.2	0.65	1.01	0.78	1.79	2.02
GWIN-124N 30 cm		0.13	2.92	0.34	0.44	1.66	2.33	9.87	1.18	1.03	0.89	1.55	1.31

K_d Value (L/kg)

*Kd values were calculated using the following pairing between water and sediment: Surface K_d values were calculated with the lake water sample at the sample location (ng L^{-1}) and 0-5 cm depth sediment sample (ng/kg); 15 cm K_d values were calculated with pore water from 15 cm depth (ng L^{-1}) and sediment from 10-15 cm depth (ng kg^{-1}) for all samples except GWOUT-L-N, which was from 12-17 cm depth; 30 cm K_d values were calculated with pore water from 30 cm depth (ng L^{-1}) and sediment from 15-30 cm depth (ng kg^{-1}) for all samples except GWOUT-L-N, which was from 12-17 cm depth. Depth distance refers to depth below lake bottom.

Table B14. ICP results of Cr, Mn, Fe, Ni, Cu, Zn, and Pb ($\mu g\ g^{-1}$) extracted with 0.5 M HCl over 3 days. nd = not detected

Sample	Sediment Depth (cm)	Cr	Mn	Fe	Ni	Cu	Zn	Pb
GWOUT-R-N	0 - 5	0.22	55.37	181.18	0.23	0.34	1.94	2.25
GWOUT-R-N	5 - 10	0.32	18.01	84.99	0.17	0.28	1.22	1.15
GWOUT-R-N	10 - 15	0.32	7.42	64.47	0.15	0.35	1.42	1.62
GWOUT-R-N	15 - 30	0.50	4.33	112.63	0.27	0.28	1.32	0.94
GWOUT-L-N	0 - 5	0.06	43.01	136.86	0.14	0.32	1.12	2.07
GWOUT-L-N	5 - 10	0.20	29.08	72.18	0.17	0.30	1.26	1.82
GWOUT-L-N	12 - 17	0.22	13.58	51.83	0.12	0.30	1.04	1.25
GWOUT-L-N	17 - 32	0.48	18.36	84.38	0.20	0.38	1.53	2.56
GWIN131N	0 - 5	0.35	1705.43	1007.75	0.34	0.46	1.22	3.57
GWIN131N	5 - 10	0.19	930.82	333.75	0.32	0.41	0.80	11.91
GWIN131N	10 - 15	nd	155.51	89.81	0.12	0.22	0.27	17.46
GWIN131N	15 - 30	0.00	181.46	119.13	0.16	0.26	0.26	2.72
GWIN124N	0 - 5	0.25	1951.22	284.55	0.94	1.26	1.23	29.27
GWIN124N	5 - 10	0.12	156.83	83.17	0.56	1.41	0.49	10.53
GWIN124N	10 - 15	nd	27.87	52.13	0.33	0.63	0.36	1.22
GWIN124N	15 - 30	nd	32.68	28.98	0.31	0.54	0.10	0.31
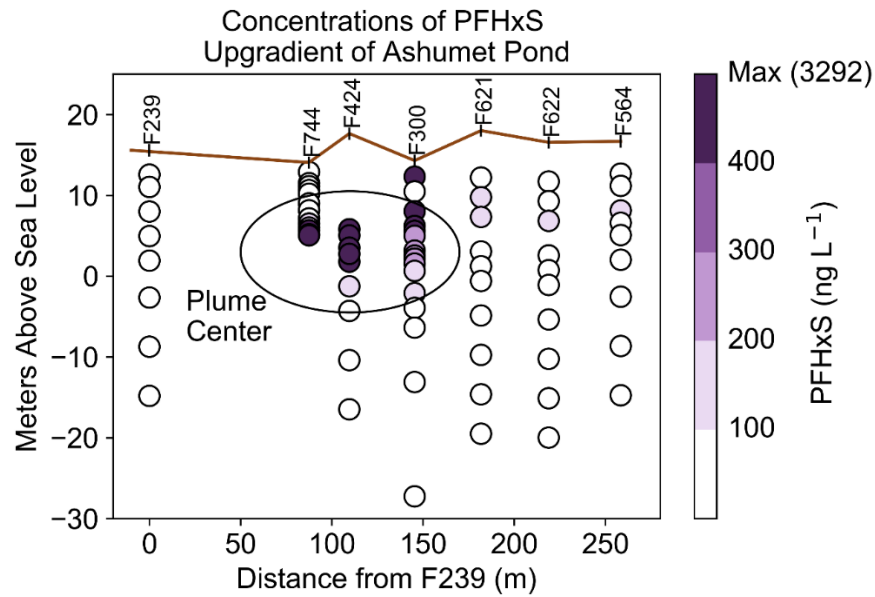
Figure B1. PFHxS concentrations in the array of groundwater wells located upgradient of Ashumet Pond.
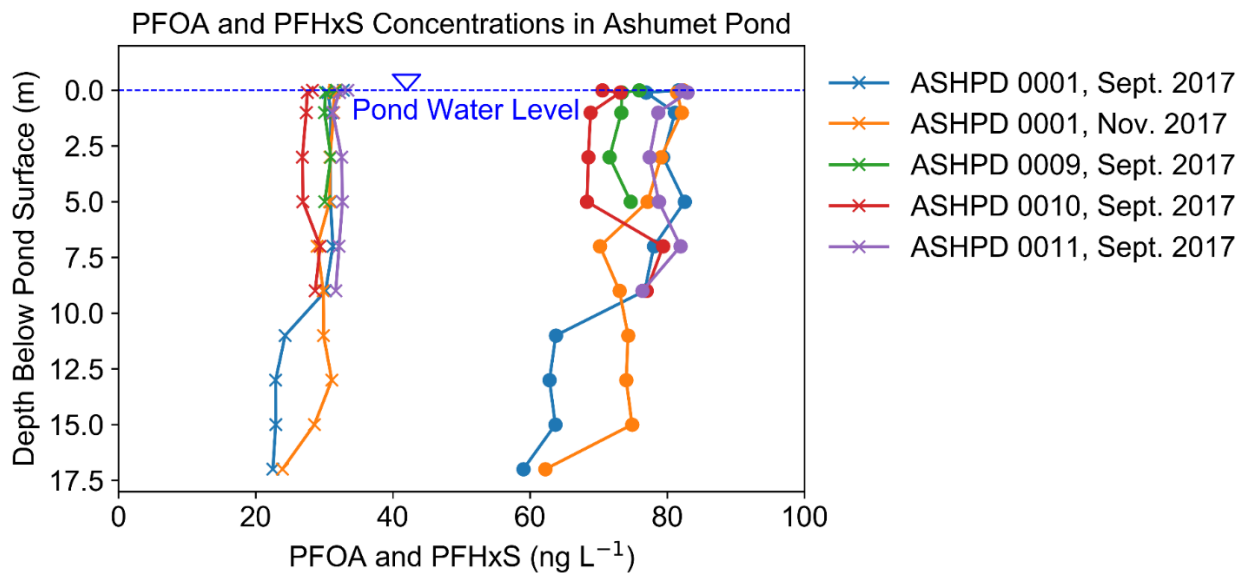
Figure B2. PFOA (x markers) and PFHxS (circle markers) concentrations in Ashumet Pond.
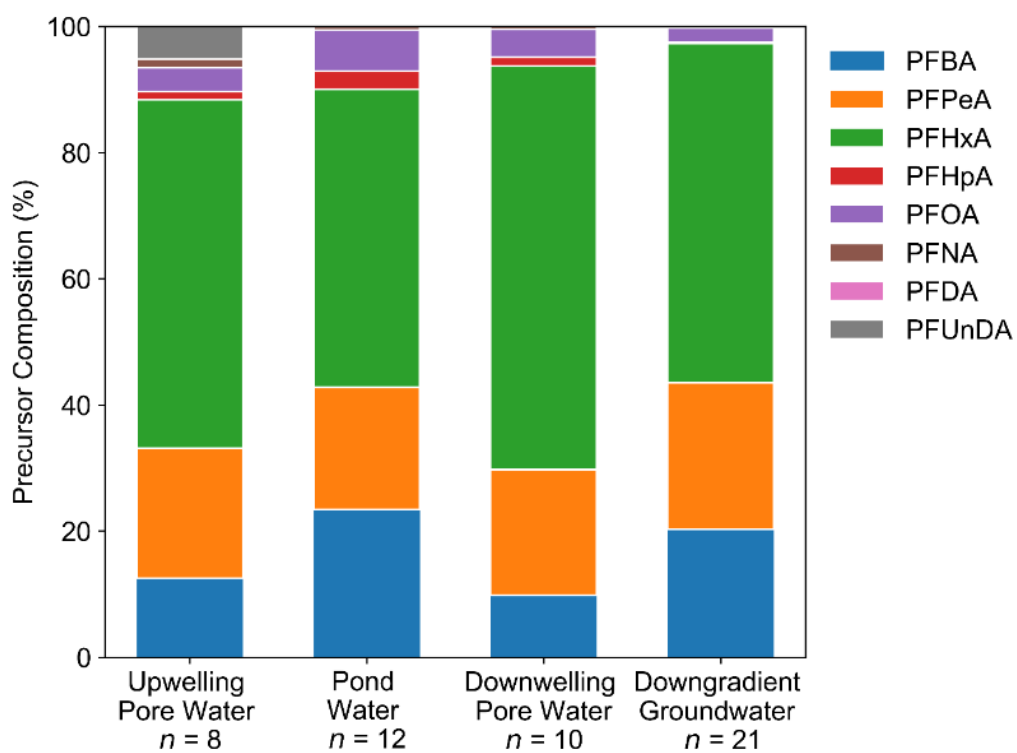
Figure B3. Average composition (%) of perfluoroalkyl carboxylates generated from oxidation in upwelling pore water, pond water, downwelling pore water, and downgradient pore water.
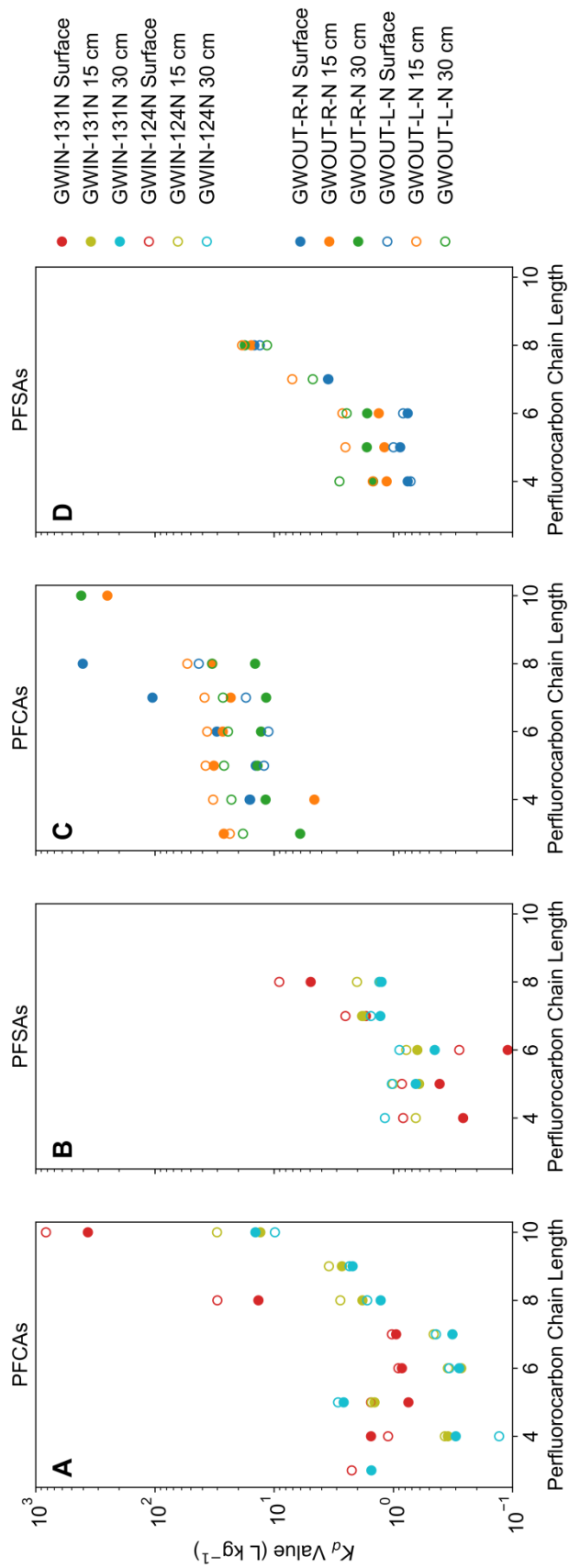
Figure B4. Sediment/water distribution coefficients (K_d) with chain length for the upwelling sites (A, B) and downwelling sites (C, D) at the surface, 15 cm, and 30 cm depth below pond bottom. See Table B13 for pore water and sediment depth pairing.

169
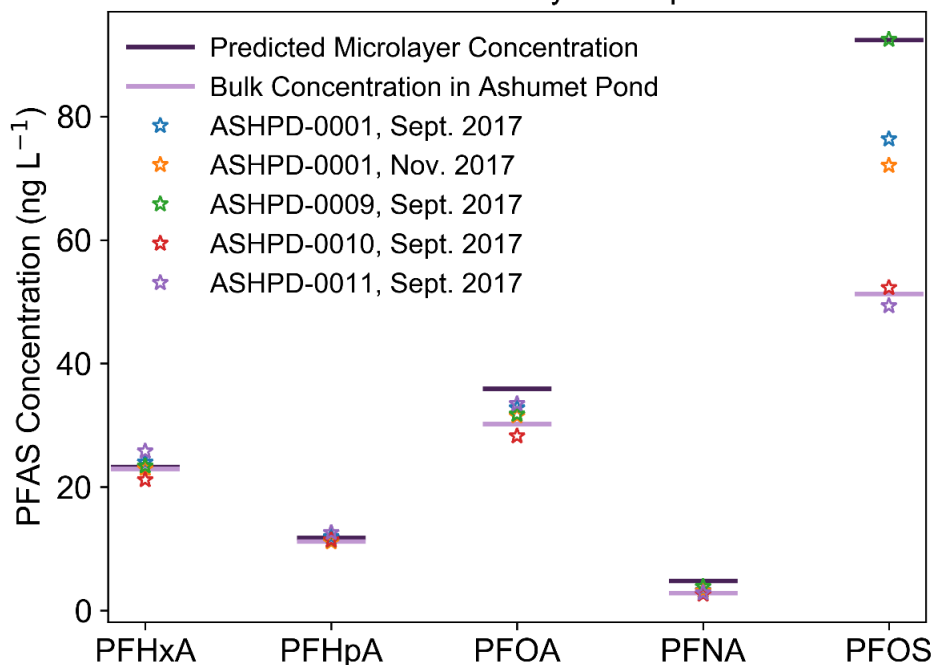
Figure B5. Predicted and measured microlayer concentrations in Ashumet Pond. Stars represent microlayer samples taken at different locations and dates in Ashumet Pond. The dark purple bar is the estimated microlayer concentration (see Microlayer Enrichment Theoretical Calculation section). The light purple bar is the bulk concentration in Ashumet Pond (median concentration of non-microlayer samples).

Appendix C

SUPPLEMENTARY INFORMATION FOR CHAPTER 4

C.1   METHODS

C.1.1   MATERIALS.

A Thermo Scientific™ Barnstead™ GenPure™ xCAD Plus (Lake Balboa, CA, U.S.A.) UV-TOC provided ultrapure deionized water (DI) with a resistivity of >18 MΩ cm^{-1}. LC-MS grade methanol (J.T. Baker, Center Valley, PA, U.S.A.), reagent grade formic acid and BioUltra ammonium acetate were obtained from Sigma Aldrich (St. Louis, MO, U.S.A.).

C.1.2   LC-MS/MS EXTRACTION.

The methanol extraction was adapted from previous studies.[20, 125] For this study, 1 ± 0.03 g subsamples (when possible) were cut with methanol-cleaned scissors and added to 15 mL polypropylene centrifuge tubes. Then, 12 mL of methanol was added to each centrifuge tube. Each sample was placed on a rotating shaker table for 1 hour and bath sonicated at 40 ^{0}C for 2 hours. Samples were then centrifuged at 4,000 rcf for 10 minutes and the supernatant was decanted into a new 15 mL polypropylene centrifuge tube and kept at 4 ^{0}C until analysis. One blank centrifuge tube was extracted within every set of 12 samples. We also assessed the sample area:weight ratio to convert concentrations into units of nmol m^{-2} (Table C4).

C.1.3   LC-MS/MS ANALYSIS.

Before LC-MS/MS analysis, the methanol extracts were warmed to room temperature and inverted before subsampling. An aliquot of methanol extract (705 µL) was combined with DI Water (750 µL) and 10 ng mL^{-1} internal standard solution (45 µL) in a polypropylene microcentrifuge tube. Samples were then briefly vortexed, centrifuged at 13,000 rpm, and then the supernatant was transferred to a polypropylene autosampler vial for analysis with an Agilent (Santa Clara, CA) 6460 triple quadrupole LC-MS/MS with electrospray ionization in negative ion mode. LC-MS/MS analysis followed the procedure outlined in Weber et al.[15] The injection volume was 300 µL. All calibration samples were prepared in a 50:50 methanol:water solution to match the sample composition. In this study, the linear calibration ranged from ~2 ng L^{-1} - 1200 ng L^{-1}, contained up to 8 points, and was forced through zero and 1/x weighted. All compounds were required to have r^2 > 0.99 for the calibration. N-EtFOSAA and N-MeFOSAA were added to the compounds measured by Weber et al.[15] (see Table C3 for parameters). If samples exceeded the calibration range by over 15% they were diluted and re-analyzed.

The limit of quantification was defined as the average sample concentration at which the signal-to-noise ratio was 10, plus the concentration of any LC-MS/MS blank (50:50 DI water:methanol with internal standards) above this value. The method quantification limit (MQL) was corrected for dilution. All blanks included in the extraction procedure were below the MQL.

C.1.4   QUALITY ASSURANCE/QUALITY CONTROL.

Duplicate injections of ~20% of the samples were completed and the results were averaged (average relative percent difference <25% except for N-EtFOSAA, which was 74% for a single sample). Recovery and precision experiments were performed on 3 samples (1 food contact material: plate, 1 textile: carpet, 1 domestic product: curtain) that had initial PFAS concentrations below the MQL to evaluate the effectiveness of the extraction method. Briefly,

four 1 ± 0.03 g samples were cut from the chosen samples and added to individual 15 mL polypropylene centrifuge tubes. All 12 samples were spiked with 7.2 ng of the native stock solution in methanol. The stock solution was added directly onto the sample and left to equilibrate for 30 minutes at room temperature. The extraction and analysis followed the methods outlined in the LC-MS/MS Extraction section. See Table C6 for results. Percent recoveries were within ±30% of expected values except for PFBS (66.3% recovery, plate), FOSA (69% recovery, plate and 69.7% recovery, carpet) and 8:2 FtS, which was removed from further consideration due to recoveries of only 22.6% for the carpet sample. Recoveries of 8:2 FtS may have been low due to matrix effects. PFDS was removed from further consideration due to poor reproducibility of continuing calibration checks.

C.1.5   XPS ANALYSIS.

The peak deconvolution and atomic ratio were calculated using the Thermo Scientific Avantage software. The accuracy of the C 1s peak fitting is ±2%. The pass energy was 50 eV for the high-resolution scans and 200 eV for the survey. At least 2 scans were performed for each data point for both the survey and the high-resolution scan. For food contact materials the food contact side was measured, whereas for textiles, the outer surface was measured (outer lining of jackets, the surface that humans would come into contact with for upholstery, etc.). For domestic products, the surface that was presumed to come into contact with humans most frequently was measured. Depth profiles were completed by etching with a monatomic argon ion beam (ion gun energy = 250 eV) with 10 seconds intervals. The material etching rate was 0.15 nm sec^{-1}, based on a tantalum pentoxide reference material. Therefore, 1.5 nm of material was etched between each XPS data point. However, because consumer products likely are not etched at the same rate as tantalum pentoxide, we estimated an etching rate of 15 nm sec^{-1} (see below section on Sputtering Yield for Consumer Products).

C.1.6   METHANOL EXTRACTION FOR XPS.

To reduce variability, a small section (<1 cm^2) of material was removed for pre-extraction XPS, and then a second subsample neighboring the first subsample was removed for post-extraction XPS. Samples were extracted following the LC-MS/MS extraction procedure outlined above, and then air-dried before analysis with XPS. Four samples with no fluorine pre-extraction were also included as controls. One of these controls (sample 9) had detectable fluorine post-extraction. The extraction was repeated, but sample 9 still displayed a small fluorine peak (<1.5% F) in the post-extraction sample. In both experiments, sample 9 had no fluorine detected via XPS pre-extraction. The other samples included as blank controls had no fluorine pre- or post-extraction. Sample 9 has a polylactic acid lining (Table C1). Methanol extraction may have removed this lining, exposing an underlying fluorine-containing surface. This is supported by the LC-MS/MS results, which show PFHxA and PFOA were present in sample 9.

C.1.7   LC-QTOF-MS ANALYSIS.

A Shimadzu high performance reverse-phase liquid chromatography (HPLC) system coupled with a Sciex 5600 Triple Quadrupole Time-of-Flight (QTOF) MS was used to analyze methanol extracts from the 11 samples that had detectable fluorine with XPS. Samples were extracted as outlined in the LC-MS/MS Extraction section, but with ACS-grade methanol. This analysis was completed to determine whether there were structures not captured with LC-MS/MS analysis prevalent in the samples. The HPLC was fitted with a Kinetex EVO C18 (2x.1 x 100 mm, 5 µm, 100 Å) column kept at 40 ºC and equipped with a Phenomenex AF0-8497 filter. The injection volume was 50 µL for each sample and mobile phases were water with 0.15% acetic acid (A) and 20 mM ammonium acetate in methanol (B). Samples were scanned in both positive and

negative ESI scan modes, and data acquisition and processing were performed using Analyst

TF 1.6 and PeakView 2.2 software, respectively.

C.2   CALCULATIONS

C.2.1   SPUTTERING YIELD FOR CONSUMER PRODUCTS.

We determined the depth of etching achieved in each step based on the sputtering yield

(atoms/argon ion) of the material.[136, 145, 146] The XPS etching rate is based on a tantalum

pentoxide reference material (0.15 nm s^{-1}, with 10 seconds of etching between each data point),

which is likely not similar to the consumer products measured here due to differences between

organic and inorganic materials.[136] A formula derived in previous work[136] was applied here, and

the etching rate of the consumer products was estimated to be less than 2 orders of magnitude

larger than the etching rate for tantalum pentoxide, assuming the samples are similar to

organics like polystyrene or polycarbonate. We consider 2 orders of magnitude an upper bound,

since fluoropolymers like PTFE and PVDF were found to have sputtering yields less than

polystyrene or polycarbonate,[147] and these samples are known to contain carbon-fluorine

bonds. This results in a maximum estimated etching depth of ~10 µm for the depth profiles

shown here (Figures C1) and in the manuscript.

C.2.2   XPS AND LC-MS/MS WEIGHT PERCENT.

XPS results in atomic percent fluorine were converted to weight percent fluorine as follows:

$$wt\% \, F = \frac{at\% \, F * A_r(F)}{at\% \, F * A_r(F) + \sum_{i=element} at \% \, i * A_r(i)} * 100$$

Where A_r(element) is the atomic weight of the element and i cycles through all elements detected in the sample in addition to fluorine.

Assuming all fluorine originated from the top 10 nm of materials, LC-MS/MS results were converted to weight percent. The following equation uses PFOA as an example:

$$wt.\%\ F = \frac{nmol_{PFOA\ extracted}}{g_{mat}} * \frac{mol}{10^9\ nmol} * \frac{15\ mol_F}{1\ mol\ _{PFOA}} * \frac{19\ g_F}{1\ mol_F} * \frac{Sample\ Thickness\ (nm)}{10nm}$$

Where g_{mat} is the total weight of the material extracted.

Table C1. Sample inventory. FCM = Food contact material.

Sample #	Weight of Material Extracted (g)	Weight/ Area Ratio (g m⁻²)	Category	Sub-Category	New/ Used	Country of Origin	Compostable	Material
1	1.00	339.0	FCM	Bowl	New		yes	Molded Fiber
2	1.01	234.0	FCM	Plate	New		yes	Molded Fiber
3	1.01	338.7	FCM	Plate	New		yes	Plant Fiber
4	1.00	458.9	FCM	Takeout Box	New		yes	
5	0.99	391.4	FCM	Takeout Box	New		yes	Plant Fiber
6	1.00	359.0	FCM	Takeout Box	New		yes	Plant Fiber
7	1.00	365.3	FCM	Takeout Box	New		yes	Plant-Based
8	1.01	402.8	FCM	Takeout Box	New		yes	Plant-Based, Polylactic Acid Lining
9	1.00	414.1	FCM	Takeout Box	New		yes	
10	1.01	396.3	FCM	Takeout Box	New		yes	
11	1.00	373.0	FCM	Takeout Box	New		Unknown	
12	1.00	415.6	FCM	Bowl	New		Unknown	
13	1.01	90.97	FCM	Popcorn Bag	New	USA	Unknown	
14	1.02	29.71	FCM	Food Bag	New		Unknown	
15	0.99	1545	FCM	Utensil	New		yes	
16	0.99	402.5	FCM	Cup	New		yes	Plant-Based Lining
17	1.01	398.8	FCM	Takeout Box	New		yes	Plant Fiber, Post Consumer Material Paper, Plant-Based Lining
18	1.01	306.3	FCM	Cup	New		yes	Palm Leaves
19	1.01	895.6	FCM	Plate	New		yes	Palm Leaves
20	1.01	605.5	FCM	Tray	New		yes	Polylactic Acid
21	1.00	346.6	FCM	Takeout Box	New		yes	Paper, Plant-Based Lining
22	1.00	336.1	FCM	Bowl	New		yes	Plant-Based
23	0.99	347.6	FCM	Bowl	New		yes	Plant-Based
24	0.99	352.0	FCM	Cup	New	USA	yes	Polylactic Acid
25	1.00	287.5	FCM	Cup	New	USA	yes	Polylactic Acid
26	0.98	354.4	FCM	Lid	New	USA	yes	Polylactic Acid

177

Table C1 (Continued)

Sample #	Weight of Material Extracted (g)	Weight/ Area Ratio (g m⁻²)	Category	Sub-Category	New/ Used	Country of Origin	Compostable	Material
27	1.01	302.4	FCM	Cup	New		yes	Paper, Plant-Based Lining
28	1.01	377.7	FCM	Lid	New		yes	Polylactic Acid
29	1.00	304.9	FCM	Takeout Box	New		yes	Polylactic Acid
30	0.99	296.3	FCM	Takeout Box	New		yes	
31	1.00	333.2	FCM	Takeout Box	New		Unknown	
32	1.01	372.6	FCM	Cup	New		Unknown	
33	0.99	249.2	FCM	Cup	New		Unknown	
34	1.01	38.92	FCM	Food Bag	New		Unknown	
35	1.01	340.6	FCM	Bowl	New		Unknown	
36	0.99	276.1	FCM	Cup	New		Unknown	
37	1.02	266.5	FCM	Cup	New		Unknown	Polypropylene Polyethylene Terephthalate Polyethylene
38	0.99	344.8	FCM	Lid	New		Unknown	Terephthalate Polystyrene
39	1.01	355.1	FCM	Lid	New		Unknown	
40	0.99	386.1	FCM	Cup	New		Unknown	
41	0.99	49.78	FCM	Food Bag	New		Unknown	
42	1.01	755.1	FCM	Food Stick	New		Unknown	
43	1.00	268.2	FCM	Plate	New		Unknown	Paper
44	1.02	218.2	FCM	Cup	New	USA	Unknown	
45	1.01	39.06	FCM	Food Paper	New	USA	Unknown	
46	1.02	3017	Textile	Carpet	New			Nylon Fiber
47	1.01	394.7	Textile	Upholstery	New			Polyester, Dyed Nylon, Acrylic
48	1.02	2721	Textile	Carpet	New			Nylon Fiber
49	1.01	2303	Textile	Carpet	New			Polyester Fiber
50	1.00	2655	Textile	Carpet	New			Nylon Fiber
51	1.00	383.5	Textile	Upholstery	New	USA		Nylon, Polyester, Acrylic
52	0.99	2348	Textile	Carpet	New			Nylon Fiber
53	0.98	2513	Textile	Carpet	New			Polyester, Polytrimethylene Terephthalate Fiber
54	1.00	522.7	Textile	Upholstery	New	USA		Cotton, Nylon, Polyester, Acrylic

Table C1 (Continued)

Sample #	Weight of Material Extracted (g)	Weight/Area Ratio (g m⁻²)	Category	Sub-Category	New/Used	Country of Origin	Compostable	Material
55	0.98	2375	Textile	Carpet	New			Polytrimethylene Terephthalate Fiber
56	1.01	2500	Textile	Carpet	New			Nylon Fiber
57	0.99	226.6	Textile	Backpack	New	China		Nylon, Polyester
58	0.99	259.6	Textile	Backpack	New	Vietnam		Nylon, Polyester
59	1.02	154.0	Textile	Mattress Pad	New			
60	1.01	3500	Textile	Carpet	Used			
61	1.00	245.0	Textile	Upholstery	Used	Taiwan		Leather
62	0.57	555.6	Textile	Upholstery	Used			Polyurethane Shell
63	1.02	280.7	Textile	Jacket	Used	China		Leather
64	0.60	844.2	Textile	Upholstery	Used	USA		
65	0.87	416.6	Textile	Upholstery	Used	USA		Cotton, Polyester
66	1.02	329.1	Textile	Jacket	Used	Pakistan		Nylon
67	1.01	65.16	Textile	Jacket	Used	Taiwan		
68	0.99	81.00	Textile	Jacket	Used			Nylon Fibers
69	0.99	3802	Textile	Carpet	New			
70	0.98	3677	Textile	Carpet	New			Ethylene-Vinyl Acetate
71	1.00	27.48	Textile	Jacket	New	China		Nylon Fiber
72	0.99	2336	Textile	Carpet	New			Nylon Fiber
73	1.00	2194	Textile	Carpet	New			Nylon Fiber
74	1.01	2692	Textile	Carpet	New			Wool, Olefin, Polypropylene
75	1.01	2314	Textile	Carpet	New			Wool, Olefin, Polypropylene
76	0.98	2367	Textile	Carpet	New			Polypropylene, Polyester,
77	1.01	2222	Textile	Carpet	New			Polypropylene, Polyester,
78	1.00	2200	Textile	Carpet	New			Polypropylene, Polytrimethylene Terephthalate, Polypropylene
79	1.02	2967	Textile	Carpet	New			Cotton
80	1.01	476.0	Textile	Backpack	New	China		Nylon, Polyester
81	1.00	476.7	Textile	Backpack	New	China		
82	1.00	350.1	Textile	Jacket	Used			Polyurethane, Viscose,

Table C1 (Continued)

Sample #	Weight of Material Extracted (g)	Weight/ Area Ratio (g m⁻²)	Category	Sub-Category	New/ Used	Country of Origin	Compostable	Material
83	1.01	298.2	Domestic Prod.	Bandage	New	China		Polyester
84	1.03	46.52	Domestic Prod.	Lens Wipes	New	China		Microfiber
85	1.00	813.7	Domestic Prod.	Boot	Used	China		
86	1.00	66.67	Domestic Prod.	Mask	New	China		Polypropylene
87	0.99	770.4	Domestic Prod.	Bandage	New	Hungary		
88	1.00	166.1	Domestic Prod.	Folder	New	USA		
89	1.02	92.12	Domestic Prod.	Label	New	Mexico		
90	1.00	438.7	Domestic Prod.	Notebook Cover	New	Vietnam		
91	1.02	265.9	Domestic Prod.	Dry Erase Tape	New	USA		
92	1.01	259.0	Domestic Prod.	Folder	New	China		
93	1.01	220.7	Domestic Prod.	Shower Curtain	New			Polyurethane Foam, Polypropylene, Polyester
94	1.01	293.0	Domestic Prod.	Mask	New	USA		

Table C2. Compound names, abbreviations, internal standards, molecular formulas and molecular weights. Modified from Weber et al.[15]

Compound Name	Abbreviation	Internal Standard	Mol. Formula	Mol. Weight
Perfluorinated Carboxylates				
Perfluorobutanoate	PFBA	[$^{13}C_4$] PFBA	$C_3F_7COO^-$	213
Perfluoropentanoate	PFPeA	[$^{13}C_2$] PFHxA	$C_4F_9COO^-$	263
Perfluorohexanoate	PFHxA	[$^{13}C_2$] PFHxA	$C_5F_{11}COO^-$	313
Perfluoroheptanoate	PFHpA	[$^{13}C_2$] PFHxA	$C_6F_{13}COO^-$	363
Perfluorooctanoate	PFOA	[$^{13}C_4$] PFOA	$C_7F_{15}COO^-$	413
Perfluorononanoate	PFNA	[$^{13}C_5$] PFNA	$C_8F_{17}COO^-$	463
Perfluorodecanoate	PFDA	[$^{13}C_2$] PFDA	$C_9F_{19}COO^-$	513
Perfluoroundecanoate	PFUnDA	[$^{13}C_2$] PFUnDA	$C_{10}F_{21}COO^-$	563
Perfluorododecanoate	PFDoDA	[$^{13}C_2$] PFDoDA	$C_{11}F_{23}COO^-$	613
Perfluorinated Sulfonates				
Perfluorobutane sulfonate	PFBS	[$^{18}O_2$] PFHxS	$C_4F_9SO_3^-$	299
Perfluorohexane sulfonate	PFHxS	[$^{18}O_2$] PFHxS	$C_6F_{13}SO_3^-$	399
Perfluorooctane sulfonate	PFOS	[$^{13}C_4$] PFOS	$C_8F_{17}SO_3^-$	499
Perfluorodecane sulfonate	PFDS	[$^{13}C_4$] PFOS	$C_{10}F_{21}SO_3^-$	599
Perfluoroalkyl Sulfonamides				
Perfluorooctane sulfonamide	FOSA	[$^{13}C_8$] FOSA	$C_8F_{17}SO_2NH_2$	498
Perfluoroalkyl Sulfonamidoacetic Acids				
N-Methyl perfluorooctane sulfonamidoacetic acid	N-MeFOSAA	d5-N-MeFOSAA	$C_8F_{17}SO_2N(CH_3)CH_2COO^-$	570
N-Ethyl perfluorooctane sulfonamidoacetic acid	N-EtFOSAA	d3-N-EtFOSAA	$C_8F_{17}SO_2N(C_2H_5)CH_2COO^-$	584
Fluorotelomer Sulfonates				
6:2 fluorotelomer sulfonate	6:2 FtS	[$^{13}C_2$] 6:2 FtS	$C_6F_{13}CH_2CH_2SO_3^-$	427
8:2 fluorotelomer sulfonate	8:2 FtS	[$^{13}C_2$] 6:2 FtS	$C_8F_{17}CH_2CH_2SO_3^-$	527

Table C3. LC-MS/MS parameters for N-EtFOSAA and N-MeFOSAA. All other parameters were as defined in Weber et al.[15]

Analyte	Type	Internal Standard	Precursor Ion Mass	Product Ion Mass	Fragmentor Voltage (V)	Collision Energy (V)
Perfluoroalkyl Sulfonamidoacetic Acids						
N-EtFOSAA	Target	d3-N-EtFOSAA	584	419	110	15
N-EtFOSAA (Q1)				526		20
N-MeFOSAA	Target	d5-N-MeFOSAA	570	419	120	20
N-MeFOSAA (Q1)				512		20
Internal Standards						
d3-N-EtFOSAA	ISTD			589	419	120	15
d5-N-MeFOSAA	ISTD			573	419	120	20

182

Table C4. LC-MS/MS results for all PFASs quantified (nmol m^{-2}). Samples above the MQL, but with qualifiers out of range are labeled QH (qualifier above ±30% range) or QL (qualifier below ±30% range). PFCAs = perfluorinated carboxylates, PFSAs = perfluorinated sulfonates, precursors = perfluoroalkyl acid precursors.

Sample #	PFCAs									PFSAs			Precursors			
	PFBA	PFPeA	PFHxA	PFHpA	PFOA	PFNA	PFDA	PFUnDA	PFDoDA	PFBS	PFHxS	PFOS	6:2 FtS	N-MeFOSAA	N-EtFOSAA	FOSA
1	958	76.6	837	28.5	6.98	<MQL	0.719	<MQL	<MQL	<MQL	<MQL	<MQL	<MQL	<MQL	0.203	<MQL
2	645	<MQL	538	16.9	4.01	0.199	0.606	<MQL	0.184	<MQL	<MQL	<MQL	0.247	0.323	0.279	<MQL
3	2.56	2.31	10.8	4.77	31.4	4.54	37.9	3.19	25.0	<MQL	<MQL	<MQL	<MQL	<MQL	<MQL	<MQL
4	17.6	11.1	59.9	3.44	<MQL	<MQL	<MQL	<MQL	<MQL	<MQL	<MQL	<MQL	<MQL	<MQL	<MQL	<MQL
5	<MQL	<MQL	4.90	3.78	34.9	3.28	25.3	2.00	9.86	<MQL	<MQL	<MQL	<MQL	<MQL	<MQL	<MQL
6	<MQL	1.85	8.24	3.49	26.3	2.57	19.6	1.34	7.88	<MQL	<MQL	<MQL	<MQL	<MQL	<MQL	<MQL
7	<MQL	<MQL	5.75	1.73	6.35	0.682	4.08	QH	2.31	<MQL	<MQL	<MQL	<MQL	<MQL	<MQL	<MQL
8	<MQL	<MQL	9.28	1.70	<MQL	<MQL	<MQL	<MQL	<MQL	<MQL	<MQL	<MQL	<MQL	<MQL	<MQL	<MQL
9	<MQL	<MQL	1.96	<MQL	0.281	<MQL	<MQL	<MQL	<MQL	<MQL	<MQL	<MQL	<MQL	<MQL	<MQL	<MQL
10	<MQL	<MQL	QL	QL	0.429	0.354	QH	<MQL	<MQL	<MQL	<MQL	<MQL	<MQL	<MQL	0.161	<MQL
11	<MQL	<MQL	38.1	QL	0.408	0.321	0.479	QL	0.542	<MQL	<MQL	<MQL	<MQL	<MQL	QL	<MQL
12	<MQL	<MQL	32.4	0.965	0.465	0.452	0.698	0.823	0.749	<MQL	<MQL	<MQL	<MQL	<MQL	<MQL	<MQL
13	<MQL	<MQL	1.73	<MQL	<MQL	<MQL	<MQL	<MQL	<MQL	<MQL	<MQL	<MQL	<MQL	<MQL	<MQL	<MQL
14	<MQL	<MQL	0.226	<MQL	<MQL	<MQL	<MQL	<MQL	<MQL	<MQL	<MQL	<MQL	<MQL	<MQL	<MQL	<MQL
15	<MQL	<MQL	<MQL	<MQL	<MQL	<MQL	<MQL	<MQL	<MQL	<MQL	<MQL	<MQL	<MQL	<MQL	<MQL	<MQL
16	<MQL	<MQL	<MQL	<MQL	<MQL	<MQL	<MQL	<MQL	<MQL	<MQL	<MQL	<MQL	<MQL	<MQL	<MQL	<MQL
17	<MQL	<MQL	QL	<MQL	<MQL	<MQL	<MQL	<MQL	<MQL	<MQL	<MQL	<MQL	<MQL	<MQL	<MQL	<MQL
18	<MQL	<MQL	QL	<MQL	<MQL	<MQL	<MQL	<MQL	<MQL	<MQL	<MQL	<MQL	<MQL	<MQL	<MQL	<MQL
19	<MQL	<MQL	<MQL	<MQL	<MQL	<MQL	<MQL	<MQL	<MQL	<MQL	<MQL	<MQL	<MQL	<MQL	<MQL	<MQL
20	<MQL	<MQL	<MQL	<MQL	<MQL	<MQL	<MQL	<MQL	<MQL	<MQL	<MQL	<MQL	<MQL	<MQL	<MQL	<MQL
21	<MQL	<MQL	<MQL	<MQL	<MQL	<MQL	<MQL	<MQL	<MQL	<MQL	<MQL	<MQL	<MQL	<MQL	<MQL	<MQL

Table C4 (Continued)

Sample #	PFCAs									PFSAs			Precursors			
	PFBA	PFPeA	PFHxA	PFHpA	PFOA	PFNA	PFDA	PFUnDA	PFDoDA	PFBS	PFHxS	PFOS	6:2 FtS	N-MeFOSAA	N-EtFOSAA	FOSA
22	<MQL	<MQL	<MQL	<MQL	<MQL	<MQL	<MQL	<MQL	<MQL	<MQL	<MQL	<MQL	<MQL	<MQL	<MQL	<MQL
23	<MQL	<MQL	<MQL	<MQL	<MQL	<MQL	<MQL	<MQL	<MQL	<MQL	<MQL	<MQL	<MQL	<MQL	<MQL	<MQL
24	<MQL	<MQL	<MQL	<MQL	<MQL	<MQL	<MQL	<MQL	<MQL	<MQL	<MQL	<MQL	<MQL	<MQL	<MQL	<MQL
25	<MQL	<MQL	<MQL	<MQL	<MQL	<MQL	<MQL	<MQL	<MQL	<MQL	<MQL	<MQL	<MQL	<MQL	<MQL	<MQL
26	<MQL	<MQL	<MQL	<MQL	<MQL	<MQL	<MQL	<MQL	<MQL	<MQL	<MQL	<MQL	<MQL	<MQL	<MQL	<MQL
27	<MQL	<MQL	QH	<MQL	<MQL	<MQL	<MQL	<MQL	<MQL	<MQL	<MQL	<MQL	<MQL	<MQL	<MQL	<MQL
28	<MQL	<MQL	<MQL	<MQL	<MQL	<MQL	<MQL	<MQL	<MQL	<MQL	<MQL	<MQL	<MQL	<MQL	<MQL	<MQL
29	<MQL	<MQL	<MQL	<MQL	<MQL	<MQL	<MQL	<MQL	<MQL	<MQL	<MQL	<MQL	<MQL	<MQL	<MQL	<MQL
30	<MQL	<MQL	<MQL	<MQL	<MQL	<MQL	<MQL	<MQL	<MQL	<MQL	<MQL	<MQL	<MQL	<MQL	<MQL	<MQL
31	<MQL	<MQL	<MQL	<MQL	<MQL	<MQL	<MQL	<MQL	<MQL	<MQL	<MQL	<MQL	<MQL	<MQL	<MQL	<MQL
32	<MQL	<MQL	<MQL	<MQL	<MQL	<MQL	<MQL	<MQL	<MQL	<MQL	<MQL	<MQL	<MQL	<MQL	<MQL	<MQL
33	<MQL	<MQL	<MQL	<MQL	<MQL	<MQL	<MQL	<MQL	<MQL	<MQL	<MQL	<MQL	<MQL	<MQL	<MQL	<MQL
34	<MQL	QL	<MQL	<MQL	<MQL	<MQL	<MQL	<MQL	<MQL	<MQL	<MQL	<MQL	<MQL	<MQL	<MQL	<MQL
35	<MQL	<MQL	<MQL	<MQL	<MQL	<MQL	<MQL	<MQL	<MQL	<MQL	<MQL	<MQL	<MQL	<MQL	<MQL	<MQL
36	<MQL	<MQL	<MQL	<MQL	<MQL	<MQL	<MQL	<MQL	<MQL	<MQL	<MQL	<MQL	<MQL	<MQL	<MQL	<MQL
37	<MQL	<MQL	<MQL	<MQL	<MQL	<MQL	<MQL	<MQL	<MQL	<MQL	<MQL	<MQL	<MQL	<MQL	<MQL	<MQL
38	<MQL	<MQL	<MQL	<MQL	<MQL	<MQL	<MQL	<MQL	<MQL	<MQL	<MQL	<MQL	<MQL	<MQL	<MQL	<MQL
39	<MQL	<MQL	<MQL	<MQL	<MQL	<MQL	<MQL	<MQL	<MQL	<MQL	<MQL	<MQL	<MQL	<MQL	<MQL	<MQL
40	<MQL	<MQL	<MQL	<MQL	<MQL	<MQL	<MQL	<MQL	<MQL	<MQL	<MQL	<MQL	<MQL	<MQL	<MQL	<MQL
41	<MQL	<MQL	<MQL	<MQL	<MQL	<MQL	<MQL	<MQL	<MQL	<MQL	<MQL	<MQL	<MQL	<MQL	<MQL	<MQL
42	<MQL	QL	<MQL	<MQL	<MQL	<MQL	<MQL	<MQL	<MQL	<MQL	<MQL	<MQL	<MQL	<MQL	<MQL	<MQL
43	<MQL	<MQL	<MQL	<MQL	<MQL	<MQL	<MQL	<MQL	<MQL	<MQL	<MQL	<MQL	<MQL	<MQL	<MQL	<MQL
44	<MQL	QL	<MQL	<MQL	<MQL	<MQL	<MQL	<MQL	<MQL	<MQL	<MQL	<MQL	<MQL	<MQL	<MQL	<MQL
45	<MQL	<MQL	<MQL	<MQL	<MQL	<MQL	<MQL	<MQL	<MQL	<MQL	<MQL	<MQL	<MQL	<MQL	<MQL	<MQL

Table C4 (Continued)

Sample #	PFCAs									PFSAs			Precursors			
	PFBA	PFPeA	PFHxA	PFHpA	PFOA	PFNA	PFDA	PFUnDA	PFDoDA	PFBS	PFHxS	PFOS	6:2 FtS	N-MeFOSAA	N-EtFOSAA	FOSA
46	32.1	26.8	137	30.0	<MQL	<MQL	<MQL	<MQL	<MQL	<MQL	<MQL	<MQL	1.05	<MQL	<MQL	<MQL
47	5.15	5.42	47.3	12.1	<MQL	QL	<MQL	<MQL	<MQL	<MQL	QL	QL	0.17	<MQL	<MQL	<MQL
48	9.22	<MQL	37.0	<MQL	<MQL	<MQL	<MQL	<MQL	<MQL	<MQL	<MQL	<MQL	<MQL	<MQL	<MQL	<MQL
49	35.0	<MQL	<MQL	<MQL	<MQL	<MQL	<MQL	<MQL	<MQL	QL	QL	<MQL	<MQL	<MQL	<MQL	<MQL
50	<MQL	<MQL	QH	<MQL	3.12	<MQL	<MQL	<MQL	<MQL	21.3	<MQL	<MQL	<MQL	<MQL	<MQL	<MQL
51	6.51	2.77	10.2	0.465	0.524	<MQL	0.248	<MQL	<MQL	<MQL	<MQL	QL	QH	<MQL	<MQL	<MQL
52	<MQL	<MQL	9.82	<MQL	QL	<MQL	<MQL	<MQL	<MQL	6.00	<MQL	<MQL	<MQL	<MQL	<MQL	<MQL
53	9.04	<MQL	<MQL	<MQL	<MQL	<MQL	<MQL	<MQL	<MQL	5.74	QL	<MQL	QH	<MQL	<MQL	<MQL
54	5.43	<MQL	7.08	0.569	0.364	QL	<MQL	<MQL	<MQL	<MQL	<MQL	<MQL	<MQL	<MQL	<MQL	<MQL
55	6.25	<MQL	<MQL	<MQL	<MQL	<MQL	<MQL	<MQL	<MQL	4.83	QL	<MQL	<MQL	<MQL	<MQL	<MQL
56	<MQL	<MQL	6.46	<MQL	<MQL	<MQL	<MQL	<MQL	<MQL	<MQL	<MQL	<MQL	<MQL	<MQL	<MQL	<MQL
57	<MQL	<MQL	0.951	<MQL	4.37	<MQL	1.01	<MQL	<MQL	<MQL	<MQL	<MQL	<MQL	<MQL	<MQL	<MQL
58	<MQL	<MQL	<MQL	<MQL	1.09	<MQL	QH	<MQL	<MQL	<MQL	<MQL	<MQL	<MQL	<MQL	<MQL	<MQL
59	<MQL	<MQL	<MQL	<MQL	0.101	<MQL	<MQL	<MQL	0.120	<MQL	<MQL	<MQL	<MQL	<MQL	<MQL	<MQL
60	<MQL	15.3	157	67.6	3200	61.6	1230	23.4	306	<MQL	<MQL	6.97	12.4	1.64	10.1	0.990
61	281	<MQL	0.872	<MQL	3.66	19.9	QH	5.33	QH	9.17	<MQL	QL	QH	<MQL	QL	0.0859
62	<MQL	<MQL	4.97	4.05	6.91	2.99	QH	QL	1.36	QH	<MQL	12.4	2.89	QH	QL	<MQL
63	<MQL	<MQL	1.55	0.730	3.72	0.435	QH	<MQL	0.188	QH	0.505	2.90	<MQL	0.169	1.37	<MQL
64	<MQL	<MQL	<MQL	QL	2.33	QL	<MQL	<MQL	<MQL	<MQL	QL	<MQL	<MQL	<MQL	4.27	<MQL
65	<MQL	<MQL	QL	<MQL	2.50	QH	QH	QH	0.869	<MQL	<MQL	1.80	1.08	<MQL	QH	<MQL
66	<MQL	<MQL	0.482	<MQL	1.74	<MQL	1.63	<MQL	0.811	<MQL	<MQL	<MQL	<MQL	<MQL	<MQL	<MQL
67	<MQL	<MQL	<MQL	<MQL	0.378	0.0405	0.175	<MQL	0.0518	QL	<MQL	<MQL	<MQL	<MQL	0.0397	<MQL
68	<MQL	<MQL	<MQL	<MQL	0.0915	<MQL	<MQL	<MQL	<MQL	<MQL	<MQL	<MQL	0.09	<MQL	QL	<MQL
69	<MQL	<MQL	<MQL	<MQL	<MQL	<MQL	<MQL	<MQL	<MQL	<MQL	<MQL	<MQL	<MQL	<MQL	<MQL	<MQL

Table C4 (Continued)

Sample #	PFCAs									PFSAs			Precursors			
	PFBA	PFPeA	PFHxA	PFHpA	PFOA	PFNA	PFDA	PFUnDA	PFDoDA	PFBS	PFHxS	PFOS	6:2 FtS	N-MeFOSAA	N-EtFOSAA	FOSA
70	<MQL	<MQL	<MQL	<MQL	<MQL	<MQL	<MQL	<MQL	<MQL	<MQL	<MQL	<MQL	<MQL	<MQL	<MQL	<MQL
71	<MQL	<MQL	<MQL	<MQL	<MQL	<MQL	<MQL	<MQL	<MQL	<MQL	<MQL	<MQL	<MQL	<MQL	<MQL	<MQL
72	<MQL	<MQL	<MQL	<MQL	<MQL	<MQL	<MQL	<MQL	<MQL	<MQL	<MQL	<MQL	<MQL	<MQL	<MQL	<MQL
73	<MQL	<MQL	<MQL	<MQL	<MQL	<MQL	<MQL	<MQL	<MQL	<MQL	<MQL	<MQL	<MQL	<MQL	<MQL	<MQL
74	<MQL	<MQL	<MQL	<MQL	<MQL	<MQL	<MQL	<MQL	<MQL	<MQL	<MQL	<MQL	<MQL	<MQL	<MQL	<MQL
75	<MQL	<MQL	<MQL	<MQL	<MQL	<MQL	<MQL	<MQL	<MQL	<MQL	<MQL	<MQL	<MQL	<MQL	<MQL	<MQL
76	<MQL	<MQL	<MQL	<MQL	<MQL	<MQL	<MQL	<MQL	<MQL	<MQL	<MQL	<MQL	<MQL	<MQL	<MQL	<MQL
77	<MQL	<MQL	<MQL	<MQL	<MQL	<MQL	<MQL	<MQL	<MQL	<MQL	<MQL	<MQL	<MQL	<MQL	<MQL	<MQL
78	<MQL	<MQL	<MQL	<MQL	<MQL	<MQL	<MQL	<MQL	<MQL	QL	QL	<MQL	<MQL	<MQL	<MQL	<MQL
79	<MQL	<MQL	<MQL	<MQL	<MQL	<MQL	<MQL	<MQL	<MQL	<MQL	<MQL	<MQL	<MQL	<MQL	<MQL	<MQL
80	<MQL	<MQL	<MQL	<MQL	<MQL	<MQL	<MQL	<MQL	<MQL	<MQL	<MQL	<MQL	<MQL	<MQL	<MQL	<MQL
81	<MQL	<MQL	<MQL	<MQL	<MQL	<MQL	<MQL	<MQL	<MQL	<MQL	<MQL	<MQL	<MQL	<MQL	<MQL	<MQL
82	<MQL	<MQL	QL	<MQL	QL	<MQL	<MQL	<MQL	<MQL	<MQL	<MQL	<MQL	<MQL	<MQL	<MQL	<MQL
83	<MQL	<MQL	0.816	0.397	1.68	QH	0.679	<MQL	<MQL	<MQL	<MQL	<MQL	<MQL	<MQL	<MQL	<MQL
84	<MQL	<MQL	<MQL	<MQL	<MQL	<MQL	<MQL	<MQL	<MQL	<MQL	<MQL	0.0199	<MQL	<MQL	<MQL	<MQL
85	<MQL	<MQL	QL	<MQL	2.40	<MQL	<MQL	<MQL	<MQL	<MQL	<MQL	0.979	<MQL	<MQL	1.47	0.242
86	<MQL	<MQL	<MQL	<MQL	<MQL	<MQL	<MQL	<MQL	<MQL	<MQL	<MQL	<MQL	<MQL	<MQL	<MQL	<MQL
87	<MQL	<MQL	<MQL	<MQL	<MQL	<MQL	<MQL	<MQL	<MQL	<MQL	<MQL	<MQL	<MQL	<MQL	<MQL	<MQL
88	<MQL	<MQL	<MQL	<MQL	<MQL	<MQL	<MQL	<MQL	<MQL	<MQL	<MQL	<MQL	<MQL	<MQL	<MQL	<MQL
89	<MQL	<MQL	<MQL	<MQL	<MQL	<MQL	<MQL	<MQL	<MQL	<MQL	QL	<MQL	<MQL	<MQL	<MQL	<MQL
90	<MQL	<MQL	<MQL	<MQL	<MQL	<MQL	<MQL	<MQL	<MQL	<MQL	<MQL	<MQL	<MQL	<MQL	<MQL	<MQL
91	<MQL	<MQL	<MQL	<MQL	<MQL	<MQL	<MQL	<MQL	<MQL	<MQL	<MQL	<MQL	<MQL	<MQL	<MQL	<MQL
92	<MQL	<MQL	<MQL	<MQL	<MQL	<MQL	<MQL	<MQL	<MQL	<MQL	<MQL	<MQL	<MQL	<MQL	<MQL	<MQL
93	<MQL	<MQL	<MQL	<MQL	<MQL	<MQL	<MQL	<MQL	<MQL	<MQL	<MQL	<MQL	<MQL	<MQL	<MQL	<MQL

Table C4 (Continued)

Sample #	PFCAs									PFSAs			Precursors			
	PFBA	PFPeA	PFHxA	PFHpA	PFOA	PFNA	PFDA	PFUnDA	PFDoDA	PFBS	PFHxS	PFOS	6:2 FtS	N-MeFOSAA	N-EtFOSAA	FOSA
94	<MQL	<MQL	<MQL	<MQL	<MQL	<MQL	<MQL	<MQL	<MQL	<MQL	<MQL	<MQL	<MQL	<MQL	<MQL	<MQL

Table C5. LC-MS/MS method quantification limits (MQL). The range of MQLs is presented below. MQL was separately determined for each batch of analyses to account for any variation in LC-MS/MS conditions.

Compound	MQL Range (ng g^{-1})
PFBA	0.32 - 1.1
PFPeA	0.080 - 1.5
PFHxA	0.43 - 1.8
PFHpA	0.11 - 1.9
PFOA	0.22 - 0.58
PFNA	0.15 - 1.6
PFDA	0.29 - 2.0
PFUnDA	0.40 - 2.6
PFDoDA	0.41 - 3.7
PFBS	0.063 - 0.31
PFHxS	0.078 - 0.40
PFOS	0.20 - 2.9
6:2 FtS	0.082 - 0.14
N-MeFOSAA	0.24 - 1.3
N-EtFOSAA	0.22 - 1.6
FOSA	0.063 - 0.45

Table C6. LC-MS/MS recovery and precision results. Average percent recovery, and relative standard deviation (RSD) of native PFAS spikes (7.2 ng) added to a plate (n = 4), curtain (n = 4), and carpet (n = 4) before extraction. PFAS concentrations were <MQL in the plate, curtain, and carpet before spiking.

	Plate (n = 4)		Curtain (n = 4)		Carpet (n = 4)	
	Average % Recovery	% RSD	Average % Recovery	% RSD	Average % Recovery	% RSD
PFBA	109	2.55	103	3.55	102	2.07
PFPeA	104	1.75	92.7	2.93	96	1.80
PFHxA	111	2.12	103	3.17	103	1.56
PFHpA	119	2.88	104	3.29	109	2.07
PFOA	109	1.51	103	2.53	105	1.59
PFNA	111	4.13	104	4.34	107	6.12
PFDA	123	5.47	113	3.74	114	4.38
PFUnDA	112	7.40	104	6.02	108	8.08
PFDoDA	110	8.22	105	7.26	108	3.64
PFBS	66.3	4.78	80.3	1.54	78.6	5.58
PFHxS	73.4	5.37	84.5	2.47	97.0	5.43
PFOS	85.8	4.33	93.9	4.77	88.3	6.12
6:2 FtS	99.3	28.4	80.2	4.09	84.9	5.53
8:2 FtS	104	5.42	139	8.52	22.6	6.75
N-MeFOSAA	106	5.82	101	8.52	97.9	7.54
N-EtFOSAA	126	8.97	109	4.99	116	7.85
FOSA	69.0	5.51	78.5	7.54	69.7	4.58

Table C7. XPS results. The limit of detection (LOD) is 1 atomic percent.

Sample	Average Atomic % F Pre-Extraction	Minimum/ Maximum Atomic % F	Average Weight % F Pre-Extraction	Minimum/ Maximum Weight % F	Average Atomic % F Post-Extraction	Minimum/ Maximum Atomic % F
1	9.74	8.76/10.7	13.3	12.0/14.6	12.8	12.0/14.2
2	8.45	7.09/9.80	11.6	9.76/13.4	14.2	13.7/14.7
4	17.7	16.4/19.1	23.2	21.5/24.9	18.8	17.6/20.0
7	<LOD		<LOD		N/A	
8	14.2	13.7/14.8	19.2	18.5/20.0	24.3	23.3/25.2
9	<LOD		<LOD		1.32	1.21/1.42
10	<LOD		<LOD		N/A	
11	<LOD		<LOD		N/A	
12	<LOD		<LOD		N/A	
14	28.3	27.0/29.6	36.0	34.5/37.4	18.5	18.2/18.8
15	<LOD		<LOD		N/A	
16	<LOD		<LOD		<LOD	
17	<LOD		<LOD		N/A	
18	<LOD		<LOD		N/A	
19	<LOD		<LOD		N/A	
20	<LOD		<LOD		N/A	
32	<LOD		<LOD		N/A	
33	<LOD		<LOD		N/A	
47	34.5	32.7/36.3	42.5	40.7/44.3	31.9	30.6/35.1
51	44.9	43.6/46.2	54.6	54.0/55.2	31.8	31.6/31.9
54	31.1	30.8/31.5	38.5	38.1/39.0	20.4	18.2/21.6
59	<LOD		<LOD		N/A	
61	6.38	5.64/7.12	8.60	7.63/9.48	3.91	3.25/4.56
62	<LOD		<LOD		N/A	
64	<LOD		<LOD		N/A	
65	<LOD		<LOD		N/A	
66	<LOD		<LOD		N/A	
67	7.39	6.83/7.94	9.96	9.25/10.7	5.71	5.25/6.17
68	3.70	3.61/3.79	4.99	4.81/5.16	2.32	2.17/2.46
71	<LOD		<LOD		N/A	
79	<LOD		<LOD		N/A	
81	<LOD		<LOD		<LOD	
82	<LOD		<LOD		<LOD	
83	<LOD		<LOD		N/A	
84	<LOD		<LOD		N/A	
85	<LOD		<LOD		N/A	
86	<LOD		<LOD		<LOD	
87	<LOD		<LOD		N/A	
88	<LOD		<LOD		N/A	
89	<LOD		<LOD		N/A	
90	<LOD		<LOD		N/A	
91	<LOD		<LOD		N/A	
92	<LOD		<LOD		N/A	
93	<LOD		<LOD		N/A	
94	<LOD		<LOD		N/A	

Table C8. LC-QTOF-MS results. Name, family, molecular formula, theoretical m/z, and peak area for sample methanol extracts. Data analyzed at Purdue University, Department of Agronomy, Interdisciplinary Ecological Science and Engineering.

Sample	Name	Family	Molecular Formula	Theoretical m/z	Area
		Negative Mode			
1	2-perfluorohexyl ethanoic acid (FHEA)	Fluorotelomer carboxylic acids (FTCAs)	C8H3F13O2	376.98472	2880
	Perfluoro-n-pentanoic acid (PFPeA)	Perfluoroalkyl carboxylic acids (PFCAs)	C5HF9O2	262.97546	2186
	Perfluoro-n-hexanoic acid (PFHxA)	Perfluoroalkyl carboxylic acids (PFCAs)	C6HF11O2	312.97226	44303
	3-Perfluoropentyl propanoic acid (FPePA)	Fluorotelomer carboxylic acids (FTCAs)	C8H5F11O2	341.00356	1822
	2H-perfluoro-2-octenoic acid (FHUEA)	Fluorotelomer unsaturated acids (FTUA)	C8H2F12O2	356.97849	15413
	10:2 fluorotelomer sulfonate (10:2 FTS)	Fluorotelomer sulfonic acids (FTSs)	C12H5F21O3S	626.95458	596
	6:2 fluorotelomer sulfonate (6:2 FTS)	Fluorotelomer sulfonic acids (FTSs)	C8H5F13O3S	426.96736	294
	Perfluoro-n-octanoic acid (PFOA)	Perfluoroalkyl carboxylic acids (PFCAs)	C8HF15O2	412.96588	1575
2	2-perfluorohexyl ethanoic acid (FHEA)	Fluorotelomer carboxylic acids (FTCAs)	C8H3F13O2	376.98472	1948
	Perfluoro-n-pentanoic acid (PFPeA)	Perfluoroalkyl carboxylic acids (PFCAs)	C5HF9O2	262.97546	1820
	Perfluoro-n-hexanoic acid (PFHxA)	Perfluoroalkyl carboxylic acids (PFCAs)	C6HF11O2	312.97226	45527
	2H-perfluoro-2-octenoic acid (FHUEA)	Fluorotelomer unsaturated acids (FTUA)	C8H2F12O2	356.97849	9946
	Perfluoro-n-butanoic acid (PFBA)	Perfluoroalkyl carboxylic acids (PFCAs)	C4HF7O2	212.97865	4261
	10:2 fluorotelomer sulfonate (10:2 FTS)	Fluorotelomer sulfonic acids (FTSs)	C12H5F21O3S	626.95458	439
	6:2 fluorotelomer sulfonate (6:2 FTS)	Fluorotelomer sulfonic acids (FTSs)	C8H5F13O3S	426.96736	321
	Perfluoro-n-octanoic acid (PFOA)	Perfluoroalkyl carboxylic acids (PFCAs)	C8HF15O2	412.96588	706
	3-Perfluoropentyl propanoic acid (FPePA)	Fluorotelomer carboxylic acids (FTCAs)	C8H5F11O2	341.00356	1216
4	2H-perfluoro-2-octenoic acid (FHUEA)	Fluorotelomer unsaturated acids (FTUA)	C8H2F12O2	356.97849	2635
	Perfluoro-n-hexanoic acid (PFHxA)	Perfluoroalkyl carboxylic acids (PFCAs)	C6HF11O2	312.97226	6597
	Perfluoro-n-butanoic acid (PFBA)	Perfluoroalkyl carboxylic acids (PFCAs)	C4HF7O2	212.97865	286
	Perfluoro-n-pentanoic acid (PFPeA)	Perfluoroalkyl carboxylic acids (PFCAs)	C5HF9O2	262.97546	512
8	Perfluoro-n-hexanoic acid (PFHxA)	Perfluoroalkyl carboxylic acids (PFCAs)	C6HF11O2	312.97226	327
14	Not Detected				
47	Perfluoro-n-pentanoic acid (PFPeA)	Perfluoroalkyl carboxylic acids (PFCAs)	C5HF9O2	262.97546	267

Table C8 (Continued)

Negative Mode

Sample	Name	Family	Molecular Formula	Theoretical m/z	Area
51	6:2, 8:2 fluorotelomer phosphate diester	Polyfluoroalkyl phosphoric acid diesters (diPAPs)	C18H9F30O4P	888.96811	483
	Perfluoro-n-hexanoic acid (PFHxA)	Perfluoroalkyl carboxylic acids (PFCAs)	C6HF11O2	312.97226	607
	Perfluoro-n-octanoic acid (PFOA)	Perfluoroalkyl carboxylic acids (PFCAs)	C8HF15O2	412.96588	170
	6:2, 6:2 fluorotelomer phosphate diester	Polyfluoroalkyl phosphoric acid diesters (diPAPs)	C16H9F26O4P	788.97450	371
	8:2, 8:2 fluorotelomer phosphate diester	Polyfluoroalkyl phosphoric acid diesters (diPAPs)	C20H9F34O4P	988.96173	175
54	Perfluoro-n-hexanoic acid (PFHxA)	Perfluoroalkyl carboxylic acids (PFCAs)	C6HF11O2	312.97226	297
61	Perfluorononane sulfonate (PFNS)	Perfluoroalkyl sulfonic acids (PFSAs)	C9HF19O3S	548.92647	100681
	Perfluoro-n-butanoic acid (PFBA)	Perfluoroalkyl carboxylic acids (PFCAs)	C4HF7O2	212.97865	838
	Perfluoro-n-nonanoic acid (PFNA)	Perfluoroalkyl carboxylic acids (PFCAs)	C9HF17O2	462.96268	1179
	Perfluoro-n-undecanoic acid (PFUnDA)	Perfluoroalkyl carboxylic acids (PFCAs)	C11HF21O2	562.95629	845
	6:2, 6:2 fluorotelomer phosphate diester	Polyfluoroalkyl phosphoric acid diesters (diPAPs)	C16H9F26O4P	788.97450	39
67	8:2, 8:2 fluorotelomer phosphate diester	Polyfluoroalkyl phosphoric acid diesters (diPAPs)	C20H9F34O4P	988.96173	301
	Perfluoro-n-octanoic acid (PFOA)	Perfluoroalkyl carboxylic acids (PFCAs)	C8HF15O2	412.96588	348
	8:2, 10:2 fluorotelomer phosphate diester	Polyfluoroalkyl phosphoric acid diesters (diPAPs)	C22H9F38O4P	1088.95534	143
	6:2, 8:2 fluorotelomer phosphate diester	Polyfluoroalkyl phosphoric acid diesters (diPAPs)	C18H9F30O4P	888.96811	61
68	6:2, 6:2 fluorotelomer phosphate diester	Polyfluoroalkyl phosphoric acid diesters (diPAPs)	C16H9F26O4P	788.97450	780
	6:2, 8:2 fluorotelomer phosphate diester	Polyfluoroalkyl phosphoric acid diesters (diPAPs)	C18H9F30O4P	888.96811	236

Positive Mode

Sample	Name	Family	Molecular Formula	Theoretical m/z	Area
47	Perfluoropentane sulfonamido propyl dimethyl quaternary amine propanoate	Perfluoroalkyl sulfonamide amino carboxylates (PFSaAmA)	C13H17F11N2O4S	507.08116	2239
54	Perfluoropentane sulfonamido propyl dimethyl quaternary amine propanoate	Perfluoroalkyl sulfonamide amino carboxylates (PFSaAmA)	C13H17F11N2O4S	507.08116	445
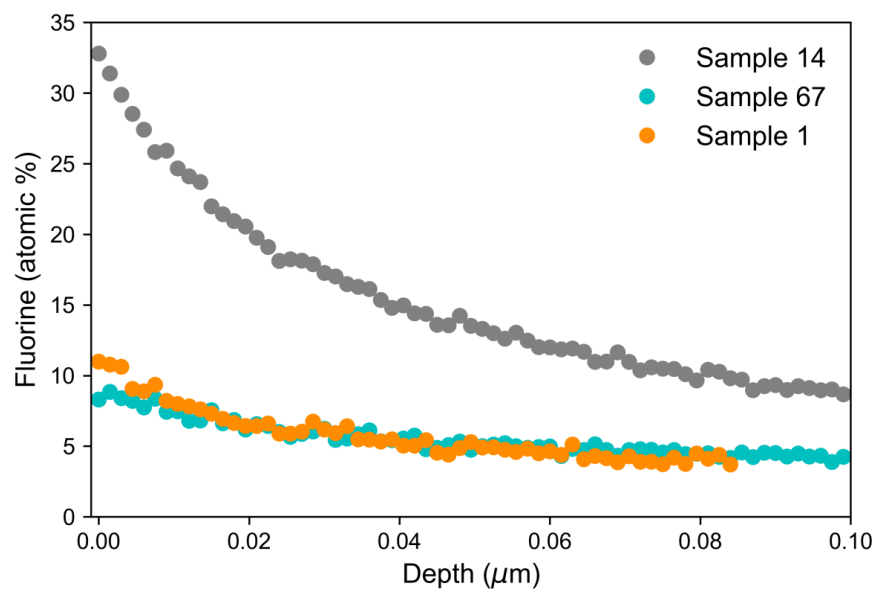
Figure C1. Depth profiles of sample 14 (food bag), sample 67 (used jacket), and sample 1 (bowl). Each point is an XPS measurement taken in between etching intervals (etching completed with an argon ion beam with 10 second intervals). The depth of etching for a tantalum pentoxide reference is plotted.
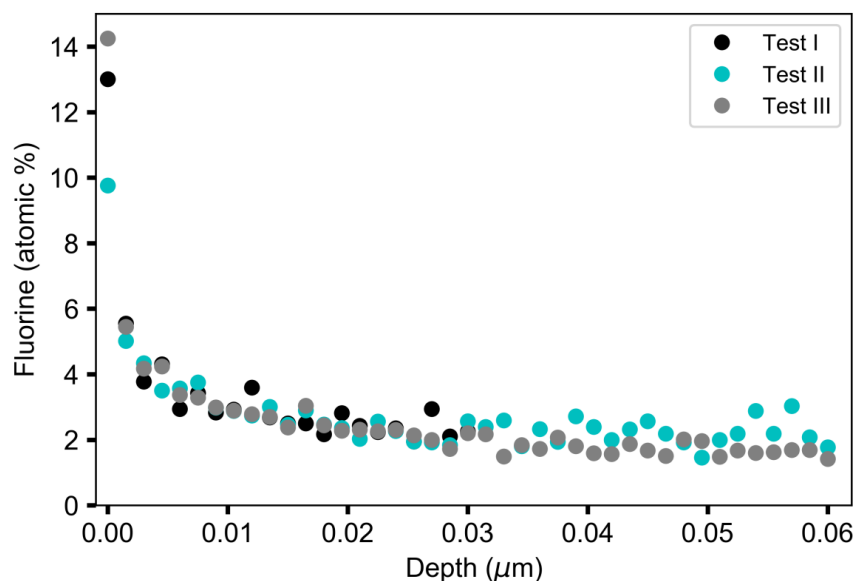
Figure C2. Repetitive depth profile analysis of sample 4 (a takeout box). Each point is an XPS measurement taken in between etching intervals (etching completed with an argon ion beam with 10 second intervals). The depth of etching for a tantalum pentoxide reference is plotted.
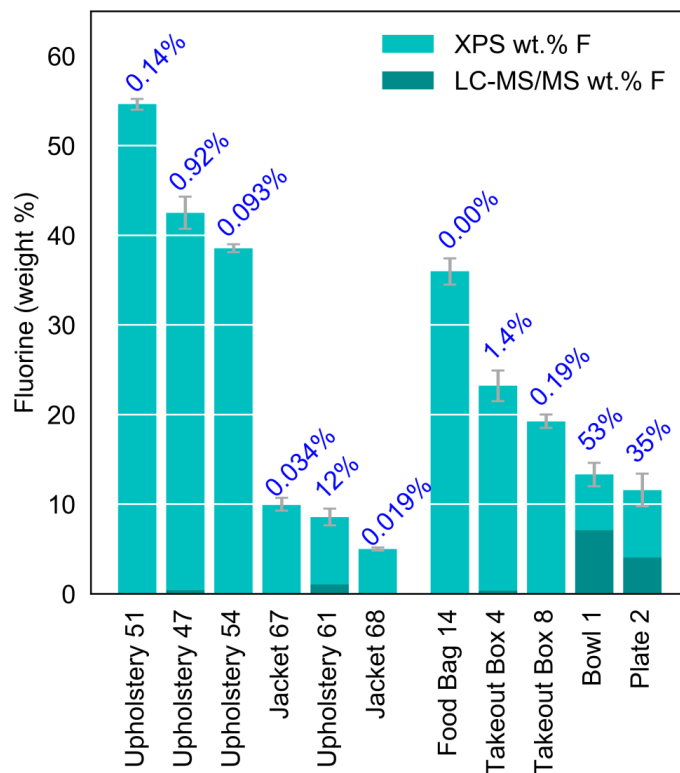
Figure C3. XPS wt.% F and LC-MS/MS wt.% F comparison. Whiskers are the minimum and maximum wt.% F from XPS, the bar is the average wt.% F. The percent of fluorine in the XPS explained by LC-MS/MS is labeled in blue at the top of each bar.
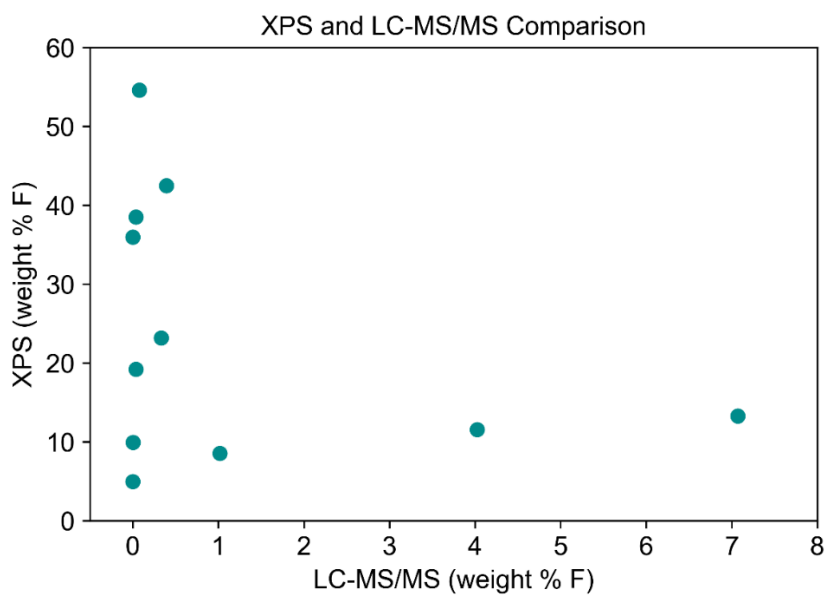
Figure C4. Comparison of LC-MS/MS and XPS data.

References

(1) Buck, R. C.; Franklin, J.; Berger, U.; Conder, J. M.; Cousins, I. T.; de Voogt, P.; Jensen, A. A.; Kannan, K.; Mabury, S. A.; van Leeuwen, S. P. J. Perfluoroalkyl and polyfluoroalkyl substances in the environment: Terminology, classification, and origins. *Integr. Environ. Assess. Manage.* **2011,** *7* (4), 513-541, DOI: 10.1002/ieam.258

(2) Wang, Z.; DeWitt, J. C.; Higgins, C. P.; Cousins, I. T. A never-ending story of per- and polyfluoroalkyl substances (PFASs)? *Environ. Sci. Technol.* **2017,** *51* (5), 2508-2518, DOI: 10.1021/acs.est.6b04806

(3) OECD. *Toward a New Comprehensive Global Database of Per- and Polyfluoroalkyl Substances (PFASs): Summary Report on Updating the OECD 2007 List of Per - and Polyfluoroalkyl Substances (PFASs)*; OECD Environment Directorate, Environment, Health and Safety Division: Paris, France, 2018.

(4) Halldorsson, T. I.; Rytter, D.; Haug, L. S.; Bech, B. H.; Danielsen, I.; Becher, G.; Henriksen, T. B.; Olsen, S. F. Prenatal exposure to perfluorooctanoate and risk of overweight at 20 years of age: A prospective cohort study. *Environ. Health Perspect.* **2012,** *120* (5), 668-673, DOI: 10.1289/ehp.1104034

(5) Barry, V.; Winquist, A.; Steenland, K. Perfluorooctanoic acid (PFOA) exposures and incident cancers among adults living near a chemical plant. *Environ. Health Perspect.* **2013,** *121* (11-12), 1313-1318, DOI: 10.1289/ehp.1306615

(6) Grandjean, P.; Andersen, E. W.; Budtz-Jørgensen, E.; Nielsen, F.; Mølbak, K.; Weihe, P.; Heilmann, C. Serum vaccine antibody concentrations in children exposed to perfluorinated compounds. *J. Am. Med. Assoc.* **2012,** *307*, 391-397, DOI: 10.1001/jama.2011.2034

(7) Geiger, S. D.; Xiao, J.; Ducatman, A.; Frisbee, S.; Innes, K.; Shankar, A. The association between PFOA, PFOS and serum lipid levels in adolescents. *Chemosphere* **2014,** *98*, 78-83, DOI: 10.1016/j.chemosphere.2013.10.005

(8) EPA, U. S. *Drinking Water Health Advisory for Perfluorooctanoic Acid (PFOA)*; 822-R-16-005; U.S. Environmental Protection Agency: Washington, DC, 2016.

(9) EPA, U. S. *Drinking Water Health Advisory for Perfluorooctane Sulfonate (PFOS)*; 822-R-16-004; U.S. Environmental Protection Agency: Washington, DC, 2016.

(10) Wang, Z.; Cousins, I. T.; Scheringer, M.; Hungerbuehler, K. Hazard assessment of fluorinated alternatives to long-chain perfluoroalkyl acids (PFAAs) and their precursors: Status quo, ongoing challenges and possible solutions. *Environ. Int.* **2015,** *75*, 172-179, DOI: 10.1016/j.envint.2014.11.013

(11) Gebbink, W. A.; van Asseldonk, L.; van Leeuwen, S. P. J. Presence of emerging per- and polyfluoroalkyl substances (PFASs) in river and drinking water near a fluorochemical production plant in the Netherlands. *Environmental science & technology* **2017,** *51* (19), 11057-11065, DOI: 10.1021/acs.est.7b02488

(12) Davis, K. L.; Aucoin, M. D.; Larsen, B. S.; Kaiser, M. A.; Hartten, A. S. Transport of ammonium perfluorooctanoate in environmental media near a fluoropolymer manufacturing facility. *Chemosphere* **2007,** *67* (10), 2011-2019, DOI: 10.1016/j.chemosphere.2006.11.049

(13) Moody, C. A.; Field, J. A. Perfluorinated surfactants and the environmental implications of their use in fire-fighting foams. *Environ. Sci. Technol.* **2000,** *34* (18), 3864-3870, DOI: 10.1021/es991359u

(14) Mejia-Avendaño, S.; Munoz, G.; Sauvé, S.; Liu, J. Assessment of the influence of soil characteristics and hydrocarbon fuel cocontamination on the solvent extraction of perfluoroalkyl and polyfluoroalkyl substances. *Anal. Chem.* **2017,** *89* (4), 2539-2546, DOI: 10.1021/acs.analchem.6b04746

(15) Weber, A. K.; Barber, L. B.; LeBlanc, D. R.; Sunderland, E. M.; Vecitis, C. D. Geochemical and hydrologic factors controlling subsurface transport of poly- and perfluoroalkyl substances, Cape Cod, Massachusetts. *Environ. Sci. Technol.* **2017,** *51* (8), 4269-4279, DOI: 10.1021/acs.est.6b05573

(16) McGuire, M. E.; Schaefer, C.; Richards, T.; Backe, W. J.; Field, J. A.; Houtz, E.; Sedlak, D. L.; Guelfo, J. L.; Wunsch, A.; Higgins, C. P. Evidence of remediation-induced alteration of subsurface poly- and perfluoroalkyl substance distribution at a former firefighter training area. *Environ. Sci. Technol.* **2014,** *48* (12), 6644-6652, DOI: 10.1021/es5006187

(17) Houtz, E. F.; Higgins, C. P.; Field, J. A.; Sedlak, D. L. Persistence of perfluoroalkyl acid precursors in AFFF-impacted groundwater and soil. *Environ. Sci. Technol.* **2013,** *47* (15), 8187-8195, DOI: 10.1021/es4018877

(18) Kotthoff, M.; Müller, J.; Jürling, H.; Schlummer, M.; Fiedler, D. Perfluoroalkyl and polyfluoroalkyl substances in consumer products. *Environ. Sci. Pollut. Res.* **2015,** *22* (19), 14546-14559, DOI: 10.1007/s11356-015-4202-7

(19) Ahrens, L.; Bundschuh, M. Fate and effects of poly- and perfluoroalkyl substances in the aquatic environment: A review. *Environ. Tox. Chem.* **2014,** *33* (9), 1921-1929, DOI: 10.1002/etc.2663

(20) Robel, A. E.; Marshall, K.; Dickinson, M.; Lunderberg, D.; Butt, C.; Peaslee, G.; Stapleton, H. M.; Field, J. A. Closing the mass balance on fluorine on papers and textiles. *Environ. Sci. Technol.* **2017,** *51* (16), 9022-9032, DOI: 10.1021/acs.est.7b02080

(21) Schultz, M. M.; Higgins, C. P.; Huset, C. A.; Luthy, R. G.; Barofsky, D. F.; Field, J. A. Fluorochemical mass flows in a municipal wastewater treatment facility. *Environ. Sci. Technol.* **2006,** *40* (23), 7350-7357, DOI: 10.1021/es061025m

(22) Hoffman, K.; Webster Thomas, F.; Bartell Scott, M.; Weisskopf Marc, G.; Fletcher, T.; Vieira Verónica, M. Private drinking water wells as a source of exposure to perfluorooctanoic acid (PFOA) in communities surrounding a fluoropolymer production facility. *Environmental health perspectives* **2011,** *119* (1), 92-97, DOI: 10.1289/ehp.1002503

(23) Vestergren, R.; Cousins, I. T.; Trudel, D.; Wormuth, M.; Scheringer, M. Estimating the contribution of precursor compounds in consumer exposure to PFOS and PFOA. *Chemosphere* **2008,** *73* (10), 1617-1624, DOI: 10.1016/j.chemosphere.2008.08.011

(24) Haug, L. S.; Huber, S.; Becher, G.; Thomsen, C. Characterisation of human exposure pathways to perfluorinated compounds — Comparing exposure estimates with biomarkers of exposure. *Environ. Int.* **2011,** *37* (4), 687-693, DOI: 10.1016/j.envint.2011.01.011

(25) Tian, Z.; Kim, S.-K.; Shoeib, M.; Oh, J.-E.; Park, J.-E. Human exposure to per- and polyfluoroalkyl substances (PFASs) via house dust in Korea: Implication to exposure pathway. *The Science of the total environment* **2016,** *553*, 266-275, DOI: 10.1016/j.scitotenv.2016.02.087

(26) Lau, C.; Anitole, K.; Hodes, C.; Lai, D.; Pfahles-Hutchens, A.; Seed, J. Perfluoroalkyl acids: A review of monitoring and toxicological findings. *Toxicol. Sci.* **2007,** *99* (2), 366-394, DOI: 10.1093/toxsci/kfm128

(27) Wallington, T. J.; Hurley, M. D.; Xia, J.; Wuebbles, D. J.; Sillman, S.; Ito, A.; Penner, J. E.; Ellis, D. A.; Martin, J.; Mabury, S. A.; Nielsen, O. J.; Anderson, M. P. S. Formation of $C_7F_{15}COOH$ (PFOA) and other perfluorocarboxylic acids during the atmospheric oxidation of 8:2 fluorotelomer alcohol. *Environ. Sci. Technol.* **2006,** *40*, 924-930, DOI: 10.1021/es051858x

(28) *Fire extinguishing agent, aqueous film forming foam (AFFF) liquid concentrate, for fresh and seawater*; Naval Research Laboratory; Naval Technology Center for Safety and Survivability: Washington, DC, 2004.

(29) Melzer, D.; Rice, N.; Depledge, M. H.; Henley, W. E.; Galloway, T. S. Association between serum perfluorooctanoic acid (PFOA) and thyroid disease in the U.S. National Health and Nutrition Examination Survey. *Environ. Health Perspect.* **2010,** *118* (5), 686-692, DOI: 10.1289/ehp.0901584

(30) Maupin, M. A.; Kenny, J. F.; Hutson, S. S.; Lovelace, J. K.; Barber, N. L.; Linsey, K. S. *Estimated use of water in the United States in 2010*; U.S. Geological Survey Circular 1405; U.S. Geological Survey: Reston, VA, 2014.

(31) Vecitis, C. D.; Wang, Y.; Cheng, J.; Park, H.; Mader, B. T.; Hoffmann, M. R. Sonochemical degradation of perfluorooctanesulfonate in aqueous film-forming foams. *Environ. Sci. Technol.* **2010,** *44* (1), 432-438, DOI: 10.1021/es902444r

(32) Anderson, R. H.; Long, G. C.; Porter, R. C.; Anderson, J. K. Occurrence of select perfluoroalkyl substances at U.S. Air Force aqueous film-forming foam release sites other than fire-training areas: Field-validation of critical fate and transport properties. *Chemosphere* **2016,** *150*, 678-685, DOI: 10.1016/j.chemosphere.2016.01.014

(33) Moody, C. A.; Hebert, G. N.; Strauss, S. H.; Field, J. A. Occurrence and persistence of perfluorooctanesulfonate and other perfluorinated surfactants in groundwater at a fire-training area at Wurtsmith Air Force Base, Michigan, USA. *J. Environ. Monit.* **2003,** *5* (2), 341-345, DOI: 10.1039/B212497A

(34) Filipovic, M.; Woldegiorgis, A.; Norström, K.; Bibi, M.; Lindberg, M.; Österås, A.-H. Historical usage of aqueous film forming foam: A case study of the widespread distribution of perfluoroalkyl acids from a military airport to groundwater, lakes, soils and fish. *Chemosphere* **2015,** *129*, 39-45, DOI: 10.1016/j.chemosphere.2014.09.005

(35) Schultz, M. M.; Barofsky, D. F.; Field, J. A. Quantitative determination of fluorotelomer sulfonates in groundwater by LC MS/MS. *Environ. Sci. Technol.* **2004,** *38* (6), 1828-1835, DOI: 10.1021/es035031j

(36) Moody, C. A.; Field, J. A. Determination of perfluorocarboxylates in groundwater impacted by fire-fighting activity. *Environ. Sci. Technol.* **1999,** *33* (16), 2800-2806, DOI: 10.1021/es981355+

(37) *Estimated quantities of aqueous film forming foam (AFFF) in the United States*; Prepared for the Fire Fighting Foam Coalition: Arlington, VA; Darwin, R. L.; Hughes Associates, Inc.: Baltimore, MD, 2004.

(38) Liu, J.; Mejia Avendaño, S. Microbial degradation of polyfluoroalkyl chemicals in the environment: A review. *Environ. Int.* **2013,** *61*, 98-114, DOI: 10.1016/j.envint.2013.08.022

(39) Harding-Marjanovic, K. C.; Houtz, E. F.; Yi, S.; Field, J. A.; Sedlak, D. L.; Alvarez-Cohen, L. Aerobic biotransformation of fluorotelomer thioether amido sulfonate (Lodyne) in AFFF-amended microcosms. *Environ. Sci. Technol.* **2015,** *49* (13), 7666-7674, DOI: 10.1021/acs.est.5b01219

(40) Mejia Avendaño, S.; Liu, J. Production of PFOS from aerobic soil biotransformation of two perfluoroalkyl sulfonamide derivatives. *Chemosphere* **2015,** *119*, 1084-1090, DOI: 10.1016/j.chemosphere.2014.09.059

(41) Zhang, S.; Szostek, B.; McCausland, P. K.; Wolstenholme, B. W.; Lu, X.; Wang, N.; Buck, R. C. 6:2 and 8:2 fluorotelomer alcohol anaerobic biotransformation in digester sludge from a WWTP under methanogenic conditions. *Environ. Sci. Technol.* **2013,** *47* (9), 4227-4235, DOI: 10.1021/es4000824

(42) Zhang, S.; Lu, X.; Wang, N.; Buck, R. C. Biotransformation potential of 6:2 fluorotelomer sulfonate (6:2 FTSA) in aerobic and anaerobic sediment. *Chemosphere* **2016,** *154*, 224-230, DOI: 10.1016/j.chemosphere.2016.03.062

(43) Plumlee, M. H.; McNeill, K.; Reinhard, M. Indirect photolysis of perfluorochemicals: Hydroxyl radical-initiated oxidation of N-ethyl perfluorooctane sulfonamido acetate (N-EtFOSAA) and other perfluoroalkanesulfonamides. *Environ. Sci. Technol.* **2009,** *43* (10), 3662-3668, DOI: 10.1021/es803411w

(44) Sinclair, E.; Kannan, K. Mass loading and fate of perfluoroalkyl surfactants in wastewater treatment plants. *Environ. Sci. Technol.* **2006,** *40* (5), 1408-1414, DOI: 10.1021/es051798v

(45) Loganathan, B. G.; Sajwan, K. S.; Sinclair, E.; Senthil Kumar, K.; Kannan, K. Perfluoroalkyl sulfonates and perfluorocarboxylates in two wastewater treatment facilities in Kentucky and Georgia. *Water Res.* **2007,** *41* (20), 4611-20, DOI: 10.1016/j.watres.2007.06.045

(46) U.S. Geological Survey. Cape Cod Toxic Substances Hydrology Research Site; http://ma.water.usgs.gov/MMRCape//. DOI:

(47) Barber, L. B., II. Sorption of chlorobenzenes to Cape Cod aquifer sediments. *Environ. Sci. Technol.* **1994,** *28* (5), 890-897, DOI: 10.1021/es00054a021

(48) Barber, L. B.; Keefe, S. H.; LeBlanc, D. R.; Bradley, P. M.; Chapelle, F. H.; Meyer, M. T.; Loftin, K. A.; Kolpin, D. W.; Rubio, F. Fate of sulfamethoxazole, 4-nonylphenol, and 17beta-estradiol in groundwater contaminated by wastewater treatment plant effluent. *Environ. Sci. Technol.* **2009,** *43* (13), 4843-4850, DOI: 10.1021/es803292v

(49) Böhlke, J. K.; Smith, R. L.; Miller, D. N. Ammonium transport and reaction in contaminated groundwater: Application of isotope tracers and isotope fractionation studies. *Water Resour. Res.* **2006,** *42* (5), 1-19, DOI: 10.1029/2005WR004349

(50) Barbaro, J. R.; Walter, D. A.; LeBlanc, D. R. *Transport of Nitrogen in a Treated-Wastewater Plume to Coastal Discharge Areas, Ashumet Valley, Cape Cod, Massachusetts*; U.S. Geological Survey Scientific Investigations Report 2013–5061; U.S. Geological Survey: Reston, VA, 2013.

(51) Repert, D. A.; Barber, L. B.; Hess, K. M.; Keefe, S. H.; Kent, D. B.; LeBlanc, D. R.; Smith, R. L. Long-term natural attenuation of carbon and nitrogen within a groundwater plume after removal of the treated wastewater source. *Environ. Sci. Technol.* **2006,** *40* (4), 1154-1162, DOI: 10.1021/es051442j

(52) Parkhurst, D. L.; Stollenwerk, K. G.; Colman, J. A. *Reactive-transport simulation of phosphorus in the sewage plume at the Massachusetts Military Reservation, Cape Cod, Massachusetts*; U.S. Geological Survey Water-Resources Investigations Report 03-4017; U. S. Geological Survey: Reston, VA, 2003.

(53) Savoie, J. G.; LeBlanc, D. R.; Fairchild, G. M.; Smith, R. L.; Kent, D. B.; Barber, L. B.; Repert, D. A.; Hart, C. P.; Keefe, S. H.; Parsons, L. A. *Groundwater-quality data for a treated-wastewater plume near the Massachusetts Military Reservation, Ashumet Valley, Cape Cod, Massachusetts, 2006–08*; U.S. Geological Survey Data Series; 648; U.S. Geological Survey: Reston, VA, 2012.

(54) Barber, L. B., II; Thurman, E. M.; Runnells, D. D. Geochemical heterogeneity in a sand and gravel aquifer: Effect of sediment mineralogy and particle size on the sorption of chlorobenzenes. *J. Contam. Hydrol.* **1992,** *9*, 35-54, DOI: 10.1016/0169-7722(92)90049-K

(55) Barber, L. B., II; Thurman, E. M.; Schroeder, M. P.; LeBlanc, D. R. Long-term fate of organic micropollutants in sewage-contaminated groundwater. *Environ. Sci. Technol.* **1988,** *22* (2), 205-211, DOI: 10.1021/es00167a012

(56) LeBlanc, D. R. *Sewage plume in a sand and gravel aquifer, Cape Cod, Massachusetts*; U. S. Geological Survey Water-Supply Paper 2218; U. S. Geological Survey: Reston, VA, 1984.

(57) *Soil thermal treatment program remedial action summary report*; Prepared for AFCEE/MMR Installation Restoration Program: Otis ANGB, MA; Harding Lawson Associates: Portland, ME, 1999.

(58) *Final supplemental remedial investigation/feasibility study work plan for 1,4-dioxane and perfluorinated compounds at Ashumet Valley, Joint Base Cape Cod, MA*; 658003-EC-AV-QAPP-003; Prepared for AFCEC/JBCC Installation Restoration Program: Otis ANGB, MA; CH2M: Otis ANGB, MA, 2016.

(59) *Final closure report, FTA-1 site*; AFC-J23-35G09901-M17-0021; Prepared for AFCEE/MMR Installation Restoration Program: Otis ANGB, MA; Jacobs Engineering Group, Inc.: Bourne, MA, 2000.

(60) Glöckner, V.; Lunkwitz, K.; Prescher, D. Zur chemischen und thermischen Stabilität von Fluortensiden. *Tenside Surf. Det.* **1989,** *26*, 376-380, DOI:

(61) Wang, F.; Lu, X.; Shih, K.; Liu, C. Influence of calcium hydroxide on the fate of perfluorooctanesulfonate under thermal conditions. *J. Hazard. Mater.* **2011,** *192* (3), 1067-1071, DOI: 10.1016/j.jhazmat.2011.06.009

(62) Krusic, P. J.; Marchione, A. A.; Roe, D. C. Gas-phase NMR studies of the thermolysis of perfluorooctanoic acid. *J. Fluorine Chem.* **2005,** *126* (11–12), 1510-1516, DOI: 10.1016/j.jfluchem.2005.08.016

(63) LeBlanc, D. R.; Hess, K. M.; Kent, D. B.; Smith, R. L.; Barber, L. B.; Stollenwerk, K. G.; Campo, K. W. *Natural restoration of a sewage plume in a sand and gravel aquifer, Cape Cod, Massachusetts*; U.S.

Geological Survey Water-Resources Investigations Report 99-4018C; U. S. Geological Survey: Reston, VA, 1999.

(64) Garabedian, S. P.; LeBlanc, D. R.; Gelhar, L. W.; Celia, M. A. Large-scale natural gradient tracer test in sand and gravel, Cape Cod, Massachusetts: 2. Analysis of spatial moments for a nonreactive tracer. *Water Resour. Res.* **1991,** *27* (5), 911-924, DOI: 10.1029/91WR00242

(65) LeBlanc, D. R.; Garabedian, S. P.; Hess, K. M.; Gelhar, L. W.; Quadri, R. D.; Stollenwerk, K. G.; Wood, W. W. Large-scale natural gradient tracer test in sand and gravel, Cape Cod, Massachusetts: 1. Experimental design and observed tracer movement. *Water Resour. Res.* **1991,** *27* (5), 895-910, DOI: 10.1029/91WR00241

(66) Walter, D. A.; McCobb, T. D.; Masterson, J. P.; Fienen, M. N. *Potential effects of sea-level rise on the depth to saturated sediments of the Sagamore and Monomoy flow lenses on Cape Cod, Massachusetts*; U.S. Geological Survey Scientific Investigations Report; 2016–5058; U. S. Geological Survey: Reston, VA, 2016.

(67) *National field manual for the collection of water-quality data: U.S. Geological Survey Techniques of Water-Resources Investigations*; Book 9; Chaps. A1-A10; U. S. Geological Survey: Reston, VA, variously dated; http://pubs.water.usgs.gov/twri9A.

(68) Barber, L. B.; Weber, A. K.; LeBlanc, D. R.; Hull, R. B.; Sunderland, E. M.; Vecitis, C. D. *Poly- and Perfluoroalkyl Substances in Contaminated Groundwater, Cape Cod, Massachusetts, 2014-2015*; U.S. Geological Survey Data Release; U.S. Geological Survey: Reston, VA, 2017. https://doi.org/10.5066/F7Z899KT.

(69) Steinle-Darling, E.; Reinhard, M. Nanofiltration for trace organic contaminant removal: Structure, solution, and membrane fouling effects on the rejection of perfluorochemicals. *Environ. Sci. Technol.* **2008,** *42* (14), 5292-5297, DOI: 10.1021/es703207s

(70) Goss, K.-U. The pKa values of PFOA and other highly fluorinated carboxylic acids. *Environ. Sci. Technol.* **2008,** *42* (2), 456-458, DOI: 10.1021/es702192c

(71) Guelfo, J. L.; Higgins, C. P. Subsurface transport potential of perfluoroalkyl acids at aqueous film-forming foam (AFFF)-impacted sites. *Environ. Sci. Technol.* **2013,** *47* (9), 4164-4171, DOI: 10.1021/es3048043

(72) Higgins, C. P.; Luthy, R. G. Sorption of perfluorinated surfactants on sediments. *Environ. Sci. Technol.* **2006,** *40*, 7251-7256, DOI: 10.1021/es061000n

(73) Ahrens, L.; Yeung, L. W. Y.; Taniyasu, S.; Lam, P. K. S.; Yamashita, N. Partitioning of perfluorooctanoate (PFOA), perfluorooctane sulfonate (PFOS) and perfluorooctane sulfonamide (PFOSA)

between water and sediment. *Chemosphere* **2011,** *85* (5), 731-737, DOI:
10.1016/j.chemosphere.2011.06.046

(74) McKenzie, E. R.; Siegrist, R. L.; McCray, J. E.; Higgins, C. P. Effects of chemical oxidants on
perfluoroalkyl acid transport in one-dimensional porous media columns. *Environ. Sci. Technol.* **2015,** *49*
(3), 1681-1689, DOI: 10.1021/es503676p

(75) Ahrens, L.; Taniyasu, S.; Yeung, L. W. Y.; Yamashita, N.; Lam, P. K. S.; Ebinghaus, R. Distribution of
polyfluoroalkyl compounds in water, suspended particulate matter and sediment from Tokyo Bay,
Japan. *Chemosphere* **2010,** *79* (3), 266-272, DOI: 10.1016/j.chemosphere.2010.01.045

(76) Sepulvado, J. G.; Blaine, A. C.; Hundal, L. S.; Higgins, C. P. Occurrence and fate of perfluorochemicals
in soil following the land application of municipal biosolids. *Environ. Sci. Technol.* **2011,** *45* (19), 8106-
8112, DOI: 10.1021/es103903d

(77) Houtz, E. F.; Sedlak, D. L. Oxidative conversion as a means of detecting precursors to perfluoroalkyl
acids in urban runoff. *Environ. Sci. Technol.* **2012,** *46* (17), 9342-9349, DOI: 10.1021/es302274g

(78) Higgins, C. P.; Field, J. A.; Criddle, C. S.; Luthy, R. G. Quantitative determination of
perfluorochemicals in sediments and domestic sludge. *Environ. Sci. Technol.* **2005,** *39*, 3946-3956, DOI:
10.1021/es048245p

(79) Smith, R. L.; Repert, D. A.; Barber, L. B.; LeBlanc, D. R. Long-term groundwater contamination after
source removal-The role of sorbed carbon and nitrogen on the rate of reoxygenation of a treated-
wastewater plume on Cape Cod, MA, USA. *Chem. Geol.* **2013,** *337–338*, 38-47, DOI:
10.1016/j.chemgeo.2012.11.007

(80) Lamborg, C. H.; Kent, D. B.; Swarr, G. J.; Munson, K. M.; Kading, T.; O'Connor, A. E.; Fairchild, G. M.;
LeBlanc, D. R.; Wiatrowski, H. A. Mercury speciation and mobilization in a wastewater-contaminated
groundwater plume. *Environ. Sci. Technol.* **2013,** *47* (23), 13239-13249, DOI: 10.1021/es402441d

(81) Prevedouros, K.; Cousins, I. T.; Buck, R. C.; Korzeniowski, S. H. Sources, fate and transport of
perfluorocarboxylates. *Environ. Sci. Technol.* **2006,** *40* (1), 32-44, DOI: 10.1021/es0512475

(82) Furl, C. V.; Meredith, C. A.; Strynar, M. J.; Nakayama, S. F. Relative importance of wastewater
treatment plants and non-point sources of perfluorinated compounds to Washington State rivers. *Sci.
Total Environ.* **2011,** *409* (15), 2902-2907, DOI: 10.1016/j.scitotenv.2011.04.035

(83) Kim, S. K.; Im, J. K.; Kang, Y. M.; Jung, S. Y.; Kho, Y. L.; Zoh, K. D. Wastewater treatment plants
(WWTPs)-derived national discharge loads of perfluorinated compounds (PFCs). *J. Hazard. Mater.* **2012,**
201-202, 82-91, DOI: 10.1016/j.jhazmat.2011.11.036

(84) Colman, J. A. *Response curves for phosphorous plume lengths from reactive-solute-transport simulations of onland disposal of wastewater in noncarbonate sand and gravel aquifers*; U.S. Geological Survey Scientific Investigations Report; 2004-5299; U.S. Geological Survey: Reston, VA, 2005.

(85) Tang, C. Y.; Shiang Fu, Q.; Gao, D.; Criddle, C. S.; Leckie, J. O. Effect of solution chemistry on the adsorption of perfluorooctane sulfonate onto mineral surfaces. *Water Res.* **2010,** *44* (8), 2654-2662, DOI: 10.1016/j.watres.2010.01.038

(86) McCobb, T. D.; LeBlanc, D. R.; Walter, D. A.; Hess, K. M.; Kent, D. B.; Smith, R. L. *Phosphorus in a ground-water contaminant plume discharging to Ashumet Pond, Cape Cod, Massachusetts, 1999*; U.S. Geological Survey Water-Resources Investigations Report 02-4306; U. S. Geological Survey: Reston, VA, 2003.

(87) Ololade, I. A.; Zhou, Q.; Pan, G. Influence of oxic/anoxic condition on sorption behavior of PFOS in sediment. *Chemosphere* **2016,** *150*, 798-803, DOI: 10.1016/j.chemosphere.2015.08.068

(88) Wang, F.; Shih, K.; Leckie, J. O. Effect of humic acid on the sorption of perfluorooctane sulfonate (PFOS) and perfluorobutane sulfonate (PFBS) on boehmite. *Chemosphere* **2015,** *118*, 213-218, DOI: 10.1016/j.chemosphere.2014.08.080

(89) Houtz, E. F.; Sutton, R.; Park, J.-S.; Sedlak, M. Poly- and perfluoroalkyl substances in wastewater: Significance of unknown precursors, manufacturing shifts, and likely AFFF impacts. *Water Res.* **2016,** *95*, 142-149, DOI: 10.1016/j.watres.2016.02.055

(90) Place, B. J.; Field, J. A. Identification of novel fluorochemicals in aqueous film-forming foams used by the US military. *Environ. Sci. Technol.* **2012,** *46* (13), 7120-7127, DOI: 10.1021/es301465n

(91) Liu, C.; Liu, J. Aerobic biotransformation of polyfluoroalkyl phosphate esters (PAPs) in soil. *Environ. Pollut.* **2016,** *212*, 230-237, DOI: 10.1016/j.envpol.2016.01.069

(92) Mejia-Avendaño, S.; Vo Duy, S.; Sauvé, S.; Liu, J. Generation of perfluoroalkyl acids from aerobic biotransformation of quaternary ammonium polyfluoroalkyl surfactants. *Environ. Sci. Technol.* **2016,** *50* (18), 9923-9932, DOI: 10.1021/acs.est.6b00140

(93) Nelson, J. W.; Hatch, E. E.; Webster, T. F. Exposure to polyfluoroalkyl chemicals and cholesterol, body weight, and insulin resistance in the general U.S. population. *Environmental health perspectives* **2010,** *118* (2), 197-202, DOI: 10.1289/ehp.0901165

(94) Sun, Q.; Zong, G.; Valvi, D.; Nielsen, F.; Coull, B.; Grandjean, P. Plasma concentrations of perfluoroalkyl substances and risk of Type 2 diabetes: A prospective investigation among U.S. women. *Environ. Health Perspect.* **2018,** *126* (3), DOI: 10.1289/EHP2619

(95) Hu, X. C.; Andrews, D. Q.; Lindstrom, A. B.; Bruton, T. A.; Schaider, L. A.; Grandjean, P.; Lohmann, R.; Carignan, C. C.; Blum, A.; Balan, S. A.; Higgins, C. P.; Sunderland, E. M. Detection of poly- and perfluoroalkyl substances (PFASs) in U.S. drinking water linked to industrial sites, military fire training areas, and wastewater treatment plants. *Environ Sci Technol Letters* **2016**, DOI: 10.1021/acs.estlett.6b00260

(96) Vestergren, R.; Cousins, I. T. Tracking the pathways of human exposure to perfluorocarboxylates. *Environmental science & technology* **2009,** *43* (15), 5565-5575, DOI: 10.1021/es900228k

(97) Barzen-Hanson, K. A.; Roberts, S. C.; Choyke, S.; Oetjen, K.; McAlees, A.; Riddell, N.; McCrindle, R.; Ferguson, P. L.; Higgins, C. P.; Field, J. A. Discovery of 40 classes of per- and polyfluoroalkyl substances in historical aqueous film-forming foams (AFFFs) and AFFF-impacted groundwater. *Environmental science & technology* **2017,** *51* (4), 2047-2057, DOI: 10.1021/acs.est.6b05843

(98) D'Agostino, L. A.; Mabury, S. A. Identification of novel fluorinated surfactants in aqueous film forming foams and commercial surfactant concentrates. *Environ. Sci. Technol.* **2014,** *48* (1), 121-129, DOI: 10.1021/es403729e

(99) Yi, S.; Harding-Marjanovic, K. C.; Houtz, E. F.; Gao, Y.; Lawrence, J. E.; Nichiporuk, R. V.; Iavarone, A. T.; Zhuang, W.-Q.; Hansen, M.; Field, J. A.; Sedlak, D. L.; Alvarez-Cohen, L. Biotransformation of AFFF component 6:2 fluorotelomer thioether amido sulfonate generates 6:2 fluorotelomer thioether carboxylate under sulfate-reducing conditions. *Environ. Sci. Technol. Lett.* **2018,** *5* (5), 283-288, DOI: 10.1021/acs.estlett.8b00148

(100) Winter, T. C.; Harvey, J. W.; Franke, O. L.; Alley, W. M. *Ground water and surface water a single resource*; U.S. Geological Survey Circular 1139; U.S. Geological Survey: Denver, CO, 1998.

(101) Lewandowski, J.; Meinikmann, K.; Nützmann, G.; Rosenberry, D. O. Groundwater – the disregarded component in lake water and nutrient budgets. Part 2: effects of groundwater on nutrients. *Hydrological Processes* **2015,** *29* (13), 2922-2955, DOI: 10.1002/hyp.10384

(102) Harvey, R. W.; Metge, D. W.; LeBlanc, D. R.; Underwood, J. C.; Aiken, G. R.; Butler, K. D.; McCobb, T. D.; Jasperse, J. Importance of the colmation layer in the transport and removal of cyanobacteria, viruses, and dissolved organic carbon during natural lake-bank filtration. *Journal of Environmental Quality* **2015,** *44* (5), 1413-1423, DOI: 10.2134/jeq2015.03.0151

(103) Lee, R. W.; Bennett, P. C. Reductive dissolution and reactive solute transport in a sewage-contaminated glacial outwash aquifer. *Ground Water* **1998,** *36* (4), 583-595, DOI:

(104) Li, F.; Fang, X.; Zhou, Z.; Liao, X.; Zou, J.; Yuan, B.; Sun, W. Adsorption of perfluorinated acids onto soils: Kinetics, isotherms, and influences of soil properties. *The Science of the total environment* **2019,** *649*, 504-514, DOI: 10.1016/j.scitotenv.2018.08.209

(105) Lyu, Y.; Brusseau, M. L.; Chen, W.; Yan, N.; Fu, X.; Lin, X. Adsorption of PFOA at the air–water interface during transport in unsaturated porous media. *Environ. Sci. Technol.* **2018**, DOI: 10.1021/acs.est.8b02348

(106) Brusseau, M. L. Assessing the potential contributions of additional retention processes to PFAS retardation in the subsurface. *The Science of the total environment* **2018,** *613-614*, 176-185, DOI: 10.1016/j.scitotenv.2017.09.065

(107) Stoliker, D. L.; Repert, D. A.; Smith, R. L.; Song, B.; LeBlanc, D. R.; McCobb, T. D.; Conaway, C. H.; Hyun, S. P.; Koh, D.-C.; Moon, H. S.; Kent, D. B. Hydrologic controls on nitrogen cycling processes and functional gene abundance in sediments of a groundwater flow-through lake. *Environ. Sci. Technol.* **2016,** *50* (7), 3649-3657, DOI: 10.1021/acs.est.5b06155

(108) Walter, D. A.; Masterson, J. P. *Estimated hydrologic budgets of kettle-hole ponds in coastal aquifers of southeastern Massachusetts*; 2011-5137; Reston, VA, 2011.

(109) Ju, X.; Jin, Y.; Sasaki, K.; Saito, N. Perfluorinated surfactants in surface, subsurface water and microlayer from Dalian coastal waters in China. *Environ. Sci. Technol.* **2008,** *42* (10), 3538-3542, DOI: 10.1021/es703006d

(110) Taniyasu, S.; Kannan, K.; Yeung, L. W. Y.; Kwok, K. Y.; Lam, P. K. S.; Yamashita, N. Analysis of trifluoroacetic acid and other short-chain perfluorinated acids (C2–C4) in precipitation by liquid chromatography–tandem mass spectrometry: Comparison to patterns of long-chain perfluorinated acids (C5–C18). *Anal. Chim. Acta* **2008,** *619* (2), 221-230, DOI: 10.1016/j.aca.2008.04.064

(111) Walter, D. A.; LeBlanc, D. R. *Geochemical and hydrologic considerations in remediating phosphorus-contaminated ground water in a sewage plume near Ashumet Pond, Cape Cod, Massachusetts*; U.S. Geological Survey; Report 97-202; U.S. Geological Survey: Reston, VA, 1997.

(112) LeBlanc, D. R.; Böhlke, J. K.; Hull, R. B.; Tokranov, A. K.; McCobb, T. D. Isotopic mapping of "lake shadows" in groundwater and their effects on the paths of VOC and PFAS contaminant plumes in the Cape Cod aquifer. *In Preparation*, DOI: N/A

(113) Ceazan, M. L.; Thurman, E. M.; Smith, R. L. Retardation of ammonium and potassium transport through a contaminated sand and gravel aquifer: the role of cation exchange. *Environ. Sci. Technol.* **1989,** *23* (11), 1402-1408, DOI: 10.1021/es00069a012

(114) Nightingale, E. R. Phenomenological Theory of Ion Solvation. Effective Radii of Hydrated Ions. *The Journal of Physical Chemistry* **1959,** *63* (9), 1381-1387, DOI: 10.1021/j150579a011

(115) Jeon, J.; Kannan, K.; Lim, B. J.; An, K. G.; Kim, S. D. Effects of salinity and organic matter on the partitioning of perfluoroalkyl acid (PFAs) to clay particles. *J. Environ. Monit.* **2011,** *13* (6), 1803-1810, DOI: 10.1039/C0EM00791A

(116) Hellsing, M. S.; Josefsson, S.; Hughes, A. V.; Ahrens, L. Sorption of perfluoroalkyl substances to two types of minerals. *Chemosphere* **2016,** *159*, 385-391, DOI: 10.1016/j.chemosphere.2016.06.016

(117) Davis, J. A.; Gloor, R. Adsorption of dissolved organics in lake water by aluminum oxide. Effect of molecular weight. *Environ. Sci. Technol.* **1981,** *15* (10), 1223-1229, DOI: 10.1021/es00092a012

(118) Coston, J. A.; Fuller, C. C.; Davis, J. A. Pb2+ and Zn2+ adsorption by a natural aluminum- and iron-bearing surface coating on an aquifer sand. *Geochimica et Cosmochimica Acta* **1995,** *59* (17), 3535-3547, DOI: 10.1016/0016-7037(95)00231-N

(119) Gao, X.; Chorover, J. Adsorption of perfluorooctanoic acid and perfluorooctanesulfonic acid to iron oxide surfaces as studied by flow-through ATR-FTIR spectroscopy. *Environmental Chemistry* **2012,** *9* (2), 148-157, DOI: 10.1071/EN11119

(120) Gu, B.; Schmitt, J.; Chen, Z.; Liang, L.; McCarthy, J. F. Adsorption and desorption of natural organic matter on iron oxide: mechanisms and models. *Environmental science & technology* **1994,** *28* (1), 38-46, DOI: 10.1021/es00050a007

(121) Grandjean, P.; Heilmann, C.; Weihe, P.; Nielsen, F.; Mogensen, U. B.; Timmermann, A.; Budtz-Jørgensen, E. Estimated exposures to perfluorinated compounds in infancy predict attenuated vaccine antibody concentrations at age 5-years. *J. Immunotoxicol.* **2017,** *14* (1), 188-195, DOI: 10.1080/1547691X.2017.1360968

(122) Liu, G.; Dhana, K.; Furtado, J. D.; Rood, J.; Zong, G.; Liang, L.; Qi, L.; Bray, G. A.; DeJonge, L.; Coull, B.; Grandjean, P.; Sun, Q. Perfluoroalkyl substances and changes in body weight and resting metabolic rate in response to weight-loss diets: A prospective study. *PLoS Med.* **2018,** *15* (2), e1002502, DOI: 10.1371/journal.pmed.1002502

(123) Begley, T. H.; White, K.; Honigfort, P.; Twaroski, M. L.; Neches, R.; Walker, R. A. Perfluorochemicals: Potential sources of and migration from food packaging. *Food Addit. Contam.* **2005,** *22* (10), 1023-1031, DOI: 10.1080/02652030500183474

(124) Begley, T. H.; Hsu, W.; Noonan, G.; Diachenko, G. Migration of fluorochemical paper additives from food-contact paper into foods and food simulants. *Food Addit. Contam., Part A* **2008,** *25* (3), 384-390, DOI: 10.1080/02652030701513784

(125) Yuan, G.; Peng, H.; Huang, C.; Hu, J. Ubiquitous occurrence of fluorotelomer alcohols in eco-friendly paper-made food-contact materials and their implication for human exposure. *Environ. Sci. Technol.* **2016,** *50* (2), 942-950, DOI: 10.1021/acs.est.5b03806

(126) CEC. *Furthering the Understanding of the Migration of Chemicals from Consumer Products – A Study of Per- and Polyfluoroalkyl substances (PFASs) in Clothing, Apparel, and Children's Items*; Montreal, Canada, 2017; p 201.

(127) *Polyfluoroalkyl Substances (PFASs) in Textiles for Children*; Survey of chemical substances in consumer products No. 136, 2015; The Danish Environmental Protection Agency: Copenhagen, Denmark, 2015.

(128) Ritter, E. E.; Dickinson, M. E.; Harron, J. P.; Lunderberg, D. M.; DeYoung, P. A.; Robel, A. E.; Field, J. A.; Peaslee, G. F. PIGE as a screening tool for per- and polyfluorinated substances in papers and textiles. *Nucl. Instrum. Methods Phys. Res., Sect. B* **2017,** *407*, 47-54, DOI: 10.1016/j.nimb.2017.05.052

(129) Schaider, L. A.; Balan, S. A.; Blum, A.; Andrews, D. Q.; Strynar, M. J.; Dickinson, M. E.; Lunderberg, D. M.; Lang, J. R.; Peaslee, G. F. Fluorinated compounds in U.S. fast food packaging. *Environ. Sci. Technol. Lett.* **2017,** *4* (3), 105-111, DOI: 10.1021/acs.estlett.6b00435

(130) Vickerman, J. C.; Gilmore, I. S., *Surface Analysis, The Principal Techniques*. 2nd ed.; John Wiley & Sons Ltd: West Sussex, U.K., 2009.

(131) Ye, F.; Zushi, Y.; Masunaga, S. Survey of perfluoroalkyl acids (PFAAs) and their precursors present in Japanese consumer products. *Chemosphere* **2015,** *127*, 262-268, DOI: 10.1016/j.chemosphere.2015.02.026

(132) van der Veen, I.; Weiss, J. M.; Hanning, A.-C.; de Boer, J.; Leonards, P. E. G. Development and validation of a method for the quantification of extractable perfluoroalkyl acids (PFAAs) and perfluorooctane sulfonamide (FOSA) in textiles. *Talanta* **2016,** *147*, 8-15, DOI: 10.1016/j.talanta.2015.09.021

(133) Ferraria, A. M.; Lopes da Silva, J. D.; Botelho do Rego, A. M. XPS studies of directly fluorinated HDPE: problems and solutions. *Polymer* **2003,** *44* (23), 7241-7249, DOI: 10.1016/j.polymer.2003.08.038

(134) *Direct Contact Risk-Based Soil Concentration: Perfluorooctanoic Acid: CAS #335-67-1* New Hampshire Department of Environmental Services, Environmental Health Program: Concord, NH, 2016.

(135) Nansé, G.; Papirer, E.; Fioux, P.; Moguet, F.; Tressaud, A. Fluorination of carbon blacks: An X-ray photoelectron spectroscopy study: I. A literature review of XPS studies of fluorinated carbons. XPS

investigation of some reference compounds. *Carbon* **1997,** *35* (2), 175-194, DOI: 10.1016/S0008-6223(96)00095-4

(136) Seah, M. P. Universal equation for argon gas cluster sputtering yields. *J. Phys. Chem. C* **2013,** *117* (24), 12622-12632, DOI: 10.1021/jp402684c

(137) Smith, R. L.; Harvey, R. W.; LeBlanc, D. R. Importance of closely spaced vertical sampling in delineating chemical and microbiological gradients in groundwater studies. *J. Contam. Hydrol.* **1991,** *7* (3), 285-300, DOI: 10.1016/0169-7722(91)90032-V

(138) Zapico, M. M.; Vales, S.; Cherry, J. A. A wireline piston core barrel for sampling cohesionless sand and gravel below the water table. *Ground Water Monit. Remediat.* **1987,** *7* (3), 74-82, DOI: 10.1111/j.1745-6592.1987.tb01077.x

(139) Eberl, D. D. User's guide to RockJock -- A program for determining quantitative mineralogy from powder X-Ray diffraction data; U.S.Geological Survey Open-File Report 2003-78; http://pubs.usgs.gov/of/2003/of03-078/. DOI:

(140) Benskin, J. P.; Silva, A. O. D.; Martin, J. W. Isomer profiling of perfluorinated substances as a tool for source tracking: A review of early findings and future applications. *Rev. of Environ. Contam. and Toxicol.* **2010,** *208*, 111-160, DOI: 10.1007/978-1-4419-6880-7_2

(141) Greaves, A. K.; Letcher, R. J. Linear and branched perfluorooctane sulfonate (PFOS) isomer patterns differ among several tissues and blood of polar bears. *Chemosphere* **2013,** *93* (3), 574-580, DOI: 10.1016/j.chemosphere.2013.07.013

(142) Agemian, H.; Chau, A. S. Y. A study of different analytical extraction methods for nondetrital heavy metals in aquatic sediments. *Archives of Environmental Contamination and Toxicology* **1977,** *6* (1), 69-82, DOI: 10.1007/bf02097751

(143) Tuccillo, M. E.; Cozzarelli, I. M.; Herman, J. S. Iron reduction in the sediments of a hydrocarbon-contaminated aquifer. *Applied Geochemistry* **1999,** *14* (5), 655-667, DOI: 10.1016/S0883-2927(98)00089-4

(144) Chen, W.; Zhang, X.; Mamadiev, M.; Wang, Z. Sorption of perfluorooctane sulfonate and perfluorooctanoate on polyacrylonitrile fiber-derived activated carbon fibers: in comparison with activated carbon. *RSC Advances* **2017,** *7* (2), 927-938, DOI: 10.1039/C6RA25230C

(145) Seah, M. P. Argon cluster size-dependence of sputtering yields of polymers: Molecular weights and the universal equation. *Surf. Interface Anal.* **2015,** *47* (1), 169-172, DOI: 10.1002/sia.5656

(146) Seah, M. P.; Nunney, T. S. Sputtering yields of compounds using argon ions. *J. Phys. D: Appl. Phys.* **2010,** *43* (25), 253001, DOI: 10.1088/0022-3727/43/25/253001

(147) Cumpson, P. J.; Portoles, J. F.; Sano, N. Material dependence of argon cluster ion sputter yield in polymers: Method and measurements of relative sputter yields for 19 polymers. *J. Vac. Sci. Technol., A* **2013,** *31* (2), 020605, DOI: 10.1116/1.4791669